2023

UNRAVELING THE CONSEQUENCE OF ADULT ONSET SULFATIDE DEPLETION: ITS IMPLICATIONS IN MYELIN AND AXONAL HEATH IN THE CONTEXT OF NEURODEGENERATIVE DISEASE

Elizabeth Dustin
Virginia Commonwealth University

UNRAVELING THE CONSEQUENCE OF ADULT ONSET SULFATIDE DEPLETION: ITS IMPLICATIONS IN MYELIN AND AXONAL HEATH IN THE CONTEXT OF NEURODEGENERATIVE DISEASE

A dissertation submitted in partial fulfillment of the requirements for the degree of

Doctor of Philosophy at Virginia Commonwealth University.

By

Elizabeth Dustin

B.S. North Carolina State University, 2016

Director: Jeffrey L. Dupree, Ph.D.

Associate Professor

Department of Anatomy and Neurobiology

Virginia Commonwealth University

Richmond, Virginia

May 2023

ACKNOWLEDGEMENTS

To begin with, I would like to thank Dr. Jeff Dupree who embodied mentorship by providing guidance and support while allowing me to develop my independence as a scientist. He taught me persistence, resilience, and to be open to where the data takes you.

I would also like to thank Dr. Rory McQuiston who taught me electrophysiology and allowed me to use his rig over the years to collect invaluable data. A special thanks to my committee member Dr. Carmen Sato-Bigbee who provided encouragement and mentorship in teaching myelin isolations and how to isolate adult oligodendrocytes from mice. And all my committee members who provided invaluable guidance and mentorship over the years. I would also like to thank the VCU Department of Anatomy and Neurobiology Microscopy Facility, including Dr. Tytus Bernas, Judy Williamson, Terry Smith, and Fran White for their assistance with training and image collection over the years.

Thank-you to the members of the Dupree lab, former and present. I would like to especially thank Dr. Edna Suarez-Pozos, who taught me western blotting, and supported me during all the highs and lows of research.

Finally, I would like to thank my family for their unconditional love and support, especially my fiancé, Nick, who provided a light at the end of the tunnel. Lastly, this thesis work is dedicated to my father who suffered from neurological disease. His disease is what motivated me to pursue neuroscience research here at VCU.

TABLE OF CONTENTS

LIST OF FIGURES **PAGE**

LIST OF TABLES

LIST OF ABBREVIATIONS

Ca^{2+}	Calcium
CAM	Cell Adhesion Molecule
CAP	Compound Action Potential
Caspr1	Contactin-Associated protein 1
CGT	Ceramide Galactosyltransferase
cKO	conditional knock out
CNP	2',3'-Cyclic Nucleotide 3'-Phosphodiesterase
CNS	Central Nervous System
CSF	Cerebral Spinal Fluid
CST	Ceramide Sulfotransferase
DIS	Dissemination In Space
DIT	Dissemination In Time
DMT	Disease-Modifying Therapy
DRM	Detergent Resistant Membranes
EBV	Epstein-Barr Virus
ECM	Extracellular Matrix
EM	Electron Microscopy
ER	Endoplasmic Reticulum
Gal3st1	galactose 3-O-sulfotransferase1

GalCer	Galactosylceramide
GlcCer	Glucosylceramide
GPI	Glycosylphosphatidylinositol
GSL	Glycosphingolipid
IP	Immunoprecipitation
KO	Knock-Out
Kv1.1	Voltage Gated Potassium Channel Kv1.1
LDL	Low-Density Lipoprotein
m	month
MAG	Myelin-Associated Glycoprotein
MBP	Myelin Basic Protein
MOG	Myelin Oligodendrocyte Glycoprotein
MRI	Magnetic Resonance Imaging
MS	Multiple Sclerosis
MWM	Morris Water Maze
Na^+	Sodium
Nav1.6	Voltage-gated sodium channel $Na_v1.6$
NAWM	Normal Appearing White Matter
NCX	Sodium-Calcium Exchanger
Nfasc155	Neurofascin 155
Nfasc155H	Neurofascin 155 high

Nfasc155L	Neurofascin 155 low
Nfasc186	Neurofascin 186
NgR2	Nogo-66 receptor
NK	Natural Killer
NOR	Novel Object Recognition
NoR	Node of Ranvier
OL	Oligodendrocyte
OPC	Oligodendrocyte Precursor Cell
PDGF	Platelet Derived Growth Factor
PI	Post-Injection
PLP	Proteolipid Protein
SPT	Serine Palmitoyltransferase
Sulfatide	3-O-sulfogalactosylceramide
TAG-1	Transient Axonal Glycoproteintype-1
TCR	T-cell Receptor
TGN	Trans-Golgi Network
TREM2	Triggering Receptor Expressed on Myeloid Cells-2

ABSTRACT

UNRAVELING THE CONSEQUENCE OF ADULT ONSET SULFATIDE DEPLETION: ITS IMPLICATIONS IN MYELIN AND AXONAL HEATH IN THE CONTEXT OF NEURODEGENERATIVE DISEASE

By Elizabeth Dustin, B.S

A dissertation submitted in partial fulfillment of the requirements for the degree of Doctor of Philosophy at Virginia Commonwealth University.

Virginia Commonwealth University, 2023

Director: Jeffrey L. Dupree, Ph.D.
Associate Professor
Department of Anatomy and Neurobiology
Deputy Associate Chief of Staff for Research and Development
Richmond VA Medical Center

Multiple Sclerosis is an immune mediated disease of the CNS. MS is diagnosed through detection of demyelinated regions. However, recent studies demonstrate that Normal Appearing White Matter (NAWM) contains substantial pathology. One such pathology observed in the NAWM is the reduction of sulfatide. The proper stoichiometry of lipids in myelin acts to maintain rapid conduction velocity, provide trophic support to the neuron, and protect the axon from degeneration. We previously characterized a mouse lacking sulfatide's synthesizing enzyme, CST through constitutive gene disruption and demonstrate that sulfide is required for proper stability of the myelin sheath. However, since MS is typically diagnosed in adults, the constitutive CST KO mouse has limited clinical relevance since these mice lack sulfatide embryonically. To generate a more clinically relevant model, our lab generated a "floxed" CST mouse, mating it to the PLP-cre^{ERT} driver to provide spatial and temporal ablation of sulfatide. I demonstrate that there is no change in g-ratios or myelin abnormalities, but there is presence of axonal degeneration. In addition, ion channels and Caspr1 become mis-localized, with loss of contactin-neurofascin155 binding. Subsequently, EP activity of myelinated fibers is disrupted. I also demonstrate lack of neurofascin155 stability within the myelin sheath, which is likely due to

loss of sulfatide stability. Together, my studies show that adult onset sulfatide depletion is sufficient to drive axonal pathology while maintaining myelin integrity. These findings have significant implications in understanding the clinical presentation of MS indicating that loss of CNS function may precede demyelination in this devastating disease.

CHAPTER ONE

INTRODUCTION

1.1 The Central Nervous System

The central nervous system (CNS) serves as an information processing center and coordinated outputs. The CNS consists of the brain and spinal cord and contains highly specialized cells known as neurons and glia (astrocytes, microglia, and oligodendrocytes). Neurons of the CNS are highly polarized, having dendrites to receive information from other neurons, an axon to propagate electrical signal, and synaptic terminals to transmit the signal (Holcomb et al., 2013; Britt et al., 2016). Astrocytes are highly diverse and have a wide variety of roles such as forming synapses, supplying energy to neurons, regulating blood flow, mediating ion buffering, and modulating disease (Y. Kim et al., 2019; N.-S. Kim & Chung, 2023; Z. Chen et al., 2023). Microglia are CNS myeloid derived cells. Microglia are highly adaptive cells to their environment and function to immunologically regulate the CNS environment (Borst et al., 2021; L. Zhang et al., 2023). Oligodendrocytes are highly specialized cells which contribute to the white matter through the production of myelin, which will be discussed below.

1.2 Brief History of the Myelin Sheath

The term “myelin” was first coined by Rudolf Ludwig Virchow in 1858. Stating this “medullary matter” has the consistency of egg yolk, he was correct in that myelin is a lipid rich substance. (Boullerne, 2016). It was not until 1922 when Pío del Río-Hortega, together with his colleague Wilder Graves Penfield, hypothesized that myelin could be made by oligodendrocytes (del Rio-Hortega, 1924; Penfield, 1924). Since then, the biochemical composition and function of the myelin sheath continues to be discovered. Here, I will briefly discuss the biochemical composition of the myelin sheath and how its unique composition is critical to function and consequential for disease.

1.3 Oligodendrocyte Lineage

Oligodendrocytes are unique in that their development consists of a lineage of cells with each stage having their own function (J.-Q. Wang et al., 2023). Neural stem cells commit to the oligodendrocyte lineage and become oligodendrocyte precursor cells (OPCs) under the influence of *Olig1/2, NKX2.2*, and *Sox10* (Emery, 2010; van Tilborg et al., 2018) and platelet derived growth factor (PDGF) promotes proliferation and inhibits differentiation. The main functions of OPCs are to migrate, proliferate, and differentiate into myelin producing cells during development (Hughes et al., 2013); however, they also have a wide variety of functions in the adult brain that includes ion buffering, launching immune response, and modulating signal transduction (Lin & Bergles, 2004; Káradóttir et al., 2008; Larson et al., 2018; Falcão et al., 2018; Madsen et al., 2020). Under the regulatory control of *Myrf*, OPCs mature into pre-oligodendrocytes (Bujalka et al., 2013) and then continue to differentiate into premyelinating oligodendrocytes that begin to express enzymes required for synthesis of myelin specific lipids such as galactosylceramide. Finally, the maturing oligodendrocytes extend membranous processes that contact and initiate that wrapping around the axon. These membranous extensions of the mature, myelin competent oligodendrocytes, which express a unique complement of myelin specific constituents such as proteolipid protein (PLP), myelin basic protein (MBP), myelin oligodendrocyte glycoprotein (MOG), and sulfatide, continue to wrap the axon resulting in a multilayer lamellar structure that constitutes the immature myelin sheath. With continuous wrapping and extrusion of the oligodendrocytic cytoplasm, membrane compaction occurs resulting in the mature myelin sheath. (Trapp et al., 1997; Trajkovic et al., 2006).

1.4.1 Biochemical Composition of Myelinating Oligodendrocytes

While the myelin sheath is contiguous with the plasma membrane of the oligodendrocyte cell body, it has a unique biochemical composition that consists of 70% lipid and 30% protein, whereas most plasma membranes contain a 50/50 ratio (Williams et al., 1993; Morell & Quarles, 1999). MBP and PLP are the major myelin proteins, making up about 30% and 50% of the protein composition of myelin, respectively (Jahn et al., 2009). The remaining composition of myelin proteins consist of over 300 proteins. A few prominent myelin-specific proteins, which will be discussed in this thesis, are; 2',3'-cyclic nucleotide 3'-phosphodiesterase (CNP), myelin-

associated glycoprotein (MAG), myelin oligodendrocyte glycoprotein (MOG), and Neurofascin 155 (Nfasc 155). Myelin membrane lipids consist of about 30% cholesterol, 40% phospholipids and 30% glycosphingolipids (GSL), whereas plasma membrane composition has much lower glycosphingolipid content but higher phospholipids (O'brien, 1965; Casares et al., 2019).

1.4.2 Myelin Lipids

As stated above, the myelin membrane is composed of about 40% phospholipids, 30% cholesterol, and 30% glycosphingolipids (Casares et al., 2019). Phospholipids are found in most plasma membranes; however, the myelin membrane is uniquely enriched with plasmalogens, a class of ether-linked phospholipids (Nagan & Zoeller, 2001; Chrast et al., 2011) and are localized to the inner leaflet of the myelin bilayer (Aggarwal et al., 2011). Cholesterol is a well-known class of lipid that has many essential functions in the myelin sheath including membrane compaction, fluidity, and localization of myelin proteins, as well as limiting ion leakage through membranes, which facilitates efficient conduction (Haines, 2001; Ohvo-Rekilä et al., 2002). Once cholesterol is produced, it is trafficked to the trans-Golgi network (TGN) and clustered with GSLs to form microdomains. GSLs can be divided into glucosylceramides (GlcCer) and galactosylceramides (GalCer), differing by the addition of a glucose versus a galactose head group, respectively. De novo synthesis of GSLs begins on the cytoplasmic leaflet of the endoplasmic reticular (ER) membrane (Wigger et al., 2019). Condensation of L-serine and palmitoyl-CoA catalyzed by L-serine palmitoyl transferase forms 3-ketosphinganine, which is then reduced to sphinganine via 3-ketosphinganine reductase. The ceramide synthases (CerS) form dihydroceramide with a carrying chain length. Ceramide synthases consist of a family ranging from CerS1 to CerS6, each having selective substrates for addition of a variety of chain lengths. Generally, CerS1-3 catalyzes the addition of a loner chain C20-24 and CerS4-6 catalyzes the addition of a shorter chain length. These chain lengths have a variety of differential function including development, immune response, and cellular signaling (Hirahara et al., 2000; Jahng et al., 2004; Laviad et al., 2008; Maricic et al., 2014; Hirahara et al., 2017). Dihydroceramide is the precursor to the GSL backbone known as ceramide, which varies in alkyl chain length due to the CerS, hydroxylation state, and desaturation, contributing to

increased variation of GSLs population. After formation of ceramide, the lipid can be decorated with various moieties resulting in the synthesis of the above-mentioned lipids. These final synthetic steps occur within both the ER and the Golgi.

The myelin sheath is enriched in GSLs compared to other membranes, which allows the sheath to have a higher degree of organization. (Poduslo, 1975; Norton & Cammer, 1984). GSLs consist of a sugar residue with a ceramide backbone, having an acyl chain. These physical properties of a larger head group and fatty acid backbone induces membrane curvature, giving structural stability to the spiraling myelin around the axon (Curatolo & Neuringer, 1986; Castro et al., 2014; Alonso & Goñi, 2018).

1.4.2.2 Microdomains

The enrichment of the myelin sheath with GSLs facilitates the formation of unique membrane domains known as microdomains (Fiedler et al., 1993; Bieberich, 2018). Microdomains form through weak associations between the carbohydrate head groups of adjacent GSLs and the tight clustering characteristic of rafts is further facilitated by the close packing of their frequently saturated acyl chains. Microdomains are small in size rarely larger than 200nm; they are heterogeneous, highly dynamic, cholesterol and sphingolipid rich domains that compartmentalize cellular processes (K. Simons & Ikonen, 1997). For many years, the presence of microdomains was highly debated due to the limited methods of study. A prime approach for the isolation and analysis of lipid rats was the use of detergents, such as Triton X-100, Triton X-102, CHAPs, or Brij98 (Hope & Pike, 1996; Cubí et al., 2013). Membranes were exposed to detergents and the non-soluble fraction was collected and termed detergent resistant membranes (DRMs), which were considered analogous to microdomains (Fiedler et al., 1993; Hope & Pike, 1996; T. Kim & Pfeiffer, 1999; Taylor et al., 2002; Lichtenberg, 2005; Cubí et al., 2013; Caritá et al., 2017). Although this approach was frequently used for raft isolation, significant concerns surrounded this approach based on the potential for artificial associations that resulted from the vigorous homogenization and centrifugation methods required for DRM harvesting. Presently, microdomains are well accepted consequential of improved methods of analysis including super resolution

imaging techniques that allow for the discrimination of structures smaller than 200nm (Klar et al., 2001; Rust et al., 2006; Sezgin, 2017).

Microdomains regulate vital cellular processes by serving as platforms for cellular communication and transduction by spatially regulating protein associations (Hope & Pike, 1996; K. Simons & Ikonen, 1997; Subczynski & Kusumi, 2003; García-Arribas et al., 2016; Roy & Patra, 2023). Proteins that are associated with rafts are typically post-translationally modified by the addition of glycosylphosphatidylinositol (GPI) anchors, fatty acids (e.g., palmitoyl-residues), or isoprenylated or acylated groups (Benjamins et al., 2012). These long carbon chains enable the protein to form close associations with the carbon chain of the GSLs, resulting in the sequestering of specific proteins based on their post-translational modifications (Melkonian et al., 1999; Mollinedo & Gajate, 2020). Apart from post-translationally modified sites, little is known about raft targeting motifs in proteins. Most recently however, it was found that sulfatide can bind directly to a myelin protein, Neurofascin 155 (Nfasc155) (McKie et al., 2023) at multiple binding sites on the extracellular domain. Although Nfasc155 is known to be palmitoylated which facilitates raft inclusion (Ren & Bennett, 1998), this current paper provides an alternative mechanism for neurofascin association with raft enriched lipids. Therefore, further work needs to be conducted to provide a more complete understanding of how proteins associate with these unique lipid domains.

1.4.2.3 importance of glycosphingolipids in the myelin membrane

As discussed above, GSLs are enriched in microdomains and this raft association provides GSLs with the unique opportunity to mediate a variety of cellular functions. However, myelin GSLs may also regulate myelin membrane structure and function through mechanisms that may be independent of raft association (Pasquini et al., 1989; Yamashita et al., 1999; M. Simons et al., 2000; Furukawa et al., 2001; Fewou et al., 2010; McGonigal et al., 2019). The major glycosphingolipids of the myelin sheath are galactosylceramide (GalCer), and it's sulfated derivative, 3-O-sulfogalactosylceramide (sulfatide) (O'Brien & Sampson, 1965; Grassi et al., 2016). GalCer and sulfatide comprise up to 16% and 4% of myelin lipids, respectively (Bosio et al., 1998;

Dasgupta et al., 2002). Together, they interact across apposed membranes on the myelin sheath potentially forming the “glycosynapse”, which stabilizes compact myelin but also may aid in transmitting signals throughout the myelin sheath (Boggs et al., 2004; Boggs, 2014). The synthesis of these 2 lipids is dependent on the transfer of a galactose head group from UDP-galactose to ceramide, a synthetic step that is catalyzed by the UDP-galactose:ceramide galactosyltransferase (CGT) to form GalCer (Morell & Radin, 1969; Sprong et al., 1998; Hanada et al., 2009) . To form sulfatide, GalCer is transported to the Golgi and the enzyme cerebroside sulfotransferase (CST) catalyzes the addition of a sulfate group to the galactose resulting in the formation of the GalCer derivation sulfatide (Yaghootfam et al., 2007).

Sulfatide is a highly multi-functional lipid involved in myelin development and maintenance, cellular proliferation and differentiation, structural stability, molecular organization, and even regulating immune response (Bansal et al., 1999; Marcus et al., 2002; Shroff et al., 2009; Hayashi et al., 2013a; A. Pomicter et al., 2013; Su et al., 2021). Largely, these functions of sulfatide were determined through the creation of a constitutive knock-out (KO) of the CST gene, galactose3-O-sulfotransferase 1 (*Gal3st1*). CST is expressed in oligodendrocytes, but also in non-neural tissues such as kidney, liver, and testis (Honke et al., 2002). Our current studies build off of decades of work that focused on the constitutive CST KO mouse in an attempt to better understand the role of sulfatide in the myelin sheath in regards to MS onset.

The CST KO mouse was created and published in 2002 by Dr. Koichi Honke. An extensive characterization of the constitutive KO mouse revealed extensive and progressive myelin pathology such as inverted paranodal loops, myelin splitting, and axonal swelling at 12 weeks of age. These pathologies are likely what contributed to the concomitant motor dysfunction such as a whole body tremor and hindlimb weakness (Honke et al., 2002). Noticing structural abnormalities at the level of the paranode, our group continued to use this mouse to further understand the role that sulfatide plays in the formation and maintenance of the myelin sheath. Ishibashi et al., (2002a) used this mouse and discovered that voltage gated potassium channels, Kv1.1, and voltage gated sodium channels, Nav1.6, were mis-localized and also the stereotypic clustering of these

channels progressively disappeared in the aged CST KO mouse. Due to the sodium and potassium channels initially being localized properly, with subsequent mis-localization, our group deemed sulfatide has a role in myelin maintenance. Although sulfatide loss is along a developmental timeline, the myelin domains localized normally. However by week six they are significantly diminished (Ishibashi et al., 2002a). This data suggests that sulfatide is essential for maintaining the ion channel domains.

In addition, qualitative assessment of the myelin sheath indicated demyelination was not occurring. Subsequent ultrastructural analyses determined that although widespread myelin loss was not evident, myelin integrity was compromised, and resulted in progressive loss of myelin integrity (Marcus et al., 2006) and that sulfatide regulated the oligodendrocyte population (Shroff et al., 2009). Together, the use of the constitutive CST KO demonstrated that sulfatide is essential for the development and maintenance of the myelin sheath.

Sulfatide in the myelin sheath is present in different “species” having a variation in acyl chain length ranging from C16-C24. Although not completely elucidated, evidence indicates that the different chain lengths may mediate unique functions. The chain length varies with maturation of the oligodendrocyte, with C16 and 18 being prominent in OPCs and C24:0 and 24:1 being the most prominent in mature oligodendrocytes (Hirahara et al., 2017). The C24 chains combined with the lipid’s large head groups positioned on the extracellular side of the membrane leaflet are together, thought to aid in the curvature required for myelin to wrap around the axon (Chrast et al., 2011). Other studies have demonstrated different chain lengths of sulfatide can have different immunogenic responses, and different chain lengths of sulfatide are found in the serum of MS patients compared to healthy controls (Jeon et al., 2008; Moyano et al., 2013; Maricic et al., 2014).

In microdomains, sulfatide maintains protein associations in the myelin sheath. Using Triton X-100 as a detergent, our lab determined that sulfatide is required for certain myelin proteins, such as MAG and neurofascin 155 high (Nfasc155H), a novel form of neurofascin 155, to be stabilized in the membrane (A. D. Pomicter et al., 2010a; A. Pomicter et al., 2013). This had clinical significance as in tissue from multiple sclerosis patients, Nfasc155H was also reduced after exposure to triton (A. D. Pomicter et al., 2010a).

1.4.3 Myelin Proteins

Myelin basic protein (MBP) is a major myelin protein found in the compact myelin sheath. It has four isoforms in the mouse and has several post-translational modifications such as deamidation, citrullination, phosphorylation, and methylation (Poduslo, 1975; Chou et al., 1976; Zand et al., 1998). Because of its highly positive charge, expression of MBP at the myelin sheath interacts with the negatively charged cytoplasmic membrane surface that brings the two layers together at their cytoplasmic sides forming the MBP-rich major dense line, resulting in myelin compaction (Aggarwal et al., 2011). MBP has long thought to be considered an autoantigen for the onset of MS. Interestingly, MS patients present with altered post-translational modifications of MBP, which may have pathogenic significance (Steinman, 2001; J. K. Kim et al., 2003).

The other major myelin protein, proteolipid protein (PLP), is a hydrophobic, transmembrane protein that spans the membrane four times and can be palmitoylated and acylated (Bizzozero et al., 2002). Similar to MBP, PLP is a major constituent of the myelin sheath and is considered a marker of mature oligodendrocytes. In contrast to its role as a marker of maturation, PLP's smaller splice variant, DM20, is synthesized early in development with a gradual decline in expression with maturation and is a minor constituent of myelin although it presents with similar properties to PLP (Milner et al., 1985; K. A. Nave et al., 1987; Campagnoni & Skoff, 2001). Also similar to MBP, PLP's major functions include assembly and stabilization of the myelin sheath but in contrast to MBP, which mediates the formation of the major dense line, PLP acts to bring together the correct apposition of the extracellular leaflets of the membrane resulting in the formation of the intraperiod line (Boison & Stoffel, 1994; Boison et al., 1995).

Myelin-Oligodendrocyte Glycoprotein (MOG) is an integral membrane protein located in the extracellular leaflet of the noncompact myelin (Burger et al., 1993). The function of MOG is not fully understood, but due to its extracellular domain, it may be involved in cell surface receptor or cell signaling (Johns & Bernard, 1999; Martini & Schachner, 1986). It is found in detergent resistant membranes, likely forming protein-lipid

interactions through n-linked glycosylation (T. Kim & Pfeiffer, 1999). N-linked glycosylation has been shown to impact the folding and antigenicity of proteins (Gardinier et al., 1992; Burska et al., 2014). Further, MOG is also considered an autoantigen for demyelinating diseases (for review see(Berger & Reindl, 2015) and repairing MOG glycosylation provides a potential therapeutic approach for promoting remyelination (Sharma et al., 2022), further demonstrating the importance and function of post-translational modifications.

Myelin Associated Glycoprotein (MAG) is a member of the immunoglobulin superfamily and is located in non-compact myelin, and is highly enriched at the adaxonal membrane along the internode and also at the mesaxon and paranodal loops (Trapp & Quarles, 1982; Bartsch et al., 1989; Quarles, 2007; Lopez, 2014). MAG serves as a ligand of gangliosides on neuronal cell surfaces and promotes differentiation, maintenance and survival of oligodendrocytes (L. J. Yang et al., 1996). MAG has several post-translational modifications such as N-linked glycosylation, C-mannosylation and palmitoylation (Pedraza et al., 1990; Tropak & Roder, 1997; Pronker et al., 2016). Of particular interest to our research is palmitoylation as this modification allows proper formation of tight associations with lipids and sequestration into lipid domains (Dai, 2022; Uchida et al., 2022). Previously, our group reported a related function of MAG with myelin GSLs (Marcus et al., 2002) and demonstrated a specific association between sulfatide and MAG that is required for the stable anchorage of MAG within the myelin sheath (Marcus et al., 2002; A. Pomicter et al., 2013). Based on the ease of extraction using Triton X-100 in the absence or sulfatide, we hypothesized that the acyl chains of sulfatide forms tight associations with the acyl chain of the palmitate group and in the absence of this interaction, MAG stability was compromised.

Cyclic Nucleotide Phosphodiesterase (CNP, also known as CNPase) is an enzymatic protein in the myelin sheath localized to the paranode that accounts for 4% of myelin proteins and is expressed very early in developmental lineage of OLs (Trapp et al., 1988; Scherer et al., 1994; Aggarwal et al., 2011). CNP has remained enigmatic as the actual enzymatic function of CNP is not entirely known, but several studies have begun to understand its enzymatic role in the central nervous system (CNS) (J. Lee et al., 2001; Verrier et al.,

2013). CNP is an early oligodendrocyte marker, involved in process outgrowth. It traffics to the periphery by association with microfilaments and juxtanodin, a cytoskeletal protein. It is involved in oligodendrocyte process outgrowth and it is associated with the cytoskeletal network (B. Zhang et al., 2005). Once in the myelin sheath, CNP plays an essential role in localizing sodium channels (Rasband et al., 2005). CNP is found in DRMs along with cytoskeletal elements, indicating they are sequestered in microdomains (De Angelis & Braun, 1996).

Neurofascin 155 (Nfasc155) is the myelin specific splice variant of the neurofascin gene. It is a member of the IgG superfamily and plays essential roles in development and myelination (Klingseisen et al., 2019). Nfasc155 is localized to the paranodes where it binds with the axonal protein complex of contactin and contactin-associated protein 1 (Caspr1) (Tait et al., 2000; Charles et al., 2002a). Disruption of Nfasc155 leads to paranodal disruption (Pillai et al., 2009) and neurological disease (Smigiel et al., 2018). Nfasc 155 is stabilized in the paranodes through associations with glycosphingolipids (Susuki et al., 2007; McGonigal et al., 2019; Baba & Ishibashi, 2019). More specifically, specific forms of Nfasc155 has sulfatide-dependent associations in the myelin sheath (A. Pomicter et al., 2013). Pomicter et al. (2010) demonstrated that there are two forms of Nfasc155, which were termed Nfasc 155 high (H) and Nfasc 155 low (L) based on their electrophoretic separation (A. D. Pomicter et al., 2010a). The specific functions and localizations of these forms is not known, but Nfasc155H is dependent on sulfatide for proper stability in the myelin sheath and it is postulated that this form is localized to the paranodes (A. Pomicter et al., 2013). Moreover, these forms are regulated through development, with Nfasc155H presenting as the predominant form during development particularly during periods of myelin formation while Nfasc155L reveals a progressive increase in expression in adulthood (A. D. Pomicter et al., 2010a), indicating Nfasc155H and L may have differential roles throughout development.

A major goal of this thesis is to provide a better understanding of how sulfatide regulates myelin protein stability within the myelin sheath in adulthood. All of these myelin proteins contain unique post-translational modifications. Post-translational modifications give proteins a variety of functions including signaling, folding, localization, and function and can regulate associations to cytoskeletal elements and microdomains dependent or independent of sulfatide.

1.5.1 Organization of the Myelin Sheath

Oligodendrocytes (OLs) are the myelinating glia of the CNS producing a multilayered membrane system called the myelin sheath. The myelin sheath extends from the cell body, making multiple wraps around an axon forming layers of uniformly electron-dense and electron-light layers (the major dense line and the intraperiod line, respectively) in electron microscopic images (Hartline, 2008). One oligodendrocyte can extend up to 80 myelin processes to multiple axons (Zalc, 2006; M. Simons & Trotter, 2007). Myelin acts to maintain rapid conduction velocity, provide trophic support to the neuron, and protect the axon from degeneration (K.-A. Nave, 2010; Fünfschilling et al., 2012; Saab & Nave, 2017). These specific and critical functions give rise to its complex and heterogenous membrane structure.

The structure can further be broken down into distinct domains known as the internode, the juxtaparanode, the paranode, and the Node of Ranvier. The structure of the myelin sheath gives way to it's function, properly insulating the axon while localizing the polarizing and hyper polarizing current at a distance suitable for optimal signal transduction. These distinct domains allow functional diversity of the myelin sheath.

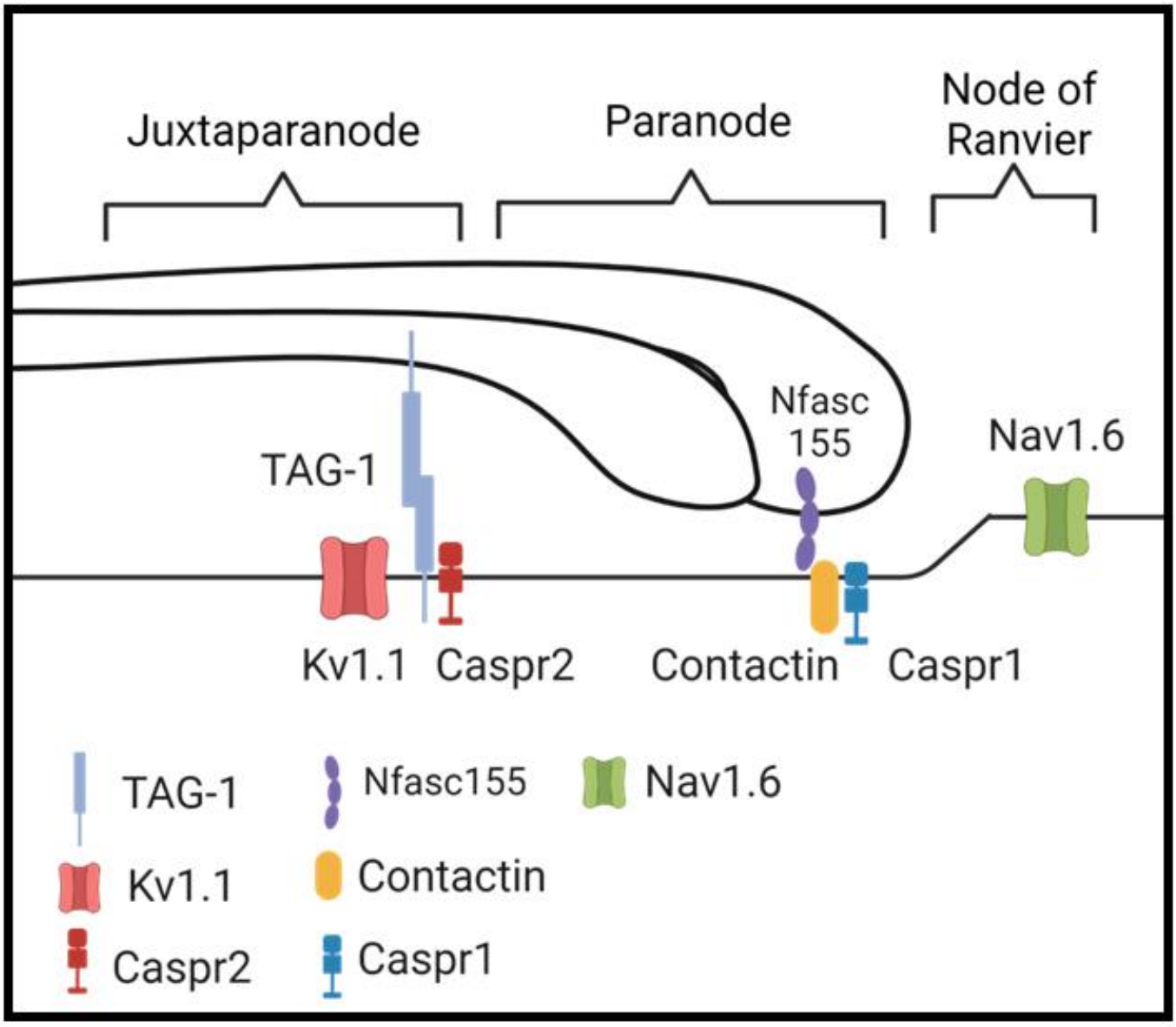

Figure 1.1: Schematic of relevant proteins localized to their proper domains. Made with Biorender.com

1.5.2 The internode

The internode contains compact myelin and spans about 99% of the myelinated segment length and consists of the characteristic periodic structure of the major dense line and the intraperiod line. The major dense line arises from compaction of cytoplasmic surfaces mediated by MBP and the intraperiod line is formed by the compaction of the outer membranes coming together where PLP plays a role (Klugmann et al., 1997; Baron & Hoekstra, 2010).

Within the internode are cytoplasmic channels, which provide a functional connection to the leading edge of the myelin sheath, which is in direct contact with the axon. These channels serve to provide transport of glial metabolites and organelles such as lysosomes through the internode (Richert et al., 2014; Snaidero et al., 2017). During development, cytoplasmic channels are much more prominent, having a crucial function in enabling myelin growth (Snaidero et al., 2014).

Throughout the internodal region the leading edge of the myelin sheath contacts the axon and can regulate signaling through distinct molecules including cell adhesion molecule 4 (Cadm4) and MAG. Cadm4 binds to axonal Cadm2 and Cadm3 (Maurel et al., 2007; Elazar, Vainshtein, Golan, et al., 2019) and MAG binds neuronal gangliosides as well as Nogo-66 receptor(NgR1) as well as NgR2 (Domeniconi et al., 2002; Venkatesh et al., 2005). Deletion of both Cadm4 and MAG leads to redundant myelin and multimyelinated axons (Elazar, Vainshtein, Rechav, et al., 2019). Therefore, Cadm4 and MAG binding to the neuron likely plays a role in signaling during onset of myelination and regulating myelin sheath growth. MAG also exerts signals that modulate the axon caliber of myelinated axons mediated through fyn signaling (Yin et al., 1998; Biffiger et al., 2000).

The internode aids in proper action potential conduction due to the lipid rich sheath maintaining a close apposition with the axon. The maintenance of these close myelin-axonal associations is important for proper action potential as myelin reduces ion loss along the internode thus facilitating electrical signal propagation by thus reducing capacitance and increasing membrane resistance (Bakiri et al., 2011; Ford et al., 2015; Micheva et al., 2021).

1.5.3 The paranode

A key contact site of myelin to the axon is the paranode. The paranode is structurally demarcated by the presence of the cytoplasmic loops that form attachments with the axon. By ultrastructural analysis these sites

of attachment present as regularly arrayed electron densities that span the periaxonal space. These densities are known as transverse bands and they are a prominent component of the paranodal axon-glial junctions (Rosenbluth et al., 2003a). Transverse bands are formed by the binding of Nfasc155 on the glial side with the heterodimer protein complex of contactin and Caspr1 on the axonal side (Rios et al., 2000; Charles et al., 2002a). In addition to anchoring the myelin sheath to the axon, transverse bands function as a “picket fence” that restricts lateral migration of proteins clustered in adjacent axonal domains. This lateral movement restriction maintains the distance between voltage gated sodium channels that cluster in the node of Ranvier and the voltage gated potassium channels of the juxtaparanode (Mierzwa et al., 2010a; Susuki et al., 2013; Amor et al., 2014). Therefore, the paranode is highly conserved, maintaining a length of about 3.5 µm in length (Shepherd et al., 2012a) and ensuring efficient saltatory conduction (Bhat et al., 2001; Pillai et al., 2009).

These paranodal adhesion molecules make associations with the underlying cytoskeletal network, further stabilizing their localization in the paranode. (C. Zhang et al., 2013). Caspr1 binds directly to protein 4.1B, which associates with the underlying cytoskeletal elements such as Ankyrin B and αII/βII spectrin (Ogawa et al., 2006; Einheber et al., 2013). These cytoskeletal elements, in addition to Caspr1, help anchor voltage gated sodium channels and voltage gated potassium channels in the axolemma and in their respective domains (Poliak et al., 2003; Amor et al., 2017). On the glial side, Nfasc155 interacts with Ankyrin B (Chang et al., 2014) and most recently, sulfatide (McKie et al., 2023). Loss of sulfatide leads to increase susceptibility of extraction of Nfasc155 as well as increased nodal length variability (Marcus et al., 2006). Therefore, binding of sulfatide to neurofascin likely plays a critical role in proper stability of neurofascin155 (Marcus et al., 2002; A. Pomicter et al., 2013; McKie et al., 2023).

1.5.4 The juxtaparanode

Just next to the paranode and flanking the internode lies the juxtaparanode. It houses potassium channels, transient axonal glycoprotein type-1 (TAG-1), and Caspr2 (Poliak et al., 1999, 2003). Specifically, two rectifying *Shaker*-like potassium channels, Kv1.1 and Kv1.2 are enriched in the juxtaparanode. These channels

function to return the membrane potential to its resting state following depolarization. The myelin juxtaparanode also has contact sites to the axon. TAG-1 is found both on the glial and axonal side and glial TAG-1 forms a cis complex with TAG-1 and Caspr2 on the axonal side (Traka et al., 2002, 2003; Thaxton & Bhat, 2009) . Caspr 2 is stabilized through the same scaffolding proteins as in the paranode through associations to protein 4.1B and αII/βII spectrin (Poliak et al., 1999). The TAG-1/Caspr-2 complex aids in localization of Kv1.1 and Kv1.2 as mutation of either of these proteins leads to mis-localization of the channels (Poliak et al., 2003).

1.5.5 The Node of Ranvier

The Node of Ranvier (NoR) is classically known for having a high density of voltage gated sodium channels (Rasband & Trimmer, 2001; Amor et al., 2017; Yermakov et al., 2019). This myelin-bare region is where the propagation of action potential occurs through the opening of the sodium channels, allowing robust depolarization of the axon. This potential can propagate quickly down the axon due to the myelin sheath flanking the NOR, creating what is known as “saltatory conduction” (Huxley & Stämpeli, 1949; Lim & Rasband, 2020). Therefore, sodium channel clustering is necessary for rapid and efficient action potential propagation in myelinated axons. While the transverse bands act as a barrier for sodium channels, sodium channels are also anchored in place by interactions with the cytoskeleton via AnkyrinG (Gasser et al., 2012). AnkyrinG is a major component of the membrane cytoskeleton and is essential for the clustering of sodium channels at the NoR (Gasser et al., 2012). AnkyrinG associates with the underlying cytoskeletal network through interacting with βIV-spectrin, further stabilizing the sodium channels as well as binging Neurofascin 186 (Nfasc186) (Y. Yang et al., 2004). Nfasc186, the neuronal specific isoform of the neurofascin gene (Alpizar et al., 2019) creates further stability by associating with proteoglycans in the extracellular matrix (ECM) (Hedstrom et al., 2007; I. Song & Dityatev, 2018). Therefore, there are multiple mechanisms at play which properly anchor myelin and axonal proteins to their proper location.

1.6 Myelin Sheath in the context of Multiple Sclerosis

Charot described multiple sclerosis (MS) as axons spared from degeneration in the presence of demyelination (Charcot, 1868). Over the years, evidence from MS tissue and myelin mutants demonstrated that disruption of the myelin ultrastructure is responsible for downstream effects that culminate in axonal pathology (Owen, 1957; Fruttiger et al., 1995; Griffiths et al., 1998). While overt myelin pathology likely disrupts the myelin sheath's ability to properly insulate and conduct electricity and thus leading to axonal degeneration, increasing evidence suggests that molecularly disrupting the myelin sheath can disturb the axo-glial communication leading to axonal pathology (Y. Lee et al., 2012; Joseph et al., 2019; Buscham et al., 2022). Further, tissues from the normal appearing white matter (NAWM) of MS patients demonstrated significant axonal pathology such as axonal swelling and mis-localization of ion channels, suggesting that considerable pathology is already occurring prior to demyelination (Gallego-Delgado et al., 2020a; Luchicchi et al., 2021b). Further lipidomic and proteomic studies have looked at the NAWM of MS patients and found that sulfatide is reduced, while there is an increase in sphingosine, a metabolite of sulfatide breakdown (Moscatelli & Isaacson, 1969; Yahara et al., 1982; Marbois et al., 2000). More recently, a study reported that there is an increase in the phospholipid/sphingolipid ratio in both normal appearing white and normal appearing grey matter in MS brains as compared to non-MS brains, indicating an overall disruption of lipid homeostasis (Wheeler et al., 2008a). While our studies do not attempt to recapitulate MS, we do aim to understand how reduction of sulfatide may have a causative role in the onset of MS symptoms. Therefore, it is important to discuss the MS epidemiology, diagnostic markers, and treatment options for MS.

MS is an autoimmune, demyelinating disorder of the CNS that is commonly diagnosed between 20 and 30 years of age, with a 2 or 3 times greater prevalence in women compared to their male counterparts. (Thompson et al., 2018; Gbaguidi et al., 2022). However, recently, cases of pediatric MS are on the rise and have a more severe disease course (Fisher et al., 2020; Krysko et al., 2020). It is estimated that this disease affects 2.8 million people world-wide and nearly one million in the United States (Wallin et al., 2019; Walton et al., 2020). The etiology is relative unknown having complex genetic and environmental factors (Ward & Goldman, 2022), which is likely what contributes to the highly heterogenous nature of this disease. A recent paper claimed Epstein-Barr virus (EBV) "greatly increased the risk of subsequent multiple sclerosis" which

generated controversy in its claims (Soldan & Lieberman, 2023). This was a longitudinal study that used blood samples from active-duty soldiers. Out that of the 801 people who developed MS, only one tested negative for EBV while the 1,500 matched controls had a much lower rate of EBV infection, calculating that people infected with EBV were 32 times as likely to develop MS as uninfected people (Bjornevik et al., 2022). While this finding needs further corroboration, it demonstrates a strong association between EBV infection and MS onset.

MS is diagnosed using the revised McDonald criteria, which uses a combination of findings to show disease activity over dissemination in space and time (Thompson et al., 2018). Dissemination in space (DIS) can be demonstrated by characteristic T2-hyperintense lesions that are in one or more of the following locations: periventricular, juxtacortical, brainstem and cerebellum, and spinal cord, or clinical evidence of two or more lesions involving a different CNS site. Dissemination in time (DIT) includes more than two attacks, separated by at least one month, simultaneous presence of gadolinium-enhancing lesions at any time, or a new T2 lesion on follow-up, or demonstration of cerebral spinal fluid (CSF) oligoclonal bands (Thompson et al., 2018; K. Zhang et al., 2020). Therefore, by the time of diagnosis, lesions (demyelination) have already occurred and likely subsequent axonal degeneration is well under way. Current therapies available are largely immune modulating such as blocking recruitment of lymphocytes into the brain, modulating cytokine/chemokine responses, T cell modulatory, and B cell depleting therapies (McGinley & Cohen, 2021; Ovchinnikov & Findling, 2022; Verreycken et al., 2022). While some of these therapies lower the annualized relapse rate, efficacy is limited and there is no effective cure of MS (Piehl, 2021). Therefore, it is important to continue to understand this complex and heterogeneous disease, particularly its pathogenesis to diagnose in its earlier stages.

1.7 Summary

Ultimately, while our lab and others have shown sulfatide is essential for myelin development, maintenance, and stability of nodal domains, the role sulfatide plays in adulthood, in the myelin sheath and oligodendrocytes, has not been addressed (Ishibashi et al., 2002a; Marcus et al., 2002; A. Pomicter et al., 2013). The constitutive

CST KO model ablated sulfatide production embryonically and in all tissues, therefore, the resulting pathologies observed are along a developmental timeline. MS is generally considered an adult-onset disease; therefore, I created a mouse model that allows for temporal and spatial ablation of sulfatide. This mouse model is used in all subsequent studies. In these studies, we attempted to understand the consequence that adult-onset depletion of sulfatide would have on the CNS. I also explored regional differences since MS lesions occur both in the brain and spinal cord (Moccia et al., 2019). In Chapter 2, I examine the structural and functional consequence of loss of sulfatide in adulthood and begin to understand molecular mechanisms that are at play. In Chapter 3 I begin to understand how sulfatide stabilizes the myelin sheath through associations with myelin proteins and I further explore regional differences in the CNS. The findings of these studies significantly enhance our understanding of the consequence of adult onset sulfatide depletion and provide conclusive evidence that sulfatide depletion, independent of demyelination, is sufficient to drive axonal degeneration and loss of axonal function. These findings are significant as they indicate that the underlying cause of the clinical presentation associated with MS may be initiated long before a patient presents in the clinic.

CHAPTER TWO

Adult-onset depletion of sulfatide leads to axonal degeneration with relative myelin sparing

Dustin et al., 2023 *Glia*

2.1 Abstract

3-O-Sulfogalactosylceramide (sulfatide) constitutes a class of sphingolipids that comprise about 4% of myelin lipids in the central nervous system. Previously, our group characterized a mouse with sulfatide's synthesizing enzyme, cerebroside sulfotransferase (CST), constitutively disrupted. Consequently, these constitutive CST knockout (KO) mice were incapable of synthesizing sulfatide. Using these mice, we demonstrated that sulfatide is required for establishment and maintenance of myelin, axoglial junctions, and axonal domains and that sulfatide depletion results in structural pathologies commonly observed in Multiple Sclerosis (MS). Interestingly, sulfatide is reduced in regions of normal appearing white matter (NAWM) of MS patients. Sulfatide reduction in NAWM suggests depletion occurs early in disease development and consistent with functioning as a driving force of disease progression. To more closely model MS, an adult-onset disease, our lab generated a "floxed" CST mouse and mated it against the PLP-cre^{ERT} mouse, resulting in a double transgenic mouse that provides temporal and cell-type specific ablation of the Cst gene (*Gal3st1*). Using this mouse, we demonstrate adult-onset sulfatide depletion has limited effects on myelin structure but results in the loss of axonal integrity including deterioration of domain organization accompanied by axonal degeneration. Moreover, the structurally preserved myelinated axons progressively lose the ability to function as myelinated axons, indicated by the loss of the N1 peak. Together, our findings indicate that sulfatide depletion, which occurs in the early stages of MS progression, is sufficient to drive the loss of axonal function independent of demyelination and that axonal pathology, which is responsible for the irreversible loss of neuronal function that is prevalent in MS, may occur earlier than previously recognized.

2.2 Introduction

Multiple Sclerosis (MS), a demyelinating, autoimmune disorder of the central nervous system (CNS) that is mostly commonly diagnosed in the third and fourth decades of life (Gbaguidi et al., 2022; Walton et al., 2020), is characterized by sensory, motor, and cognitive dysfunction. MS affects nearly one million people in the United States (Wallin et al., 2019) and nearly 2.8 million worldwide (Walton et al., 2020). Currently, there is no cure for MS and treatments exhibit limited efficacy (Piehl, 2021). While our understanding of MS pathogenesis is largely immune focused (O'Connor et al., 2001; Rodríguez Murúa et al., 2022), the exact disease etiology remains unknown. Although immune activation is a consistent aspect of MS, other factors implicated in disease onset and progression include environment, gender, genetics, and viral exposure (Bjornevik et al., 2022; Olsson et al., 2017).

Although a multifaceted disease, an interesting and consistent observation is the dysregulation of lipid metabolism in the CNS (Podbielska et al., 2022; Wheeler et al., 2008). Marbois et al., (2000) using ion electrospray mass spectrometry, reported a 25% reduction specifically of the myelin sphingolipid sulfatide in normal appearing white matter (NAWM) compared to non-MS brains confirming a much earlier report of specific sulfatide depletion in MS (Yahara et al., 1982). Additionally, Wheeler et al. (2008) reported a significant increase in the phospholipid/sphingolipid ratio in both normal appearing white and normal appearing grey matter in MS brains as compared to non-MS brains while Moscatelli and Issacson (1969) reported an increase in sphingosine, a metabolite of sulfatide breakdown. Together, these findings indicate that altered sphingolipid metabolism and sulfatide depletion in MS occurs prior to demyelination temporally positioning sulfatide loss as a causative event in disease onset and progression.

Myelin is essential for proper transduction of electrical signals in axons by acting as an insulator through its unique lipid rich biochemical composition (Huxley & Stämpeli, 1949). In addition to its structural role, myelin metabolically supports the axon and maintains overall axonal integrity (Babetto & Beirowski, 2022; G. J. Duncan et al., 2021; Griffiths et al., 1998; Y. Lee et al., 2012). During MS onset, the myelin sheath is attacked by CD4+ myelin reactive T cells resulting in demyelination and/or axonal loss, creating areas of plaque matter;

while areas of NAWM supposedly are undisturbed. However, a growing body of literature suggests the NAWM contains axonal pathologies suggesting that the irreversible functional loss that has been attributed to axonal degeneration (Trapp et al., 1998) may precede demyelination in contrast to axonal pathology being a consequence of myelin loss (Gallego-Delgado et al., 2020; Luchicchi et al., 2021). Therefore, it is imperative to develop a better understanding of the pathological events that occur in the earliest stages of disease.

To delineate the role that sulfatide plays in both a healthy and diseased CNS, our group generated (Honke et al., 2002) and characterized a mouse with a disruption in the cerebroside sulfotransferase (CST) gene, galactose3-O-sulfotransferase 1 (*Gal3st1*) (which will be referred to as Cst as is commonly used in the literature) (Ishibashi et al., 2002; Marcus et al., 2006; A. Pomicter et al., 2013; Shroff et al., 2009), which encodes the enzyme that catalyzes the final step of sulfatide synthesis (Yaghootfam et al., 2007; Honke et al., 1997). This global, constitutive CST knockout (KO) mouse displays progressive myelin pathologies that are observed in MS brains (Gallego-Delgado et al., 2020; Luchicchi et al., 2021; Suzuki et al., 1969; York et al., 2021) including (1) thin, unstable, and uncompacted myelin sheaths (Marcus et al., 2006); (2) ultrastructurally compromised nodal and paranodal domains (Honke et al., 2002; Marcus et al., 2006); (3) abnormal and unstable clustering of nodal and juxtaparanodal ion channels (Ishibashi et al., 2002) and (4) reduction of major myelin proteins and lipids (Palavicini et al., 2016). Thus, sulfatide is implicated in the establishment and maintenance of myelin and axonal structure and function (Hayashi et al., 2013). Although a valuable resource for elucidating functions of sulfatide, the constitutive CST KO mouse develops in the absence of the lipid. To overcome potential developmental confounds, we have generated a Cst floxed (flanking loxP; $Cst^{fl/fl}$) mouse capable of age- and cell type- specific sulfatide depletion. We mated the $Cst^{fl/fl}$ mouse with a mouse that expresses tamoxifen-inducible cre recombinase under the control of the oligodendrocyte (OL)-specific proteolipid protein (PLP) promoter (Belachew et al., 2001; Mallon et al., 2002; Wight & Dobretsova, 2004). Here, we exploit this novel double transgenic mouse to determine the causal relationship between adult onset sulfatide depletion and myelin and axonal structure and function

2.3 Materials and Methods

Animal Model

Male and female CST inducible knockout mice, generated on the c57black/6J background (see below), were bred, housed and aged in the Central Virginia Veterans Affairs Health Care Systems AAALAC accredited vivarium on a 12-hour light/dark cycle with food and water provided *ad libitum*.

Generation of CST conditional knockout mouse

Using CRISPR technology, we generated cerebroside sulfotransferase (Cst) floxed (flanking loxP) mice (Applied StemCell, Inc, Milpitas, CA). Based on transcript sequence information in Ensembl (Transcript ID MGP_C57BL6NJ_T0028206.1), and consistent with published sequence analysis (Hirahara et al., 2000; Honke et al., 2002), the Cst gene (*Gal3st1*) consists of 3 exons. Exon 1 is non-coding with variable regions termed 1a- 1g. Exons 2 and 3 constitute the coding regions. LoxP sequences were inserted in introns up and down stream of exons 2 and 3 (Fig. 1A). Guide RNAs, two single-stranded oligodeoxynucleotide donors and designed Cas-9 mRNA, were injected into the cytoplasm of c57black/6J embryos. Resulting pups were screened for loxP sites at the designated locations using PCR followed by sequencing to confirm that the Cst gene locus contained the loxP sites in the correct location and orientation (not shown). To specifically target ablation of the Cst gene in oligodendrocytes in the CNS, we purchased $Plp^{Cre\mathit{ERT}}$ mice (Jax Labs; stock # 005975) to induce recombination and mated them to the homozygous Cst floxed ($Cst^{fl/fl}$) line. The PLP^{CreERT}line was chosen as the Cre driver line since this line has been routinely used to efficiently induce adult-onset gene ablation in the CNS in chronic studies (Pillai et al., 2009; Mei et al., 2013; Jablonska et al., 2016; De Logu et al., 2017, 2020; Thomason et al., 2022; Borges et al., 2023). In the original report of the generation of these mice, Doerflinger et al., (2003) showed that in the absence of tamoxifen, Cre remained cytoplasmic and there was no evidence of recombination. Moreover, behavioral and histological analyses at chronic post tamoxifen injection time points have revealed no signs of functional impairment or myelin or axonal pathology independent of target gene ablation (T. Li et al., 2018; Mierzwa et al., 2013; Zhao et al., 2020). Additionally, Peacock et al. (2018) used this line to compare distinct floxed genes and observed no consistent pathologies between lines indicating that developed pathologies were independent of PLP induced Cre expression.

To generate mice used in all subsequent studies, we mated homozygous $Cst^{fl/fl}$ mice with heterozygous $Plp^{CreERT-/+}$;$Cst^{fl/fl}$ mice, creating both $PLP^{CreERT-/-}$ (no cre):$Cst^{l/fl}$ and $Plp^{CreERT-/+}$;$Cst^{fl/fl}$. All experimental mice were $Plp^{CreERT-/+}$;$Cst^{fl/fl}$ (abbreviated as CST-cKO); $PLP^{CreERT-/-}$;$Cst^{fl/fl}$ were used as controls (abbreviated as CTL). All mice received tamoxifen treatment (see below). *Tamoxifen treated $PLP^{CreERT-/-}$;$Cst^{fl/fl}$ mice were used to control for potential side effects of tamoxifen treatment* (Denk et al., 2015; Valny et al., 2016; Barratt et al., 2016).

Induction of Cre-mediated Recombination with Tamoxifen

Mice were intraperitoneally injected with 60mg/kg of tamoxifen based on previous work from our group (Qiu et al., 2021). Tamoxifen was diluted in corn oil, and delivered through intraperitoneal injection into 10-week-old $Plp^{CreERT-/+}$;$Cst^{fl/fl}$ and $PLP^{CreERT-/-}$;$Cst^{fl/fl}$ mice for four consecutive days.

Polymerase Chain Reaction – Cst gene ablation assessment

To confirm Cre-mediated recombination, genomic DNA was extracted from the corpus callosum of 6-week post tamoxifen injected mice using Qiagen DNeasy Mini kit (Qiagen, Germantown, MD; cat # 69504) according to the manufacturer's instructions. Briefly, mice were deeply anesthetized using 0.016 mL/gm body weight of a 2.5% solution of avertin (2, 2, 2 tribromoethanol; Sigma-Aldrich; St. Louis, MO; cat#T48402) in 0.9% sodium chloride (Sigma-Aldrich, St. Louis, MO) and transcardially perfused with ice-cold saline for 3 minutes. The brain was harvested; sectioned into 1mm coronal slices, which were used for corpus callosum isolation; snap-frozen in liquid nitrogen and stored at -80C. Snap frozen tissue was used for DNA ablation assessment and mRNA quantitation. DNA fragments spanning genomic target sites were amplified by PCR using the following primers:

Gal3st1 Forward (5'- GATTGTAGCCTTCCGTATGAACCG -3')
Gal3st1 Reverse 1 (5'- CGAACTCAACTCAAAGAGAGCAGG -3') and
Gal3st1 Reverse 2 (5'- TAATCTCTGCTCTAACCTGGTCGC -3').

The *Gal3st1* Forward primer targets upstream of the first flanking loxP site and *Gal3st1* Reverse 1 primer targets downstream of the first flanking loxP site; the *Gal3st1* Reverse 2 primer targets downstream of the

second flanking loxP site, such that when recombination does not occur, the size of the potential product between Forward and Reverse 2 primers is too large to amplify. However, after Cre-mediated recombination, the distance between these primer target sites is shortened and a 432bp band is detected (Fig. 1A). If no recombination occurs, the Forward and Reverse 1 primer will detect a product of 246bp (Fig. 1A). Cycling parameters were one cycle at 95°C (3 min), 40 cycles of 95°C (30 s), 60°C (30 s), and 72°C (1 min 30 s), then 72°C (5 min), and a final hold at 4°C. PCR amplified products were analyzed by agarose gel electrophoresis (Fig. 1B).

Real Time-Polymerase Chain Reaction – Cst mRNA quantitation

Total RNA was extracted from isolated corpus callosi using a Qiagen RNeasy Micro kit (Qiagen, Germantown, MD; cat# 74004) according to manufacturer's instructions. Contaminating DNA was eliminated through treatment with Ambion DNase I (Invitrogen Life Technologies, Grand Island, NY; cat# AM2222). Omniscript Reverse Transcription Supermix (BioRad, Hercules, CA; cat# 205113) was used to create cDNA from the isolated RNA (150µL/sample). Quantitative RT-PCR was performed with a CFX96 (BioRad, Hercules, CA) RT-PCR detection system using 1µL of cDNA, SsoFast Evagreen Supermix (BioRad; cat# 1725201), and the following primers (20µM):

Gal3st1 Forward (5'- GCAGCACACTGCTCAACATC -3')

Gal3st1 Reverse (5'- ACCAGGCTTCGTGCAAAGTA -3')

Cyclophilin A Forward (5'- CTAGAGGGCATGGATGTGGT -3')

Cyclophilin A Reverse (5'- TGACATCCTTCAGTGGCTTG-3')

Phosphoglycerate kinase 1 Forward (5'- ATGCAAAGACTGGCCAAGCTA -3')

Phosphoglycerate kinase 1 Reverse (5'-AGCCACAGCCTCAGCATATTT-3')

Cycling parameters were: one cycle at 95°C (5 min), 39 cycles of 95°C (5s) and 56°C (5s) followed by a melt curve measurement consisting of 5s 0.5°C incremental increases from 65°C to 95°C. The fold changes in expression of the Cst gene in corpus callosum samples were calculated using the formula RQ 5 22DDCt, using

Cyclophilin and Phosphoglycerate kinase 1. For statistical analysis, a Student's t-test was performed using GraphPad Prism software version 9.4.1 for Windows.

Lipid Mass Spectrometry

Multidimensional mass spectrometry-based shotgun lipidomics analysis was performed as described in Qiu et al. (2021). Briefly, mice were injected with Avertin and perfused with ice cold saline. The brains were sliced into 1mm coronal slices and corpus callosi was dissected and flash frozen in liquid nitrogen. Tissue was homogenized and protein concentrations was determined using Bio-Rad protein assay (Bio-Rad, Hercules, CA, USA). In the presence of internal standards, lipids were extracted following a modified procedure of Bligh and Dyer. Lipids were measured using a triple-quadrupole mass spectrometer (TSQ Altis, (Thermo Scientific, Rockford, IL) equipped with a Nanomate device (Advion Ithaca, NY, USA) and Xcalibur system. Data were processed using ion peak selection, baseline correction, data transfer, peak intensity comparison, ^{13}C deisotoping. Data were analyzed using a custom-programmed Microsoft Excel macro

Immunohistochemistry

Tissue was processed as previously described (Dupree et al., 1999; Shepherd et al., 2012; Clark et al., 2016). Briefly, mice were deeply anesthetized using 0.016 mL/gm body weight of a 2.5% solution of avertin in 0.9% sodium chloride, and transcardially perfused with 4% paraformaldehyde (Ted Pella, Redding, CA; cat#18501) in 0.1M Millonigs buffer (Dupree et al., 1999; Shepherd et al., 2012). Following perfusion, the brains were cryopreserved in 1X PBS containing 30% sucrose for 48 hours, frozen in Optimal Cutting Temperature compound (Fisher Scientific; Hampton, NH, cat# 23-730-571), and serially sectioned, spanning 1.1 mm anterior to bregma to 2.5 mm posterior to bregma, at 40µm in a coronal orientation using a Leica CM 1850 cryostat (Leica, Buffalo Grove, IL). Fifteen sets of six sections were collected and placed on ProbeOn Plus slides (Fisher Scientific, Loughborough, UK; cat# 15-188-51) and stored at −80°C. Adapted from Dupree et al. (1999) and Shepherd et al. (2012), coronally sectioned brains were triple labelled with Caspr1 at a dilution of 1:500 (rabbit polyclonal, Abcam cat# ab34151), Kv1.1 at a dilution of 1:750 (mouse monoclonal IgG2b, Antibodies Inc cat#75-105) and Nav1.6 at a dilution of 1:250 (mouse monoclonal IgG1, Antibodies Inc., cat

#75-026); per manufacturer's description, each antibody is knock-out validated. After overnight primary antibody incubation at 4°C, the sections were rinsed in PBS, blocked in blocking solution (0.5% triton X-100, 10% cold water fish skin gelatin (Aurion, Netherlands; cat# 900.033) in PBS) as previously described (Benusa et al., 2017; Clark et al., 2016) and incubated with the appropriate, fluorescently tagged Alexa™fluor secondary antibodies (Invitrogen Life Technologies, Grand Island, NY) diluted 1:500. Slides were cover slipped with Vectashield™ (Vector Laboratories, Newark, CA, cat# H-1000) and stored at -80°C until imaged. For immunohistochemistry (IHC) analysis, an n=3-7 mice were used per sex per genotype per timepoint (see Table 1).

Image collection and Quantitation

All images were collected using a Zeiss LSM 880 with AiryScan confocal laser scanning microscope (Carl Zeiss Microscopy, LLC; White Plains, NY), housed in the VCU Microscopy and Imaging Facility. Confocal z-stacks, each spanning 3µm, using a pin hole of 1 Airy disc unit and Nyquist sampling, were collected from the corpus callosum at the level of the fornix. Six images were collected per animal and a minimum of 150 nodal domains were quantitatively analyzed per animal. Images were captured using a 63X oil-immersion objective with a numerical aperture of 0.55; optical slice thickness was 0.21µm using a line scanning average of 4. X, Y, and Z dimensions were 67µm × 67µm × 3µm, respectively. The magnification was digitally increased by a factor of 2 using the zoom feature. The gain and offset were kept consistent for all images. The 405nm laser detector gain was approximately 700; the 488nm laser set at 750 detector gain, and the 594nm laser set at 780 detector gain. For quantitation, criteria were established to quantify overlapping, absent, and/or aberrant placement of nodal protein fluorescent signals. Nodal abnormalities were quantified using ImageJ analysis software by manually marking overlapping fluorescent labels from maximum intensity projection images. All analyses were conducted blinded from experimental group and sex. Fluorescently labelled domains that touched the edge of the image were excluded from analysis. We quantitatively analyzed age-matched CST-cKO and control mice at 3-, 6-, and 11-month post tamoxifen injection. Analysis was performed using a 2-way ANOVA comparing genotypes across time. All graphing and statistical analyses were performed using GraphPad Prism version 9.4.1 for Windows (GraphPad Software, San Diego, CA).

Electron Microscopy

For ultrastructural quantitation, mice were processed for transmission electron microscopic analyses as previously described by (Dupree et al., 1998a; Dupree et al., 1998b; Dupree et al., 1999; Marcus et al., 2006). Briefly, mice were deeply anesthetized, as described above, and transcardially perfused with a solution of 0.1M Millonigs buffer containing 4% paraformaldehyde and 5% glutaraldehyde (EM sciences, Hatfield, PA cat#16310). Perfusions were followed by a 2-week incubation in the same fixative solution at 4°C. Brains were harvested, vibratome- sectioned at 100µm to generate both coronally and sagittally oriented samples of the *corpus callosum at the level of the fornix*. The cervical region of the spinal cords was harvested and sliced into 1mm sections. Comparable sections were selected and postfixed in 1% osmium tetroxide (EM Sciences, Hatfield, PA; cat# 20816-12-0), dehydrated in increasing concentrations of ethanol, followed by incubation in the transition solvent propylene oxide (EM Sciences, Hatfield, PA cat# 20412) and embedded in PolyBed epoxy resin (PolySciences, Warrington, PA; cat#08791-500). One micron and ultrathin (70nm) sections were stained with toluidine blue or the heavy metals uranyl acetate and lead citrate, respectively. One-micron sections were imaged using a Nikon ECLIPSE E800M upright light microscope (Nikon Instruments, Melville, NY), which is housed in the VCU Microscopy and Imaging Facility, to confirm region of interest and quality of tissue preservation. The ultrathin sections were used for myelin and axonal analyses and imaged using a JEOL JEM-1400Plus (JEOL USA, Inc, Boston, MA) equipped with a Gatan One View 1095 T and Gatan Microscopy Suite (GMS) 3.3.2 software.

For g-ratio analysis, a minimum of 100 myelinated axons were analyzed per mouse at the level of the fornix for the corpus callosum and the dorsal column of the cervical spinal cord. Axons with a diameter > 0.3 µm (Mason et al., 2001), were used for quantitative analysis. Images were collected at magnification of 7,200X from the sagittally (corpus callosum) and transversely (cervical spinal cord) oriented sections. For each myelinated axon, 2 axon diameters (the longest and shortest), and two myelin widths (the widest and the thinnest) were measured using NIH ImageJ (Marcus et al., 2006). Only myelin regions that exhibited no sign of fixation artifact or non-compaction were used for determining myelin thickness. Also, regions containing either the

inner or outer tongues were not used for g ratio analyses. To calculate g-ratio, the average diameter for each axon was divided by the average axon diameter plus the sum of the myelin widths. For corpus callosum EM analysis, an n=3-4 was used per sex per genotype per timepoint (see Table 1). In addition to the corpus callosum, dorsal column white matter tracts from cervical spinal cords were also analyzed using a minimum of an n=3 per genotype per time point. G-ratios were statistically compared between genotypes and time points using a 1-way ANOVA for average values per animal. In addition, separate t-tests were conducted to strictly compare between genotypes at each time point. All graphing and statistical analyses were performed using GraphPad Prism version 9.4.1 for Windows (GraphPad Software, San Diego, CA).

To quantify myelin and axon integrity, a minimum of 600 axons were analyzed per mouse. These images were used to assess the percent of myelinated versus unmyelinated axons, redundant myelin, myelin uncompaction, vacuolar degeneration of the myelin sheath, and axonal degeneration as previously described (Dupree et al., 2015). Only axons with a diameter equal to or greater than 0.3µm (Marcus et al., 2006; Mason et al., 2001) were included in the quantitation. Statistical analysis was performed using a 2-way ANOVA comparing genotypes across time. All graphing and statistical analyses were performed using GraphPad Prism version 9.4.1 for Windows (GraphPad Software, San Diego, CA).

Coronally oriented ultrathin corpus callosum sections were imaged at 7,2000X for nodal regions. A minimum of 10 nodal regions were imaged per mouse to quantify node of Ranvier length. For statistical testing, (performed by Dr. Leroy Thacker of the VCU Biostatics Department) the fit of the two models (single variance/covariance matrix or group specific variance/covariance matrices) was compared using a likelihood ratio test (LRT). For all analyses an $\alpha = 0.05$ was used for statistical significance and SAS v9.4 was used. Variance was also calculated per mouse and variability was plotted. Qualitative assessment of paranodal-axonal junctions (transverse bands) and organization and orientation of paranodal loops were also conducted.

Tissue Prep for Immunoprecipitation and western blotting

To quantify the interaction between neurofascin and contactin, mice were injected with Avertin and perfused with ice cold saline. The brains were removed and sliced into 1mm coronal slices. The corpus callosum was excised and homogenized with 0.1mL of 1X PBS and protease inhibitor cocktail (Millipore/Sigma, St. Louis MO, cat# 539136) and phosphatase inhibitor cocktail (Rockford, IL, cat#P044-1ml) and flash frozen in liquid nitrogen and stored at -80C. Tissue was thawed on ice and protein concentrations were determined with the Micro BCA Protein Assay kit (Thermo Scientific, Rockford, IL, cat# 23235).

Immunoprecipitation

Following the instructions of Pierce ™ Crosslink Magnetic IP/Co-IP Kit (Thermo Scientific, Rockford, IL, cat# 88805) 250µg of protein was loaded onto magnetic beads with neurofascin antibody, FIGQY, (courtesy of Dr. Matthew Rasband) bound. Homogenate was incubated overnight at 4C rotating on a platform. Neurofascin enriched elute was collected and 4X LICOR buffer was added. Samples were heated to 70C for 5 min and aliquots were frozen in -80C until used for western blotting.

Western Blotting

50 µg of proteins were loaded into 4-20% tris\glycine gels (Bio-Rad, cat# 4561094, Hercules, CA) for the IP samples and 30 µg was loaded for total corpus callosum homogenate and run for 30 minutes at 70V followed by an additional 25 minutes at 150V. The protein ladder used was Chameleon Duo pre-stained protein ladder (LI-COR, Lincoln, NE cat#928-60000). Samples were transferred to Immobilon-P transfer membrane (Millipore, St. Louis, MO, cat#IPVH00010) for one hour at 100V on ice. Membranes were rinsed briefly in 1X PBS with 0.1% Tween-20 (Millipore/Sigma, St. Louis, MO, cat#1379) and stained for total protein with Revert 700 Total Protein Stain (Lincoln, NE, cat#926-11011). Total protein was visualized using an Odyssey Clx LICOR system (LI-COR, Lincoln, NE, cat#1928) with Image Studio software version 5.2 (LICOR Lincoln, NE) for normalization. Total protein was washed off with REVERT Reversal Solution (LICOR, Lincoln, NE, cat#629-11013) and blocked for one hour in 2.5% dry milk in PBS-T. The blot was briefly washed with PBS-T and incubated overnight at 4°C in Intercept Blocking Buffer (LICOR Lincoln, NE, cat#927-70001) with contactin

antibody (Antibodies Inc, Davis, CA, cat# K73/20) 1:1000 for the IP tissue or pan anti-Neurofascin (1:500) (R&D Systems, Minneapolis, MN, cat#AF3235). The following day, the primary antibody was discarded and the blot was rinsed in PBS-T and incubated with secondary antibody for one hour at room temperature. After one-hour incubation in the appropriate secondary antibody from LICOR diluted at 1:10,000 (IRDye 680 anti-mouse (cat# 926-68070) and IRDye 800 anti-chicken (cat#926-32218). The blot was rinsed in PBS-T and western blot was visualized with Odyssey Clx LICOR system. Blots were analyzed using Image Studio software version 5.2.

Protein Mass Spectrometry

To confirm neurofascin 155 was being enriched by the IP reaction, we performed proteomic analysis on observed protein bands. Briefly, IP elute was diluted to 100ug of protein in 4x Protein Loading Buffer (LICOR Lincoln, NE, cat# 928-40004) heated to 70C for 5 minutes and loaded onto 4-20% gel for electrophoretic separation for 30 minutes at 70V and 25 minutes at 150V. The gel was then stained with Silver stain (Thermo scientific, Rockford, IL, Pierce Silver Stain cat#24600) following manufacturer's instructions. Band of interest was excited and processed for mass spectrometry courtesy of Charles Lyons at the Massey Cancer Center Proteomics Shared Resource. Upon confirming validity of IP approach, we moved onto immunoprecipitation experiments using CTL and CST-cKO corpus callosal tissue.

Electrophysiology

Mice were initially anesthetized with the volatile anesthetic isoflurane followed by an intraperitoneal injection of ketamine (200 mg/kg) and xylazine (20 mg/kg). Mice were then transcardially perfused with ice-cold sucrose artificial cerebrospinal fluid (sucrose-aCSF), which contained (in mM): 206 sucrose, 25 glucose, 25 $NaHCO_3$, 4 $MgSO_4$, 3 KCl, 1.25 NaH_2PO_4, 1.2 $CaCl_2$ saturated with 95% O_2 and 5% CO_2. Following perfusion, mice were decapitated and the brain removed to produce *ex vivo* brain slices. Coronal brain slices of 350μm thickness were sectioned in the same ice-cold sucrose-aCSF using a vibratome (Leica VT1200, Leica Biosystems, Deer Park, IL). Slices between 1.4 mm posterior and 2.5 mm posterior to bregma were collected for recording and maintained in an incubation chamber for at least 30 min before recording. The incubation chamber contained room temperature aCSF (~21° C) consisting of (in mM): 125 NaCl, 25 $NaHCO_3$, 25 glucose, 3 KCl, 1.2

NaH_2PO_4, 1.2 $CaCl_2$, 1.2 MgSO4 bubbled with 95% O_2 and 5% CO_2. For recording, slices were transferred to a recording chamber mounted on the stage of an Olympus BX51WI microscope (Olympus Life Science Solutions, Bartlett, TN) equipped with a 10x (0.3 NA) water immersion objective and perfused with oxygenated room temperature aCSF. For electrophysiology studies, an n = 3-5 mice per sex per genotype per timepoint was used (Table 2.1).

To stimulate corpus callosal fibers, a bipolar stimulating electrode (FHC Neural Microtargeting, Bowdoin, ME; matrix electrode; cat #30250) was placed approximately 1 mm from a glass micropipette recording electrode filled with extracellular solution (1.65 mm OD, 1.0 mm ID, 8250 capillary glass, King Precision Glass, Claremont, CA). Micropipettes were pulled on a horizontal electrode puller (P1000; Sutter Instruments, Novato, CA) to produce tip diameters of approximately 2µm that resulted in ~3 MΩ resistances when filled with aCSF. Compound action potentials (CAPs) were evoked with a DS3 Isolated Current Stimulator (Digitimer, Ft. Lauderdale, FL) and measured with a Model 2400 patch clamp amplifier (A-M Systems; Sequim, WA). The resultant extracellular analog signals were converted into a digital signal by a PCI-6040E A/D board (National Instruments, Austin, TX), and stored and analyzed on a PC computer using WCP Strathclyde Software (courtesy of Dr. J Dempster, Strathclyde University, Glasgow, Scotland). CAPs were elicited using a stimulation protocol consisting of five consecutive sweeps, 100µs in duration, with a 10s delay between sweeps ranging from 100µA to 500µA. An average of three recordings from one slice was used to reduce signal to noise ratio. CAPs were analyzed using the WinWCP program (courtesy of Dr. J Dempster, Strathclyde University, Glasgow, Scotland). Graphpad prism (San Diego, CA) was used to graph the ratio of N1 (myelinated axons) to N2 (unmyelinated axons) and for statistical analysis. Analysis was performed using a 2-way ANOVA comparing genotypes across stimulus current. Representative traces were superimposed using Origin2020b software (Origin, Northampton, MA).

2.4 Results

Confirmation of gene ablation and lipid reduction following tamoxifen injection of the conditional CST knock-out model

Studies have reported that MS patients present with a significant reduction of the myelin lipid known as sulfatide even in regions of NAWM (Marbois et al., 2000; Yahara et al., 1982). To determine the consequence of adult-onset sulfatide reduction, we generated a conditional CST knockout (CST-cKO) mouse using CRISPR technology. Fig. 2.1A depicts the modified Cst gene with loxP sites inserted in non-coding regions and flanking exons 2 and 3. We designed and positioned primers up- and downstream of the loxP sites to detect ablation. Fig. 2.1A displays gene products after tamoxifen injection of both the CST-cKO and control with the CST-cKO yielding a PCR product of 432 bp, which is the product size consistent with gene ablation. Fig. 2.1B demonstrates successful ablation of the Cst gene in the CST-cKO mice having both ablated and non-ablated products. The presence of both ablated and non-ablated products is expected and consistent with: 1. starting material of the corpus callous, which also contains non-oligodendrocytic cells and 2. less than 100% ablation efficiency of oligodendrocyte lineage cells. To further assess ablation efficiency, we isolated mRNA. Fig. 2.1C demonstrates significantly reduced transcript levels for Cst message in the CST-cKO corpus callosum compared to message levels of the control animals. Our gene and message analyses demonstrate gene ablation accompanied with >60% message reduction.

Although our findings confirm both appropriate gene ablation and message reduction, these data do not directly assess lipid levels. To quantify sulfatide amounts, multidimensional mass spectrometry-based shotgun lipidomics was performed as previously described (Qiu et al., 2021). We isolated corpus callosi from CST-cKO and control mice at 3-, 6-, and 11-month (m) post tamoxifen injection (PI). These time points were chosen since sulfatide requires ~4 months to turnover (Hayes & Jungawala, 1976; Norton & Cammer, 1984). At 3m PI, there was no significant difference in relative sulfatide levels between the CST-cKO and control mice (Fig. 2.1D). By 6m PI, we observed a significant and consistent reduction of the lipid with sulfatide levels in the CST-cKO mice only reaching 40% of the sulfatide levels in the controls. By 11m PI, sulfatide levels remained

significantly depleted and the mice presented with an additional 10% reduction indicating a sustained and progressive loss of the lipid. Importantly, consistent with our group's previous analyses (Qiu et al., 2021), these findings confirm sulfatide reduction and reveal no difference in the levels of galactocerebroside, the precursor of sulfatide (Morell & Radin, 1969) at any of the PI time points (data not shown). Taken together, our findings demonstrate that the novel Cst floxed mouse provides a unique opportunity to ablate the Cst gene and specifically reduce sulfatide levels in the adult CNS.

Progressive axonal pathology with myelin sparing

Previously, our group reported that in constitutive CST KO mice, myelin sheaths were significantly thinner than in their wildtype littermates. We also observed a variety of myelin pathologies including uncompacted, degenerating, and redundant myelin profiles (Marcus et al., 2006). To determine if adult-onset sulfatide depletion resulted in similar pathologies, we used EM analysis to calculate g ratios in the corpus callosum. Fig. 2.2A i-vi presents representative electron micrographs for each genotype at each PI time point.

To determine if demyelination or myelin instability occurs following adult-onset sulfatide depletion, we compared the percent of myelinated and unmyelinated axons in the corpus callosi of mice with normal and depleted levels of sulfatide. Across all timepoints, there was no significant difference in the percent of unmyelinated fibers between the two genotypes (Fig. 2.2B) (3m p=0.9891, 6m p=0.6478, 11m p=0.5010). We conducted separate t tests at each timepoint and determined that there was no significant difference between genotypes at any timepoint (3m p=0.6359 6m p=0.3963 11m p=0.2737).

Fig. 2.2C compares the average g ratio values obtained for individual mice and individual axons. Using a 2-way ANOVA, there was no significant difference among the genotypes at each timepoint (3m p=0.6541, 6m p=0.7676, 11m p=0.2247). In addition, separate t-tests were conducted to strictly compare genotypes at each time point, of which there was no significant difference (3m p=0.2659, 6m p=0.4402, 11m p=0.0980). Since

sulfatide is reduced in MS and MS is 3 times more prevalent in females than males (Koch-Henriksen & Sørensen, 2010), we further assessed g ratio, with sex as a biological variable. Binning the values per sex, also revealed no sex differences at any of the experimental endpoints (data not shown).

Previous studies have reported that myelin and axon defects are more prone to axons of specific caliber (Thomason et al., 2022). Therefore, we used a similar binning approach (increments of 0.1µm) to assess axonal caliber-specific pathologies; however, no difference in axon caliber, or myelin thickness was detected (Figure 2.3 And 2.4, respectively).

To further assess the consequence of adult onset sulfatide depletion on CNS integrity, we quantified myelin and axonal pathologies including: 1. myelin un-compaction, 2. Vacuolar degeneration, 3. redundant myelin profiles and 4. degenerating axonal fibers. The compilation of these pathologies revealed a significant increase in the CST-cKO mice reaching statistical significance at 11m post injection (Fig. 2.5B) ($p=0.0018$) indicating a loss of overall myelin/axon integrity following sulfatide depletion. Interestingly, when separating the four pathologies, there was no statistical difference at any of the time points including 11m PI for any of the myelin pathologies ((un-compaction $p=0.9541$; vacuolar degeneration ($p=0.9996$); redundant myelin ($p=0.9986$) (Fig. 2.5C-E)). These data imply that physiological sulfatide levels in adulthood are not essential for proper myelin structural maintenance. However, there was a robust and significant difference in the extent of axonal degeneration at 11m PI (Fig. 2.5F) ($p=<0.0001$) (3m $p= 0.9988$, 6m $p= 0.3068$) suggesting that loss of sulfatide facilitates axonal pathology independent of myelin loss. (See Fig. 2.2A for low magnification overview where neurodegeneration is observed at 6m and 11m PI.) This analysis was repeated in the dorsal columns of the cervical spinal cord and we also observed a significant increase in axonal degeneration at 11m in the CST-cKO compared to CTL ($p=0.0022$). There was no difference in myelin abnormalities at any of the timepoints between genotypes nor any difference in the percentage of unmyelinated fiber or g-ratio (Fig. 2.4-2.6).

Variation in Nodal Length

Although no significant difference in myelin integrity was observed by our myelin ultrastructural analyses, axonal pathology was abundant. Consistent with sulfatide playing a role in maintaining axonal integrity, our previous analyses of the constitutive CST KO mice revealed abnormal lengths of the nodes of Ranvier (Marcus et al., 2006). Therefore, using a similar approach, we measured the length of the nodes of Ranvier in the conditional CST KO mice at the three PI time points. As shown in Fig. 2.7C, no difference in nodal length was observed between the CST-cKO and CTL mice at 3, 6, or 11m PI (3m control 1.548μm ± 0.175μm vs. 3m CST-cKO 1.236μm ± 0.106μm; p=0.8269; 6m control, 1.065μm ± 0.096μm vs. 6m CST-cKO, 1.038μm ± 0.120μm; p=0.9999; and 11m control, 1.047μm ± 0.111 vs. 1.575μm ±0.479 p=0.3780), with all of them exhibiting a similar mean nodal length. Using a variability analysis to analyze the rage of nodal lengths observed, we observed no significant difference in length variability at 3m or 6m PI (3m p=0.7047 and 6m p=0.8607). However, at 11m PI, there was a significant increase in variability (p<0.0001). Similarly, calculating variability per mouse per time point (Fig. 2.7D), demonstrated a significant increase in the variance at the 11m timepoint in the CST-cKO mice. To further investigate this increased variability in node length, we focused our attention on the structural integrity of the paranode, which flanks the node of Ranvier defining the nodal gap (Peters, 1966). Paranodes are important for node assembly and maintenance, restricting the movement of the flanking sodium and potassium channels in the node of Ranvier and juxtaparanode, respectively (Rasband et al., 1999). The axonal cytoskeleton contains a network of spectrin (αII spectrin, and βII spectrin) and ankyrinB which aid in anchoring these ion channels. (Ogawa et al., 2006; Susuki et al., 2018; C. Zhang et al., 2013). A prominent structural component of the paranodal junctions are the electron dense transverse bands, which are composed of glial and neuronal adhesion molecules (Schnapp et al., 1976; Tait et al., 2000; Charles et al., 2002a) We and others have previously proposed that a function of the transverse bands is to maintain adherence between the myelin sheath and the axon resulting in the maintenance of myelin integrity and axon-myelin communication, organized axonal domains and overall axonal health (Coman et al., 2006; Dupree et al., 1998a; Mierzwa et al., 2010; Pillai et al., 2009; Rosenbluth et al., 2003; Susuki et al., 2018). Additionally, we reported compromised paranodal junctions in the constitutive CST KO mice (Honke et al., 2002; Marcus et al., 2006). Therefore, we proposed that increased variability in nodal length could be a consequence of compromised junctions as evidenced by a deterioration of transverse bands. In the healthy CNS, EM analysis

reveals transverse bands as regularly spaced electron densities that span the periaxonal space of the paranode (Peters et al., 1992) (Fig. 2.7E) Consistent with our previous analyses of the constitutive CST KO mice and with the loss of axonal integrity, we observed a frequent loss or irregular spacing of these densities that constitute the myelin/axon paranodal junctions in the CST-cKO mice (Fig. 2.7F).

Disruption of Contactin-Neurofascin binding

In order to quantify the binding relationship of the axo-glial paranodal junction, we used immunoprecipitation followed by western blotting to quantitatively compare the relative amount of contactin bound to neurofascin in the corpus callosum of CTL and CST-cKO at 3-month and 11-month PI. We found that at 3-months PI, there was no significant difference in amount of contactin between the CTL and CST-cKO. However, at 11-months PI we found a significant reduction of contactin in the IP eluant (Figure 2.8A). These data demonstrate that there is lower abundance of contactin in the CST-cKO compared to CTL per the same amount of neurofascin protein. To further corroborate these findings, we performed western blot analysis on neurofascin in corpus callosal tissue and determined there is no significant difference in neurofascin protein at the 3- or 11-month PI timepoints (Figure 2.8C).

Progressive nodal protein domain abnormalities

Our ultrastructural analyses demonstrate an increase in variability in the length of the nodal gap and a loss of paranodal integrity at the 11m timepoint. Since axo-glial junctions play a role in the establishment and maintenance of the distribution of the axonal proteins that are specifically clustered in the node of Ranvier, the paranode and the juxtaparanode, the disruption of regularly spaced transverse bands may result in compromised domain organization (Coman et al., 2006; Dupree et al., 1998b; Einheber et al., 2006; Garcia-Fresco et al., 2006; Kojima & Hayashi, 2018; Marcus et al., 2006; Mierzwa et al., 2010). To determine if the axonal domains are disrupted consequential of adult-onset loss of sulfatide, we immuno-labeled corpus callosum sections from CST-cKO and control mice with Nav1.6, Caspr1, and Kv1.1 to assess protein organization of the node of Ranvier, the paranode, and the juxtaparanode, respectively (Fig. 2.9A). Common

pathologies observed, but not exclusive, were: 1. binodal sodium channel clusters (Fig. 2.9B), 2. elongation of Nav1.6 and Caspr1 domains (Fig. 2.9C), 3. A combination of pathologies such as mixing of proteins from adjacent domains and binodal sodium (Fig. 2.9D). Quantification of domain organization (Fig. 2.9E) revealed no alterations by 3m post tamoxifen injection (8.3% for control vs 10.2% for CST-cKO p=0.958 n=7, 150+ nodal domains per animal), a time point when sulfatide levels remained unaltered; however, by 6 and 11m post tamoxifen injection, time points when sulfatide levels were reduced (Fig. 2.1D), the percentage of abnormal domain arrangement was significantly and progressively increased (6m – 9.6% for control vs 21.8% for CST-cKO; p=0.032 n=6 and 11m – 20.8% for control vs 81.4% for CST-cKO; p<0.0001 n=7-11, 150+ nodal domains per animal for each timepoint). These data are consistent with previous findings in the constitutive CST KO mice that demonstrated neuronal nodal domain proteins are mis-localized in the absence of sulfatide (Ishibashi et al., 2002; Hayashi et al., 2013)

Progressive shift in myelinated axonal function

Action potential conduction is mediated by appropriate clustering of ion channels in specific domains along the axon (Wang et al., 1994; (Caldwell et al., 2000) When domain organization is disrupted, axonal function is compromised (Bagchi et al., 2014; Sinha et al., 2006). Based on both our ultrastructural and immunohistochemical data, we proposed that the axons of the corpus callosum were functionally compromised. To directly assess axonal function, we employed a well-established electrophysiological approach designed to CAPs in both the myelinated and unmyelinated axons (Baker et al., 2002; Reeves et al., 2005; Yamate-Morgan et al., 2019). Typically, a CAP consists of two downward deflections referred to as N1 and N2 (Fig. 8Ai). The CAPs of myelinated axons are represented in the N1 peak, the first downward deflection across time, while the N2 peak represents the CAPs of unmyelinated axons, the second downward deflection. To compare N1 and N2 peaks across time and between genotypes, we have presented the data as a ratio of N1/N2.

At the 3m PI timepoint, there was no change in N1/N2 ratio (Fig. 2.10Aii), which is consistent with our lipidomic data showing no difference in sulfatide levels between genotypes, as well as our IHC data showing no difference in abnormal domain localization. However, consistent with our IHC data, which revealed significant disruption in ion channel domain organization, CAP analyses showed that at 6- and 11-month PI, there is a statistically significant reduction in the N1/N2 ratio in the CST-cKO mice compared to control mice (Fig. 2.10B and 2.10Cii, respectively). At the 11-month timepoint, the N1 peak is completely absent (Fig. 2.10Ci) giving a ratio of zero across all stimulation intensities. While previous studies using the constitutive CST KO mice quantified conduction velocity in the sciatic nerve (Honke et al., 2002; Hayashi et al., 2013) we provide the first direct evidence of functional loss within the CNS following sulfatide depletion and more interesting, we show a profound impaired function that parallels ion channel redistribution that precedes significant myelin disruption or myelin loss. Figures 2.2-5 demonstrate that myelin is intact, and Fig. 2.5 and Fig. 2.6 show no increase in myelin pathology, yet, the progressive loss of N1 indicates these myelinated axons are not functioning as myelinated axons at the 6- and11-month timepoint. Collectively, these findings demonstrate that loss of sulfatide in adulthood leads to increased axonal pathology with relative myelin sparing.

2.5 Discussion

In MS brains, lipid metabolism is disrupted (Moscatelli & Isaacson, 1969) even in regions of NAWM (Wheeler et al., 2008). More specifically, sulfatide, a prominent glycosphingolipid of the myelin sheath (Norton & Cammer, 1984), is decreased in NAWM while no other myelin proteins or lipids are reduced (Marbois et al., 2000; Yahara et al., 1982) indicating sulfatide loss is independent of demyelination. Previous work from our group (Marcus et al., 2006; Pomicter et al., 2013; Shroff et al., 2009) and our collaborators (Ishibashi et al., 2002) using the constitutive CST KO mouse (Honke et al., 2002) shows a plethora of myelin abnormalities accompanied by axonal abnormalities that are consistent with myelin and axonal pathologies prevalent in MS (Pomicter et al., 2010; Suzuki et al., 1969; York et al., 2021). Recognizing that CNS pathologies presented in the constitutive CST KO mouse may be consequential of disrupted development, we generated the Cst floxed mouse, which enables adult-onset sulfatide depletion. Exploiting this novel mouse, we show for the first time

that adult onset sulfatide reduction is sufficient to compromise neuronal structure and function independent of myelin loss, yet not sufficient to drive demyelination.

Adult-onset sulfatide depletion is not sufficient to drive demyelination

In our previous work, we showed a significant increase in the g ratio of myelinated axons in the CNS of adolescent and adult constitutive CST KO mice (Marcus et al., 2006). In contrast, our quantitative analyses of the conditional CST KO mice showed no change in g ratios (Fig. 2.2). We propose that this difference in g ratio data between the 2 CST mutant models reflects 1) a developmental inhibition of myelin synthesis with the absence of sulfatide during the critical period of myelin production and maturation (Foran & Peterson, 1992; Sturrock, 1980) in the constitutive CST KO mice whereas sulfatide synthesis in the conditional CST KO animals was not inhibited until 10 weeks of age and 2) the retention of a portion of the sulfatide that was synthesized prior to gene ablation**.** In addition to thin myelin, our analysis of the constitutive CST KO mice showed that early depletion of sulfatide synthesis resulted in unstable myelin sheaths as evidenced by increased and progressive myelin uncompaction and demyelination (Marcus et al., 2006). Those findings led us to conclude that the absence of sulfatide plays a prominent role in myelin loss observed in MS. However, our current findings from the conditional CST KO mice contrast with our original conclusion. Although myelin that is formed in the absence of the sphingolipid is more vulnerable to demyelination (Marcus et al., 2006), our longitudinal study of the conditional CST KO mice strongly suggests that myelin synthesized in the presence of sulfatide, but with reduced lipid after maturation, is relatively stable with regard to compaction and myelin loss. Based on our previous work, we assessed a variety of other pathologies including vacuolar degeneration of the myelin sheath (Fig. 2.5ii), myelin uncompaction (Fig. 2.5iii), frequency of myelin redundancy (Fig. 2.5iv) and axonal degeneration (Fig. 2.5v). Although all of these pathologies were observed, the only pathology that was significantly more prevalent in the sulfatide depleted mice was axonal degeneration, suggesting that adult-onset depletion of sulfatide is not sufficient to drive overt dys- or demyelination but is sufficient for the loss of axonal structure and function.

Adult-onset sulfatide depletion induces axonal pathology

Our ultrastructural analysis indicated the absence of demyelination but revealed a significant impact on axon integrity following chronic sulfatide depletion. Axonal degeneration was evidenced by abnormal electron dense bodies within the axon, the loss of organelle structure and the retention of myelin sheaths that lack the axon entirely (Fig. 2.5Av). Oligodendrocytes play important roles in metabolically and structurally supporting axons (Fünfschilling et al., 2012; Lappe-Siefke et al., 2003; Lassetter et al., 2023; Y. Lee et al., 2012; Morrison et al., 2013; Mukherjee et al., 2020). Therefore, it is not surprising that loss of an oligodendrocyte component leads to axonal pathology with myelin sparing, as this has been previously reported (Buscham et al., 2022; Griffiths et al., 1998). There are several mechanisms in which progressive loss of sulfatide could lead to axonal degeneration. One possibility is involvement of the immune system. Using the conditional sulfatide KO mouse, our group has demonstrated a significant increase in disease-associated microglial and astrocyte neuroinflammation, particularly within myelin containing regions (Qiu et al., 2021). Ultrastructural analysis revealed astrocytic processes around the myelin sheath and TREM2, which is expressed by microglia and acts as a lipid sensor, is known to interact with sulfatide. (Poliani et al., 2015; Wang et al., 2015). Since sulfatide is enriched in the outer leaflet of the myelin sheath (Boggs et al., 2008), TREM2 may sense altered lipid stoichiometry and launch an immune response (Cantoni et al., 2015; Poliani et al., 2015)

In NAWM of MS patients, activated microglia can drive disruption of axo-glial junctions, leading to elongated and mis-localized sodium and potassium channels (Howell et al., 2010). Our findings provide evidence of disruption of transverse bands and subsequent sodium and potassium channel redistribution. Transverse bands, which are formed by the binding of neurofascin155 of the myelin sheath to the contactin/Caspr1 axonal complex (Charles et al., 2002a), tether the myelin sheath to the axon. Previous work from us (Dupree et al., 1998b; Dupree et al., 1999; Pomicter et al., 2010) and others (Charles et al., 2002a; Coman et al., 2006; Rasband et al., 1999) has shown that a loss of myelin-axon interaction, particularly at the paranode region, is associated with altered axon structure and function. Consistent with these previous reports, here we observed compromised transverse band integrity and a significant increase in the variability of node of Ranvier length.

The disruption of the transverse band complex is further evidenced by the significant decrease of contactin in the neurofascin IP reaction at 11-months PI in the CST-cKO mice. This demonstrates that given the same amount of neurofascin, there is a reduction of contactin, indicating contactin is not binding to neurofascin. In addition, we observe the mis-localization of Caspr1 via IHC, an essential component of the transverse band complex (Bhat et al., 2001; Boyle et al., 2001; Sun et al., 2009). Mis-localization of Caspr1 suggests that the Caspr1-contactin complex is not appropriately binding to its glial ligand neurofascin 155. This has been confirmed in our model, we see a significant loss of neurofascin-contactin binding in our immunoprecipitation at 11m PI. Consequently, disruption of these complexes results in a loss of proper myelin-axon anchoring (Bhat et al., 2001; Boyle et al., 2001) and could result in lateral movement of the sheath along the axon providing a viable explanation for the observed variation in node of Ranvier length that we observe in the conditional CST KO mice (Fig. 2.7). Additionally, these paranodal junctions also aid in maintaining the proper clustering of the axonal proteins that constitute the node, paranode and juxtaparanode, in addition to the underlying axon cytoskeletal network (Mierzwa et al., 2010a; Susuki et al., 2013; Amor et al., 2014). Interestingly, we have previously shown, using the constitutive CST KO mice, that the loss of sulfatide results in destabilization of the paranodal axo-glial complexes and a loss of the respective protein clusters (Ishibashi et al., 2002; Pomicter et al., 2013). Since this previous work was based on studies using the constitutive CST KO mice, the possibility remained that this sulfatide-dependent regulation was limited to developmental conditions with limited relevance to an adult-onset disease. Here, we show that adult-onset sulfatide depletion is sufficient to drive protein domain disruption at both the ultrastructural and molecular levels.

Adult-onset sulfatide depletion disrupts the function of myelinated axons

In addition to possibly facilitating the “sliding” of the myelin sheath along the axon, altered transverse band integrity may result in compromised axonal domain organization. Our IHC data showed that at 6m and 11m PI, the highly conserved spatial organization of the sodium and potassium channel domains was significantly compromised. Although myelin structure was spared, mis-localization of the ion channels translated functionally into loss of the myelinated (N1) amplitude. Similar abnormal protein domain localization

pathologies have been observed using the experimental autoimmune encephalomyelitis (EAE) mouse model (Recks et al., 2013) as well as clinical studies showing substantial pathology in the NAWM, where sodium and potassium channel domains overlapped (Gallego-Delgado et al., 2020; Howell et al., 2010) and axonal degeneration preceded demyelination (Luchicchi et al., 2021).

Disruption of ion channel localization not only leads to mis-firing and inefficient functioning of the axon, but also leads to channelopathy. Craner et al. (2004) demonstrated that aberrant localization of Nav1.6 along extensive regions of a demyelinated fiber co-localizes with sodium/calcium exchangers (NCX), causing a reversion of the exchangers' function, resulting in increased intracellular calcium resulting in abnormal axonal function and ultimately axonal degeneration (Craner, Hains, et al., 2004; Stys et al., 1992). Our data show, at 6 months PI, an increase in protein domain mis localization and a functional ratio shift from N1 to N2; however, there is no significant difference in axonal degeneration. Consistent with limited axonal pathology in the sulfatide conditional CST KO mice is the retention of the myelin sheath. In contrast to demyelinated axons, dysmyelinated axons express Nav1.2 (Boiko et al., 2001; Westenbroek et al., 1992) and are less sensitive to this type of injury. Presently, it is unknown if the myelinated axons in the conditional CST KO mice present with a re-expression of the immature sodium channel isoform. Ultrastructural axonal degeneration reaches significance at 11m PI coinciding with an increase in the frequency of elongated Nav1.6 channel domains. It will be of interest to determine if the myelinated axons in the conditional CST KO mice present with an upregulation of Nav1.2, which has been reported following myelin disruption (Craner et al., 2004; Dupree et al., 2004). Perhaps there is a differential expression of Nav1.6 and Nav1.2 in the conditional CST KO, with Nav1.6 expression associated with the 10% axonal degeneration we observed and Nav1.2 is expressed in the axons with intact structure. An upregulation of Nav1.2 expression might provide protection from degeneration, expanding the window for myelin repair and ultimately axonal function.

Loss of function of N1 axons likely contributes to disrupted motor function. Our group has previously extensively assessed neuromotor function in the conditional CST KO mice (see Qiu et al., 2021 for more

information). In these studies, Qiu et al. (2021) used nine paradigms to assess neuromotor function including; righting reflex, hindlimb clasping, crossed extensor reflex, forelimb/hindlimb placing responses, grasp reflex, rooting reflex, vibrissa placing response, negative geotaxis, and auricular startle tests, of which there was no significant difference between CTL and CST-cKO at 10 months post injection. Subsequent studies also included frailty index assessment (including evaluation of the visual system and visual loss) (Whitehead et al., 2014), Morris Water Maze (MWM), and Novel Object Recognition (NOR). There was no significant difference in the frailty index between CTL and CST-cKO at 10 months post injection. However, the MWM and NOR assessment showed a genotype effect (Qiu et al., 2021). Our combined studies provide evidence that loss of sulfatide in adulthood leads to disruption of N1 amplitudes with accompanying neurobehavior dysfunction.

Technology has greatly improved the resolution of magnetic resonance imaging (MRI) allowing the detection of lesions in what otherwise was considered NAWM (Inglese et al., 2018). While our studies suggest that a significant reduction of sulfatide leads to axonal degeneration, perhaps the dysmyelination, defined by the disruption of axo-glial complexes resulting in ion channel mislocalization, that occurs consequential of sulfatide depletion may act to spare axonal integrity via expression of Nav 1.2, at least in the acute, or perhaps prodromic, stage of the disease. It remains to be determined if sulfatide depletion alone is sufficient to induce demyelination and to drive the transition of NAWM into lesion development. By the time lesions are detected, axonal pathology, which is at least in part consequential of sulfatide deletion and sufficient to result in functional deficits, has already developed. Our findings combined with the studies that have shown a loss of sulfatide in brain regions that reveal no myelin abnormalities are consistent with sulfatide depletion defining the prodromic stage of MS, the period of months or years before classic MS symptom onset (Makhani & Tremlett, 2021). It is unknown how the initial loss of sulfatide occurs, and how long sulfatide is reduced in NAWM prior to the onset of demyelination and plaque formation; however, detection of sulfatide levels should be considered as a possible diagnostic for MS in the future and may provide an indicator for initiation of therapeutic repair prior to irreversible axonal loss.

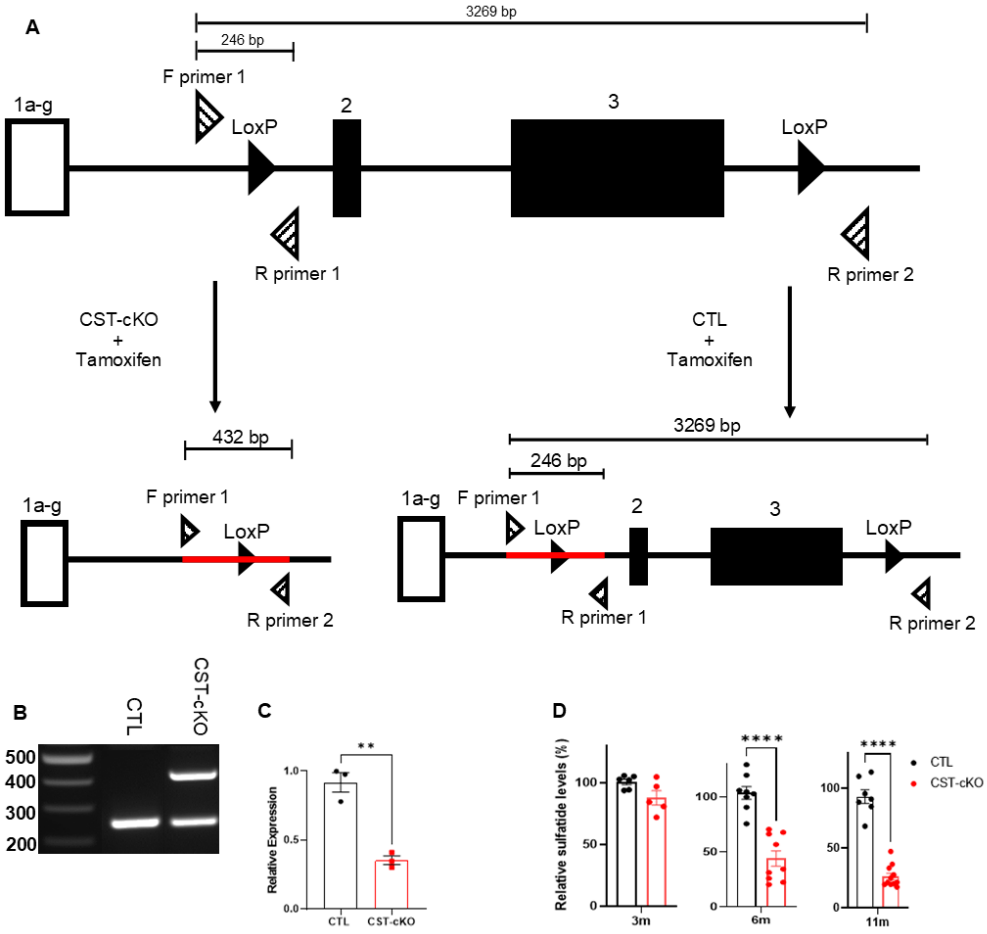
A
3269 bp
246 bp
F primer 1
1a-g
LoxP
2
3
LoxP
R primer 1
R primer 2
CST-cKO
+
Tamoxifen
CTL
+
Tamoxifen
432 bp
3269 bp
246 bp
1a-g
F primer 1
LoxP
2
3
LoxP
R primer 2
R primer 1
R primer 2
B
CTL
CST-cKO
500
400
300
200
C
**
Relative Expression
1.0
0.5
0.0
CTL
CST-cKO
D
Relative sulfatide levels (%)
****
****
100
50
0
3m
6m
11m
CTL
CST-cKO

Figure 2.1: Genetic ablation of the cerebroside sulfotransferase (Cst) gene. (A) Schematic illustrating the *Cst* gene with loxP sites (solid black triangles) upstream and downstream of coding regions exons 2 and 3. Three primers (striped triangles) were designed around the loxP sites to detect for genetic ablation: F (forward) primer 1, R (reverse) primer 2, and R (reverse) primer 1. Tamoxifen was administered to both CST-cKO and CTL mice, resulting in *Cst* gene recombination in CST-cKO mice (left; ablated gene product indicated by red line) with gene sparing (right; intact gene product indicated by red line) in CTL mice. **(B)** PCR amplification of genomic DNA from the CTL and CST-cKO mice confirmed recombination in CST-cKO mutant mouse brains 6 weeks post tamoxifen injection. **(C)** Real-Time PCR of CTL and CST-cKO mutant mouse brains 6 weeks post tamoxifen injection revealed ~50% reduction in mRNA expression. **(D)** Lipidomic analysis of total sulfatide in CST-cKO and CTL brains presented no change in sulfatide levels by 3-months PI but a significant sulfatide loss at 6 and 11 months PI. Unpaired Student's t-test. All data are presented as mean ± standard error. **p<0.005 **** p<0.0001.

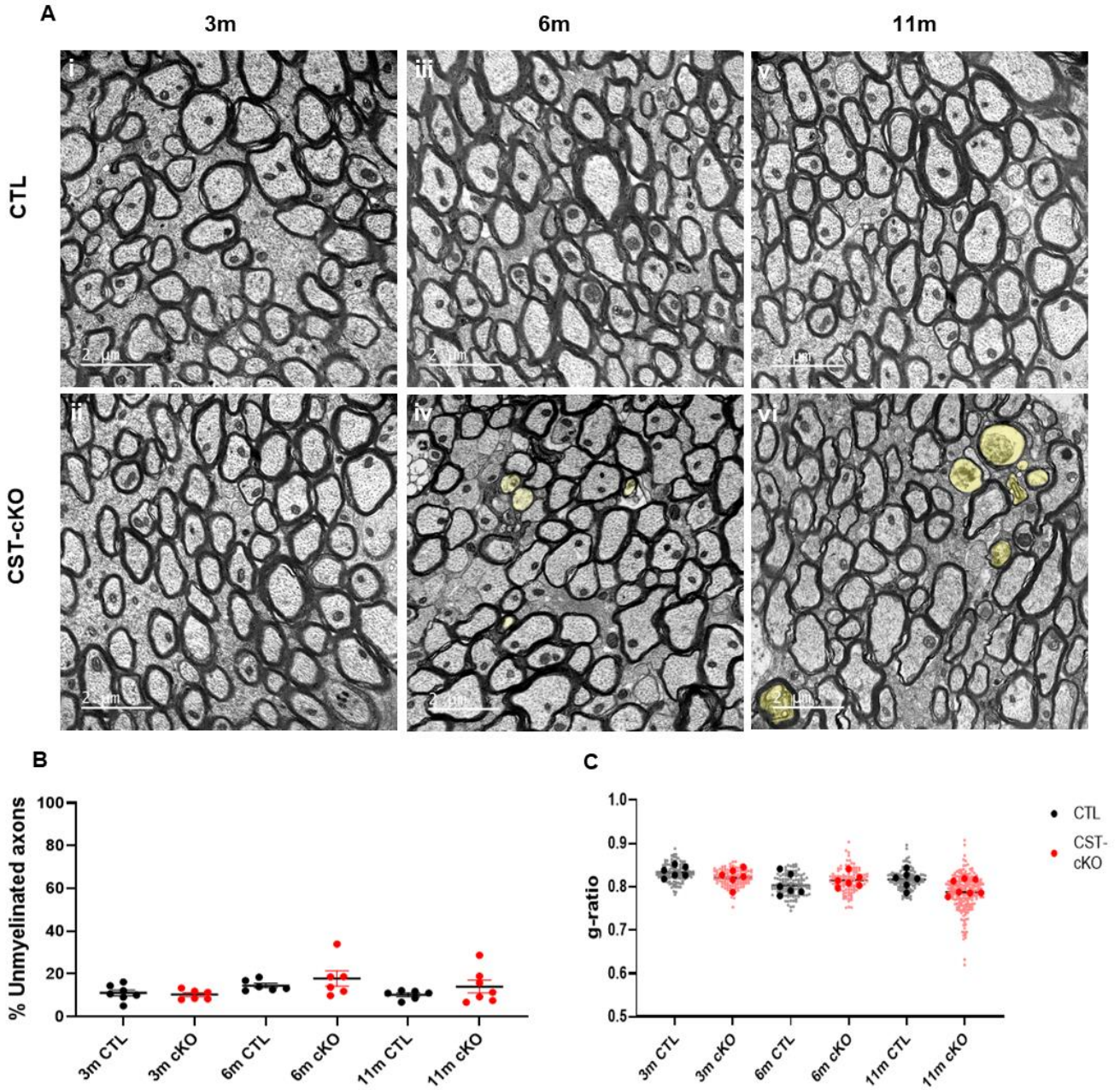
A
3m
6m
11m
CTL
CST-cKO
i
ii
iii
iv
v
vi
2 μm
B
% Unmyelinated axons
100
80
60
40
20
0
3m CTL
3m cKO
6m CTL
6m cKO
11m CTL
11m cKO
C
g-ratio
1.0
0.9
0.8
0.7
0.6
0.5
CTL
CST-cKO

Figure 2.2: No change in extent of myelination in the corpus callosum of CST-cKO mice. (A) Cross section representative images from the corpus callosum at the level of the fornix from control (CTL; Ai, Aiii and Av) and CST-cKO (Aii, Aiv and Avi) mice following 3- (Ai and Aii), 6- (Aiii and Aiv) and 11- (Av and Avi) months post injection. 3-, 6- and 11- months PI mice presented abundant myelinated axons with no difference in the percent of myelinated versus unmyelinated fibers **(B)** or in myelin thickness as quantitatively compered by g ratio analysis. **(C)** Note axonal pathology (yellow shade) in the 6m- and 11m-PI tissue. Data are presented as mean ± standard error; data statistically compared by 2-way ANOVA analysis followed by a Tukey's post-hoc multiple comparison test. Scale bar=2µm

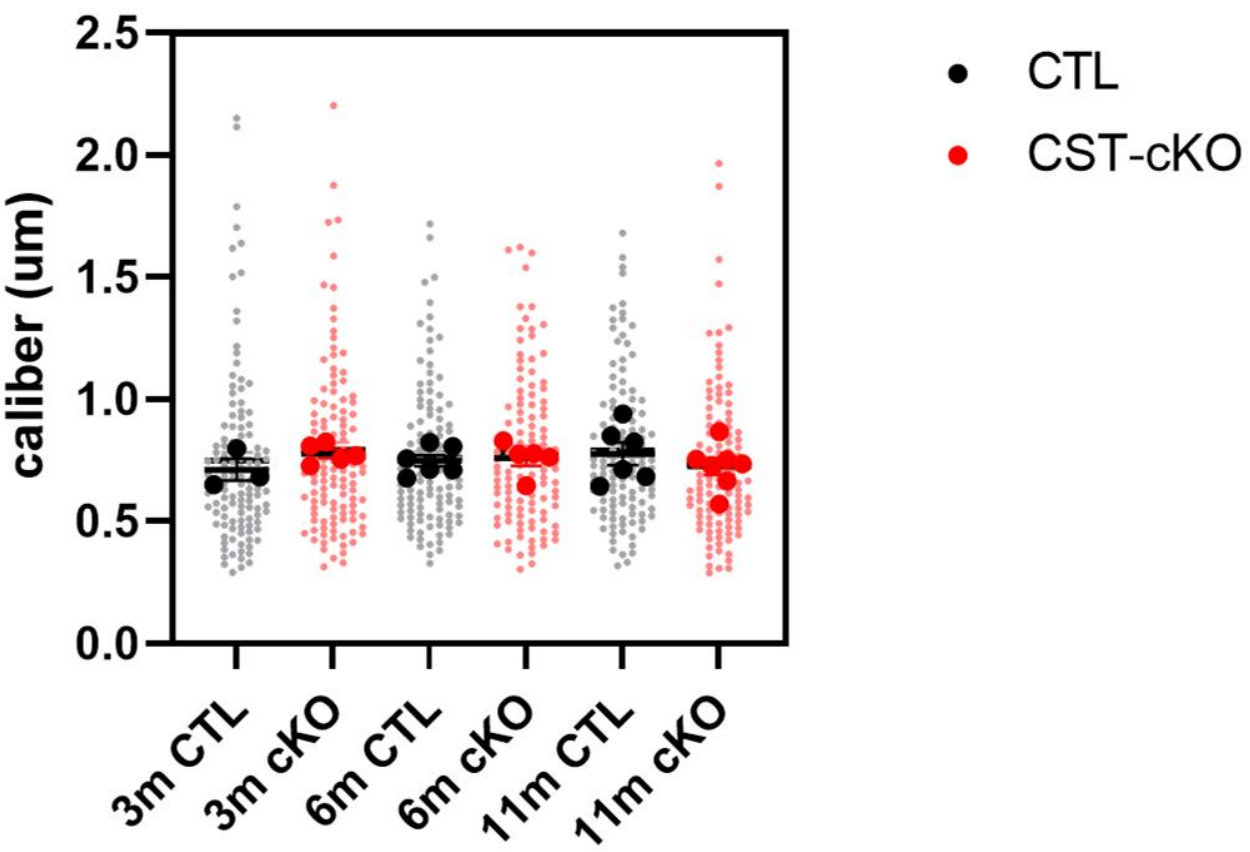
Axon Caliber
caliber (um)
2.5
2.0
1.5
1.0
0.5
0.0
3m CTL
3m cKO
6m CTL
6m cKO
11m CTL
11m cKO
CTL
CST-cKO

Figure 2.3: No change in extent of axon caliber in the corpus callosum of CST-cKO mice. Graphing individual values of axon caliber (at least 150 per mouse) and graphing the average of each mouse, yielded no significant difference in the extent of axon caliber between genotypes along any of the timepoints.

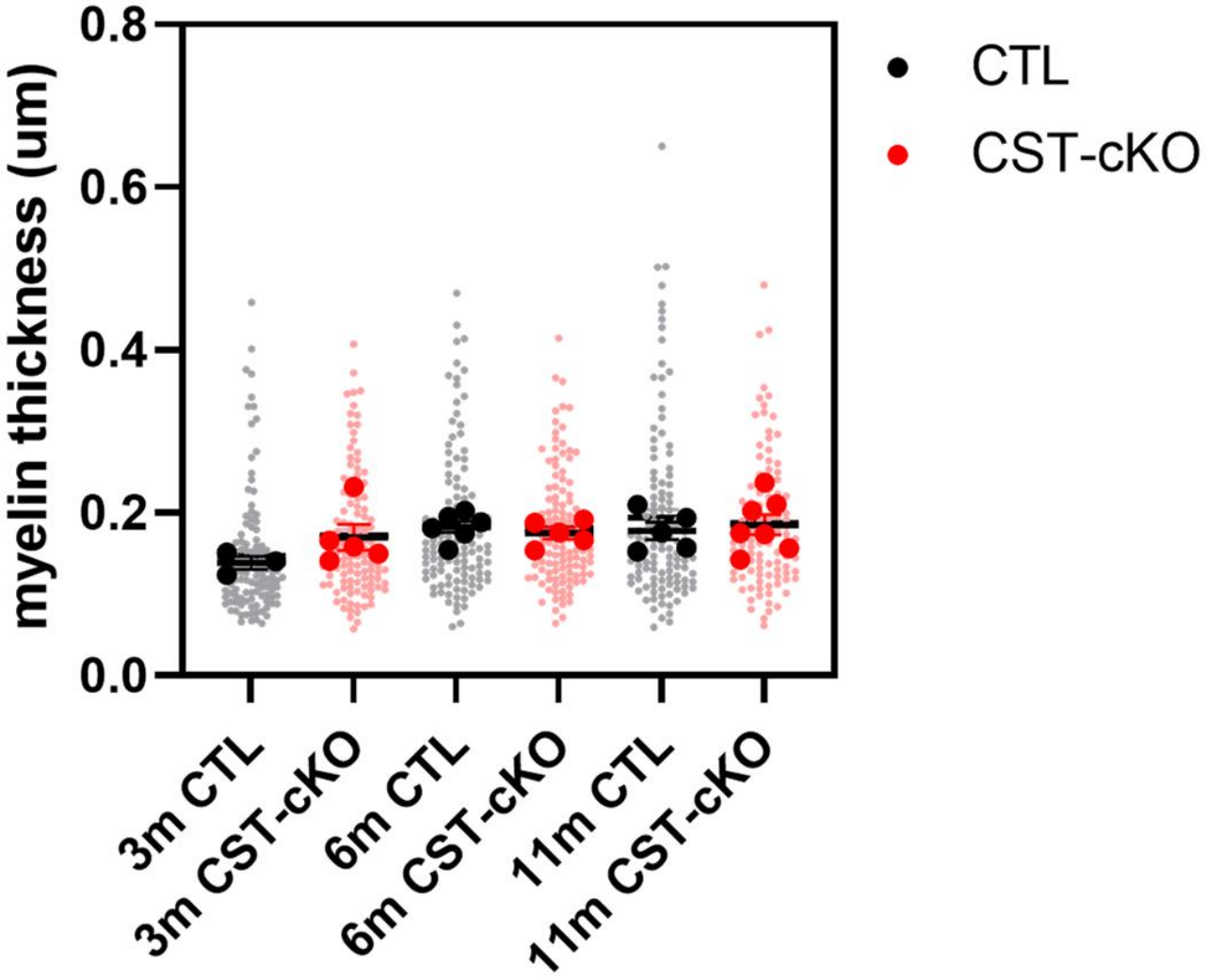
myelin thickness (um)
0.8
0.6
0.4
0.2
0.0
CTL
CST-cKO
3m CTL
3m CST-cKO
6m CTL
6m CST-cKO
11m CTL
11m CST-cKO

Figure 2.4: No change in extent of myelin thickness in the corpus callosum of CST-cKO mice. Graphing individual values of axon caliber (at least 150 per mouse) and graphing the average of each mouse, yielded no significant difference in the extent of myelin thickness between genotypes along any of the timepoints.

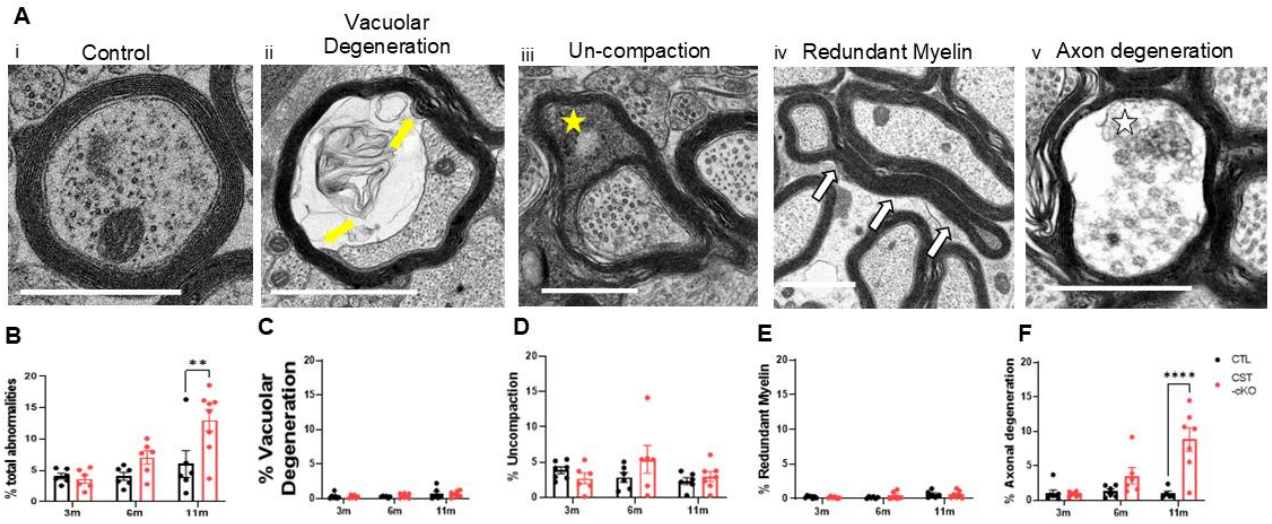
A
i Control
ii Vacuolar Degeneration
iii Un-compaction
iv Redundant Myelin
v Axon degeneration
B
% total abnormalities
**
3m
6m
11m
C
% Vacuolar Degeneration
D
% Uncompaction
E
% Redundant Myelin
F
% Axonal degeneration
****
CTL
CST -cKO

Figure 2.5. Quantification of myelin and axonal pathologies in the corpus callosum of CST-cKO mice. **(A)** Representative image of a healthy axon with an intact, compacted myelin sheath and appropriate array of neurofilament and microtubules (Ai). Representative images of various myelin and axonal abnormalities observed in the CST-cKO mouse included (from left to right): axon losing attachment to the myelin sheath (Aii; vacuolar degeneration; yellow arrows); presence of cytoplasm between compacted wraps of myelin (Aiii; un-compaction; yellow star); compact myelin out folding (Aiv; redundant myelin; white arrows) and organelle and cytoskeletal degeneration within the axon (Av; axon degeneration; white star). **(B)** Quantitative analysis combining all pathologies revealed a significant increase in myelin/axonal pathologies at 11m PI but not at 3- and 6- months PI. Separating out the individual pathologies revealed **(C-E)** no significant difference in myelin ultrastructure between genotypes at any of the timepoints analyzed; however, **(F)** axonal degeneration was significantly increased in the 11m CST-cKO mice. All data were statistically compared using a 2-way ANOVA; ** $p<0.005$ **** $p<0.0001$. Scale bar=1µm.

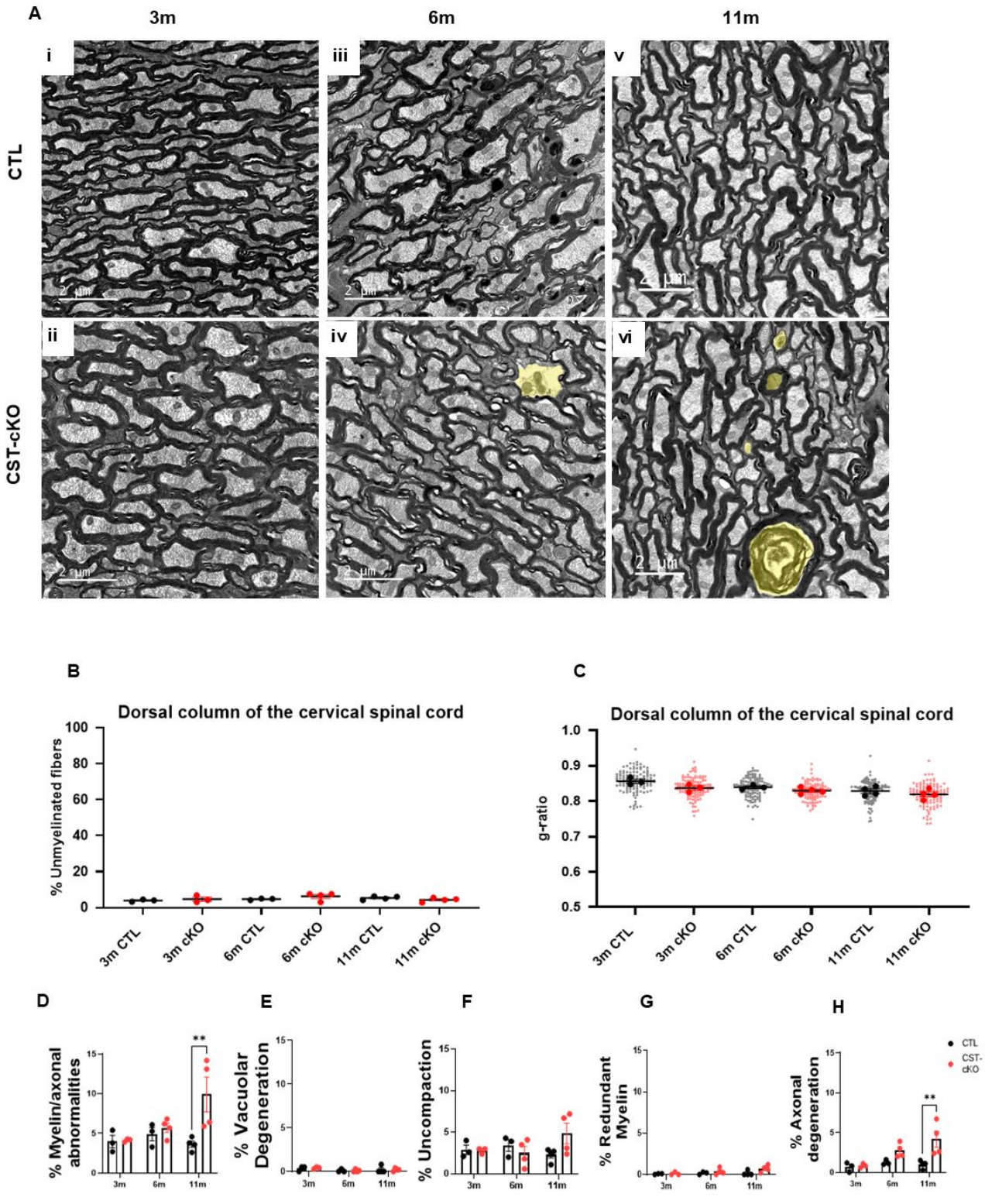
A
3m
6m
11m
i
iii
v
ii
iv
vi
CTL
CST-cKO
2 µm
B
Dorsal column of the cervical spinal cord
% Unmyelinated fibers
3m CTL
3m cKO
6m CTL
6m cKO
11m CTL
11m cKO
C
Dorsal column of the cervical spinal cord
g-ratio
D
% Myelin/axonal abnormalities
E
% Vacuolar Degeneration
F
% Uncompaction
G
% Redundant Myelin
H
% Axonal degeneration
CTL
CST-cKO

Figure 2.6: No change in extent of myelination in the dorsal column of the cervical spinal cord following adult-onset sulfatide depletion. (A) Cross section representative images from the dorsal column of the cervical spinal cord from control (CTL; Ai, Aiii and Av) and CST-cKO (Aii, Aiv and Avi) mice following 3- (Ai and Aii), 6- (Aiii and Aiv) and 11- (Av and Avi) months post injection. Quantitative analysis of the dorsal column of the spinal cord revealed no difference in the percent of myelinated versus unmyelinated axon **(B)**, or myelin thickness as calculated by g ratios (**C**). Similar to the corpus callosum, quantitative analysis of the combined axonal and myelin pathologies revealed a significant increase in the CST-cKO mice at PI 11-months but not at 3- and 6-months PI (**D**). However, when the individual pathologies were compared, myelin pathologies were comparable between genotypes (**E-G**) while axonal degeneration was significantly more abundant in the CST-cKO at 11-months PI compared to 11-months PI CTL mice (**H**). All data were statistically compared using a 2-way ANOVA; ** $p<0.005$ ****$p<0.0001$.

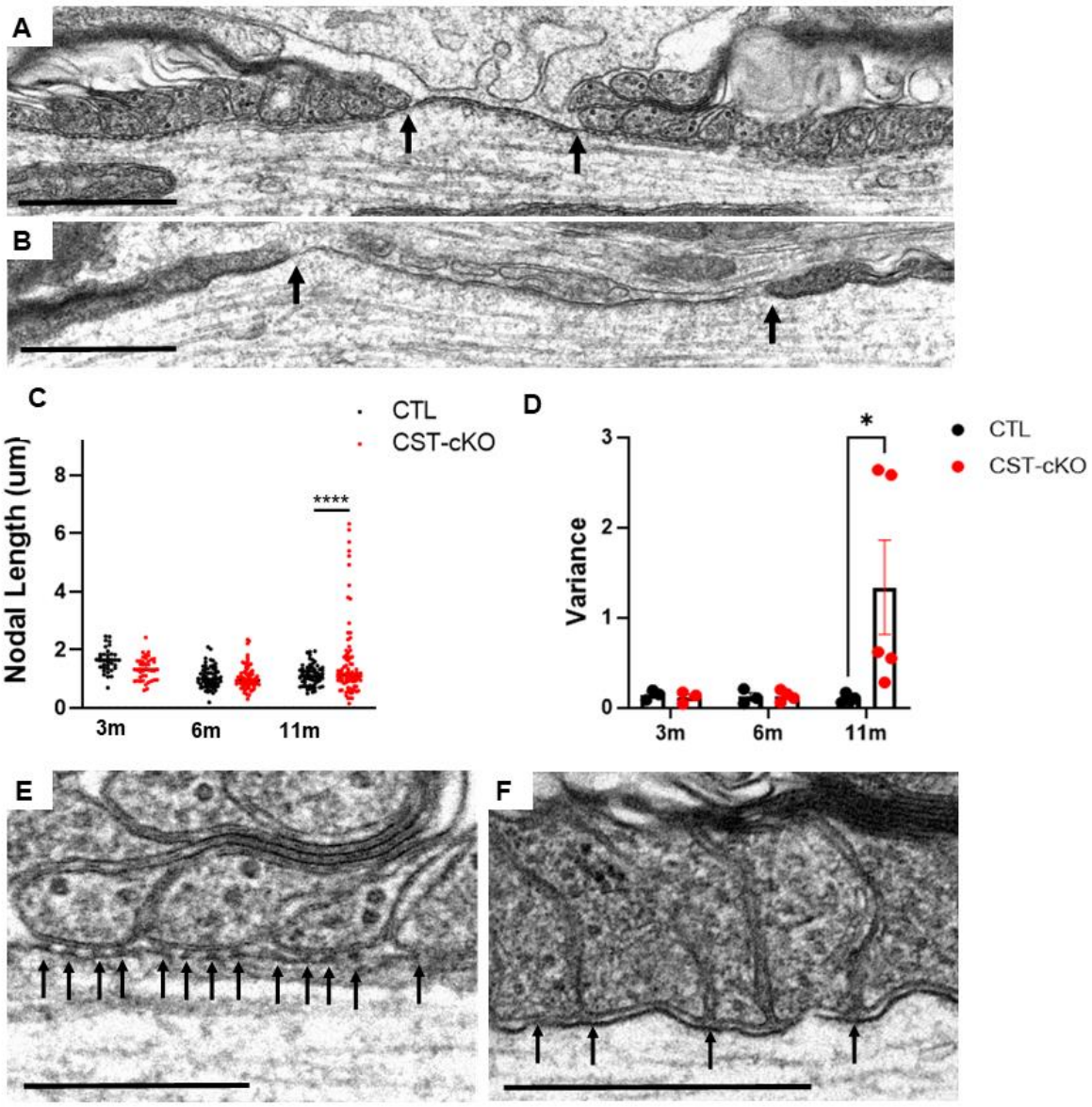
A
B
C
CTL
CST-cKO
Nodal Length (um)
8
6
4
2
0
****
3m
6m
11m
D
CTL
CST-cKO
Variance
3
2
1
0
*
3m
6m
11m
E
F

Figure 2.7. Increase in nodal length variability and loss of transverse bands following adult onset sulfatide depletion. (A) Normal ultrastructure of a node of Ranvier (bound indicated by black arrows) including nodal length (~1 micron) and flanking paranodal regions with lateral loops closely apposed to the axolemma. **(B)** CST-cKO mice revealed nodes of Ranvier with varying lengths including abnormally long nodal gaps (nodal bounds indicated by arrows). **(C)** Overall, node quantitation revealed no significant change in average nodal length between genotypes at any of the time points analyzed; however, a significant difference was observed in length variability in the 11-months post tamoxifen injected CST-cKO mice with nodes of Ranvier presenting both shorter and longer than 1 micron. **(D)** Calculating the nodal length variance per mouse further confirmed this variability at 11-months PI with a significant increase in length variance with no difference in variance at the earlier PI time points. All data were statistically compared using a 2-way ANOVA. **(E)** CTL mice revealed equally spaced electron densities, known as transverse bands (arrows), at the interface between the lateral loops of the myelin sheath and the axolemma. **(F)** In contrast, transverse bands were unevenly spaced and structurally disrupted (arrows) in the CST-cKO. For analysis, the fit of the two models (single variance/covariance matrix or group specific variance/covariance matrices) was compared using a likelihood ratio test. A-B Scale bars = 1µm. *$p<0.05$ ****$p<0.0001$. E-F Scale bars=0.5µm

A

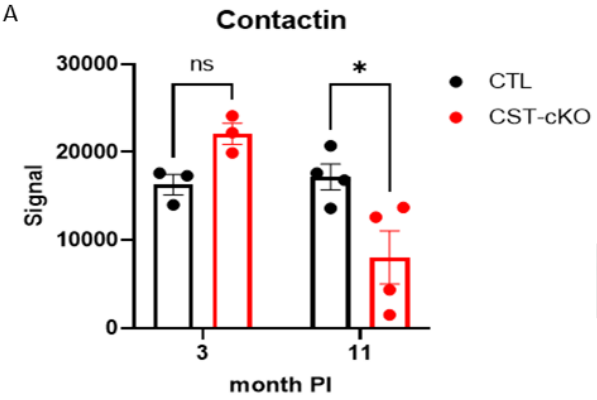
Contactin
30000
20000
10000
0
Signal
ns
*
3
11
month PI
CTL
CST-cKO

B

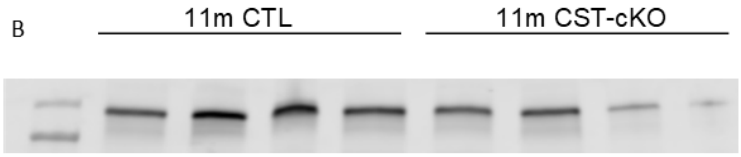
11m CTL
11m CST-cKO

C

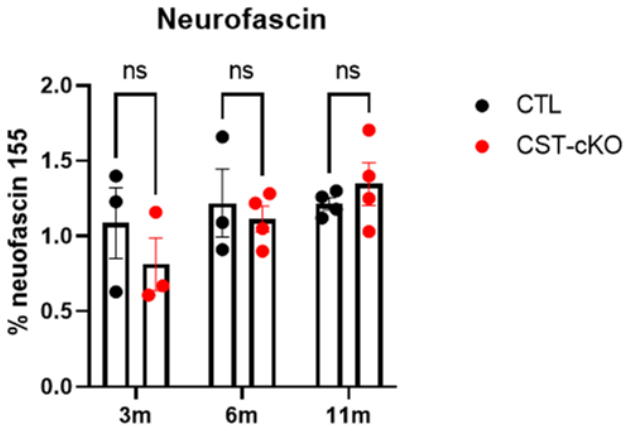
Neurofascin
2.0
1.5
1.0
0.5
0.0
% neuofascin 155
ns
ns
ns
3m
6m
11m
CTL
CST-cKO

Figure 2.8 Loss of neurofascin-contactin contact in 11m PI CST-cKO mice

(A) At 3m PI, there is no significance between the amount of contactin present after an immunoprecipitation with neurofascin between CTL and CST-cKO. However, at 11m PI, we see a significant loss of contactin in the CST-CKO **(B)** Image of the western blot probed for contactin after the neurofascin IP reaction **(C)** Demonstrates there is no significant difference in amount of neurofascin between any of the timepoints or genotypes

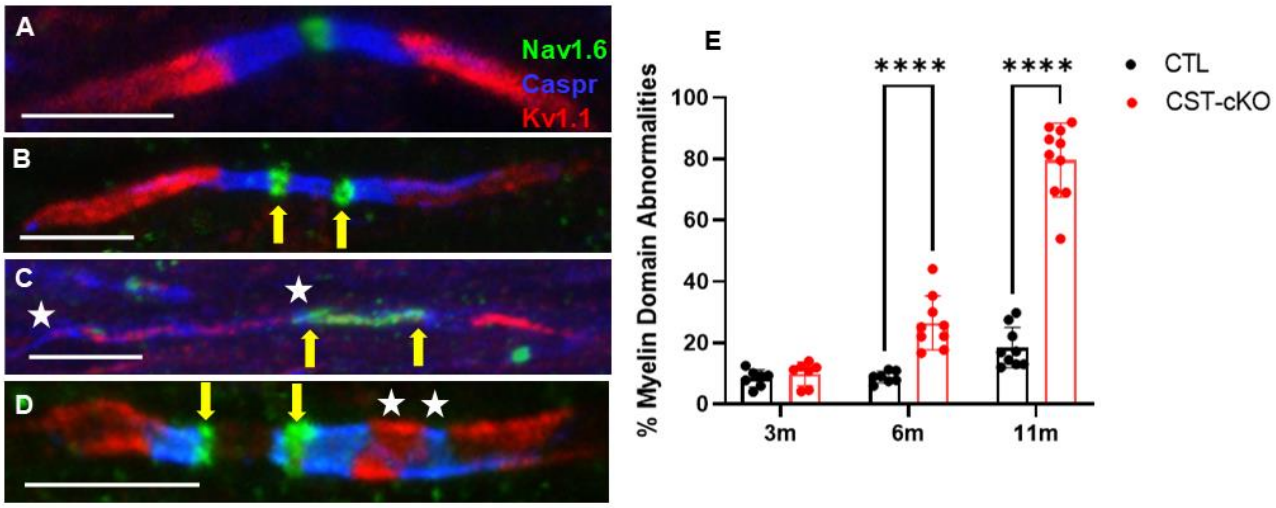
A
Nav1.6
Caspr
Kv1.1
B
C
D
E
% Myelin Domain Abnormalities
100
80
60
40
20
0
3m
6m
11m
****
****
CTL
CST-cKO

Figure 2.9. Mis-localization of axonal domain proteins following adult-onset sulfatide depletion. **(A)** An axon from a CTL mouse demonstrates proper ion channel and axonal domain protein organization in the corpus callosum with Nav1.6 (green) localized to the node of Ranvier; caspr (blue) localized to the paranode; and Kv1.1 (red) localized to the juxtaparanode. Common, but not exclusive pathologies, observed included **(B)** binodal Nav1.6 (green; yellow arrows); **(C)** elongated Nav1.6 (green; yellow arrows indicating bounds of Nav1.6 distribution); and elongated caspr (blue) with Kv1.1 (red) intermixed (white stars flank region of intermixing). **(D)** A combination of several pathologies such as binodal Nav1.6 (yellow arrows) and Kv1.1 and caspr intermixing (white stars) was also observed. **(E)** Quantification of protein organization revealed preservation of protein domain at 3-months PI but a significant loss of axonal domain organization at 6- and 11-month PI. Data are presented as mean ± standard error and analyzed using a 2-way ANOVA; **** $p<0.0001$. Scale bars = 5µm

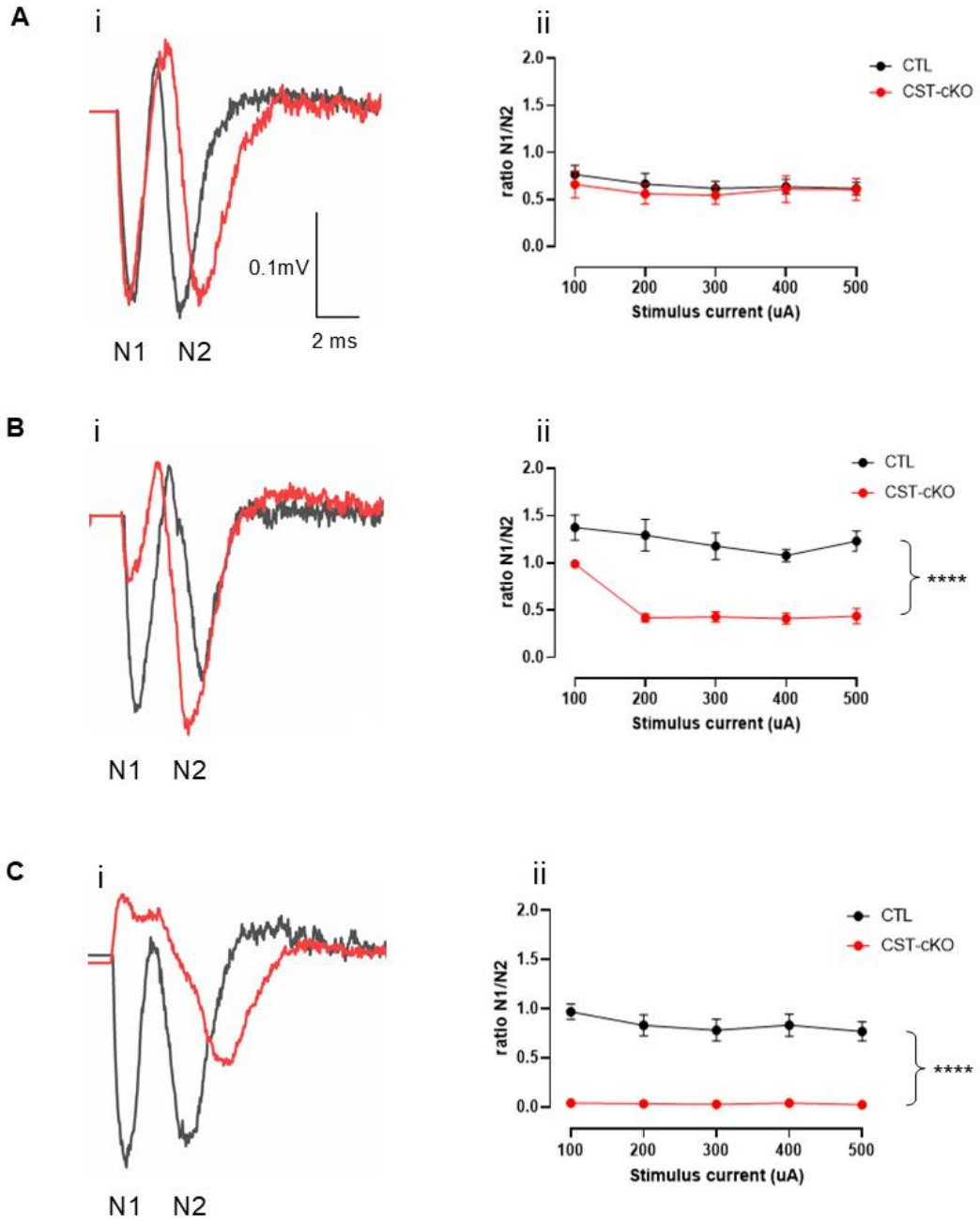
A
i
ii
0.1mV
2 ms
N1
N2
ratio N1/N2
Stimulus current (uA)
CTL
CST-cKO
B
C
****

Figure 2.10. Decrease of N1 peak following adult-onset sulfatide depletion. **(Ai)** Compound action potential (CAP) recordings demonstrate comparable and robust N1 and N2 peaks between the CTL and CST-cKO mice 3-months PI. **(Aii)** Quantification of the ratio of N1/N2 from ascending stimulus currents in the CTL and CST-cKO mouse at 3-months PI shows no significant difference between genotypes. **(Bi)** By 6-months PI CST-cKO mice present with a reduced N1 peak and **(Bii)** a significant reduction in the N1/N2 ratio between cKO and CTL mice. **(Ci)** By 11-months PI, N1 peaks were not observed in the CST cKO mice but N2 peaks were spared. **(Cii)** The loss of the N1 peak resulted in further separation of N1/N2 ratios between CTL and CST-cKO mice at 11-months PI with the ratios being zero due to loss of N1 peak. Analyzed using a 2-way ANOVA. ****$p<0.0001$

Sample size breakdown per timepoint

Timepoint	Genotype	Sex	EM	IHC	EP
3	CTL	Female	3	3	3
		Male	3	4	4
	CST-cKO	Female	3	3	3
		Male	3	4	3
6	CTL	Female	3	3	4
		Male	3	4	3
	CST-cKO	Female	3	3	4
		Male	3	6	5
11	CTL	Female	3	3	4
		Male	3	4	3
	CST-cKO	Female	3	4	3
		Male	4	7	5

EM: Electron Microscopy
IHC: Immunohistochemistry
EP: Electrophysiology

CHAPTER THREE

Compromised myelin and axonal molecular organization following adult-onset sulfatide depletion

Dustin et al. (accepted pending minor revisions) *Biomedicines*

3.1 Abstract

3-O-sulfogalactosylceramide, or sulfatide, is a microdomain-associated glycosphingolipid reduced in the normal appearing white matter (NAWM) of Multiple Sclerosis (MS), indicating that the loss of this lipid is specific and not a consequence of demyelination. Using a mouse model that is constitutively depleted of sulfatide, we previously presented data that revealed essential functions of sulfatide during development such as the requirement of this lipid for the establishment and maintenance of myelin and axonal integrity. Here, using an adult-onset depletion model of sulfatide, which is more reminiscent of adult-onset disease, we observe mis-localized ion channels, variation in nodal length, and axon degeneration with myelin sparing and aim to understand the molecular mechanisms regulating protein membrane organization at the level of the spinal cord. Using an in-situ extraction procedure, we previous showed that embryonic inhibition of sulfatide production resulted in increased extraction susceptibility of neurofascin 155 high and myelin-associated glycoprotein. Here, we employ a similar approach to elucidate the molecular mechanisms of sulfatide-dependent myelin membrane stability following adult-onset lipid depletion. Our study shows that myelin proteins are maintained in the sheath through sulfatide-dependent and -independent mechanisms and that the mechanisms employed by myelin proteins may change dependent on the stage of development and maturation.

3.2 Introduction

The canonical function of the myelin sheath is to insulate axons to propagate a rapid signal through saltatory conduction. However, the myelin sheath is not merely a static insulator, but a dynamic membrane that provides axonal support through glia-neuron communication (Y. Lee et al., 2012; Saab & Nave, 2017; Stadelmann et al., 2019). Its insulatory properties are derived both from specific domains of the myelin sheath and its biochemical composition (Moore et al., 1978; Hayashi et al., 2013b; Chiu et al., 1999; Kister & Kister, 2022). The myelin sheath is unique in that it is composed of 70% lipids and 30% proteins, whereas most plasma membranes have an equal ratio of lipids to proteins (Morell & Quarles, 1999). Of those lipids, glycosphingolipids constitute about 20% of total lipids, the majority being galactosylceramide and sulfatide (O'Brien & Sampson, 1965; Grassi et al., 2016). These lipids create membrane stability due to the presence of long saturated acyl chains, which allow for tight molecular packing, and a high degree of hydroxylation, which enables hydrogen bond formation facilitating even tighter lipid clustering. The combination of this tight packing and rigid carbon chain structure allows for efficient conduction of the electrical signal down the axon (Bazan et al., 2002; Quarles et al., 2006; Zöller et al., 2008; J. L. Dupree & Pomicter, 2010).

The stereotypical region of the myelin sheath is the internodal domain that presents with tightly compacted concentric wraps of the myelin membranes. In addition to the internode, the myelin sheath can be further divided into separate domains that each have distinct functions and biochemical composition. Similar to the internode, the juxtaparanode also presents with compacted myelin. The juxtaparanode is positioned at the lateral most extent of the internode and concentrates the adhesion molecule transient axonal glycoprotein-1 (TAG-1) (Traka et al., 2002, 2003). The axonal juxtaparanodal membrane clusters TAG-1 and Caspr2, facilitating homophilic and heterophilic binding with myelin TAG-1 to tether the myelin sheath to the axolemma (Tsiotra et al., 1996; Kunz et al., 2002; Traka et al., 2002). In addition to TAG-1 and Caspr2, voltage gated potassium channels, which play a role in repolarizing the axon membrane (Poliak et al., 2003; Hivert et al., 2016), also cluster in the juxtaparanode. The sheath also establishes and maintains regions of noncompacted myelin including the paranode and the cytoplasmic channels. The paranode is positioned between the node of Ranvier and the juxtaparanode and is demarcated by the presence of the cytoplasmic sacs that align along the axonal membrane (Peters et al., 1992). The basal membrane of these loops clusters neurofascin155

(Nfasc155) while the axonal paranode clusters Caspr1 and contactin, which form a heterodimer that binds the myelin specific isoform of neurofascin to form the paranodal junctional complexes that are partially indicated by transverse bands (Tait et al., 2000; Chang et al., 2014; Rosenbluth et al., 2012; Faivre-Sarrailh, 2020). The cytoplasmic channels include the inner tongue, which is the leading edge of the myelin sheath, the outer tongue, which is the trailing edge of the myelinating membrane and is connected to the oligodendrocyte cell body, and these cytoplasmic channels run through the compact myelin (Rhodes et al., 1997; Hivert et al., 2016).

The specific mechanisms that regulate the trafficking, sorting and retention of these proteins to their unique destinations of these various domains are not completely defined. Previous work from our group has shown that the myelin sphingolipids, galactosylceramide and its sulfated derivative sulfatide, play a role in these processes (A. D. Pomicter et al., 2010b; A. Pomicter et al., 2013) and in the absence of these lipids, these domains, particularly the noncompacted myelin domains, are compromised (J. L. Dupree, Coetzee, Suzuki, et al., 1998; J. L. Dupree et al., 1999; Marcus et al., 2006). One plausible explanation for how sphingolipids regulate domain establishment and maintenance involves lipid ordered membrane domains known as microdomains (reviewed in (Bieberich, 2018). Microdomains are enriched in glycosphingolipids and have been implicated in a variety of cellular functions including signal transduction, intercellular adhesion and specific protein sequestering and sorting (Taylor et al., 2002; Schafer, 2004; T. Kim & Pfeiffer, 1999; Diaz-Rohrer et al., 2023; Grassi et al., 2020; Isik & Cizmecioglu, 2023) . Although microdomains may play a role in molecular sorting and ultimately in domain formation and maintenance, it is unclear how certain proteins are included while others are excluded. Our previous studies using the constitutive knock-out of sulfatide's synthesizing enzyme, ceramide sulfotransferase (CST), demonstrated that sulfatide, a prominent lipid component of myelin microdomains (Arvanitis et al., 2005) is required for stabilization of certain proteins, namely MAG and neurofascin 155 high, within the myelin sheath during development (A. Pomicter et al., 2013). Both neurofascin 155 and MAG are known myelin specific mediators of axon-glial communication (L. J. Yang et al., 1996; Charles et al., 2002b; Schnaar, 2010; Janssen, 2018), and have been shown to be prominent components of microdomains (Vinson et al., 2003; Schaeren-Wiemers et al., 2004).

The identification of these specific proteins is of interest since they have been shown to directly mediate axon-myelin interactions (L. J. Yang et al., 1996; Charles et al., 2002b; Schnaar, 2010; Janssen, 2018). We hypothesized that these proteins associate with sulfatide in microdomains via post translational lipid modifications including the addition of long saturated fatty chains that form hydrophobic associations with the acyl chain of sulfatide (Grassi et al., 2016).

However, this previous work utilized a constitutive knockout of CST, ablating sulfatide production in all tissues embryonically (Honke et al., 2002; A. Pomicter et al., 2013). To determine if the adult sheath utilizes similar mechanisms to maintain myelin stability, here, we exploit the LoxP/creERT system combined with cell-type specific cre expression to deplete sulfatide specifically in oligodendrocytes in adulthood (Palavicini et al., 2022; Qiu et al., 2021). Our studies demonstrate that disruption of the myelin membrane, independent of overt changes in myelin ultrastructure, leads to significant axonal pathology indicating that correct myelin composition is essential for proper neuron-glia communication.

The importance of these findings is accentuated by the fact that sulfatide is significantly reduced in the earliest stages of MS (Yahara et al., 1982; Marbois et al., 2000). Interestingly, in both MS (Howell et al., 2006b; Gallego-Delgado et al., 2020a) and in the adult-onset sulfatide depleted mouse, axonal protein domain organization is disrupted in the NAWM. Since the commonality between the human disease and the adult-onset sulfatide depleted mouse is the early loss of the lipid, we propose that loss of axolemmal organization is a downstream consequence of sulfatide depletion. We further propose that sulfatide depletion is responsible for axolemmal disorganization by the loss of stability of specific myelin proteins that mediate axon-glial adhesion and interaction. Therefore, we propose that the loss of sulfatide, from the adult myelin sheath, will also result in destabilization of specific myelin proteins that are microdomain associated and that are known to regulate axon-myelin interactions.

3.3 Materials and Method

Animal model

Using CRISPR technology, we generated a cerebroside sulfotransferase (CST) floxed mouse (Applied StemCell, Inc, Milpitas, CA; (Palavicini et al., 2022; Qiu et al., 2021). The CST floxed mouse was mated with a mouse expressing Proteolipid Protein (PLP)-cre conjugated to a mutated estrogen receptor (ERT) (Doerflinger et al., 2003) (Jax Labs; stock # 005975) to generate $CST^{fl/fl}$ /PLP-$creERT^{+/-}$ mice. To induce cre translocation into the nucleus to promote CST gene ablation, 10 weeks old $CST^{fl/fl}$ /PLP-$creERT^{+/-}$ mice (referred to CST-cKO) were intraperitoneally injected with 60mg/kg body weight of tamoxifen (Millipore/Sigma; St. Louis, MO; cat# T5648) for 4 consecutive days. $CST^{fl/fl}$ /PLP-$creERT^{-/-}$ mice, which were also injected with tamoxifen, were used as controls (CTLs). Since sulfatide requires ~3 months to turnover (Norton & Cammer, 1984), we analyzed the mice at 3, 6, and 11 months post tamoxifen injection (PI).

Polymerase Chain Reaction and Real-Time Polymerase Chain Reaction

DNA and RNA were extracted from the brains of 6-weeks post tamoxifen injected mice using Qiagen DNA/RNA Mini extraction kit (Qiagen, Germantown, MD, cat# 80204) according to the manufacturer's instructions. Briefly, mice were deeply anesthetized using 0.016 mL/gm body weight of a 2.5% solution of avertin (2, 2, 2 tribromoethanol; Millipore/Sigma; St. Louis, MO; cat#T48402) in 0.9% sodium chloride (Millipore/Sigma, St. Louis, MO; cat# S9888) and transcardially perfused with ice-cold saline. The cervical region of the spinal cord was harvested, snap-frozen in liquid nitrogen and stored at -80C until DNA and RNA isolation. DNA fragments spanning genomic target sites were amplified by PCR using the following primers:

Gal3st1 Forward (5'- GATTGTAGCCTTCCGTATGAACCG -3')
Gal3st1 Reverse 1 (5'- CGAACTCAACTCAAAGAGAGCAGG -3') and
Gal3st1 Reverse 2 (5'- TAATCTCTGCTCTAACCTGGTCGC -3').

After RNA isolation, contaminating DNA was eliminated through treatment with Ambion DNase I (Invitrogen Life Technologies, Grand Island, NY; cat# AM2222). Omniscript Reverse Transcription Supermix (BioRad, Hercules, CA; cat# 205113) was used to create cDNA from the isolated RNA (150µL/sample). Quantitative RT-

PCR was performed with a CFX96 (BioRad, Hercules, CA) RT-PCR detection system using 1µL of cDNA, SsoFast Evagreen Supermix (BioRad; cat# 1725201), and the following primers:

Gal3st1 Forward (5'- GCAGCACACTGCTCAACATC -3')

Gal3st1 Reverse (5'- ACCAGGCTTCGTGCAAAGTA -3')

Cyclophilin A Forward (5'- CTAGAGGGCATGGATGTGGT -3')

Cyclophilin A Reverse (5'- TGACATCCTTCAGTGGCTTG-3')

Phosphoglycerate kinase 1 Forward (5'- ATGCAAAGACTGGCCAAGCTA -3')

Phosphoglycerate kinase 1 Reverse (5'-AGCCACAGCCTCAGCATATTT-3')

Cycling parameters were: one cycle at 95°C (5 min), 39 cycles of 95°C (5s) and 56°C (5s) followed by a melt curve measurement consisting of 5s 0.5°C incremental increases from 65°C to 95°C. The fold changes in expression of the Cst gene in corpus callosum samples were calculated using the formula RQ 5 22DDCt, using Cyclophilin and Phosphoglycerate kinase 1. For statistical analysis, a Student's t-test was performed using GraphPad Prism software version 9.4.1 for Windows.

Mass Spectrometry

Multidimensional mass spectrometry-based shotgun lipidomics analysis was performed as described (Palavicini et al., 2022; Qiu et al., 2021). Briefly, mice were injected with Avertin and perfused with ice cold saline. The cervical region of the spinal cord was dissected, and flash frozen in liquid nitrogen. Tissue was homogenized and protein concentrations was determined using Bio-Rad protein assay (Bio-Rad, Hercules, CA, USA; cat# 5000201). In the presence of internal standards, lipids were extracted following a modified procedure of Bligh and Dyer (Bligh & Dyer, 1959; Qiu et al., 2021). Lipids were measured using a triple-quadrupole mass spectrometer (TSQ Altis, Thermo Fisher Scientific, Waltham, MA, USA) equipped with a Nanomate device (Advion Ithaca, NY, USA) and Xcalibur system. Data were processed using ion peak selection, baseline correction, data transfer, peak intensity comparison, ^{13}C deisotoping. Data were analyzed using a custom-programmed Microsoft Excel macro.

Electron microscopy

Mice were survived for 3, 6, and 11 months PI and cervical spinal cords were prepared for standard transmission electron microscopic analyses as previously described (J. L. Dupree, Coetzee, Blight, et al., 1998b; Marcus et al., 2006). Briefly, mice were transcardially perfused with 0.1M Millonigs buffer containing 4% paraformaldehyde and 5% glutaraldehyde and post fixed for 2 weeks. Cervical spinal cords (1mm specimens) were post fixed in 1% osmium tetroxide (Electron Microscopy Sciences, Fort Washington, PA; cat# 19150), dehydrated in ethanol and embedded in PolyBed resin (PolySciences, Warrington, PA; cat# 00552-500). Tissues were sectioned at 70nm, stained with uranyl acetate and lead citrate (Millipore/Sigma, St. Louis, MO; cat# 15326) and imaged using a JEOL JEM1400 PLUS transmission electron microscope (JEOL USA, Inc, Boston, MA) equipped with a Gatan One View digital camera (Gatan, Pleasanton, CA). Transversely sectioned tissues were used for quantifying percent of unmyelinated axons, g ratios and myelin and axonal integrity. Longitudinally sectioned tissues were used to assess node length and presence of transverse bands. For percent of unmyelinated axons, the total number of axons, greater than 0.3µm in diameter (Mason et al., 2001) were determined from a minimum of 10 electron micrographs collected at 5000x. The number of axons that lacked at least a single complete ensheathment of an oligodendrocyte process, defined as unmyelinated, was determined. The percent of unmyelinated axons, calculated by dividing the number of unmyelinated axons by the total number of axons, was determined per mouse and a one-way ANOVA was conducted with each mouse as an “n”. For g ratio analysis, the same electron micrographs were used. Avoiding areas of fixation artifact, myelin pathologies and inner and outer myelin tongues, the shortest and longest diameter for each myelinated axon was measured and the widths of the thinnest and thickest regions of the myelin sheath were recorded. Total fiber diameter was calculated by adding the average axon diameter to the two myelin thickness measurements. To calculate the g ratio, the axon diameter was divided by total fiber dimeter. A minimum of 100 myelinated axons per mouse was used for g ratio calculation. The average g ratio per mouse constituted an “n” for statistical comparison and used for analysis. In addition, all g ratios were plotted, individually per treatment group and per time point, to compare the relative subpopulations of myelinated axons with standard (defined as g ratios between 0.70 and 0.85) or very thin (>0.85) (G. J. Duncan et al., 2021) myelin sheaths.

Using all 10 electron micrographs collected in the transverse orientation, totaling at least 600 axons, the extent of myelin and axon pathology was quantified as previously described (J. L. Dupree & Feinstein, 2018). Briefly, the percent of myelinated axons that presented with specific myelin and axonal pathologies (vacuolar degeneration of the myelin sheath; redundant myelin profiles, non-compacted myelin sheaths and axonal degeneration) was calculated for each mouse and the total percent of the combined pathologies was determined per mouse.

Transverse band integrity was qualitatively assessed using longitudinally sectioned samples. A minimum of 10 nodes of Ranvier with accompanying paranodes per mouse was used for this analysis. Only the middle two thirds of the paranode was used for transverse band analysis since transverse bands are frequently, and normally, not formed between the nodal-most and juxtaparanodal-most lateral loops and the axolemma (Allt, 1969). Nodal length was determined by measuring the distance between the most nodally positioned lateral loops of adjacent myelin segments as previously described (Marcus et al., 2006). For statistical testing of the nodal length, (performed by Dr. Leroy Thacker of the VCU Biostatistics Department), the fit of the two models (single variance/covariance matrix or group specific variance/covariance matrices) was compared using a likelihood ratio test (LRT). For all analyses an $\alpha = 0.05$ was used for statistical significance and SAS v9.4 was used.

For all ultrastructural analyses, 4-7 mice per treatment and time point were used and all analyses were limited to the ventral columns of the cervical spinal cord. Quantitative analysis for g ratios and node length was conducted using Image J. Analyses were performed using Student's t-test when comparing between treatments within a single time point or a 2-way ANOVA when comparing genotypes across time. All graphing and statistical analysis were performed using GraphPad Prism version 9.4.1 for Windows (GraphPad Software, San Diego, CA).

Immunohistochemistry:

Mice 3, 6, and 11 months PI were prepared and imaged as previously described (Clark et al., 2016; Benusa et al., 2017). Briefly, mice were perfused as above with the exception that perfusion fixative did not contain glutaraldehyde. Cervical spinal cords were cryopreserved in 30% sucrose in 1X phosphate buffered saline (PBS), frozen in Tissue Tek Optimal Cutting Temperature media (Clark et al., 2016), sectioned at 40 µm and triple immunolabeled with antibodies directed against voltage gated sodium channel type 1.6 (Nav1.6; 1:250, mouse monoclonal IgG1, Antibodies Inc., Davis CA; cat# 75-026), Caspr1 (1:500, rabbit polyclonal, Abcam cat# ab34151) and voltage gated potassium channel 1.1 (1:750; (Kv1.1; mouse monoclonal IgG2b, Antibodies Inc., cat# 75-105). Sections were imaged using a Zeiss LSM 880 laser scanning confocal microscope. Images were collected using a 63X oil-immersion objective (N.A. of 0.55) employing Nyquist sampling, with digital zoom of 2, pin hole of 1 Airy unit, optical slice thickness of 0.21 µm and line scan average of 4. X, Y, and Z dimensions were 67µm × 67µm × 3µm, respectively. 6-9 mice per genotype per time point were used. With a blinded approach, Image J analysis software was used to assess nodal/paranodal/juxtaparanodal abnormalities by marking overlapping fluorescent labels from maximum intensity projection images. All graphing and statistical analysis were performed using GraphPad Prism version 9.4.1 for Windows (GraphPad Software, San Diego, CA).

In situ detergent extraction

In situ protein extraction was performed as previously described with some modification (A. Pomicter et al., 2013). Briefly, cervical spinal cords from 3-, 6-, and 11-months PI mice were harvested, diced into small pieces, and incubated in extraction buffer consisting of 20 mM Tris-HCl (pH 8.0), 10 mM EDTA, 150 mM NaCl, and protease inhibitor cocktail (Millipore/Sigma, St. Louis, MO, cat# 539136) with or without Triton X-100 (1%; non-ionic) (Millipore/Sigma, St. Louis, MO, cat# X100-5ML) at 4C for two hours with constant gentle shaking. After two hours, tissue was removed from the extraction buffer and rinsed in 1XPBS. Optimal incubation time for detergent penetration was determined to be two hours as indicated by Pomicter et al. (2013). Tissue was homogenized in 200uL of 1% sodium dodecyl sulfate (SDS) (Millipore/Sigma, St. Louis, MO, cat# L3771) in PBS with 5 µl of protease inhibitor cocktail (Millipore/Sigma, St. Louis MO, cat# 539136) for one minute. Homogenates were aliquoted and stored at -80°C.

Western Blot analysis

For western blot analysis, tissue aliquots were thawed on ice and protein concentrations were determined with the Micro BCA Protein Assay kit (Thermo Scientific, Rockford, IL, cat# 23235). 2X Laemmeli Sample Buffer (Bio-Rad, Hercules, CA; cat#1610737) containing 5% β-mercaptoethanol (Millipore/Sigma, St. Louis, MO, cat# M6250) was added to aliquots at a 1:1 ratio. Samples were heated at 70C for five minutes. 30µg of protein was used per sample except for MBP where 10ug of protein was used. Samples were run on 4-20% tris\glycine gels (Bio-Rad, cat# 4561094, Hercules, CA) for 30 minutes at 70V followed by an additional 25 minutes at 150V. For separation of Neurofascin 155 high and low, proteins were run on 10% gels (Bio-Rad, Hercules, CA, cat# 4561034) for 30 minutes at 70V then 120 minutes at 150V as previously described (A. Pomicter et al., 2013; A. D. Pomicter et al., 2010b)The protein ladder used was Chameleon Duo pre-stained protein ladder (LI-COR, Lincoln, NE cat#928-60000). Samples were transferred to Immobilon-P transfer membrane (Millipore, St. Louis, MO, cat#IPVH00010) for one hour at 100V on ice. Membranes were rinsed briefly in 1X PBS with 0.1% Tween-20 (Millipore/Sigma, St. Louis, MO, cat#1379) (PBS-T) and stained for total protein with Revert 700 Total Protein Stain (Lincoln, NE, cat#926-11011). Total protein was visualized using an Odyssey Clx LICOR system (LI-COR, Lincoln, NE, cat#1928) with Image Studio software version 5.2 (LICOR Lincoln, NE) for normalization. Total protein was washed off with REVERT Reversal Solution (LICOR, Lincoln, NE, cat#629-11013) and blocked for one hour in 2.5% dry milk in PBS-T. The blot was briefly washed with PBS-T and incubated overnight at 4°C in Intercept Blocking Buffer with appropriate antibody (LICOR Lincoln, NE, cat#927-70001). The following day, the primary antibody was discarded and the blot was rinsed in PBS-T and incubated with secondary antibody for one hour at room temperature. After one-hour incubation in the appropriate secondary antibody, the blot was rinsed in PBS-T and western blot was visualized with Odyssey Clx LICOR system. Blots were analyzed using Image Studio software version 5.2.

Antibodies used for Western Blot analysis

The primary antibodies used for western blot analysis are as follows: pan anti-Neurofascin (1:500) (R&D Systems, Minneapolis, MN, cat#AF3235); anti-Myelin Associated Glycoprotein (MAG) (1:500) (Thermo

Scientific, Rockford, IL, cat#34-6200); anti-Myelin Basic Protein (MBP) (1:100) (Thermo Scientific, Rockford, IL, cat#386); anti-Cyclin Nucleotide Phosphodiesterase (CNP) (1:500) (Thermo Scientific, Rockford, IL, cat#836404); anti-Myelin Oligodendrocyte Glycoprotein (MOG) (1:500) (Millipore, St. Louis, MO, cat#MAB5680); anti-Glyceraldehyde 3-phosphate dehydrogenase (GAPDH) (1:10,000) (Millipore, St. Louis, MO, cat#MAB374); anti-contactin associated protein 1 (Caspr1) (1:500) (Abcam Cambridge, UK cat# ab34151). Secondaries from LICOR were diluted at 1:10,000 and are as follows: IRDye 680 anti-rabbit (cat# 926-68073); IRDye 800 anti-rat (cat# 925-32219); IRDye 680 anti-mouse (cat# 926-68070); and IRDye 800 anti-chicken (cat#926-32218).

3.4 Results

Confirmation of gene ablation and sulfatide depletion

Figure 3.1A represents our paradigm for injections and tissue collection timepoints. As described in Qiu et al. (2021), the CST floxed mouse was generated with loxP sites flanking the coding regions of the CST gene (Figure 3.1B). Here, a similar approach, as described by Qiu et al. (2021), was used to assess gene ablation and sulfatide reduction in the spinal cord. With tamoxifen injection, cre recombinase is induced to enter the nucleus resulting in excision of the floxed region of the gene. Figure 3.1C confirms successful CST gene ablation in the spinal cord, which is the region of the CNS used in the present study. Amplification of the ablated gene results in a PCR product of 432 bp and amplification of the unablated gene results in a PCR product of 246 bp. Since whole spinal cord was used as starting material, both ablated and unablated products are expected since non-oligodendrocytes would present non-ablated genes. The presence of the unablated product could also result from less than 100% efficient oligodendrocyte gene ablation. The use of whole spinal cord precludes quantifying oligodendrocyte ablation efficiency; however, the true indicator of success of the approach is the analysis of sulfatide levels. As shown in Figure 3.1D, mass spectrometric analyses reveal no sulfatide reduction by 3 months PI; however, there is ~50% reduction by 6 months PI and ~70% reduction by 11 months PI. These results are similar to the previously reported lipid reduction in the brain (Qiu et al., 2021) and this significant and consistent reduction of sulfatide confirms that the CST floxed mouse is a viable model for analyzing adult-onset depletion of sulfatide in the spinal cord.

Myelin thinning and axon ultrastructural pathology

To quantify the consequence of adult onset sulfatide depletion on myelin structure, we initially determined the percent of unmyelinated axons in the ventral column of the cervical spinal cord of CST-cKO and CTL mice 3-, 6- and 11-months PI (n= 4-6 and a minimum of 650 axons was quantified per animal). No difference in the percent of unmyelinated axons was observed at any of the survival time points (3m CTL = 7.9 ± 1.2 versus CST-cKO = 6.6 ± 0.8; p= 0.903 6m CTL = 5.8 ± 0.7 versus CST-cKO = 9.0 ± 0.8; p=0.316; 11m CTL = 6.5 ± 1.0 versus CST-cKO = 10.3 ± 2.1; p= 0.16; Figure 3.2G). We have previously reported that ~7% of the axons in the ventral column of the cervical spinal cord of c57black6/J wild type mice are unmyelinated (Marcus et al., 2006). Therefore, these counts are consistent with previous analysis.

Myelinated axons from the spinal cords of the CST-cKO mice presented with no difference in myelin thickness, as quantified by g ratios at 3 months PI (n=4,4 for CTL and CST-cKO respectively, a minimum of 108 axons per animal) (CTL = 0.779 ± 0.003 vs CST-cKO = 0.770 ± 0.011; p=0.67; Figure 3.2 A&B) and 6 months PI (n=4,5 for CTL and CST-cKO respectively, a minimum of 110 axons per animal) (CTL = 0.774 ± 0.003 vs CST-cKO = 0.790 ± 0.005; p = 0.22; Figure 3.2C&D). However, by 11 months PI, a modest but significant increase was observed in g ratios (thinner myelin) (n=4,5 for CTL and CST-cKO respectively, a minimum of 103 axons per animal) (CTL = 0.763 ± 0.006 vs CST-cKO = 0.804 ± 0.006; p=0.002; Figure 3.2E&F). Although most myelinated axons revealed myelin thickness in the normal range, based on axon caliber (g ratios between 0.70 and 0.85), a subset of the axons in the 11 months, PI CST-cKO mice, presented with abnormally thin myelin sheaths (g ratios >0.85) (I. D. Duncan et al., 2018). Axons with very thin myelin sheaths are presented in Figure 3.2F (inset) and the prevalence of axons with extremely thin myelin sheaths is indicated by the scatter plot in Figure 3.2H. Next, to analyze the integrity of myelinated axons, we quantified frequency of myelin non-compaction, vacuolar degeneration, redundant myelin, as well as axonal degeneration. At 3 months PI, there was no difference in integrity of the myelinated axons between the sulfatide deficient and control mice (CTL = 3.6% ± 1.4%; versus CST-cKO = 3.8% ±1.3%; p = 0.99). By 6 months PI there was an apparent progressive increase in compromised integrity (CTL = 3.2% ± 0.6%; versus CST-cKO = 9.7% ± 2.8%; p = 0.21) that

reached significance by 11 months PI (CTL = 3.9% ± 0.9%; versus CST-cKO= 14.7% ± 3.4%; n = 6; p = 0.01) (Figure 3.3B). Interestingly, when we graphed these individual pathologies, we did not see a significant difference in myelin non-compaction nor vacuolar degeneration, but we did see a significant increase in redundant myelin (Figure 3.3E) at 11m PI as well as axonal degeneration both at 6- and 11-months PI (Figure 3.3F). These data indicate that axonal pathology occurs independent of myelin loss with possible demyelination/remyelination occurring at 11m PI. Although it is not possible to definitively state that demyelination/remyelination has occurred, the presence of very thin myelin sheaths (g ratios >0.85) provides strong supportive evidence of remyelination (Figure 3.2F inset) (I. D. Duncan et al., 2018). Demyelination followed by remyelination also provides an explanation for the overall increase in g ratios at 11 months PI.

Compromised nodal structure

Since the constitutive CST KO mice presented with altered node/paranode organization, (Marcus et al., 2006) we next analyzed these domains in the CST-cKO mice. In contrast to our findings in the constitutive CST KO mice, we did not observe everted or disorganized lateral loops in the paranode at any of the time points analyzed. Although not observed in the mice 3m PI, qualitative assessment revealed frequent disruption of transverse bands in the periaxonal space of 6m and 11m PI mice (Figure 3.4B). However, we observed a variaiton in nodal length, having both longer (Figure 3.4D) and shorter nodes. We analyzed the length of the nodal gap (n=4-6, minimum of 10 nodes per animal). At 3m PI, the nodal length was similar between the treatment groups (CTL = 1.20µm ± 0.33µm; nodes versus CST-cKO = 1.08µm ± 0.34µm; p = 0.74). By 6m and 11m PI, we observed an increase in variability, with the CST-cKO having both longer and shorter nodes. The variance test statistically confirmed that 6 and 11 months PI mice had a significant difference in variability ($p<0.001$). (Figure 3.4E).

Compromised molecular organization of the nodal regions

Together, demyelination followed by remyelination, as indicated by g ratios greater than 0.85, disruption of transverse bands, axonal pathology, and variable nodal gap length are consistent with compromised axonal domain organization. To directly quantify domain organization, we employed triple immunohistochemical

labeling. As shown in Figure 3.5, Nav1.6, Caspr1, and Kv1.1 are restricted to their appropriate axonal domains, which are the node of Ranvier, the paranode and the juxtaparanode, respectively, in the CTL mice at all ages analyzed. While there was no significant difference at the 3m timepoint, (CTL = 11.6% ± 1.0%; versus CST-cKO = 10.3% ± 0.9%; p= 0.99), which is expected due to sulfatide's turnover rate, domain disruption was observed at 6m PI (CTL = 12.9% ± 1.2%; versus CST-cKO = 28.9% ± 4.5%; p=0.003) and 11m PI (CTL = 16.3% ± 1.4%; versus CST-cKO = 64.8% ± 7.4%; p<0.0001). We observed a significant and progressive deterioration of the protein domains highlighted by an invasion of Kv1.1 into paranode (Figure 3.5B), Nav1.6 elongation without evidence of either a downstream paranode or juxtaparanode, which is suggestive of heminode formation (Figure 3.5C), Caspr1 length elongation (Figure 3.5D), bi-nodal Nav1.6 and intermixing of Kv1.1 channels and Caspr1 (Figure 3.5E). This loss of protein domain organization is consistent with previous findings from the constitutive CST KO mice (Ishibashi et al., 2002b; A. Pomicter et al., 2013; A. D. Pomicter et al., 2010b); however, in contrast to the constitutive CST KO mice, the conditional CST KO mice developed with normal levels of sulfatide removing the possibility that impaired development was a causative factor in domain disorganization and deterioration.

Disruption of membrane stability

Based on these observations and consistent with our previous work (Pomicter et al., 2013), we hypothesized that the reduction of sulfatide in the myelin membrane resulted in less stable anchoring of specific proteins within the sheath. To test this hypothesis, we used our extraction method of exposing tissue to 1% Triton-X 100. To assess effectiveness of detergent penetration, we used GAPDH, a cytoplasmic protein, to compare tissue exposed to no triton versus tissue exposed to 1% Triton X-100 and found that GAPDH was consistently extracted at about 50% regardless of timepoints or genotype (Figure 3.6, Table 3.1A). Upon confirming the validity of this approach, we applied this method to our CTL and CST-cKO tissues and found no difference in the membrane stability of MBP, MOG, MAG, Nfasc155 low, or Caspr1 regardless of genotype or time PI (Figure 3.6, Table 3.1B-D, 1F, H). In contrast, Nfasc 155 high was significantly more susceptible to extraction in the CST-cKO mice at 6- and 11-months PI (72.9% protein remaining, p=0.0002 and 82.6% protein remaining, p=0.0024, respectively) (Table 3.1G) while CNP was more susceptible to extraction at 11 months PI

(71.5% protein remaining, p=0.0014) (Figure 3.6, Table 3.1E). See supplementary figure 3.1 for total protein levels of each representative blot.

3.5 Discussion

After observing a variation in nodal length, and mis-localized myelin domains, we employed a previously published biochemical approach (A. Pomicter et al., 2013; Rodi et al., 2014; Caritá et al., 2017) to begin to elucidate the mechanistic consequence of sulfatide loss on myelin sheath integrity. In our studies, we observe both ultrastructural and molecular differences between the constitutive CST KO and our adult-onset sulfatide deficient models. One possible explanation for this difference is a differential dependency on sulfatide for myelin integrity during development versus adulthood consistent with sulfatide playing a greater role in active myelination than in myelin maintenance. The constitutive CST KO mice exhibit a complete lack of sulfatide while the conditional CST KO mice maintain a low level of sulfatide, which may be sufficient to partially preserve myelin structure but not sufficient to maintain axonal health.

How does sulfatide regulate myelin stability?

Our initial ultrastructural studies demonstrated that adult-onset loss of sulfatide leads to axonal pathology with relative sparing of the myelin sheath. This is in contrast to the constitutive CST KO mice which showed an increase in g-ratios as early as 15 days of age (Marcus et al., 2006) as well as an increase in myelin pathologies such as vacuolar degeneration, redundant myelin, and progressive uncompacted myelin that was first observed at 1 month of age. In order to understand this disparity of sulfatide dependencies on the myelin sheath integrity during development versus adulthood, we utilized the triton extraction approach to perturb the membrane. The triton X-100 detergent extraction method selectively removes proteins and lipids from the membrane that are not securely tethered in place (Taylor et al., 2002; Caritá et al., 2017). This approach provides a biochemically based strategy to identify membrane proteins that are differentially bound within the membrane.

The extraction method showed both genotypic and age-related differences between the constitutive CST KO and the CST-cKO mice. The constitutive CST KO mice at 15 days of age showed an effect of triton extractions independent of genotype for MOG with the protein being equally susceptible to extraction in both the WT and constitutive CST KO mice (A. Pomicter et al., 2013). However, in adult mice MOG was not susceptible to extraction in either the CTL or the CST-cKO mice indicating the MOG anchorage within the adult sheath is regulated by different mechanisms compared to the adolescent sheath and that anchorage in the adult sheath is not dependent on sulfatide. Unlike MOG, MAG was susceptible to detergent extraction in the adolescent constitutive CST KO mice but extraction required sulfatide depletion (A. Pomicter et al., 2013). In contrast, MAG was not readily extracted from either the CTL or the adult-onset sulfatide depleted mice. This demonstrates that while MAG is sulfatide dependent for proper stabilization into the myelin sheath during development, MAG employs sulfatide independent means to stabilize in the adult myelin sheath. The extracellular domain structures such as Nogo-66 receptor (NgR2) on MAG allows it to have binding properties and as such may facilitate binding to gangliosides on the neuronal membrane (Y. Chen et al., 2006; Janssen, 2018). Perhaps in mature myelin sheaths, MAG is able to employ this mechanism to stabilize its incorporation within the myelin sheath.

In contrast to the constitutive CST KO mouse studies, we observed that CNP was significantly extracted at the 11m PI timepoint in the CST-cKO mice suggesting the employment of differential stabilization mechanisms in the developing and adult myelin sheath. CNP is commonly found in Triton X-100 insoluble microdomains (Hinman et al., 2008) and our studies confirmed CNP is resistant to extraction at the 3 and 6m timepoint in both CTL and CST-cKO. However, at the 11m timepoint we see a significant extraction of CNP in the CST-cKO mice. CNP is localized to the regions of non-compact myelin, particularly the leading edge, where sulfatide is enriched (Braun et al., 1988; Brunner et al., 1989; Maier et al., 2008; Trapp et al., 1988). CNP has post-translational modifications including iso-prenylation, and phosphorylation, (Agrawal et al., 1994; Braun et al., 1991), which may aid in its incorporation into and stability within microdomains, and also has associations with the underlying cytoskeleton (Dyer & Benjamins, 1989). CNP is an early oligodendrocyte marker and expressed in pre-myelinating oligodendrocytes (Knapp et al., 1988). During process extension, CNP

associates with microfilaments but in later stages, once membranes sheets have formed, CNP co-localization with microfilaments disappears (Wilson & Brophy, 1989). Perhaps once process extension is complete and the microfilaments depolymerize, CNP remains in the non-compact myelin via sulfatide associations. CNP's instability in the myelin sheath due to sulfatide loss may contribute to the observed pathologies. CNP is a part of the cytoplasmic channels, such as the leading edge, which are known to support axons (Snaidero et al., 2017). Perhaps disruption of the axo-glial complex at the level of CNP alters feedback mechanisms for the oligodendrocyte (Rasband et al., 2005) resulting in axolemmal disorganization. Further, CNP-null mice exhibit structurally intact myelin with subsequent axonal pathology (Lappe-Siefke et al., 2003; Edgar et al., 2009). So, while CNP is still being expressed and produced, perhaps its instability is sufficient to contribute to the axonal pathology presented by the CST-cKO animals.

Similar to the constitutive CST KO mice, our data show that Nfasc 155 high (H) is more susceptible to extraction in the CST-cKO mice than from the CTL mice. Our lab discovered that Nfasc 155 exists in two forms that we identified as Nfasc155 H and Nfasc 155 low (L) (A. D. Pomicter et al., 2010b). While it is unknown if there are differential functions or localizations of Nfasc 155 H and L, one hypothesis to how sulfatide may regulate Nfasc155H stability is through incorporation within microdomains. Microdomains are enriched in cholesterol and glycosphingolipids that contain long acyl carbon chains (Brown & Rose, 1992; Hirano et al., 2022). Neurofascin proteins contain post-translational modifications such as palmitoylation which facilitates recruitment into rafts. Studies which cleaved the palmitate residue of neurofascin using hydroxyl amine facilitated extraction of Nfasc155 while Caspr1 was unaffected (J. L. Dupree & Pomicter, 2010). Therefore, the position and post-translational modifications of Nfasc155H may form sulfatide-dependent associations within the membrane. Most recently however it was discovered that sulfatide is able to bind directly to Nfasc155 (McKie et al., 2023). Therefore, it is still possible removing the palmitate residue disrupts associations with other long chain glycosphingolipids, but is not the sole mechanism of sulfatide association to Nfasc155. This also explains why in the constitutive CST KO mouse and in our CST-cKO, we see an increase in extractability of Nfasc 155H, but not complete extraction. Nfasc 155H is likely still being anchored through weaker associations to other long chain glycosphingolipids, but is not completey extrcted due to loss of sulfatide. We

predict that this disorganization of Nfasc155H at the level of the paranode is responsible for the disruption of transverse bands. Adult-onset depletion of Nfasc155 resulted in the gradual loss of Caspr1 clustering (Pillai et al., 2009; Thaxton et al., 2011). Therefore, if Nfasc 155 H is not properly stabilized within the myelin sheath, it is unable to find its binding partner.Thus, leading to disruption of the axo-glial complex. These studies have clinical relevance to MS patients as our lab used the extraction method on plaque matter from MS tissue and found similarly, that Nfasc155H is more extracted than in control tissue (A. D. Pomicter et al., 2010b).

The axo-glial complex is composed of Neurofascin 155 on the myelin side and contactin and Caspr1 on the neuronal side (Charles et al., 2002b). These proteins are sorted to their determined location (Charles et al., 2002b; Mierzwa et al., 2010b; Susuki et al., 2013; Amor et al., 2014; Susuki et al., 2018) and bind to form complexes that appear as electron densities in the paranode. Potentially, as a consequence of protein mislocalization and compromised axo-glial junctional complexes, myelin sheath tethering is undermined, thus facilitating node length variability at both 6- and 11-month PI mice.

Accompanying the change in nodal length is the movement of the ion channels that are specifically clustered in the node and juxtaparanode. Using immunohistochemical labeling, we observed at both 6 and 11 months PI an increase in Caspr1 length (Fig. 3.5D), elongated and binodal (Fig 3.5C& E) sodium channel clusters, which is consistent with reduced stability, or presence, of Nfasc 155 within the myelin sheath that has been shown to bind to the contactin-Caspr1 complex and facilitate compromised ion channel clustering (Charles et al., 2002b; Pillai et al., 2009; Thaxton et al., 2011). Transverse bands, a component of the paranodal junctional complex, provide a mechanism to restrict sodium and potassium channels to their proper domain and disruption of the transverse bands may lead to the ion channel mis-localization we observed (Faivre-Sarrailh, 2020). This is in contrast to our ultrastructure data which did not show myelin pathology until 11m PI. Based on our findings, it would appear that ion channel mislocalization may be a more sensitive indicator of axonal health than either g-ratio measurements or myelin ultrastructural changes, which have been used for assessing myelin and axonal damage in MS patients (Yu et al., 2019). Perhaps loss of sulfatide seen in MS may contribute neurofascin cluster instability, which has been reported in early stages of demyelination (Howell et al., 2006b) and

transverse band disruption (Suzuki et al., 1969) in the human disease. Moreover, diffuse sodium channel distribution, which is accompanied by altered conduction activity, is sufficient to lead to axonal degeneration (Smith, 2007; Freeman et al., 2016). Together, our data provide evidence that molecular disorganization of the myelin sheath due to sulfatide loss is sufficient to lead to axonal pathology, and molecular disorganization is the first step before overt myelin pathology occurs. Therefore, in the case of MS, membrane disorganization through lipid dyshomeostasis may be occurring prior to clinical diagnosis thus defining the prodromic disease period of MS. If so, the loss of sulfatide may present a valuable early marker for disease diagnosis.

3.6 Conclusion

In conclusion, our studies provide evidence of sulfatide-dependent molecular mechanisms that regulate the stability of the axo-glial junction. Loss of sulfatide leads to instability of CNP and Nfasc155 H in the myelin sheath which is accompanied by subsequent axonal pathology with myelin sparing. These studies shed light on early pathogenesis in MS where sulfatide is reduced prior to demyelination consistent with the loss of sulfatide representing a prodromic period in MS before demyelination.

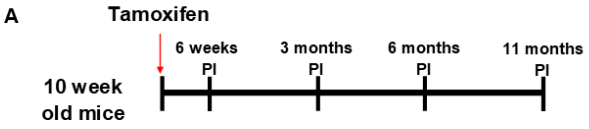
A
Tamoxifen
6 weeks
PI
3 months
PI
6 months
PI
11 months
PI
10 week
old mice

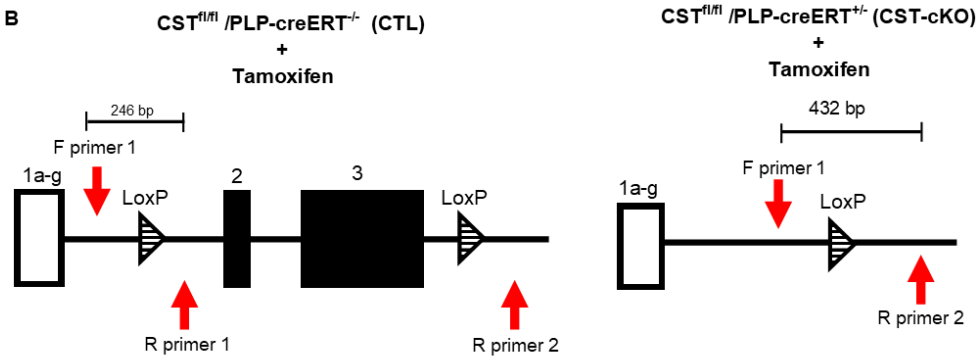
B
CST^fl/fl /PLP-creERT-/- (CTL)
+
Tamoxifen
246 bp
F primer 1
1a-g
LoxP
2
3
LoxP
R primer 1
R primer 2
CST^fl/fl /PLP-creERT+/- (CST-cKO)
+
Tamoxifen
432 bp
F primer 1
1a-g
LoxP
R primer 2

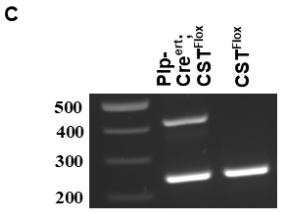
C
Plp-Cre ert, CST Flox
CST Flox
500
400
300
200

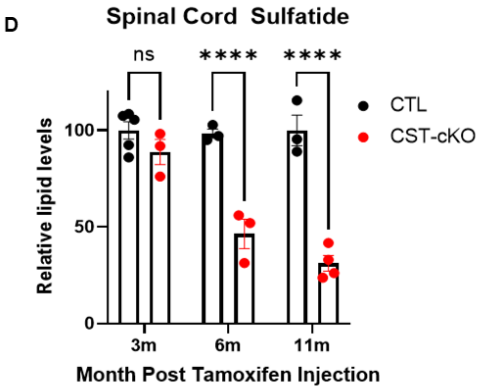
D
Spinal Cord Sulfatide
ns
****
****
CTL
CST-cKO
Relative lipid levels
100
50
0
3m
6m
11m
Month Post Tamoxifen Injection

Figure 3.1: Adult-onset sulfatide depletion model. (A) Schematic of the tamoxifen injection paradigm. Both CTL and CST-cKO littermates were aged to 10 weeks and given an intraperitoneal injection of 60mg/kg of tamoxifen for four consecutive days. Samples were collected at 6 weeks PI for ablation assessment; mice were analyzed at 3, 6 and 11 months PI **(B)** Schematic illustrating the non-coding (exon 1a-g; white rectangle) and coding (exons 2 and 3; black rectangles) of the *CST* gene with loxP sites (striped triangles) upstream and downstream of coding exons 2 and 3. Three primers (red arrows) were designed around the loxP sites to detect for genetic ablation: F (forward) primer 1, F (forward) primer 2, and R (reverse) primer 1. Tamoxifen was administered to both CST-cKO and CTL mice, resulting in *CST* gene recombination in CST-cKO mice (left) with gene sparing (right) in CTL mice. **(C)** PCR amplification of genomic DNA from the spinal cord of CTL and CST-cKO mice confirmed recombination in CST-cKO mutant mouse brains 6 weeks post tamoxifen injection. **(D)** Lipidomic analysis of total sulfatide in CST-cKO and CTL spinal cord presented no change in sulfatide levels by 3 months post injection but a significant sulfatide loss at 6- and 11-months post injection. C:**** $p<0.0001$ One-way ANOVA. All data are presented as mean ± standard error.

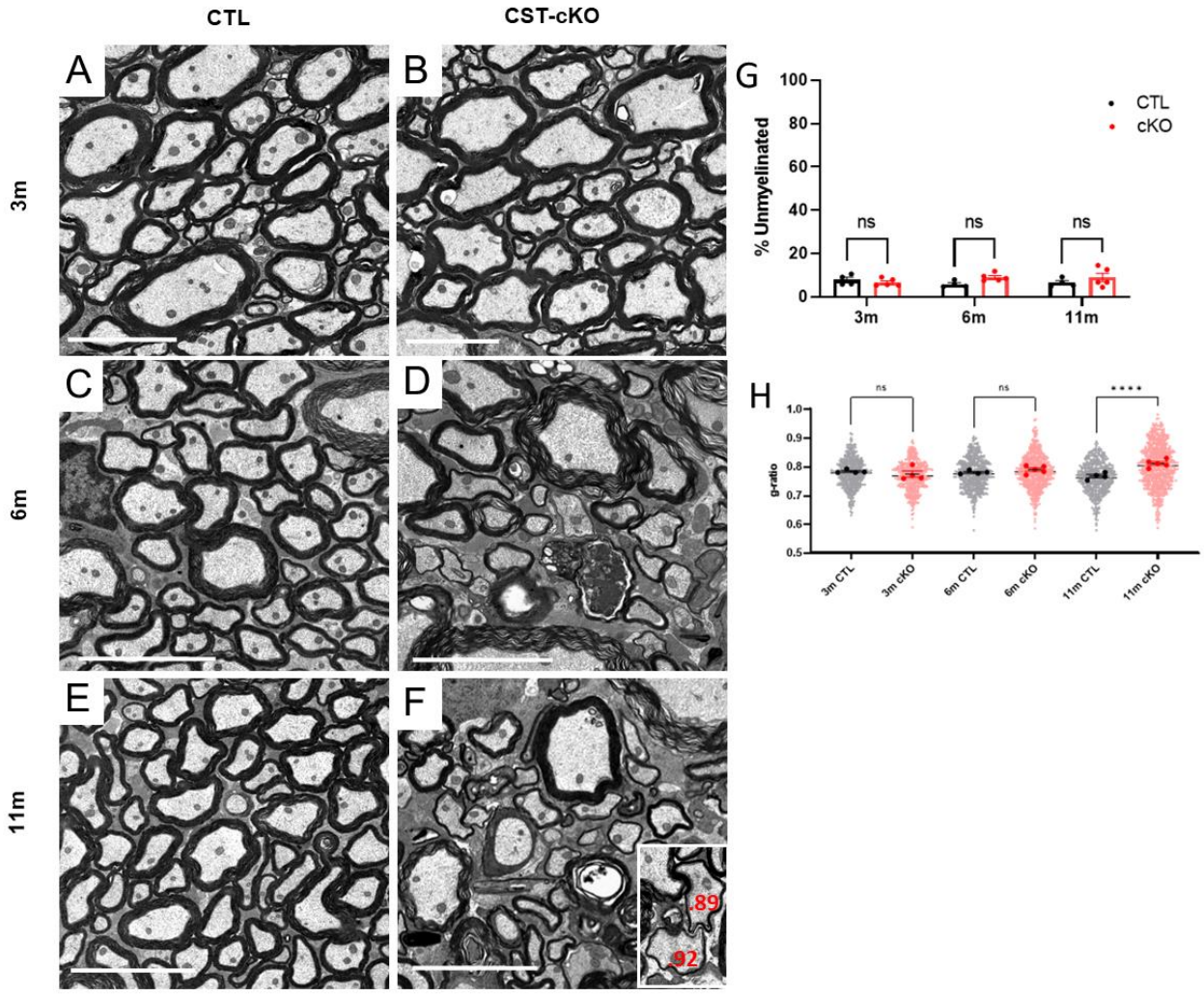
CTL
CST-cKO
3m
6m
11m
A
B
C
D
E
F
.89
.92
G
% Unmyelinated
CTL
cKO
ns
3m
6m
11m
H
g-ratio
****
3m CTL
3m cKO
6m CTL
6m cKO
11m CTL
11m cKO

Figure 3.2: Sulfatide depletion resulted in no change in the percent of unmyelinated axons and myelin thickness was only reduced at 11 months PI. (A) Cross section representative images from the ventral columns of the spinal cord from control (CTL; **A, C, E**) and CST-cKO (**B, D, F**) mice following 3- (**A** and **B**), 6- (**C** and **D**) and 11- (**E** and **F**) months post injection (PI). 3-, 6- and 11- months PI mice presented abundant myelinated axons with no difference in the percent of myelinated versus unmyelinated fibers **(G).** However, we observed an increase in g-ratios at 11m PI indicating demyelination/remyelination (**H**). Note the presence of axonal pathology in the 6m- and 11m-PI CST-cKO mice as well as evidence of demyelination/ remyelination at 11m PI (inset). Data are presented as mean ± standard error; data statistically compared by 2-way ANOVA analysis followed by a Tukey's post-hoc multiple comparison test. Scale bar=5μm

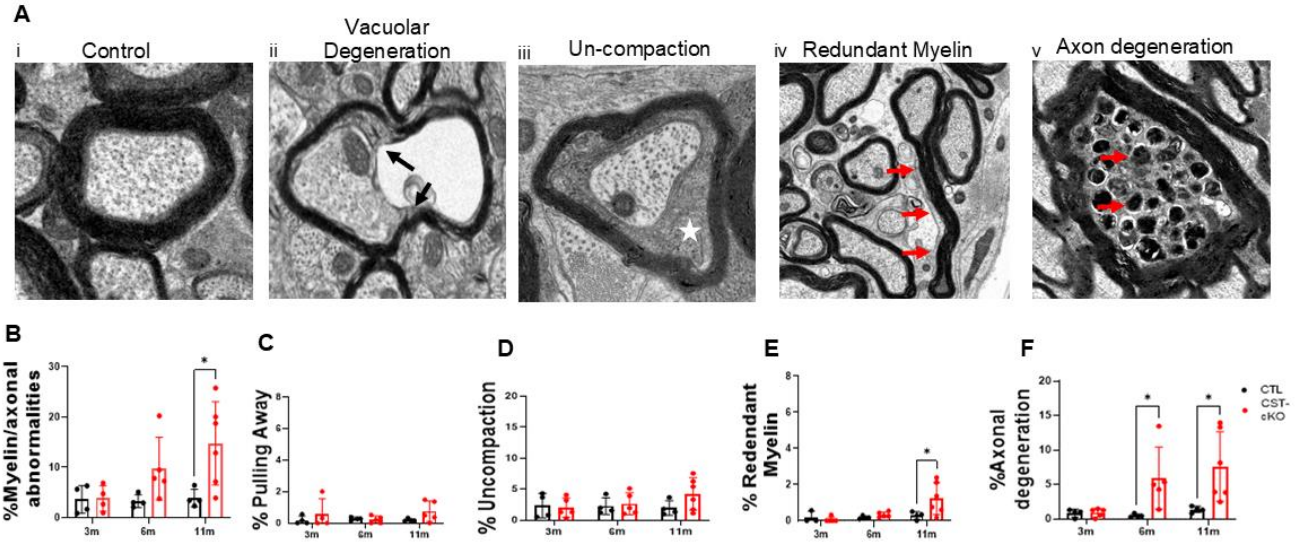
A
i Control
ii Vacuolar Degeneration
iii Un-compaction
iv Redundant Myelin
v Axon degeneration
B
%Myelin/axonal abnormalities
C
% Pulling Away
D
% Uncompaction
E
% Redendant Myelin
F
%Axonal degeneration
CTL
CST-cKO
3m
6m
11m

Figure 3.3. Quantification of myelin and axonal pathologies in the dorsal region of the cervical spinal in CST-cKO mice. (A) Representative image of a healthy axon with an intact, compacted myelin sheath and an appropriate array of neurofilament and microtubules (Ai). Representative images of various myelin and axonal abnormalities observed in the spinal cord of the CTL and CST-cKO mice: (from left to right): axon losing attachment to the myelin sheath (Aii; vacuolar degeneration; black arrows); presence of cytoplasm between compacted wraps of myelin (Aiii; un-compaction; white star); compact myelin out folding (Aiv; redundant myelin; red arrows) and organelle fluid filled swellings and cytoskeletal degeneration within the axon (Av; axon degeneration; red arrows). **(B)** Quantitative analysis combining all pathologies revealed a significant increase in myelin/axonal pathologies at 11m PI but not at 3- and 6- months PI. Separating out the individual pathologies revealed no significant difference in myelin ultrastructure except for redundant myelin **(C-E)**; **(F)** axonal degeneration was significantly increased in the 6m and 11m CST-cKO mice. All data were statistically compared using a 2-way ANOVA; * $p<0.05$.

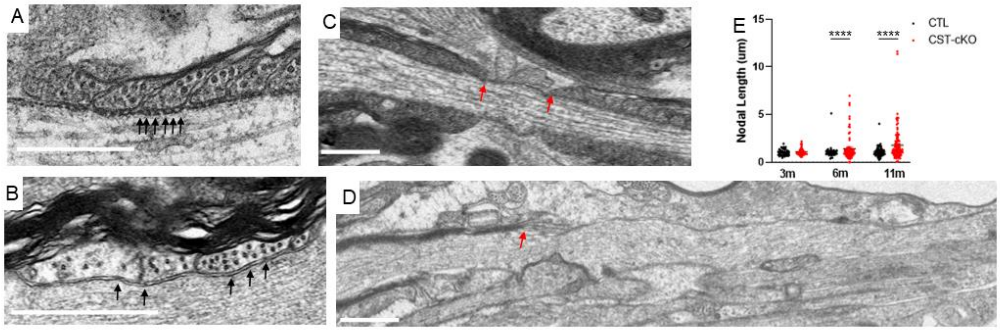
A
B
C
D
E
Nodal Length (um)
15
10
5
0
3m
6m
11m
****
****
CTL
CST-cKO

Figure 3.4. Increase in nodal length variability and loss of transverse bands following adult onset sulfatide depletion. (A) CTL mice revealed equally spaced electron densities (arrows), at the interface between the lateral loops of the myelin sheath and the axolemma. **(B)** In contrast, transverse bands were missing and structurally disrupted (note electron densities without clearly defined edges, arrows) in the periaxonal space of the CST-cKO mouse. **(C)** Normal ultrastructure of a node of Ranvier (indicated by red arrows) including nodal length (~1 micron) and flanking paranodal regions with lateral loops closely apposed to the axolemma. **(D)** CST-cKO mice revealed nodes of Ranvier with varying lengths including abnormally long nodal gaps. Heminodes, defined by a single paranode (indicated by red arrow) with no adjacent paranode in the plane of section for at last 3 microns, were also observed. (E) A significant difference was observed in length variability in the 6- and 11-months post tamoxifen injected CST-cKO mice. A-B Scale bars = 1μm. C-D Scale bars=0.5μm For analysis, the fit of the two models (single variance/covariance matrix or group specific variance/covariance matrices) was compared using a likelihood ratio test ****$p<0.0001$.

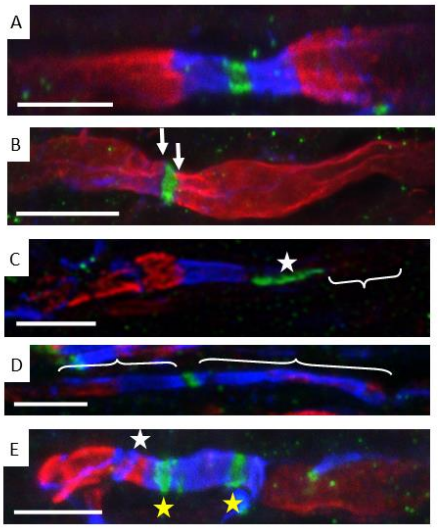
A
B
C
D
E

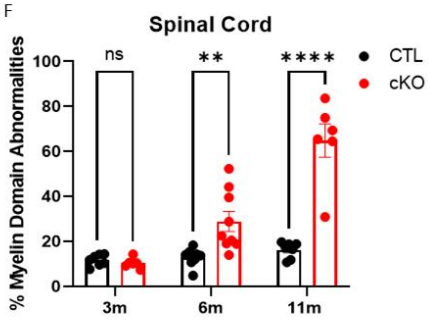
F
Spinal Cord
% Myelin Domain Abnormalities
100
80
60
40
20
0
ns
**
****
CTL
cKO
3m
6m
11m

Figure 3.5. Mis-localization of axonal domain proteins following adult-onset sulfatide depletion. **(A)** An axon from a CTL mouse demonstrates proper ion channel and axonal domain protein organization in the spinal cord with Nav1.6 (green) localized to the node of Ranvier; caspr1 (blue) localized to the paranode; and Kv1.1 (red) localized to the juxtaparanode. Common, but not exclusive, pathologies observed included **(B)** Kv1.1 invading the paranodal region, (white arrows); **(C)** elongated sodium channel domain (white star) and heminode (white bracket) (note: z-stack collected encompassed entirety of fluorescence and absent paranode was not the result of exclusion of z-stack); **(D)** elongated caspr1 localization (white brackets); **(E)** combination of several pathologies including binodal sodium channels clusters (yellow stars) and intermixing of Kv1.1 channels and caspr1. **(F)** Quantification of protein organization revealed preservation of protein domains at 3-months PI but a significant loss of axonal domain organization at 6- and 11-month PI. Data are presented as mean ± standard error and analyzed using a 2-way ANOVA; ** $p<0.01$ **** $p<0.0001$. Scale bars = 5μm

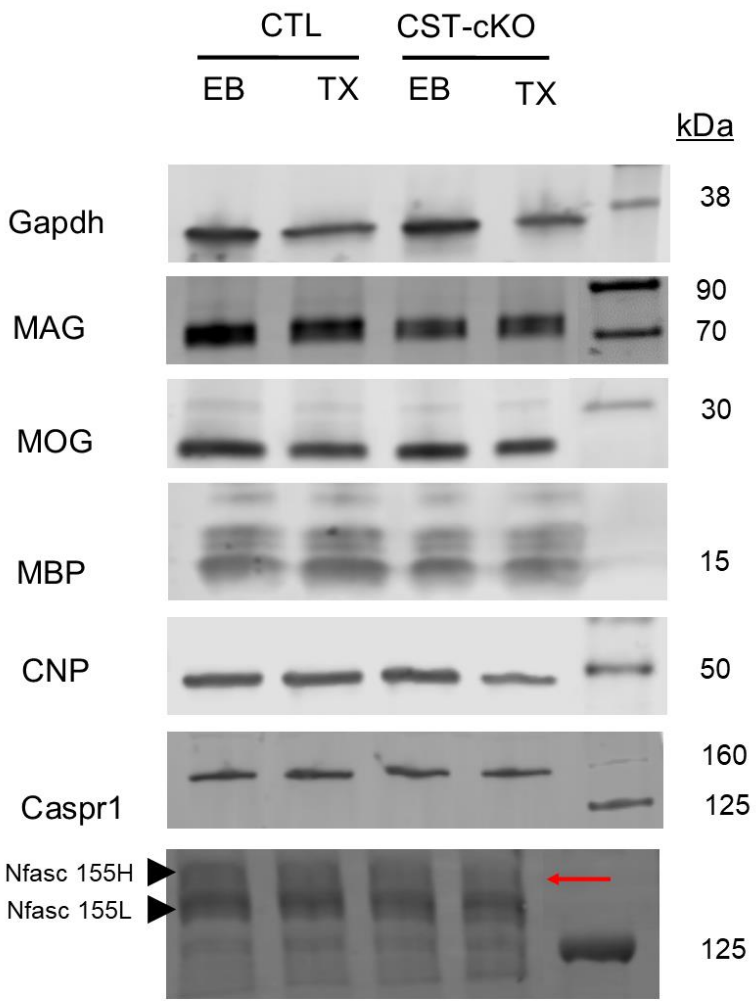
CTL
CST-cKO
EB
TX
EB
TX
kDa
Gapdh
38
MAG
90
70
MOG
30
MBP
15
CNP
50
Caspr1
160
125
Nfasc 155H
Nfasc 155L
125

Figure 3.6. Nfasc155H and CNP exhibit an increased susceptibility to detergent extraction in the absence of sulfatide. Cervical spinal cords from CTL and CST-cKO mice, incubated in extraction buffer without detergent (EB) or in buffer containing detergent Triton X-100 (TX). GAPDH was extracted independent of sulfatide at a consistent ratio across timepoints to confirm validity of technique. Nfasc155H and CNP were extracted at a greater rate in the CST-cKO mice, while MAG, MOG, MBP, and Caspr1 remain unchanged regardless of treatment or genotype

A GAPDH

PI	CTL	CST-cKO
3	46.0 ± 4.8	54.4 ± 2.9
6	43.9 ± 6.8	40.9 ± 2.3
11	49.1 ± 2.1	54.7 ± 4.6

B MAG

PI	CTL	CST-cKO
3	100 ±1.6	98.6 ±3.1
6	100 ±5.9	104.7 ±0
11	100 ±6.3	104.7 ±5.9

C MOG

PI	CTL	CST-cKO
3	100 ± 6.3	95.6 ± 4.5
6	100 ± 4.3	105.6 ± 7.8
11	100± 6.3	104.8 ± 4.9

D MBP

PI	CTL	CST-cKO
3	100 ± 10.3	71.5 ±5.7
6	100 ±18.23	74.0 ±4.6
11	100 ± 5.0	100.5 ±14.0

E CNP

	CTL	CST-cKO
3	100 ±6.8	102.7 ±4.2
6	98.0 ± 3.7	102.1 ±5.2
11	100 ±4.3	71.5 ±0.86*

F Caspr1

	CTL	CST-cKO
3	100 ± 11.5	100.7 ± 9.5
6	100 ± 11.3	104.4 ± 9.6
11	100 ± 5.7	108.8 ± 5.1

G NF155H

	CTL	CST-cKO
3	100 ±4.6	96.0 ±0.9
6	100 ±1.9	72.9 ±4.7*
11	100 ±3.8	82.6 ±5.0*

H NF155L cCST

	CTL	CST-cKO
3	100 ±1.2	93.5 ± 2.0
6	100 ± 0	99.4 ± 4.0
11	100 ±3.9	105.8 ±2.7

Table 3.1: Quantification of myelin proteins following Triton X-100 extraction

* $p<0.05$

GAPDH

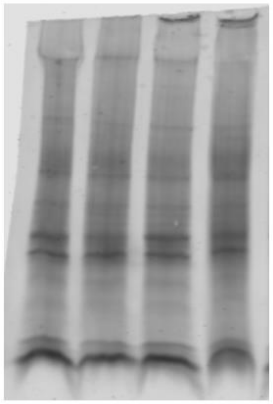

MAG

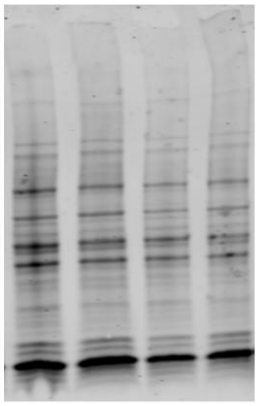

MOG

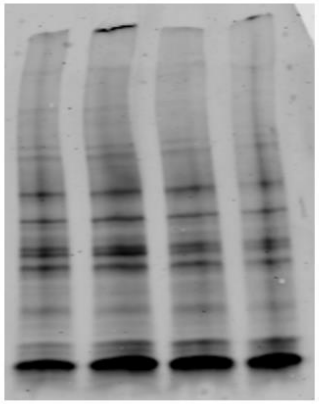

MBP

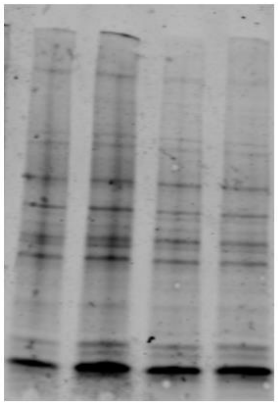

CNP

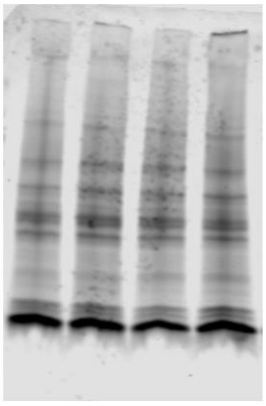

Caspr

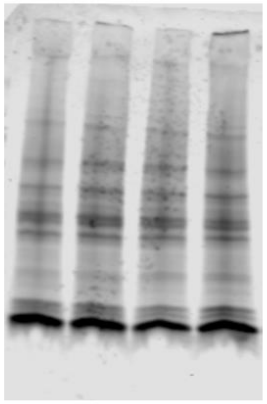

Nfasc 155H

Nfasc 155L

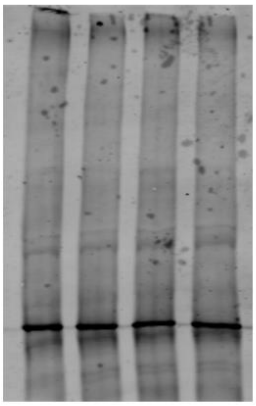

Supplement Figure 3.1: Total protein load for western blot analysis

Total protein blots, stained with REVERT total protein stain, were used to normalize protein percentages for all proteins analyzed. Note Nfasc155 total protein is lighter due to different gel conditions, see methods

CHAPTER FOUR

DISCUSSION

4.1 Summary

The focus of these studies was to better understand how adult onset sulfatide loss may affect axonal and myelin integrity in the NAWM of MS patients. While the pathogenesis of MS is largely autoimmune, our studies demonstrate lipid dyshomeostasis, through sulfatide reduction, may be a causative factor in the onset of MS, particularly with regard to axonal pathology in the absence of demyelination. Previous studies demonstrated sulfatide is essential for myelin maintenance during development, with particular emphasis of pathology present at the paranode (Honke et al., 2002; Marcus et al., 2006). The constitutive CST KO studies established the role of sulfatide in the developing CNS; however, this mouse has limited clinical relevance to onset of MS due to 1) sulfatide being disrupted embryonically and 2) sulfatide is not completely absent in the NAWM of MS patients, but rather is reduced. Therefore, our model establishes an early onset aspect of MS, allowing us to observe structural and functional differences due to reduction of sulfatide throughout the CNS.

In the present series of studies, I demonstrate for the first time that sulfatide loss in adulthood results in disruption of the contactin-neurofascin complex, ion channel mis-localization, with subsequent axonal degeneration and overt myelin sparing with slight regional differences throughout the CNS (Figure 4.1). This contrasts with what was observed in the constitutive CST KO (Honke et al., 2002; Ishibashi et al., 2002b; Marcus et al., 2006). Based on the previous work form our lab, I predicted that OL specific, sulfatide loss in adulthood would result in a similar effect of overt myelin abnormalities. These studies not only provide a more nuanced model for MS pathogenesis, but also enable us to tease apart the differential roles of sulfatide in the CNS during development versus adulthood.

Molecular observations of constitutive versus conditional CST KO

Across all CNS regions analyzed (corpus callosum, ventral and dorsal columns of the cervical spinal cord), my work demonstrates that myelin sheath ultrastructure remains intact through 6m PI. There is no significant difference between the percentage of unmyelinated axons, nor is there a change in the g-ratios or any significant difference in myelin abnormalities between the CTL and the CST-cKO mice. In the developmental model, the constitutive CST KO mice showed increased g-ratios by 15 days of age in the ventral columns of the cervical spinal cord. As these mice age, they develop a progressive tremor that first appears between 2 and 3 months of age that progresses into a significant impairment of ambulation by 7 months of age. This progressive loss of motor function is accompanied by myelin abnormalities such as vacuolar degeneration, redundant myelin, and progressive uncompacted myelin (Marcus et al., 2006). Taking a closer look at the molecular organization between these two models, there are differences between myelin proteins, lipids, and cytoskeletal elements. In the constitutive CST KO, there was a significant decrease in galactosylceramide, sphingomyelin and phospholipids in 3 month old mice. In addition, major myelin proteins such as MBP, PLP, MAG, and Nfasc155H were reduced (Palavicini et al., 2016). Studies that isolated myelin in 30 day old mice constitutive CST KO mice reported changes in expression of cytoskeletal elements, vesicular transport, and metabolomics (Fewou et al., 2010). Therefore, the resulting motor deficits and myelin pathologies reported in the constitutive CST KO mice could largely be attributed to deficits in global lipid synthesis and a severe reduction in major myelin proteins such as PLP and MBP. In contrast, the conditional CST-cKO mice present no significant difference at 3- or 6-months PI in MAG, CNP, MOG, Nfasc155, or MBP.

The constitutive and conditional CST KO models demonstrate a measurable difference in their phenotype. These dramatic differences are likely due to 1) timing of depletion with the constitutive KO mice having no sulfatide during myelin production while the conditional KO mice having sulfatide depletion during the time of myelin maintenance and 2) the degree of sulfatide reduction with the constitutive KO mice having a complete depletion of the lipid while the conditional CST KO mice only presented with reduced lipid levels and 3) Sulfatide is depleted in all cells such as kidney, colon, pancreas, liver, and gall bladder in the CST KO (Honke et al., 2002). Therefore, it is possible depletion of sulfatide in these organs can lead to differences in phenotype. As such, studies have demonstrated that embryonically disrupting sulfatide results in global protein

and lipid changes with subsequent structural pathology (Marcus et al., 2006; Fewou et al., 2010; A. Pomicter et al., 2013; Palavicini et al., 2016). Our conditional sulfatide reduction model is not depleted of sulfatide rather, it becomes progressively reduced, and it appears myelin proteins and lipids remain relatively stable (Qiu et al., 2021). The constitutive CST KO mice exhibit a complete lack of the sulfated lipid while the conditional CST KO mice maintain a low level of sulfatide, which may be sufficient to partially preserve myelin structure but not sufficient to maintain axonal function.

Structural comparisons of constitutive versus conditional CST KO

We observed a significant increase in nodal length variability at 6m PI in the ventral region of the spinal cord and an increase in nodal length variability at 11m PI in the corpus callosum and ventral region of the spinal cord. The constitutive CST KO mice also presented disrupted nodal lengths, which was accompanied by severely compromised myelin sheath integrity both in the internodal and paranodal regions (Marcus et al., 2006). In contrast, nodal disruption in the conditional CST KO mice presented with relative sparing of myelin structure. However, this maintained structural integrity is not sufficient to preserve the molecular integrity of the axonal domains. At 6m PI we see a mis-localization of ion channels in both the corpus callosum and spinal cord, suggesting a breakdown of the axo-glial complex. Improper tethering of the myelin to the axon via transverse bands could facilitate ion channel lateral diffusion along the axon, resulting in mis-firing of neurons, as seen by the loss of N1 CAP, and the resulting motor dysfunction.

While the myelin in the sulfatide conditional KO mice is relatively stable compared to the constitutive KO, myelin thinning was observed at 11-months PI in the ventral region of the spinal cord. Thin myelin indicates demyelination/remyelination occurring in the adult mouse (I. D. Duncan et al., 2018). If the adult oligodendrocytes are participating in remyelination, this newly formed myelin may more closely represent the phenotype of the developmental constitutive CST KO, as this myelin would be extending, wrapping, and compacting without sulfatide. The constitutive CST KO showed a plethora of myelin abnormalities, and while no increase was observed in in myelin-uncompaction or vacuolar degeneration, two very common myelin

abnormalities observed in the constitutive KO mice (Marcus et al., 2006), we did see an increase in redundant myelin at 11-months PI. Also referred to as “myelin outfoldings”, this myelin feature is more prevalent during development, perhaps to aid in trafficking of components to the leading edge (Rosenbluth, 1966; Snaidero et al., 2014). However, after adult-onset, these myelin outfoldings practically disappear; therefore, presence of redundant myelin during adulthood is considered pathological and is observed in other dys-myelinating neuropathologies (Previtali et al., 2007; Mierzwa et al., 2015). In our case, we are seeing axonal pathology precede this overt myelin pathology across all CNS regions analyzed.

Axonal degeneration preceding myelin pathology persists in multiple CNS regions

Our initial studies in the corpus callosum show about a 30% disruption of myelin domain structure at 6m PI with a progressive increase to ~90% by 11m PI. This significant and robust deterioration as early as 6m PI demonstrates that ion channel mis-localization may be a more sensitive indicator of overall myelin-axon health than myelin integrity. Interestingly, a similar mis-localization is also observed in the NAWM of MS patients (Howell et al., 2006a; Gallego-Delgado et al., 2020b; Luchicchi et al., 2021a) further supporting the idea that domain organization occurs early in disease progression and is not dependent on demyelination. Following ion channel mis-localization, at 11 months PI the corpus callosum of the conditional CST-KO revealed a significant increase in axonal pathology with just under 10% of the axons presenting with signs consistent with degeneration compared to 0.5% in the corpus callosum of CTL mice. To confirm this observation of axonal degeneration with the presence of intact myelin, we analyzed the dorsal column of the cervical spinal cord. Here we observed a similar trend of 4% axonal degeneration vs 1% in CTL. While the trends are similar, there is nearly double the percentage of axonal degeneration in the corpus callosum. It is known that there are regional differences in myelination and signaling molecules between the brain and spinal cord regions (Bercury et al., 2014; Wahl et al., 2014; Zeisel et al., 2018). Mature oligodendrocytes (MOLs) have distinct subpopulations, having unique functional roles in development, myelination, and disease (Marques et al., 2016). These subpopulations of MOLs, (MOL1-6) have differential expression between the corpus callosum and spinal cord. MOL2 is significantly more prevalent in dorsal SC than in CC (Floriddia et al., 2020). Floriddia

et al. (2020) demonstrated that MOL2 may be associated with circuit remodeling, resulting from sprouting of intact axons proximal to the injury site. Mature oligodendrocytes can change their transcriptional profile after injury (Falcão et al., 2018). Perhaps loss of sulfatide in these subsets of mature OLs triggers altered expression patterns, leading to differential axo-glial communication responses.

In the ventral column of the spinal cord, we observed an earlier occurrence of axonal degeneration. In both the corpus callosum and the dorsal column of the spinal cord, we did not observe significant axonal degeneration until 11m PI. In the ventral columns of the spinal cord, significant axonal degeneration presented in the CST-cKO by 6 months PI, having 5.9% of axons showing degeneration versus control having 0.5%. At 11 months PI we see a further progression of degeneration reaching ~8% versus 1.4% in aged-matched CTL mice. The ventral column houses motor axons which are larger in size, ranging from 1µm to over 9 µm (Marcus et al., 2006; Stifani, 2014; Saliani et al., 2017). Due to their larger size, trafficking of components and energetic demands are higher (Perge et al., 2009; Chamberlain & Sheng, 2019), possibly leaving them more susceptible to damage (Mahad et al., 2009).

Our studies demonstrate that loss of sulfatide in adulthood leads to axonal degeneration independent of demyelination. However, we do not know the exact mechanism by which this occurs. Likely, there are multiple mechanisms at play mediating axonal degeneration. In this discussion we will consider possible causative roles of axonal degeneration following sulfatide loss.

Channelopathy

Although the timing of domain disruption was slightly different among the 3 regions analyzed, a loss in axonal domain organization was a consistent, progressive pathologic event that occurred independent of myelin loss. Consistent with this loss of domain organization, the electrophysiological data revealed a loss of function of the

myelinated axons with a loss of the N1 peak. Previous work has indicated a correlation between altered expression and localization of Nav1.6 voltage gated channels and axonal degeneration.

Mis-localization of ion channels and axonal domains was the first pathology observed in the corpus callosum and concomitantly with axonal degeneration in the ventral column of the spinal cord at 6m PI. In the corpus callosum and spinal cord at 6m PI, there was a significant increase in mis-localization of myelin domains. Ion channels play a fundamental role in the health and function of the axon and proper localization is critical for proper action propagation. Here, we observed mis-localization of these domains results in disruption of N1 waveforms. Mis-localization of these ion channels may not only lead to disruption of action potential propagation, but channelopathies leading to axonal degeneration. Previous work in animal models of MS and in MS tissue demonstrated that in demyelinated fibers Nav1.6 migrates beyond the boundaries of the node of Ranvier and can co-localize with sodium/calcium exchangers (NCX) resulting in axonal degeneration due to a reversion of function (Craner et al., 2003; Craner, Hains, et al., 2004; Craner, Newcombe, et al., 2004; Bouafia et al., 2014; Alrashdi et al., 2019). Unlike other sodium channel isoforms, Nav1.6 is capable of producing a persistent sodium current. This buildup of sodium ions triggers a reversal of NCX function. Under normal conditions, the NCX exports calcium ions (Ca^{2+}) and imports sodium ions (Na^{+}). However, if Nav1.6 channels are diffusely expressed along the axon, causing increased depolarization near the NCX, the sodium gradient will be diminished and the electrochemical driving force will reverse triggering Ca^{2+} to enter the axon (Stys et al., 1992; Craner, Hains, et al., 2004; J.-L. Song et al., 2022). Increase in intracellular Ca^{2+} activates calpains and caspases that can degrade cytoskeletal proteins (Gutiérrez-Martín et al., 2005). Increase in calpain activation due to increased Ca^{2+} levels leading to axonal degeneration is a well-established observation in neurodegenerative diseases (Bano et al., 2005; J. Yang et al., 2013; J.-L. Song et al., 2022). Further, studies inhibiting either calpain activation or NCX function in inflammatory models, as well as demyelinating diseases, has shown to have protective effects (Kapoor et al., 2003; Bei & Smith, 2012; Omelchenko et al., 2019; Cunningham et al., 2023; McGonigal et al., 2023). These studies propose that the temporal order of events is demyelination followed by mis-localization of Nav1.6 with consequential reversal of function of NCX and ultimately Ca^{2+} accumulation and pathologic calpain activity. However, mis-localization of Nav1.6 has also

been reported in areas of NAWM in MS brains (Gallego-Delgado et al., 2020b; Luchicchi et al., 2021a). Therefore, it is possible that the initiation of the pathologies that develop downstream of demyelination actually occur prior to myelin loss.

In our model, Nav1.6 becomes mis-localized in the absence of demyelination. Therefore, we predict that elongation of the Nav1.6 domain or migration of Nav1.6 beyond the boundaries of the node of Ranvier, which we show in Chapter 2 figure 2.9C is sufficient to alter NCX activity with subsequent axonal degermation. Moving forward, it would be interesting to see if inhibition of either NCX or calpain could protect axons from subsequent damage in our sulfatide reduction model. Therefore, future studies using the CST-cKO mouse should explore co-localization of NCX with Nav1.6, Nav1.2 and a marker for axonal injury such as smi-32. Smi-32 detects non-phosphorylated neurofilaments, and non-phosphorylated neurofilament accumulation within the axon is considered a marker of acute axonal injury (Meller et al., 1994; Schirmer et al., 2012).

Sulfatide in Microdomains

Microdomains are small cholesterol and glycosphingolipid rich microdomains that function to compartmentalize proteins for a variety of processes such as signaling, stability, and aid in receptor binding (Laganowsky et al., 2014; Isik & Cizmecioglu, 2023). Sulfatide could be playing a much more global role in mediating myelin-axon interactions. Sulfatide is a major constituent in microdomains. As such disruption of the microdomain stoichiometry could disrupt proper sequestering of proteins into their proper domains for signaling. In our studies, we demonstrated perturbation of the myelin sheath through the absence of sulfatide, which resulted in increased extraction of specific myelin proteins. While this study demonstrated that sulfatide mediates protein stability within the myelin sheath, we looked at a limited panel of prominent myelin proteins. Microdomains have a multifunctional role in compartmentalizing scaffolding proteins and serving as a platform for signaling domains, and cellular processes such as proliferation and apoptosis (Wee & Wang, 2017; Kovacs et al., 2022; Gajate et al., 2009; Sankarshanan et al., 2007). Therefore, reduction of sulfatide in microdomains could lead to

a broader range of disruption in cellular processes such as development, trafficking, and proliferation/differentiation.

Using an Alzheimer's Disease gene expression panel, our collaborators found a significant difference in cellular processes such as transport, cell differentiation and development in 9m PI CST-cKO mice. In addition, it is known oligodendrocytes can communicate with neurons via exosomes (S. Li & Sheng, 2023). Exosomal membranes consist of microdomains (Skotland et al., 2019; Horbay et al., 2022). Therefore, it is possible reduction of sulfatide may be disrupting proper neuron-glia transport via disruption of exosome membrane composition, leading to neurodegeneration.

Kiss and Run mechanism

Low levels of sulfatide are found in neurons and astrocytes (Isaac et al., 2006; Van Zyl et al., 2010), however the specific function of sulfatide in these cells is not known. While studies have shown CST activity in neurons (Eckhardt et al., 2007), there is debate whether neurons synthesize sulfatide or it is imported via endocytosis (Pernber et al., 2002; Molander-Melin et al., 2004). Our group has proposed a mechanism for sulfatide transport to neurons (Han, 2004, 2007, 2010). Under normal physiological conditions, apoE4-associated lipoproteins are released from astrocytes where they acquire sulfatide from the myelin sheath through a "kiss-and-run" mechanism. They then traffic to the neuron and bind to low-density lipoprotein (LDL) receptors on the neuron. The cargo is metabolized through the endocytic pathway and incorporated into neurons (Arélin et al., 2002; Shinohara et al., 2017; Gal et al., 2022). Perhaps sulfatide reduction in our CST-cKO model leads to diminished availability of the lipid to be trafficked to neurons, leading to neurodegeneration. There is overwhelming evidence describing how oligodendrocytes metabolically support axons (Fünfschilling et al., 2012; Y. Lee et al., 2012; Saab & Nave, 2017). It is possible that sulfatide plays a direct role supporting neurons. A few possibilities include integration into microdomains to support the plasma membrane or integration into microdomains to aid in trafficking of axonal components (Sonnino et al., 2014; Grassi et al.,

2020). Therefore, reduced sulfatide in oligodendrocytes may mediate neurodegeneration through loss of sulfatide transport to the neuron.

Immune mediated mechanism

Sulfatide has differential roles in the immune system, having evidence of both inflammatory and anti-inflammatory responses (Jahng et al., 2004; Su et al., 2021; S. Li & Sheng, 2023). In our recent paper, (Qiu et al., 2021), we observed evidence of astrogliosis and microgliosis in the CST-cKO mice. Using a gene expression panel, there were differences in genes related to transport, cell differentiation/ development and immune response without infiltration of peripheral immune cells. Specifically, there is an increase in TREM2 which is a lipid sensor and promotes microglial response in areas of demyelination (Poliani et al., 2015). Considering cross-talk between oligodendrocytes, microglia, and astrocytes occurs (Domingues et al., 2016), and sulfatide is able to interact with the extracellular milieu (Baron et al., 2014; Capelluto, 2022), it is possible the absence of sulfatide's headgroup on the outer leaflet may be sensed by TREM2 or other receptors, leading to a response (Su et al., 2021). Thus loss of sulfatide could lead to inflammation-mediated neurodegeneration (Block & Hong, 2005; Choi et al., 2021; Muzio et al., 2021). However, this study did not elucidate the mechanism by which loss of sulfatide could contribute to inflammation.

Mechanisms of sulfatide reduction in MS

Our findings from the CST-cKO mice demonstrate that adult onset sulfatide depletion is sufficient to drive axonal structural and functional pathology in the absence of demyelination. This is highly significant since sulfatide is significantly reduced in MS prior to myelin loss. However, it remains unknown *how* sulfatide is reduced in the NAWM of MS patients. Considering sulfatide is located on the extracellular leaflet of the myelin sheath and forms a glyco-synapse with galactosylceramide (Boggs et al., 2008), it's head group is strategically positioned to make contact with the extracellular environment. Using a similar idea of a "kiss-and-run" mechanism by astrocytes, I predict that CD1d- restricted NK T cells bind sulfatide (Shamshiev et al., 2000; Arrenberg et al., 2010) and extract it from the membrane to present to T-cells for recognition. When sulfatide is

bound by CD1d- restricted NK T cell for presentation for T-cell recognition, the sphingosine backbone binds in the F' pocket of the CD1d molecule, and the acyl chain of varying lengths binds in the A' pocket (Zajonc et al., 2005). The 3'-sulfatide galactose headgroup projects up and away from the binding pocket and is exposed for interaction with the T-cell receptor (TCR). Thus, allowing for sulfate-specific interactions with the TCR. If this process is occurring in an aberrant fashion, perhaps the CD1d- restricted NK T cell is reducing the amount of sulfatide in the myelin sheath by continual extraction and presentation to T-cells.

However, our model does not recapitulate how sulfatide may be reduced in the NAWM. Our model reduced sulfatide genetically, and we still observed astrogliosis and microgliosis due to loss of sulfatide (Qiu et al., 2021). Several studies have published sulfatide having both inflammatory and anti-inflammatory responses (Jeon et al., 2008; Maricic et al., 2014). However, these studies share the commonality in that sulfatide specifically, and not it's precursor GalCer, was able to elicit these immunogenic responses. Therefore, moving forward, sulfatide should be considered as a mediator for inflammation in MS

Implications for MS diagnosis and treatment

As previously described, MS is diagnosed using the McDonald criteria which uses DIS and DIT to diagnose MS. Therefore, by the time of diagnosis, substantial pathology has occurred before the patient is on disease-modifying therapies (DMTs). Identifying a prodromic biomarker for MS would be beneficial to diagnose and begin treatment earlier in patients prior to demyelination.

More recent research has focused on the use of proteomics or metabolomics as a prognostic biomarker (Jafari et al., 2021) and sulfatide has been considered a marker for disease progression in MS (Moyano et al., 2013, 2016; Novakova et al., 2018) using plasma or CSF of MS patients. However, using a larger patient population, there was no difference in specific sulfatide isoforms from CSF between MS patients and healthy donors

(Novakova et al., 2023). Follow-up studies should be performed on larger patient populations assessing sulfatide in plasma as a marker for disease progression.

More recently, studies have shown there is a shift in lipid profiles in MS (Ferreira et al., 2021; Podbielska et al., 2022). In MS patients, it is likely sulfatide is not the only lipid affected, but our studies have shown that sulfatide reduction alone is sufficient to drive axonal pathology independent of demyelination. I predict the onset of MS is coincides with a global lipid dyshomeostasis, but sulfatide reduction may be the leading cause of subsequent pathology.

Concluding Remarks

Our studies have demonstrated reduction of sulfatide in the myelin sheath can lead to axonal degeneration with relative myelin sparing. The disparity between myelin and axonal health is novel as typically in myelin mutants axonal pathology follows myelin pathology (C. Li et al., 1994; Bhat et al., 2001; Rasband et al., 2005; Pillai et al., 2009; Marcus et al., 2006; Mayer et al., 2011; Steyer et al., 2023) However, growing evidence in the field demonstrates that axonal pathology can proceed with structurally intact myelin in myelin mutants (Joseph et al., 2019; Buscham et al., 2022). Here, we have added to the growing body of literature demonstrating sulfatide is highly multifunctional, playing a role in mediating axo-glial interactions, supporting axonal health, and stabilizing molecular interactions in the myelin sheath, and these roles may differ in various CNS regions. More recent studies have demonstrated the immunogenicity of sulfatide and it's implication in MS, therefore further clinical studies need to be conducted to identify sulfatide as a biomarker in the onset of MS.

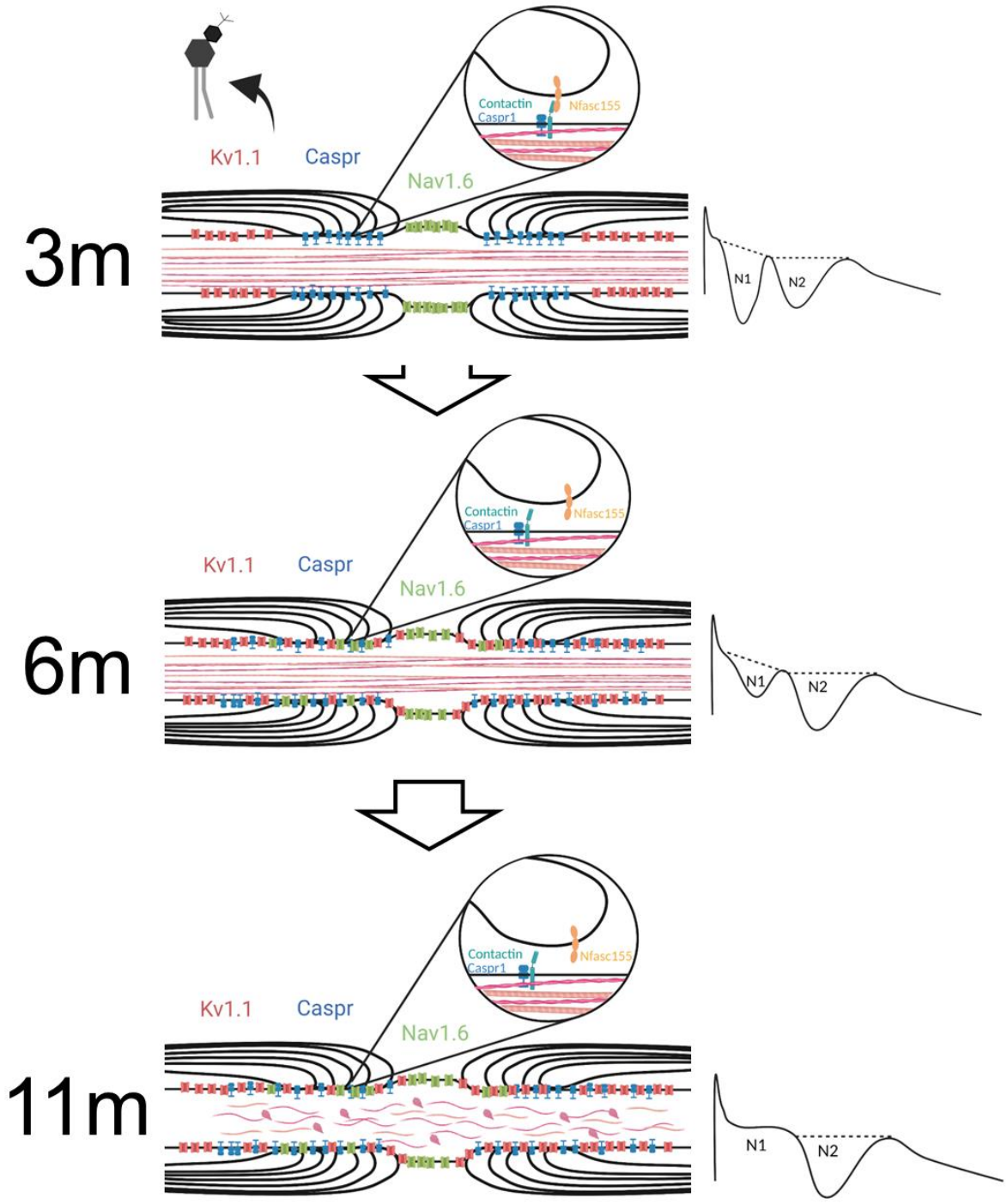
3m
Kv1.1
Caspr
Nav1.6
Contactin
Caspr1
Nfasc155
N1
N2
6m
Kv1.1
Caspr
Nav1.6
Contactin
Caspr1
Nfasc155
N1
N2
11m
Kv1.1
Caspr
Nav1.6
Contactin
Caspr1
Nfasc155
N1
N2

Figure 4.1 Schematic of proposed role of sulfatide in CNS integrity. In our current studies, we demonstrate loss of sulfatide causes molecular aberrations in the myelin sheath by loss of contactin-Neurofascin155 contact, leading to destabilization of transverse bands, thus causing an increase in variability in nodal length. The disruption of the transverse bands is likely what allows mislocalization of ion channels, thus disrupting proper functioning of the myelinated fibers. Subsequently at 11 months PI we see neurodegeneration.

REFERENCES

Aggarwal, S., Yurlova, L., Snaidero, N., Reetz, C., Frey, S., Zimmermann, J., Pähler, G., Janshoff, A., Friedrichs, J., Müller, D. J., Goebel, C., & Simons, M. (2011). A Size Barrier Limits Protein Diffusion at the Cell Surface to Generate Lipid-Rich Myelin-Membrane Sheets. *Developmental Cell*, *21*(3), 445–456. https://doi.org/10.1016/j.devcel.2011.08.001

Agrawal, H. C., Sprinkle, T. J., & Agrawal, D. (1994). In vivo phosphorylation of 2',3'-cyclic nucleotide 3'-phosphohydrolase (CNP): CNP in brain myelin is phosphorylated by forskolin- and phorbol ester-sensitive protein kinases. *Neurochemical Research*, *19*(6), 721–728. https://doi.org/10.1007/BF00967712

Allt, G. (1969). Repair of segmental dehyelination in peripheral nerves: An electron microscope study. *Brain: A Journal of Neurology*, *92*(3), 639–646. https://doi.org/10.1093/brain/92.3.639

Alonso, A., & Goñi, F. M. (2018). The Physical Properties of Ceramides in Membranes. *Annual Review of Biophysics*, *47*, 633–654. https://doi.org/10.1146/annurev-biophys-070317-033309

Alpizar, S. A., Baker, A. L., Gulledge, A. T., & Hoppa, M. B. (2019). Loss of Neurofascin-186 Disrupts Alignment of AnkyrinG Relative to Its Binding Partners in the Axon Initial Segment. *Frontiers in Cellular Neuroscience*, *13*, 1. https://doi.org/10.3389/fncel.2019.00001

Alrashdi, B., Dawod, B., Schampel, A., Tacke, S., Kuerten, S., Marshall, J. S., & Côté, P. D. (2019). Nav1.6 promotes inflammation and neuronal degeneration in a mouse model of multiple sclerosis. *Journal of Neuroinflammation*, *16*(1), 215. https://doi.org/10.1186/s12974-019-1622-1

Amor, V., Feinberg, K., Eshed-Eisenbach, Y., Vainshtein, A., Frechter, S., Grumet, M., Rosenbluth, J., & Peles, E. (2014). Long-Term Maintenance of Na+ Channels at Nodes of Ranvier Depends on Glial Contact Mediated by Gliomedin and NrCAM. *The Journal of Neuroscience*, *34*(15), 5089–5098. https://doi.org/10.1523/JNEUROSCI.4752-13.2014

Amor, V., Zhang, C., Vainshtein, A., Zhang, A., Zollinger, D. R., Eshed-Eisenbach, Y., Brophy, P. J., Rasband, M. N., & Peles, E. (2017). The paranodal cytoskeleton clusters Na+ channels at nodes of Ranvier. *ELife*, *6*, e21392. https://doi.org/10.7554/eLife.21392

Arélin, K., Kinoshita, A., Whelan, C. M., Irizarry, M. C., Rebeck, G. W., Strickland, D. K., & Hyman, B. T. (2002). LRP and senile plaques in Alzheimer's disease: Colocalization with apolipoprotein E and with activated astrocytes. *Brain Research. Molecular Brain Research*, *104*(1), 38–46. https://doi.org/10.1016/s0169-328x(02)00203-6

Arrenberg, P., Halder, R., Dai, Y., Maricic, I., & Kumar, V. (2010). Oligoclonality and innate-like features in the TCR repertoire of type II NKT cells reactive to a β-linked self-glycolipid. *Proceedings of the National Academy of Sciences*, *107*(24), 10984–10989. https://doi.org/10.1073/pnas.1000576107

Arvanitis, D. N., Min, W., Gong, Y., Heng, Y. M., & Boggs, J. M. (2005). Two types of detergent-insoluble, glycosphingolipid/cholesterol-rich membrane domains from isolated myelin. *Journal of Neurochemistry*, *94*(6), 1696–1710. https://doi.org/10.1111/j.1471-4159.2005.03331.x

Baba, H., & Ishibashi, T. (2019). The Role of Sulfatides in Axon–Glia Interactions. In K. Sango, J. Yamauchi, T. Ogata, & K. Susuki (Eds.), *Myelin* (Vol. 1190, pp. 165–179). Springer Singapore. https://doi.org/10.1007/978-981-32-9636-7_11

Babetto, E., & Beirowski, B. (2022). Of axons that struggle to make ends meet: Linking axonal bioenergetic failure to programmed axon degeneration. *Biochimica et Biophysica Acta. Bioenergetics*, *1863*(5), 148545. https://doi.org/10.1016/j.bbabio.2022.148545

Bagchi, B., Al-Sabi, A., Kaza, S., Scholz, D., O'Leary, V. B., Dolly, J. O., & Ovsepian, S. V. (2014). Disruption of myelin leads to ectopic expression of K(V)1.1 channels with abnormal conductivity of optic nerve axons in a cuprizone-induced model of demyelination. *PloS One*, *9*(2), e87736. https://doi.org/10.1371/journal.pone.0087736

Baker, A. J., Phan, N., Moulton, R. J., Fehlings, M. G., Yucel, Y., Zhao, M., Liu, E., & Tian, G. F. (2002). Attenuation of the Electrophysiological Function of the Corpus Callosum after Fluid Percussion Injury in the Rat. *Journal of Neurotrauma*, *19*(5), 587–599. https://doi.org/10.1089/089771502753754064

Bakiri, Y., Káradóttir, R., Cossell, L., & Attwell, D. (2011). Morphological and electrical properties of oligodendrocytes in the white matter of the corpus callosum and cerebellum. *The Journal of Physiology*, *589*(Pt 3), 559–573. https://doi.org/10.1113/jphysiol.2010.201376

Bano, D., Young, K. W., Guerin, C. J., Lefeuvre, R., Rothwell, N. J., Naldini, L., Rizzuto, R., Carafoli, E., & Nicotera, P. (2005). Cleavage of the plasma membrane Na+/Ca2+ exchanger in excitotoxicity. *Cell*, *120*(2), 275–285. https://doi.org/10.1016/j.cell.2004.11.049

Bansal, R., Winkler, S., & Bheddah, S. (1999). Negative Regulation of Oligodendrocyte Differentiation by Galactosphingolipids. *The Journal of Neuroscience*, *19*(18), 7913–7924. https://doi.org/10.1523/JNEUROSCI.19-18-07913.1999

Baron, W., Bijlard, M., Nomden, A., de Jonge, J. C., Teunissen, C. E., & Hoekstra, D. (2014). Sulfatide-mediated control of extracellular matrix-dependent oligodendrocyte maturation. *Glia*, *62*(6), 927–942. https://doi.org/10.1002/glia.22650

Baron, W., & Hoekstra, D. (2010). On the biogenesis of myelin membranes: Sorting, trafficking and cell polarity. *FEBS Letters*, *584*(9), 1760–1770. https://doi.org/10.1016/j.febslet.2009.10.085

Barratt, H. E., Budnick, H. C., Parra, R., Lolley, R. J., Perry, C. N., & Nesic, O. (2016). Tamoxifen promotes differentiation of oligodendrocyte progenitors in vitro. *Neuroscience*, *319*, 146–154. https://doi.org/10.1016/j.neuroscience.2016.01.026

Bartsch, U., Kirchhoff, F., & Schachner, M. (1989). Immunohistological localization of the adhesion molecules L1, N-CAM, and MAG in the developing and adult optic nerve of mice. *The Journal of Comparative Neurology*, *284*(3), 451–462. https://doi.org/10.1002/cne.902840310

Bazan, N. G., Colangelo, V., & Lukiw, W. J. (2002). Prostaglandins and other lipid mediators in Alzheimer's disease. *Prostaglandins & Other Lipid Mediators*, *68–69*, 197–210. https://doi.org/10.1016/s0090-6980(02)00031-x

Bei, F., & Smith, K. J. (2012). Axonal protection achieved by blockade of sodium/calcium exchange in a new model of ischemia in vivo. *Neuropharmacology*, *63*(3), 405–414. https://doi.org/10.1016/j.neuropharm.2012.04.019

Belachew, S., Yuan, X., & Gallo, V. (2001). Unraveling Oligodendrocyte Origin and Function by Cell-Specific Transgenesis. *Developmental Neuroscience*, *23*(4–5), 287–298. https://doi.org/10.1159/000048712

Benjamins, J. A., Murphy, E. J., & Seyfried, T. N. (2012). Chapter 5—Lipids. In S. T. Brady, G. J. Siegel, R. W. Albers, & D. L. Price (Eds.), *Basic Neurochemistry (Eighth Edition)* (pp. 81–100). Academic Press. https://doi.org/10.1016/B978-0-12-374947-5.00005-5

Benusa, S. D., George, N. M., Sword, B. A., DeVries, G. H., & Dupree, J. L. (2017). Acute neuroinflammation induces AIS structural plasticity in a NOX2-dependent manner. *Journal of Neuroinflammation*, *14*(1), 116. https://doi.org/10.1186/s12974-017-0889-3

Bercury, K. K., Dai, J., Sachs, H. H., Ahrendsen, J. T., Wood, T. L., & Macklin, W. B. (2014). Conditional Ablation of Raptor or Rictor Has Differential Impact on Oligodendrocyte Differentiation and CNS Myelination. *The Journal of Neuroscience*, *34*(13), 4466–4480. https://doi.org/10.1523/JNEUROSCI.4314-13.2014

Berger, T., & Reindl, M. (2015). Antibody biomarkers in CNS demyelinating diseases – a long and winding road. *European Journal of Neurology*, *22*(8), 1162–1168. https://doi.org/10.1111/ene.12759

Bhat, M. A., Rios, J. C., Lu, Y., Garcia-Fresco, G. P., Ching, W., St Martin, M., Li, J., Einheber, S., Chesler, M., Rosenbluth, J., Salzer, J. L., & Bellen, H. J. (2001). Axon-glia interactions and the domain organization of myelinated axons requires neurexin IV/Caspr/Paranodin. *Neuron*, *30*(2), 369–383. https://doi.org/10.1016/s0896-6273(01)00294-x

Bieberich, E. (2018). Sphingolipids and lipid rafts: Novel concepts and methods of analysis. *Chemistry and Physics of Lipids*, *216*, 114–131. https://doi.org/10.1016/j.chemphyslip.2018.08.003

Biffiger, K., Bartsch, S., Montag, D., Aguzzi, A., Schachner, M., & Bartsch, U. (2000). Severe Hypomyelination of the Murine CNS in the Absence of Myelin-Associated Glycoprotein and Fyn Tyrosine Kinase. *The Journal of Neuroscience*, *20*(19), 7430–7437. https://doi.org/10.1523/JNEUROSCI.20-19-07430.2000

Bizzozero, O. A., Malkoski, S. P., Mobarak, C., Bixler, H. A., & Evans, J. E. (2002). Mass-spectrometric analysis of myelin proteolipids reveals new features of this family of palmitoylated membrane proteins. *Journal of Neurochemistry*, *81*(3), 636–645. https://doi.org/10.1046/j.1471-4159.2002.00852.x

Bjornevik, K., Cortese, M., Healy, B. C., Kuhle, J., Mina, M. J., Leng, Y., Elledge, S. J., Niebuhr, D. W., Scher, A. I., Munger, K. L., & Ascherio, A. (2022). Longitudinal analysis reveals high prevalence of Epstein-Barr virus associated with multiple sclerosis. *Science (New York, N.Y.)*, *375*(6578), 296–301. https://doi.org/10.1126/science.abj8222

Bligh, E. G., & Dyer, W. J. (1959). A rapid method of total lipid extraction and purification. *Canadian Journal of Biochemistry and Physiology*, *37*(8), 911–917. https://doi.org/10.1139/o59-099

Block, M. L., & Hong, J.-S. (2005). Microglia and inflammation-mediated neurodegeneration: Multiple triggers with a common mechanism. *Progress in Neurobiology*, *76*(2), 77–98. https://doi.org/10.1016/j.pneurobio.2005.06.004

Boggs, J. M. (2014). Role of galactosylceramide and sulfatide in oligodendrocytes and CNS myelin: Formation of a glycosynapse. *Advances in Neurobiology*, *9*, 263–291. https://doi.org/10.1007/978-1-4939-1154-7_12

Boggs, J. M., Gao, W., & Hirahara, Y. (2008). Myelin glycosphingolipids, galactosylceramide and sulfatide, participate in carbohydrate–carbohydrate interactions between apposed membranes and may form glycosynapses between oligodendrocyte and/or myelin membranes. *Biochimica et Biophysica Acta (BBA) - General Subjects*, *1780*(3), 445–455. https://doi.org/10.1016/j.bbagen.2007.10.015

Boggs, J. M., Wang, H., Gao, W., Arvanitis, D. N., Gong, Y., & Min, W. (2004). A glycosynapse in myelin? *Glycoconjugate Journal*, *21*(3–4), 97–110. https://doi.org/10.1023/B:GLYC.0000044842.34958.f8

Boiko, T., Rasband, M. N., Levinson, S. R., Caldwell, J. H., Mandel, G., Trimmer, J. S., & Matthews, G. (2001). Compact Myelin Dictates the Differential Targeting of Two Sodium Channel Isoforms in the Same Axon. *Neuron*, *30*(1), 91–104. https://doi.org/10.1016/S0896-6273(01)00265-3

Boison, D., Bussow, H., D'Urso, D., Muller, H. W., & Stoffel, W. (1995). Adhesive properties of proteolipid protein are responsible for the compaction of CNS myelin sheaths. *Journal of Neuroscience*, *15*(8), 5502–5513. https://doi.org/10.1523/JNEUROSCI.15-08-05502.1995

Boison, D., & Stoffel, W. (1994). Disruption of the compacted myelin sheath of axons of the central nervous system in proteolipid protein-deficient mice. *Proceedings of the National Academy of Sciences of the United States of America*, *91*(24), 11709–11713.

Borges, B. C., Meng, X., Long, P., Kanold, P. O., & Corfas, G. (2023). Loss of oligodendrocyte ErbB receptor signaling leads to hypomyelination, reduced density of parvalbumin-expressing interneurons, and inhibitory function in the auditory cortex. *Glia*, *71*(2), 187–204. https://doi.org/10.1002/glia.24266

Borst, K., Dumas, A. A., & Prinz, M. (2021). Microglia: Immune and non-immune functions. *Immunity*, *54*(10), 2194–2208. https://doi.org/10.1016/j.immuni.2021.09.014

Bosio, A., Binczek, E., Haupt, W. F., & Stoffel, W. (1998). Composition and Biophysical Properties of Myelin Lipid Define the Neurological Defects in Galactocerebroside- and Sulfatide-Deficient Mice. *Journal of Neurochemistry*, *70*(1), 308–315. https://doi.org/10.1046/j.1471-4159.1998.70010308.x

Bouafia, A., Golmard, J.-L., Thuries, V., Sazdovitch, V., Hauw, J. J., Fontaine, B., & Seilhean, D. (2014). Axonal expression of sodium channels and neuropathology of the plaques in multiple sclerosis. *Neuropathology and Applied Neurobiology*, *40*(5), 579–590. https://doi.org/10.1111/nan.12059

Boullerne, A. I. (2016). The history of myelin. *Experimental Neurology*, *283*(Pt B), 431–445. https://doi.org/10.1016/j.expneurol.2016.06.005

Boyle, M. E., Berglund, E. O., Murai, K. K., Weber, L., Peles, E., & Ranscht, B. (2001). Contactin orchestrates assembly of the septate-like junctions at the paranode in myelinated peripheral nerve. *Neuron*, *30*(2), 385–397. https://doi.org/10.1016/s0896-6273(01)00296-3

Braun, P. E., De Angelis, D., Shtybel, W. W., & Bernier, L. (1991). Isoprenoid modification permits 2',3'-cyclic nucleotide 3'-phosphodiesterase to bind to membranes. *Journal of Neuroscience Research*, *30*(3), 540–544. https://doi.org/10.1002/jnr.490300311

Braun, P. E., Sandillon, F., Edwards, A., Matthieu, J. M., & Privat, A. (1988). Immunocytochemical localization by electron microscopy of 2'3'-cyclic nucleotide 3'-phosphodiesterase in developing oligodendrocytes of normal and mutant brain. *Journal of Neuroscience*, *8*(8), 3057–3066. https://doi.org/10.1523/JNEUROSCI.08-08-03057.1988

Britt, D. J., Farías, G. G., Guardia, C. M., & Bonifacino, J. S. (2016). Mechanisms of Polarized Organelle Distribution in Neurons. *Frontiers in Cellular Neuroscience*, *10*. https://www.frontiersin.org/articles/10.3389/fncel.2016.00088

Brown, D. A., & Rose, J. K. (1992). Sorting of GPI-anchored proteins to glycolipid-enriched membrane subdomains during transport to the apical cell surface. *Cell*, *68*(3), 533–544. https://doi.org/10.1016/0092-8674(92)90189-J

Brunner, C., Lassmann, H., Waehneldt, T. V., Matthieu, J. M., & Linington, C. (1989). Differential ultrastructural localization of myelin basic protein, myelin/oligodendroglial glycoprotein, and 2',3'-cyclic nucleotide 3'-phosphodiesterase in the CNS of adult rats. *Journal of Neurochemistry*, *52*(1), 296–304. https://doi.org/10.1111/j.1471-4159.1989.tb10930.x

Bujalka, H., Koenning, M., Jackson, S., Perreau, V. M., Pope, B., Hay, C. M., Mitew, S., Hill, A. F., Lu, Q. R., Wegner, M., Srinivasan, R., Svaren, J., Willingham, M., Barres, B. A., & Emery, B. (2013). MYRF Is a Membrane-Associated Transcription Factor That Autoproteolytically Cleaves to Directly Activate Myelin Genes. *PLOS Biology*, *11*(8), e1001625. https://doi.org/10.1371/journal.pbio.1001625

Burger, D., Steck, A. J., Bernard, C. C., & Kerlero de Rosbo, N. (1993). Human myelin/oligodendrocyte glycoprotein: A new member of the L2/HNK-1 family. *Journal of Neurochemistry*, *61*(5), 1822–1827. https://doi.org/10.1111/j.1471-4159.1993.tb09822.x

Burska, A. N., Hunt, L., Boissinot, M., Strollo, R., Ryan, B. J., Vital, E., Nissim, A., Winyard, P. G., Emery, P., & Ponchel, F. (2014). Autoantibodies to Posttranslational Modifications in Rheumatoid Arthritis. *Mediators of Inflammation*, *2014*, 492873. https://doi.org/10.1155/2014/492873

Buscham, T. J., Eichel-Vogel, M. A., Steyer, A. M., Jahn, O., Strenzke, N., Dardawal, R., Memhave, T. R., Siems, S. B., Müller, C., Meschkat, M., Sun, T., Ruhwedel, T., Möbius, W., Krämer-Albers, E.-M., Boretius, S., Nave, K.-A., & Werner, H. B. (2022). Progressive axonopathy when oligodendrocytes lack the myelin protein CMTM5. *ELife*, *11*, e75523. https://doi.org/10.7554/eLife.75523

Caldwell, J. H., Schaller, K. L., Lasher, R. S., Peles, E., & Levinson, S. R. (2000). Sodium channel Nav1.6 is localized at nodes of Ranvier, dendrites, and synapses. *Proceedings of the National Academy of Sciences*, *97*(10), 5616–5620. https://doi.org/10.1073/pnas.090034797

Campagnoni, A. T., & Skoff, R. P. (2001). The pathobiology of myelin mutants reveal novel biological functions of the MBP and PLP genes. *Brain Pathology (Zurich, Switzerland)*, *11*(1), 74–91. https://doi.org/10.1111/j.1750-3639.2001.tb00383.x

Cantoni, C., Bollman, B., Licastro, D., Xie, M., Mikesell, R., Schmidt, R., Yuede, C. M., Galimberti, D., Olivecrona, G., Klein, R. S., Cross, A. H., Otero, K., & Piccio, L. (2015). TREM2 regulates microglial cell activation in response to demyelination in vivo. *Acta Neuropathologica*, *129*(3), 429–447. https://doi.org/10.1007/s00401-015-1388-1

Capelluto, D. G. S. (2022). The repertoire of protein-sulfatide interactions reveal distinct modes of sulfatide recognition. *Frontiers in Molecular Biosciences*, *9*, 1080161. https://doi.org/10.3389/fmolb.2022.1080161

Caritá, A. C., Mattei, B., Domingues, C. C., de Paula, E., & Riske, K. A. (2017). Effect of Triton X-100 on Raft-Like Lipid Mixtures: Phase Separation and Selective Solubilization. *Langmuir: The ACS Journal of Surfaces and Colloids*, *33*(29), 7312–7321. https://doi.org/10.1021/acs.langmuir.7b01134

Casares, D., Escribá, P. V., & Rosselló, C. A. (2019). Membrane Lipid Composition: Effect on Membrane and Organelle Structure, Function and Compartmentalization and Therapeutic Avenues. *International Journal of Molecular Sciences*, *20*(9). https://doi.org/10.3390/ijms20092167

Castro, B. M., Prieto, M., & Silva, L. C. (2014). Ceramide: A simple sphingolipid with unique biophysical properties. *Progress in Lipid Research*, *54*, 53–67. https://doi.org/10.1016/j.plipres.2014.01.004

Chamberlain, K. A., & Sheng, Z.-H. (2019). Mechanisms for the maintenance and regulation of axonal energy supply. *Journal of Neuroscience Research*, *97*(8), 897–913. https://doi.org/10.1002/jnr.24411

Chang, K.-J., Zollinger, D. R., Susuki, K., Sherman, D. L., Makara, M. A., Brophy, P. J., Cooper, E. C., Bennett, V., Mohler, P. J., & Rasband, M. N. (2014). Glial ankyrins facilitate paranodal axoglial junction assembly. *Nature Neuroscience*, *17*(12), 1673–1681. https://doi.org/10.1038/nn.3858

Charcot, J.-M. (1868). *Histologie de la sclérose en plaques*. s.n.

Charles, P., Tait, S., Faivre-Sarrailh, C., Barbin, G., Gunn-Moore, F., Denisenko-Nehrbass, N., Guennoc, A.-M., Girault, J.-A., Brophy, P. J., & Lubetzki, C. (2002a). Neurofascin is a glial receptor for the paranodin/Caspr-contactin axonal complex at the axoglial junction. *Current Biology: CB*, *12*(3), 217–220. https://doi.org/10.1016/s0960-9822(01)00680-7

Charles, P., Tait, S., Faivre-Sarrailh, C., Barbin, G., Gunn-Moore, F., Denisenko-Nehrbass, N., Guennoc, A.-M., Girault, J.-A., Brophy, P. J., & Lubetzki, C. (2002b). Neurofascin Is a Glial Receptor for the Paranodin/Caspr-Contactin Axonal Complex at the Axoglial Junction. *Current Biology*, *12*(3), 217–220. https://doi.org/10.1016/S0960-9822(01)00680-7

Chen, Y., Aulia, S., & Tang, B. L. (2006). Myelin-associated glycoprotein-mediated signaling in central nervous system pathophysiology. *Molecular Neurobiology*, *34*(2), 81–91. https://doi.org/10.1385/MN:34:2:81

Chen, Z., Yuan, Z., Yang, S., Zhu, Y., Xue, M., Zhang, J., & Leng, L. (2023). Brain Energy Metabolism: Astrocytes in Neurodegenerative Diseases. *CNS Neuroscience & Therapeutics*, *29*(1), 24–36. https://doi.org/10.1111/cns.13982

Chiu, S. Y., Zhou, L., Chuan-Li, Z., & Messing, A. (1999). Analysis of potassium channel functions in mammalian axons by gene knockouts. *Journal of Neurocytology*, *28*(4), 349–364.

Choi, S., Guo, L., & Cordeiro, M. F. (2021). Retinal and Brain Microglia in Multiple Sclerosis and Neurodegeneration. *Cells*, *10*(6), 1507. https://doi.org/10.3390/cells10061507

Chou, F. C., Chou, C. H., Shapira, R., & Kibler, R. F. (1976). Basis of microheterogeneity of myelin basic protein. *Journal of Biological Chemistry*, *251*(9), 2671–2679. https://doi.org/10.1016/S0021-9258(17)33540-8

Chrast, R., Saher, G., Nave, K.-A., & Verheijen, M. H. G. (2011). Lipid metabolism in myelinating glial cells: Lessons from human inherited disorders and mouse models. *Journal of Lipid Research*, *52*(3), 419–434. https://doi.org/10.1194/jlr.R009761

Clark, K. C., Josephson, A., Benusa, S. D., Hartley, R. K., Baer, M., Thummala, S., Joslyn, M., Sword, B. A., Elford, H., Oh, U., Dilsizoglu-Senol, A., Lubetzki, C., Davenne, M., DeVries, G. H., & Dupree, J. L. (2016). Compromised axon initial segment integrity in EAE is preceded by microglial reactivity and contact. *Glia*, *64*(7), 1190–1209. https://doi.org/10.1002/glia.22991

Coman, I., Aigrot, M. S., Seilhean, D., Reynolds, R., Girault, J. A., Zalc, B., & Lubetzki, C. (2006). Nodal, paranodal and juxtaparanodal axonal proteins during demyelination and remyelination in multiple sclerosis. *Brain: A Journal of Neurology*, *129*(Pt 12), 3186–3195. https://doi.org/10.1093/brain/awl144

Craner, M. J., Hains, B. C., Lo, A. C., Black, J. A., & Waxman, S. G. (2004). Co-localization of sodium channel Nav1.6 and the sodium-calcium exchanger at sites of axonal injury in the spinal cord in EAE. *Brain: A Journal of Neurology*, *127*(Pt 2), 294–303. https://doi.org/10.1093/brain/awh032

Craner, M. J., Lo, A. C., Black, J. A., & Waxman, S. G. (2003). Abnormal sodium channel distribution in optic nerve axons in a model of inflammatory demyelination. *Brain: A Journal of Neurology*, *126*(Pt 7), 1552–1561. https://doi.org/10.1093/brain/awg153

Craner, M. J., Newcombe, J., Black, J. A., Hartle, C., Cuzner, M. L., & Waxman, S. G. (2004). Molecular changes in neurons in multiple sclerosis: Altered axonal expression of Nav1.2 and Nav1.6 sodium channels and Na+/Ca2+ exchanger. *Proceedings of the National Academy of Sciences of the United States of America*, *101*(21), 8168–8173. https://doi.org/10.1073/pnas.0402765101

Cubí, R., Matas, L. A., Pou, M., Aguilera, J., & Gil, C. (2013). Differential sensitivity to detergents of actin cytoskeleton from nerve endings. *Biochimica Et Biophysica Acta*, *1828*(11), 2385–2393. https://doi.org/10.1016/j.bbamem.2013.06.022

Cunningham, M. E., McGonigal, R., Barrie, J. A., Campbell, C. I., Yao, D., & Willison, H. J. (2023). Axolemmal nanoruptures arising from paranodal membrane injury induce secondary axon degeneration in murine Guillain-Barré syndrome. *Journal of the Peripheral Nervous System*, *28*(1), 17–31. https://doi.org/10.1111/jns.12532

Curatolo, W., & Neuringer, L. J. (1986). The effects of cerebrosides on model membrane shape. *The Journal of Biological Chemistry*, *261*(36), 17177–17182.

Dai, G. (2022). Neuronal KCNQ2/3 channels are recruited to lipid raft microdomains by palmitoylation of BACE1. *The Journal of General Physiology*, *154*(4), e202112888. https://doi.org/10.1085/jgp.202112888

Dasgupta, S., Levery, S. B., & Hogan, E. L. (2002). 3-O-acetyl-sphingosine-series myelin glycolipids characterization of novel 3-O-acetyl-sphingosine galactosylceramide. *Journal of Lipid Research*, *43*(5), 751–761.

De Angelis, D. A., & Braun, P. E. (1996). 2′,3′-Cyclic Nucleotide 3′-Phosphodiesterase Binds to Actin-Based Cytoskeletal Elements in an Isoprenylation-Independent Manner. *Journal of Neurochemistry*, *67*(3), 943–951. https://doi.org/10.1046/j.1471-4159.1996.67030943.x

De Logu, F., De Prá, S. D.-T., de David Antoniazzi, C. T., Kudsi, S. Q., Ferro, P. R., Landini, L., Rigo, F. K., de Bem Silveira, G., Silveira, P. C. L., Oliveira, S. M., Marini, M., Mattei, G., Ferreira, J., Geppetti, P., Nassini, R., & Trevisan, G. (2020). Macrophages and Schwann cell TRPA1 mediate chronic allodynia in a mouse model of complex regional pain syndrome type I. *Brain, Behavior, and Immunity*, *88*, 535–546. https://doi.org/10.1016/j.bbi.2020.04.037

De Logu, F., Nassini, R., Materazzi, S., Carvalho Gonçalves, M., Nosi, D., Rossi Degl'Innocenti, D., Marone, I. M., Ferreira, J., Li Puma, S., Benemei, S., Trevisan, G., Souza Monteiro de Araújo, D., Patacchini, R., Bunnett, N. W., & Geppetti, P. (2017). Schwann cell TRPA1 mediates neuroinflammation that sustains macrophage-dependent neuropathic pain in mice. *Nature Communications*, *8*(1), Article 1. https://doi.org/10.1038/s41467-017-01739-2

del Rio-Hortega, P. (1924). *La glie à radiations peu nombreuses et la cellule de Schwann sontelles homologables? 91*, 818–820.

Denk, F., Ramer, L. M., Erskine, E. L. K. S., Nassar, M. A., Bogdanov, Y., Signore, M., Wood, J. N., McMahon, S. B., & Ramer, M. S. (2015). Tamoxifen induces cellular stress in the nervous system by inhibiting cholesterol synthesis. *Acta Neuropathologica Communications*, *3*. https://doi.org/10.1186/s40478-015-0255-6

Diaz-Rohrer, B., Castello-Serrano, I., Chan, S. H., Wang, H.-Y., Shurer, C. R., Levental, K. R., & Levental, I. (2023). Rab3 mediates a pathway for endocytic sorting and plasma membrane recycling of ordered microdomains. *Proceedings of the National Academy of Sciences of the United States of America*, *120*(10), e2207461120. https://doi.org/10.1073/pnas.2207461120

Doerflinger, N. H., Macklin, W. B., & Popko, B. (2003). Inducible site-specific recombination in myelinating cells. *Genesis*, *35*(1), 63–72. https://doi.org/10.1002/gene.10154

Domeniconi, M., Cao, Z., Spencer, T., Sivasankaran, R., Wang, K. C., Nikulina, E., Kimura, N., Cai, H., Deng, K., Gao, Y., He, Z., & Filbin, M. T. (2002). Myelin-Associated Glycoprotein Interacts with the Nogo66 Receptor to Inhibit Neurite Outgrowth. *Neuron*, *35*(2), 283–290. https://doi.org/10.1016/S0896-6273(02)00770-5

Domingues, H. S., Portugal, C. C., Socodato, R., & Relvas, J. B. (2016). Oligodendrocyte, Astrocyte, and Microglia Crosstalk in Myelin Development, Damage, and Repair. *Frontiers in Cell and Developmental Biology*, *4*, 71. https://doi.org/10.3389/fcell.2016.00071

Duncan, G. J., Simkins, T. J., & Emery, B. (2021). Neuron-Oligodendrocyte Interactions in the Structure and Integrity of Axons. *Frontiers in Cell and Developmental Biology*, *9*, 653101. https://doi.org/10.3389/fcell.2021.653101

Duncan, I. D., Radcliff, A. B., Heidari, M., Kidd, G., August, B. K., & Wierenga, L. A. (2018). The adult oligodendrocyte can participate in remyelination. *Proceedings of the National Academy of Sciences of the United States of America*, *115*(50), E11807–E11816. https://doi.org/10.1073/pnas.1808064115

Dupree, J. L., Coetzee, T., Blight, A., Suzuki, K., & Popko, B. (1998a). Myelin Galactolipids Are Essential for Proper Node of Ranvier Formation in the CNS. *Journal of Neuroscience*, *18*(5), 1642–1649. https://doi.org/10.1523/JNEUROSCI.18-05-01642.1998

Dupree, J. L., Coetzee, T., Blight, A., Suzuki, K., & Popko, B. (1998b). Myelin Galactolipids Are Essential for Proper Node of Ranvier Formation in the CNS. *Journal of Neuroscience*, *18*(5), 1642–1649. https://doi.org/10.1523/JNEUROSCI.18-05-01642.1998

Dupree, J. L., Coetzee, T., Suzuki, K., & Popko, B. (1998). Myelin abnormalities in mice deficient in galactocerebroside and sulfatide. *Journal of Neurocytology*, *27*(9), 649–659. https://doi.org/10.1023/A:1006908013972

Dupree, J. L., & Feinstein, D. L. (2018). Influence of diet on axonal damage in the EAE mouse model of multiple sclerosis. *Journal of Neuroimmunology*, *322*, 9–14. https://doi.org/10.1016/j.jneuroim.2018.05.010

Dupree, J. L., Girault, J. A., & Popko, B. (1999). Axo-glial interactions regulate the localization of axonal paranodal proteins. *The Journal of Cell Biology*, *147*(6), 1145–1152. https://doi.org/10.1083/jcb.147.6.1145

Dupree, J. L., Polak, P. E., Hensley, K., Pelligrino, D., & Feinstein, D. L. (2015). Lanthionine ketimine ester provides benefit in a mouse model of multiple sclerosis. *Journal of Neurochemistry*, *134*(2), 302–314. https://doi.org/10.1111/jnc.13114

Dupree, J. L., & Pomicter, A. D. (2010). Myelin, DIGs, and membrane rafts in the central nervous system. *Prostaglandins & Other Lipid Mediators*, *91*(3), 118–129. https://doi.org/10.1016/j.prostaglandins.2009.04.005

Dupree, J., Mason, J., Marcus, J., Stull, M., Levinson, R., Matsushima, G., & Popko, B. (2004). Oligodendrocytes assist in the maintenance of sodium channel clusters independent of the myelin sheath. *Neuron Glia Biology*, *1*(3), 179–192.

Dyer, C. A., & Benjamins, J. A. (1989). Organization of oligodendroglial membrane sheets. I: Association of myelin basic protein and 2',3'-cyclic nucleotide 3'-phosphohydrolase with cytoskeleton. *Journal of Neuroscience Research*, *24*(2), 201–211. https://doi.org/10.1002/jnr.490240211

Eckhardt, M., Hedayati, K. K., Pitsch, J., Lüllmann-Rauch, R., Beck, H., Fewou, S. N., & Gieselmann, V. (2007). Sulfatide storage in neurons causes hyperexcitability and axonal degeneration in a mouse model of metachromatic leukodystrophy. *The Journal of Neuroscience: The Official Journal of the Society for Neuroscience*, *27*(34), 9009–9021. https://doi.org/10.1523/JNEUROSCI.2329-07.2007

Edgar, J. M., McLaughlin, M., Werner, H. B., McCulloch, M. C., Barrie, J. A., Brown, A., Faichney, A. B., Snaidero, N., Nave, K.-A., & Griffiths, I. R. (2009). Early ultrastructural defects of axons and axon–glia junctions in mice lacking expression of Cnp1. *Glia*, *57*(16), 1815–1824. https://doi.org/10.1002/glia.20893

Einheber, S., Bhat, M. A., & Salzer, J. L. (2006). Disrupted axo-glial junctions result in accumulation of abnormal mitochondria at nodes of ranvier. *Neuron Glia Biology*, *2*(3), 165–174. https://doi.org/10.1017/S1740925X06000275

Einheber, S., Meng, X., Rubin, M., Lam, I., Mohandas, N., An, X., Shrager, P., Kissil, J., Maurel, P., & Salzer, J. L. (2013). The 4.1B cytoskeletal protein regulates the domain organization and sheath thickness of myelinated axons. *Glia*, *61*(2), 240–253. https://doi.org/10.1002/glia.22430

Elazar, N., Vainshtein, A., Golan, N., Vijayaragavan, B., Schaeren-Wiemers, N., Eshed-Eisenbach, Y., & Peles, E. (2019). Axoglial Adhesion by Cadm4 Regulates CNS Myelination. *Neuron*, *101*(2), 224-231.e5. https://doi.org/10.1016/j.neuron.2018.11.032

Elazar, N., Vainshtein, A., Rechav, K., Tsoory, M., Eshed-Eisenbach, Y., & Peles, E. (2019). Coordinated internodal and paranodal adhesion controls accurate myelination by oligodendrocytes. *The Journal of Cell Biology*, *218*(9), 2887–2895. https://doi.org/10.1083/jcb.201906099

Emery, B. (2010). Regulation of oligodendrocyte differentiation and myelination. *Science (New York, N.Y.)*, *330*(6005), 779–782. https://doi.org/10.1126/science.1190927

Faivre-Sarrailh, C. (2020). Molecular organization and function of vertebrate septate-like junctions. *Biochimica et Biophysica Acta (BBA) - Biomembranes*, *1862*(5), 183211. https://doi.org/10.1016/j.bbamem.2020.183211

Falcão, A. M., van Bruggen, D., Marques, S., Meijer, M., Jäkel, S., Agirre, E., Samudyata, Floriddia, E. M., Vanichkina, D. P., ffrench-Constant, C., Williams, A., Guerreiro-Cacais, A. O., & Castelo-Branco, G. (2018). Disease-specific oligodendrocyte lineage cells arise in multiple sclerosis. *Nature Medicine*, *24*(12), Article 12. https://doi.org/10.1038/s41591-018-0236-y

Ferreira, H. B., Melo, T., Monteiro, A., Paiva, A., Domingues, P., & Domingues, M. R. (2021). Serum phospholipidomics reveals altered lipid profile and promising biomarkers in multiple sclerosis. *Archives of Biochemistry and Biophysics*, *697*, 108672. https://doi.org/10.1016/j.abb.2020.108672

Fewou, S. N., Fernandes, A., Stockdale, K., Francone, V. P., Dupree, J. L., Rosenbluth, J., Pfeiffer, S. E., & Bansal, R. (2010). Myelin protein composition is altered in mice lacking either sulfated or both sulfated and non-sulfated galactolipids. *Journal of Neurochemistry*, *112*(3), 599–610. https://doi.org/10.1111/j.1471-4159.2009.06464.x

Fiedler, K., Kobayashi, T., Kurzchalia, T. V., & Simons, K. (1993). Glycosphingolipid-enriched, detergent-insoluble complexes in protein sorting in epithelial cells. *Biochemistry*, *32*(25), 6365–6373. https://doi.org/10.1021/bi00076a009

Fisher, K. S., Cuascut, F. X., Rivera, V. M., & Hutton, G. J. (2020). Current Advances in Pediatric Onset Multiple Sclerosis. *Biomedicines*, *8*(4), 71. https://doi.org/10.3390/biomedicines8040071

Floriddia, E. M., Lourenço, T., Zhang, S., van Bruggen, D., Hilscher, M. M., Kukanja, P., Gonçalves dos Santos, J. P., Altınkök, M., Yokota, C., Llorens-Bobadilla, E., Mulinyawe, S. B., Grãos, M., Sun, L. O., Frisén, J., Nilsson, M., & Castelo-Branco, G. (2020). Distinct oligodendrocyte populations have spatial preference and different responses to spinal cord injury. *Nature Communications*, *11*, 5860. https://doi.org/10.1038/s41467-020-19453-x

Foran, D. R., & Peterson, A. C. (1992). Paper for timeline of myelination: Myelin acquisition in the central nervous system of the mouse revealed by an MBP-Lac Z transgene. *Journal of Neuroscience*, *12*(12), 4890–4897. https://doi.org/10.1523/JNEUROSCI.12-12-04890.1992

Ford, M. C., Alexandrova, O., Cossell, L., Stange-Marten, A., Sinclair, J., Kopp-Scheinpflug, C., Pecka, M., Attwell, D., & Grothe, B. (2015). Tuning of Ranvier node and internode properties in myelinated axons to adjust action potential timing. *Nature Communications*, *6*, 8073. https://doi.org/10.1038/ncomms9073

Freeman, S. A., Desmazières, A., Fricker, D., Lubetzki, C., & Sol-Foulon, N. (2016). Mechanisms of sodium channel clustering and its influence on axonal impulse conduction. *Cellular and Molecular Life Sciences*, *73*, 723–735. https://doi.org/10.1007/s00018-015-2081-1

Fruttiger, M., Montag, D., Schachner, M., & Martini, R. (1995). Crucial Role for the Myelin-associated Glycoprotein in the Maintenance of Axon-Myelin Integrity. *European Journal of Neuroscience*, *7*(3), 511–515. https://doi.org/10.1111/j.1460-9568.1995.tb00347.x

Fünfschilling, U., Supplie, L. M., Mahad, D., Boretius, S., Saab, A. S., Edgar, J., Brinkmann, B. G., Kassmann, C. M., Tzvetanova, I. D., Möbius, W., Diaz, F., Meijer, D., Suter, U., Hamprecht, B., Sereda, M. W., Moraes, C. T., Frahm, J., Goebbels, S., & Nave, K.-A. (2012). Glycolytic oligodendrocytes maintain myelin and long-term axonal integrity. *Nature*, *485*(7399), 517–521. https://doi.org/10.1038/nature11007

Furukawa, K., Takamiya, K., Okada, M., Inoue, M., Fukumoto, S., & Furukawa, K. (2001). Novel functions of complex carbohydrates elucidated by the mutant mice of glycosyltransferase genes. *Biochimica et Biophysica Acta (BBA) - General Subjects*, *1525*(1), 1–12. https://doi.org/10.1016/S0304-4165(00)00185-9

Gajate, C., Gonzalez-Camacho, F., & Mollinedo, F. (2009). Involvement of Raft Aggregates Enriched in Fas/CD95 Death-Inducing Signaling Complex in the Antileukemic Action of Edelfosine in Jurkat Cells. *PLOS ONE*, *4*(4), e5044. https://doi.org/10.1371/journal.pone.0005044

Gal, J., Katsumata, Y., Zhu, H., Srinivasan, S., Chen, J., Johnson, L. A., Wang, W.-X., Golden, L. R., Wilcock, D. M., Jicha, G. A., Cykowski, M. D., & Nelson, P. T. (2022). Apolipoprotein E Proteinopathy Is a Major Dementia-Associated Pathologic Biomarker in Individuals with or without the APOE Epsilon 4 Allele. *The American Journal of Pathology*, *192*(3), 564–578. https://doi.org/10.1016/j.ajpath.2021.11.013

Gallego-Delgado, P., James, R., Browne, E., Meng, J., Umashankar, S., Tan, L., Picon, C., Mazarakis, N. D., Faisal, A. A., Howell, O. W., & Reynolds, R. (2020a). Neuroinflammation in the normal-appearing white matter (NAWM) of the multiple sclerosis brain causes abnormalities at the nodes of Ranvier. *PLoS Biology*, *18*(12), e3001008. https://doi.org/10.1371/journal.pbio.3001008

Gallego-Delgado, P., James, R., Browne, E., Meng, J., Umashankar, S., Tan, L., Picon, C., Mazarakis, N. D., Faisal, A. A., Howell, O. W., & Reynolds, R. (2020b). Neuroinflammation in the normal-appearing white matter (NAWM) of the multiple sclerosis brain causes abnormalities at the nodes of Ranvier. *PLoS Biology*, *18*(12), e3001008. https://doi.org/10.1371/journal.pbio.3001008

García-Arribas, A. B., Alonso, A., & Goñi, F. M. (2016). Cholesterol interactions with ceramide and sphingomyelin. *Chemistry and Physics of Lipids*, *199*, 26–34. https://doi.org/10.1016/j.chemphyslip.2016.04.002

Garcia-Fresco, G. P., Sousa, A. D., Pillai, A. M., Moy, S. S., Crawley, J. N., Tessarollo, L., Dupree, J. L., & Bhat, M. A. (2006). Disruption of axo-glial junctions causes cytoskeletal disorganization and degeneration of Purkinje neuron axons. *Proceedings of the National Academy of Sciences of the United States of America*, *103*(13), 5137–5142. https://doi.org/10.1073/pnas.0601082103

Gardinier, M. V., Amiguet, P., Linington, C., & Matthieu, J. M. (1992). Myelin/oligodendrocyte glycoprotein is a unique member of the immunoglobulin superfamily. *Journal of Neuroscience Research*, *33*(1), 177–187. https://doi.org/10.1002/jnr.490330123

Gasser, A., Ho, T. S.-Y., Cheng, X., Chang, K.-J., Waxman, S. G., Rasband, M. N., & Dib-Hajj, S. D. (2012). An AnkyrinG-Binding Motif Is Necessary and Sufficient for Targeting Nav1.6 Sodium Channels to Axon Initial Segments and Nodes of Ranvier. *The Journal of Neuroscience*, *32*(21), 7232–7243. https://doi.org/10.1523/JNEUROSCI.5434-11.2012

Gbaguidi, B., Guillemin, F., Soudant, M., Debouverie, M., Mathey, G., & Epstein, J. (2022). Age-period-cohort analysis of the incidence of multiple sclerosis over twenty years in Lorraine, France. *Scientific Reports*, *12*(1), Article 1. https://doi.org/10.1038/s41598-022-04836-5

Grassi, S., Giussani, P., Mauri, L., Prioni, S., Sonnino, S., & Prinetti, A. (2020). Lipid rafts and neurodegeneration: Structural and functional roles in physiologic aging and neurodegenerative diseases: Thematic Review Series: Biology of Lipid Rafts. *Journal of Lipid Research*, *61*(5), 636–654. https://doi.org/10.1194/jlr.TR119000427

Grassi, S., Prioni, S., Cabitta, L., Aureli, M., Sonnino, S., & Prinetti, A. (2016). The Role of 3-O-Sulfogalactosylceramide, Sulfatide, in the Lateral Organization of Myelin Membrane. *Neurochemical Research*, *41*(1), 130–143. https://doi.org/10.1007/s11064-015-1747-2

Griffiths, I., Klugmann, M., Anderson, T., Yool, D., Thomson, C., Schwab, M. H., Schneider, A., Zimmermann, F., McCulloch, M., Nadon, N., & Nave, K. A. (1998). Axonal swellings and degeneration in mice lacking the major proteolipid of myelin. *Science (New York, N.Y.)*, *280*(5369), 1610–1613. https://doi.org/10.1126/science.280.5369.1610

Gutiérrez-Martín, Y., Martín-Romero, F. J., Henao, F., & Gutiérrez-Merino, C. (2005). Alteration of cytosolic free calcium homeostasis by SIN-1: High sensitivity of L-type Ca2+ channels to extracellular oxidative/nitrosative stress in cerebellar granule cells. *Journal of Neurochemistry*, *92*(4), 973–989. https://doi.org/10.1111/j.1471-4159.2004.02964.x

Haines, T. H. (2001). Do sterols reduce proton and sodium leaks through lipid bilayers? *Progress in Lipid Research*, *40*(4), 299–324. https://doi.org/10.1016/s0163-7827(01)00009-1

Han, X. (2004). The role of apolipoprotein E in lipid metabolism in the central nervous system. *Cellular and Molecular Life Sciences*, *61*(15), 1896–1906. https://doi.org/10.1007/s00018-004-4009-z

Han, X. (2007). Potential mechanisms contributing to sulfatide depletion at the earliest clinically recognizable stage of Alzheimer's disease: A tale of shotgun lipidomics. *Journal of Neurochemistry*, *103 Suppl 1*, 171–179. https://doi.org/10.1111/j.1471-4159.2007.04708.x

Han, X. (2010). The Pathogenic Implication of Abnormal Interaction Between Apolipoprotein E Isoforms, Amyloid-beta Peptides, and Sulfatides in Alzheimer's Disease. *Molecular Neurobiology*, *41*(2–3), 97–106. https://doi.org/10.1007/s12035-009-8092-x

Hanada, K., Kumagai, K., Tomishige, N., & Yamaji, T. (2009). CERT-mediated trafficking of ceramide. *Biochimica Et Biophysica Acta*, *1791*(7), 684–691. https://doi.org/10.1016/j.bbalip.2009.01.006

Hartline, D. K. (2008). What is myelin? *Neuron Glia Biology*, *4*(2), 153–163. http://dx.doi.org.proxy.library.vcu.edu/10.1017/S1740925X09990263

Hayashi, A., Kaneko, N., Tomihira, C., & Baba, H. (2013a). Sulfatide decrease in myelin influences formation of the paranodal axo-glial junction and conduction velocity in the sciatic nerve. *Glia*, *61*(4), 466–474. https://doi.org/10.1002/glia.22447

Hayashi, A., Kaneko, N., Tomihira, C., & Baba, H. (2013b). Sulfatide decrease in myelin influences formation of the paranodal axo-glial junction and conduction velocity in the sciatic nerve. *Glia*, *61*(4), 466–474. https://doi.org/10.1002/glia.22447

Hayes, L. W., & Jungawala, F. B. (1976). *Synthesis and Turnover of Cerebrosides and Phosphatidylserine of Myelin and Mcrosomal Fractions of Adult and Developing Rat Brain*. *160*, 10.

Hedstrom, K. L., Xu, X., Ogawa, Y., Frischknecht, R., Seidenbecher, C. I., Shrager, P., & Rasband, M. N. (2007). Neurofascin assembles a specialized extracellular matrix at the axon initial segment. *The Journal of Cell Biology*, *178*(5), 875–886. https://doi.org/10.1083/jcb.200705119

Hinman, J. D., Chen, C.-D., Oh, S.-Y., Hollander, W., & Abraham, C. R. (2008). Age-dependent accumulation of ubiquitinated 2',3'-cyclic nucleotide 3'-phosphodiesterase in myelin lipid rafts. *Glia*, *56*(1), 118–133. https://doi.org/10.1002/glia.20595

Hirahara, Y., Tsuda, M., Wada, Y., & Honke, K. (2000). CDNA cloning, genomic cloning, and tissue-specific regulation of mouse cerebroside sulfotransferase. *European Journal of Biochemistry*, *267*(7), 1909–1917. https://doi.org/10.1046/j.1432-1327.2000.01139.x

Hirahara, Y., Wakabayashi, T., Mori, T., Koike, T., Yao, I., Tsuda, M., Honke, K., Gotoh, H., Ono, K., & Yamada, H. (2017). Sulfatide species with various fatty acid chains in oligodendrocytes at different developmental stages determined by imaging mass spectrometry. *Journal of Neurochemistry*, *140*(3), 435–450. https://doi.org/10.1111/jnc.13897

Hirano, K., Kinoshita, M., & Matsumori, N. (2022). Impact of sphingomyelin acyl chain heterogeneity upon properties of raft-like membranes. *Biochimica Et Biophysica Acta. Biomembranes*, *1864*(12), 184036. https://doi.org/10.1016/j.bbamem.2022.184036

Hivert, B., Pinatel, D., Labasque, M., Tricaud, N., Goutebroze, L., & Faivre-Sarrailh, C. (2016). Assembly of juxtaparanodes in myelinating DRG culture: Differential clustering of the Kv1/Caspr2 complex and scaffolding protein 4.1B. *Glia*, *64*(5), 840–852. https://doi.org/10.1002/glia.22968

Holcomb, P. S., Deerinck, T. J., Ellisman, M. H., & Spirou, G. A. (2013). Construction of a polarized neuron. *The Journal of Physiology*, *591*(13), 3145–3150. https://doi.org/10.1113/jphysiol.2012.248542

Honke, K., Hirahara, Y., Dupree, J., Suzuki, K., Popko, B., Fukushima, K., Fukushima, J., Nagasawa, T., Yoshida, N., Wada, Y., & Taniguchi, N. (2002). Paranodal junction formation and spermatogenesis require sulfoglycolipids. *Proceedings of the National Academy of Sciences of the United States of America*, *99*(7), 4227–4232. https://doi.org/10.1073/pnas.032068299

Honke, K., Tsuda, M., Hirahara, Y., Ishii, A., Makita, A., & Wada, Y. (1997). Molecular cloning and expression of cDNA encoding human 3'-phosphoadenylylsulfate:galactosylceramide 3'-sulfotransferase. *The Journal of Biological Chemistry*, *272*(8), 4864–4868. https://doi.org/10.1074/jbc.272.8.4864

Hope, H. R., & Pike, L. J. (1996). Phosphoinositides and phosphoinositide-utilizing enzymes in detergent-insoluble lipid domains. *Molecular Biology of the Cell*, *7*(6), 843–851. https://doi.org/10.1091/mbc.7.6.843

Horbay, R., Hamraghani, A., Ermini, L., Holcik, S., Beug, S. T., & Yeganeh, B. (2022). Role of Ceramides and Lysosomes in Extracellular Vesicle Biogenesis, Cargo Sorting and Release. *International Journal of Molecular Sciences*, *23*(23), 15317. https://doi.org/10.3390/ijms232315317

Howell, O. W., Palser, A., Polito, A., Melrose, S., Zonta, B., Scheiermann, C., Vora, A. J., Brophy, P. J., & Reynolds, R. (2006a). Disruption of neurofascin localization reveals early changes preceding demyelination and remyelination in multiple sclerosis. *Brain*, *129*(12), 3173–3185. https://doi.org/10.1093/brain/awl290

Howell, O. W., Palser, A., Polito, A., Melrose, S., Zonta, B., Scheiermann, C., Vora, A. J., Brophy, P. J., & Reynolds, R. (2006b). Disruption of neurofascin localization reveals early changes preceding demyelination and remyelination in multiple sclerosis. *Brain*, *129*(12), 3173–3185. https://doi.org/10.1093/brain/awl290

Howell, Owain. W., Rundle, Jon. L., Garg, A., Komada, M., Brophy, Peter. J., & Reynolds, R. (2010). Activated microglia mediate axo-glial disruption that contributes to axonal injury in multiple sclerosis. *Journal of Neuropathology and Experimental Neurology*, *69*(10), 1017–1033. https://doi.org/10.1097/NEN.0b013e3181f3a5b1

Hughes, E. G., Kang, S. H., Fukaya, M., & Bergles, D. E. (2013). Oligodendrocyte progenitors balance growth with self-repulsion to achieve homeostasis in the adult brain. *Nature Neuroscience*, *16*(6), 668–676. https://doi.org/10.1038/nn.3390

Huxley, A. F., & Stämpeli, R. (1949). Evidence for saltatory conduction in peripheral myelinated nerve fibres. *The Journal of Physiology*, *108*(3), 315–339. https://doi.org/10.1113/jphysiol.1949.sp004335

Inglese, M., Fleysher, L., Oesingmann, N., & Petracca, M. (2018). Clinical applications of ultra-high field magnetic resonance imaging in multiple sclerosis. *Expert Review of Neurotherapeutics*, *18*(3), 221–230. https://doi.org/10.1080/14737175.2018.1433033

Isaac, G., Pernber, Z., Gieselmann, V., Hansson, E., Bergquist, J., & Månsson, J.-E. (2006). Sulfatide with short fatty acid dominates in astrocytes and neurons. *The FEBS Journal*, *273*(8), 1782–1790. https://doi.org/10.1111/j.1742-4658.2006.05195.x

Ishibashi, T., Dupree, J. L., Ikenaka, K., Hirahara, Y., Honke, K., Peles, E., Popko, B., Suzuki, K., Nishino, H., & Baba, H. (2002a). A myelin galactolipid, sulfatide, is essential for maintenance of ion channels on myelinated axon but not

essential for initial cluster formation. *The Journal of Neuroscience: The Official Journal of the Society for Neuroscience*, *22*(15), 6507–6514. https://doi.org/20026705

Ishibashi, T., Dupree, J. L., Ikenaka, K., Hirahara, Y., Honke, K., Peles, E., Popko, B., Suzuki, K., Nishino, H., & Baba, H. (2002b). A Myelin Galactolipid, Sulfatide, Is Essential for Maintenance of Ion Channels on Myelinated Axon But Not Essential for Initial Cluster Formation. *The Journal of Neuroscience*, *22*(15), 6507–6514. https://doi.org/10.1523/JNEUROSCI.22-15-06507.2002

Isik, O. A., & Cizmecioglu, O. (2023). Rafting on the Plasma Membrane: Lipid Rafts in Signaling and Disease. *Advances in Experimental Medicine and Biology*. https://doi.org/10.1007/5584_2022_759

Jablonska, B., Gierdalski, M., Chew, L.-J., Hawley, T., Catron, M., Lichauco, A., Cabrera-Luque, J., Yuen, T., Rowitch, D., & Gallo, V. (2016). Sirt1 regulates glial progenitor proliferation and regeneration in white matter after neonatal brain injury. *Nature Communications*, *7*, 13866. https://doi.org/10.1038/ncomms13866

Jafari, A., Babajani, A., & Rezaei-Tavirani, M. (2021). Multiple Sclerosis Biomarker Discoveries by Proteomics and Metabolomics Approaches. *Biomarker Insights*, *16*, 11772719211013352. https://doi.org/10.1177/11772719211013352

Jahn, O., Tenzer, S., & Werner, H. B. (2009). Myelin Proteomics: Molecular Anatomy of an Insulating Sheath. *Molecular Neurobiology*, *40*(1), 55–72. https://doi.org/10.1007/s12035-009-8071-2

Jahng, A., Maricic, I., Aguilera, C., Cardell, S., Halder, R. C., & Kumar, V. (2004). Prevention of Autoimmunity by Targeting a Distinct, Noninvariant CD1d-reactive T Cell Population Reactive to Sulfatide. *The Journal of Experimental Medicine*, *199*(7), 947–957. https://doi.org/10.1084/jem.20031389

Janssen, B. J. C. (2018). Inside-out or outside-in, a new factor in MAG-mediated signaling in the nervous system: An Editorial for “High-affinity heterotetramer formation between the large myelin-associated glycoprotein and the dynein light chain DYNLL1” on page 764. *Journal of Neurochemistry*, *147*(6), 712–714. https://doi.org/10.1111/jnc.14597

Jeon, S.-B., Yoon, H. J., Park, S.-H., Kim, I.-H., & Park, E. J. (2008). Sulfatide, A Major Lipid Component of Myelin Sheath, Activates Inflammatory Responses As an Endogenous Stimulator in Brain-Resident Immune Cells. *The Journal of Immunology*, *181*(11), 8077–8087. https://doi.org/10.4049/jimmunol.181.11.8077

Johns, T. G., & Bernard, C. C. A. (1999). The Structure and Function of Myelin Oligodendrocyte Glycoprotein. *Journal of Neurochemistry*, *72*(1), 1–9. https://doi.org/10.1046/j.1471-4159.1999.0720001.x

Joseph, S., Vingill, S., Jahn, O., Fledrich, R., Werner, H. B., Katona, I., Möbius, W., Mitkovski, M., Huang, Y., Weis, J., Sereda, M. W., Schulz, J. B., Nave, K.-A., & Stegmüller, J. (2019). Myelinating Glia-Specific Deletion of Fbxo7 in Mice Triggers Axonal Degeneration in the Central Nervous System Together with Peripheral Neuropathy. *The Journal of Neuroscience: The Official Journal of the Society for Neuroscience*, *39*(28), 5606–5626. https://doi.org/10.1523/JNEUROSCI.3094-18.2019

Kapoor, R., Davies, M., Blaker, P. A., Hall, S. M., & Smith, K. J. (2003). Blockers of sodium and calcium entry protect axons from nitric oxide-mediated degeneration. *Annals of Neurology*, *53*(2), 174–180. https://doi.org/10.1002/ana.10443

Káradóttir, R., Hamilton, N. B., Bakiri, Y., & Attwell, D. (2008). Spiking and non-spiking classes of oligodendrocyte precursor glia in CNS white matter. *Nature Neuroscience*, *11*(4), 450–456. https://doi.org/10.1038/nn2060

Kim, J. K., Mastronardi, F. G., Wood, D. D., Lubman, D. M., Zand, R., & Moscarello, M. A. (2003). Multiple sclerosis: An important role for post-translational modifications of myelin basic protein in pathogenesis. *Molecular & Cellular Proteomics: MCP*, *2*(7), 453–462. https://doi.org/10.1074/mcp.M200050-MCP200

Kim, N.-S., & Chung, W.-S. (2023). Astrocytes regulate neuronal network activity by mediating synapse remodeling. *Neuroscience Research*, *187*, 3–13. https://doi.org/10.1016/j.neures.2022.09.007

Kim, T., & Pfeiffer, S. E. (1999). Myelin glycosphingolipid/cholesterol-enriched microdomains selectively sequester the non-compact myelin proteins CNP and MOG. *Journal of Neurocytology*, *28*(4), 281–293.

Kim, Y., Park, J., & Choi, Y. K. (2019). The Role of Astrocytes in the Central Nervous System Focused on BK Channel and Heme Oxygenase Metabolites: A Review. *Antioxidants*, *8*(5), 121. https://doi.org/10.3390/antiox8050121

Kister, A., & Kister, I. (2022). Overview of myelin, major myelin lipids, and myelin-associated proteins. *Frontiers in Chemistry*, *10*, 1041961. https://doi.org/10.3389/fchem.2022.1041961

Klar, T. A., Engel, E., & Hell, S. W. (2001). Breaking Abbe's diffraction resolution limit in fluorescence microscopy with stimulated emission depletion beams of various shapes. *Physical Review. E, Statistical, Nonlinear, and Soft Matter Physics*, *64*(6 Pt 2), 066613. https://doi.org/10.1103/PhysRevE.64.066613

Klingseisen, A., Ristoiu, A.-M., Kegel, L., Sherman, D. L., Rubio-Brotons, M., Almeida, R. G., Koudelka, S., Benito-Kwiecinski, S. K., Poole, R. J., Brophy, P. J., & Lyons, D. A. (2019). Oligodendrocyte Neurofascin Independently Regulates Both Myelin Targeting and Sheath Growth in the CNS. *Developmental Cell*, *51*(6), 730-744.e6. https://doi.org/10.1016/j.devcel.2019.10.016

Klugmann, M., Schwab, M. H., Pühlhofer, A., Schneider, A., Zimmermann, F., Griffiths, I. R., & Nave, K.-A. (1997). Assembly of CNS Myelin in the Absence of Proteolipid Protein. *Neuron*, *18*(1), 59–70. https://doi.org/10.1016/S0896-6273(01)80046-5

Knapp, P. E., Skoff, R. P., & Sprinkle, T. J. (1988). Differential expression of galactocerebroside, myelin basic protein, and 2′,3′-cyclic nucleotide 3′-phosphohydrolase during development of oligodendrocytes in vitro. *Journal of Neuroscience Research*, *21*(2–4), 249–259. https://doi.org/10.1002/jnr.490210217

Koch-Henriksen, N., & Sørensen, P. S. (2010). The changing demographic pattern of multiple sclerosis epidemiology. *The Lancet. Neurology*, *9*(5), 520–532. https://doi.org/10.1016/S1474-4422(10)70064-8

Kojima, W., & Hayashi, K. (2018). Changes in the axo-glial junctions of the optic nerves of cuprizone-treated mice. *Histochemistry and Cell Biology*, *149*(5), 529–536. https://doi.org/10.1007/s00418-018-1654-0

Kovacs, T., Zakany, F., & Nagy, P. (2022). It Takes More than Two to Tango: Complex, Hierarchal, and Membrane-Modulated Interactions in the Regulation of Receptor Tyrosine Kinases. *Cancers*, *14*(4), Article 4. https://doi.org/10.3390/cancers14040944

Krysko, K. M., Graves, J. S., Rensel, M., Weinstock-Guttman, B., Rutatangwa, A., Aaen, G., Belman, A., Benson, L., Chitnis, T., Gorman, M., Goyal, M. S., Harris, Y., Krupp, L., Lotze, T., Mar, S., Moodley, M., Ness, J., Rodriguez, M., Rose, J., … Centers, the U. N. of P. M. (2020). Real-World Effectiveness of Initial Disease-Modifying Therapies in Pediatric Multiple Sclerosis. *Annals of Neurology*, *88*(1), 42–55. https://doi.org/10.1002/ana.25737

Kunz, B., Lierheimer, R., Rader, C., Spirig, M., Ziegler, U., & Sonderegger, P. (2002). Axonin-1/TAG-1 Mediates Cell-Cell Adhesion by a Cis-assisted Trans-interaction *. *Journal of Biological Chemistry*, *277*(6), 4551–4557. https://doi.org/10.1074/jbc.M109779200

Laganowsky, A., Reading, E., Allison, T. M., Ulmschneider, M. B., Degiacomi, M. T., Baldwin, A. J., & Robinson, C. V. (2014). Membrane proteins bind lipids selectively to modulate their structure and function. *Nature*, *510*(7503), Article 7503. https://doi.org/10.1038/nature13419

Lappe-Siefke, C., Goebbels, S., Gravel, M., Nicksch, E., Lee, J., Braun, P. E., Griffiths, I. R., & Nave, K.-A. (2003). Disruption of Cnp1 uncouples oligodendroglial functions in axonal support and myelination. *Nature Genetics*, *33*(3), 366–374. https://doi.org/10.1038/ng1095

Larson, V. A., Mironova, Y., Vanderpool, K. G., Waisman, A., Rash, J. E., Agarwal, A., & Bergles, D. E. (2018). Oligodendrocytes control potassium accumulation in white matter and seizure susceptibility. *ELife*, *7*, e34829. https://doi.org/10.7554/eLife.34829

Lassetter, A. P., Corty, M. M., Barria, R., Sheehan, A. E., Hill, J. Q., Aicher, S. A., Fox, A. N., & Freeman, M. R. (2023). Glial TGFβ activity promotes neuron survival in peripheral nerves. *The Journal of Cell Biology*, *222*(1), e202111053. https://doi.org/10.1083/jcb.202111053

Laviad, E. L., Albee, L., Pankova-Kholmyansky, I., Epstein, S., Park, H., Merrill, A. H., & Futerman, A. H. (2008). Characterization of Ceramide Synthase 2 TISSUE DISTRIBUTION, SUBSTRATE SPECIFICITY, AND INHIBITION BY SPHINGOSINE 1-PHOSPHATE. *Journal of Biological Chemistry*, *283*(9), 5677–5684. https://doi.org/10.1074/jbc.M707386200

Lee, J., Gravel, M., Gao, E., O'Neill, R. C., & Braun, P. E. (2001). Identification of Essential Residues in 2',3'-Cyclic Nucleotide 3'-Phosphodiesterase: CHEMICAL MODIFICATION AND SITE-DIRECTED MUTAGENESIS TO INVESTIGATE THE ROLE OF CYSTEINE AND HISTIDINE RESIDUES IN ENZYMATIC ACTIVITY *. *Journal of Biological Chemistry*, *276*(18), 14804–14813. https://doi.org/10.1074/jbc.M009434200

Lee, Y., Morrison, B. M., Li, Y., Lengacher, S., Farah, M. H., Hoffman, P. N., Liu, Y., Tsingalia, A., Jin, L., Zhang, P.-W., Pellerin, L., Magistretti, P. J., & Rothstein, J. D. (2012). Oligodendroglia metabolically support axons and contribute to neurodegeneration. *Nature*, *487*(7408), 443–448. https://doi.org/10.1038/nature11314

Li, C., Tropak, M. B., Gerlai, R., Clapoff, S., Abramow-Newerly, W., Trapp, B., Peterson, A., & Roder, J. (1994). Myelination in the absence of myelin-associated glycoprotein. *Nature*, *369*(6483), 747–750. https://doi.org/10.1038/369747a0

Li, S., & Sheng, Z.-H. (2023). Oligodendrocyte-derived transcellular signaling regulates axonal energy metabolism. *Current Opinion in Neurobiology*, *80*, 102722. https://doi.org/10.1016/j.conb.2023.102722

Li, T., Wang, J., Wang, H., Yang, Y., Wang, S., Huang, N., Wang, F., Gao, X., Niu, J., Li, Z., Mei, F., & Xiao, L. (2018). The deletion of dicer in mature myelinating glial cells causes progressive axonal degeneration but not overt demyelination in adult mice. *Glia*, *66*(9), 1960–1971. https://doi.org/10.1002/glia.23450

Lichtenberg, D. (2005). *Detergent-resistant membranes should not be identified with membrane rafts*. 7.

Lim, B. C., & Rasband, M. N. (2020). Saltatory Conduction: Jumping to New Conclusions. *Current Biology*, *30*(7), R326–R328. https://doi.org/10.1016/j.cub.2020.02.037

Lin, S.-C., & Bergles, D. E. (2004). Synaptic signaling between neurons and glia. *Glia*, *47*(3), 290–298. https://doi.org/10.1002/glia.20060

Lopez, P. H. H. (2014). Role of myelin-associated glycoprotein (siglec-4a) in the nervous system. *Advances in Neurobiology*, *9*, 245–262. https://doi.org/10.1007/978-1-4939-1154-7_11

Luchicchi, A., Hart, B., Frigerio, I., van Dam, A., Perna, L., Offerhaus, H. L., Stys, P. K., Schenk, G. J., & Geurts, J. J. G. (2021a). Axon-Myelin Unit Blistering as Early Event in MS Normal Appearing White Matter. *Annals of Neurology*, *89*(4), 711–725. https://doi.org/10.1002/ana.26014

Luchicchi, A., Hart, B., Frigerio, I., van Dam, A.-M., Perna, L., Offerhaus, H. L., Stys, P. K., Schenk, G. J., & Geurts, J. J. G. (2021b). Axon-Myelin Unit Blistering as Early Event in MS Normal Appearing White Matter. *Annals of Neurology*, *89*(4), 711–725. https://doi.org/10.1002/ana.26014

Madsen, P. M., Desu, H. L., Vaccari, J. P. de R., Florimon, Y., Ellman, D. G., Keane, R. W., Clausen, B. H., Lambertsen, K. L., & Brambilla, R. (2020). Oligodendrocytes modulate the immune-inflammatory response in EAE via TNFR2 signaling. *Brain, Behavior, and Immunity*, *84*, 132–146. https://doi.org/10.1016/j.bbi.2019.11.017

Mahad, D. J., Ziabreva, I., Campbell, G., Lax, N., White, K., Hanson, P. S., Lassmann, H., & Turnbull, D. M. (2009). Mitochondrial changes within axons in multiple sclerosis. *Brain: A Journal of Neurology*, *132*(Pt 5), 1161–1174. https://doi.org/10.1093/brain/awp046

Maier, O., Hoekstra, D., & Baron, W. (2008). Polarity Development in Oligodendrocytes: Sorting and Trafficking of Myelin Components. *Journal of Molecular Neuroscience*, *35*(1), 35–53. https://doi.org/10.1007/s12031-007-9024-8

Makhani, N., & Tremlett, H. (2021). The multiple sclerosis prodrome. *Nature Reviews. Neurology*, *17*(8), 515–521. https://doi.org/10.1038/s41582-021-00519-3

Mallon, B. S., Shick, H. E., Kidd, G. J., & Macklin, W. B. (2002). Proteolipid Promoter Activity Distinguishes Two Populations of NG2-Positive Cells throughout Neonatal Cortical Development. *The Journal of Neuroscience*, *22*(3), 876–885. https://doi.org/10.1523/JNEUROSCI.22-03-00876.2002

Marbois, B. N., Faull, K. F., Fluharty, A. L., Raval-Fernandes, S., & Rome, L. H. (2000). Analysis of sulfatide from rat cerebellum and multiple sclerosis white matter by negative ion electrospray mass spectrometry. *Biochimica et Biophysica Acta (BBA) - Molecular and Cell Biology of Lipids*, *1484*(1), 59–70. https://doi.org/10.1016/S1388-1981(99)00201-2

Marcus, J., Dupree, J. L., & Popko, B. (2002). Myelin-associated glycoprotein and myelin galactolipids stabilize developing axo-glial interactions. *The Journal of Cell Biology*, *156*(3), 567–577. https://doi.org/10.1083/jcb.200111047

Marcus, J., Honigbaum, S., Shroff, S., Honke, K., Rosenbluth, J., & Dupree, J. L. (2006). Sulfatide is essential for the maintenance of CNS myelin and axon structure. *Glia*, *53*(4), 372–381. https://doi.org/10.1002/glia.20292

Maricic, I., Halder, R., Bischof, F., & Kumar, V. (2014). Dendritic cells and anergic type I NKT cells play a crucial role in sulfatide-mediated immune regulation in experimental autoimmune encephalomyelitis. *Journal of Immunology (Baltimore, Md. : 1950)*, *193*(3), 1035–1046. https://doi.org/10.4049/jimmunol.1302898

Marques, S., Zeisel, A., Codeluppi, S., van Bruggen, D., Mendanha Falcão, A., Xiao, L., Li, H., Häring, M., Hochgerner, H., Romanov, R. A., Gyllborg, D., Muñoz Manchado, A., La Manno, G., Lönnerberg, P., Floriddia, E. M., Rezayee, F., Ernfors, P., Arenas, E., Hjerling-Leffler, J., … Castelo-Branco, G. (2016). Oligodendrocyte heterogeneity in the mouse juvenile and adult central nervous system. *Science (New York, N.Y.)*, *352*(6291), 1326–1329. https://doi.org/10.1126/science.aaf6463

Martini, R., & Schachner, M. (1986). Immunoelectron microscopic localization of neural cell adhesion molecules (L1, N-CAM, and MAG) and their shared carbohydrate epitope and myelin basic protein in developing sciatic nerve. *The Journal of Cell Biology*, *103*(6 Pt 1), 2439–2448. https://doi.org/10.1083/jcb.103.6.2439

Mason, J. L., Langaman, C., Morell, P., Suzuki, K., & Matsushima, G. K. (2001). Episodic demyelination and subsequent remyelination within the murine central nervous system: Changes in axonal calibre. *Neuropathology and Applied Neurobiology*, *27*(1), 50–58. https://doi.org/10.1046/j.0305-1846.2001.00301.x

Maurel, P., Einheber, S., Galinska, J., Thaker, P., Lam, I., Rubin, M. B., Scherer, S. S., Murakami, Y., Gutmann, D. H., & Salzer, J. L. (2007). Nectin-like proteins mediate axon Schwann cell interactions along the internode and are essential for myelination. *The Journal of Cell Biology*, *178*(5), 861–874. https://doi.org/10.1083/jcb.200705132

Mayer, J. A., Larsen, E. C., Kondo, Y., & Duncan, I. D. (2011). Characterization of a PLP-overexpressing transgenic rat, a model for the connatal form of Pelizaeus-Merzbacher disease. *Neurobiology of Disease*, *44*(2), 231–238. https://doi.org/10.1016/j.nbd.2011.07.007

McGinley, M. P., & Cohen, J. A. (2021). Sphingosine 1-phosphate receptor modulators in multiple sclerosis and other conditions. *Lancet (London, England)*, *398*(10306), 1184–1194. https://doi.org/10.1016/S0140-6736(21)00244-0

McGonigal, R., Barrie, J. A., Yao, D., McLaughlin, M., Cunningham, M. E., Rowan, E. G., & Willison, H. J. (2019). Glial Sulfatides and Neuronal Complex Gangliosides Are Functionally Interdependent in Maintaining Myelinating Axon Integrity. *Journal of Neuroscience*, *39*(1), 63–77. https://doi.org/10.1523/JNEUROSCI.2095-18.2018

McGonigal, R., Cunningham, M. E., Smyth, D., Chou, M., Barrie, J. A., Wilkie, A., Campbell, C., Saatman, K. E., Lunn, M., & Willison, H. J. (2023). The endogenous calpain inhibitor calpastatin attenuates axon degeneration in murine Guillain-Barré syndrome. *Journal of the Peripheral Nervous System: JPNS*, *28*(1), 4–16. https://doi.org/10.1111/jns.12520

McKie, S. J., Nicholson, A. S., Smith, E., Fawke, S., Caroe, E. R., Williamson, J. C., Butt, B. G., Kolářová, D., Peterka, O., Holčapek, M., Lehner, P. J., Graham, S. C., & Deane, J. E. (2023). Altered plasma membrane abundance of the sulfatide-binding protein NF155 links glycosphingolipid imbalances to demyelination. *Proceedings of the National Academy of Sciences*, *120*(14), e2218823120. https://doi.org/10.1073/pnas.2218823120

Mei, F., Wang, H., Liu, S., Niu, J., Wang, L., He, Y., Etxeberria, A., Chan, J. R., & Xiao, L. (2013). Stage-Specific Deletion of Olig2 Conveys Opposing Functions on Differentiation and Maturation of Oligodendrocytes. *Journal of Neuroscience*, *33*(19), 8454–8462. https://doi.org/10.1523/JNEUROSCI.2453-12.2013

Melkonian, K. A., Ostermeyer, A. G., Chen, J. Z., Roth, M. G., & Brown, D. A. (1999). Role of lipid modifications in targeting proteins to detergent-resistant membrane rafts. Many raft proteins are acylated, while few are prenylated. *The Journal of Biological Chemistry*, *274*(6), 3910–3917. https://doi.org/10.1074/jbc.274.6.3910

Meller, D., Eysel, U. T., & Schmidt-Kastner, R. (1994). Transient immunohistochemical labelling of rat retinal axons during Wallerian degeneration by a monoclonal antibody to neurofilaments. *Brain Research*, *648*(1), 162–166. https://doi.org/10.1016/0006-8993(94)91917-8

Micheva, K. D., Kiraly, M., Perez, M. M., & Madison, D. V. (2021). Conduction Velocity Along the Local Axons of Parvalbumin Interneurons Correlates With the Degree of Axonal Myelination. *Cerebral Cortex (New York, N.Y.: 1991)*, *31*(7), 3374–3392. https://doi.org/10.1093/cercor/bhab018

Mierzwa, A. J., Arevalo, J.-C., Schiff, R., Chao, M. V., & Rosenbluth, J. (2010a). Role of transverse bands in maintaining paranodal structure and axolemmal domain organization in myelinated nerve fibers: Effect on longevity in dysmyelinated mutant mice. *The Journal of Comparative Neurology*, *518*(14), 2841–2853. https://doi.org/10.1002/cne.22367

Mierzwa, A. J., Arevalo, J.-C., Schiff, R., Chao, M. V., & Rosenbluth, J. (2010b). Role of transverse bands in maintaining paranodal structure and axolemmal domain organization in myelinated nerve fibers: Effect on longevity in dysmyelinated mutant mice. *The Journal of Comparative Neurology*, *518*(14), 2841–2853. https://doi.org/10.1002/cne.22367

Mierzwa, A. J., Marion, C. M., Sullivan, G. M., McDaniel, D. P., & Armstrong, R. C. (2015). Components of Myelin Damage and Repair in the Progression of White Matter Pathology After Mild Traumatic Brain Injury. *Journal of Neuropathology and Experimental Neurology*, *74*(3), 218–232. https://doi.org/10.1097/NEN.0000000000000165

Mierzwa, A. J., Zhou, Y.-X., Hibbits, N., Vana, A. C., & Armstrong, R. C. (2013). FGF2 and FGFR1 Signaling Regulate Functional Recovery Following Cuprizone Demyelination. *Neuroscience Letters*, *548*, 280–285. https://doi.org/10.1016/j.neulet.2013.05.010

Milner, R. J., Lai, C., Nave, K.-A., Lenoir, D., Ogata, J., & Sutcliffe, J. G. (1985). Nucleotide sequences of two mRNAs for rat brain myelin proteolipid protein. *Cell*, *42*(3), 931–939. https://doi.org/10.1016/0092-8674(85)90289-2

Moccia, M., Ruggieri, S., Ianniello, A., Toosy, A., Pozzilli, C., & Ciccarelli, O. (2019). Advances in spinal cord imaging in multiple sclerosis. *Therapeutic Advances in Neurological Disorders*, *12*, 1756286419840593. https://doi.org/10.1177/1756286419840593

Molander-Melin, M., Pernber, Z., Franken, S., Gieselmann, V., Månsson, J.-E., & Fredman, P. (2004). Accumulation of sulfatide in neuronal and glial cells of arylsulfatase A deficient mice. *Journal of Neurocytology*, *33*(4), 417–427. https://doi.org/10.1023/B:NEUR.0000046572.53905.2c

Mollinedo, F., & Gajate, C. (2020). Lipid rafts as signaling hubs in cancer cell survival/death and invasion: Implications in tumor progression and therapy. *Journal of Lipid Research*, *61*(5), 611–635. https://doi.org/10.1194/jlr.TR119000439

Moore, J. W., Joyner, R. W., Brill, M. H., Waxman, S. D., & Najar-Joa, M. (1978). Simulations of conduction in uniform myelinated fibers. Relative sensitivity to changes in nodal and internodal parameters. *Biophysical Journal*, *21*(2), 147–160. https://doi.org/10.1016/S0006-3495(78)85515-5

Morell, P., & Quarles, R. H. (1999). Characteristic Composition of Myelin. *Basic Neurochemistry: Molecular, Cellular and Medical Aspects. 6th Edition*. https://www.ncbi.nlm.nih.gov/books/NBK28221/

Morell, P., & Radin, N. S. (1969). Synthesis of cerebroside by brain from uridine diphosphate galactose and ceramide containing hydroxy fatty acid. *Biochemistry*, *8*(2), 506–512. https://doi.org/10.1021/bi00830a008

Morrison, B. M., Lee, Y., & Rothstein, J. D. (2013). Oligodendroglia metabolically support axons and maintain structural integrity. *Trends in Cell Biology*, *23*(12). https://doi.org/10.1016/j.tcb.2013.07.007

Moscatelli, E. A., & Isaacson, E. (1969). Gas liquid chromatographic analysis of sphingosine bases in sphingolipids of human normal and multiple sclerosis cerebral white matter. *Lipids*, *4*(6), 550–555. https://doi.org/10.1007/BF02531040

Moyano, A. L., Li, G., Boullerne, A. I., Feinstein, D. L., Hartman, E., Skias, D., Balavanov, R., van Breemen, R. B., Bongarzone, E. R., Månsson, J.-E., & Givogri, M. I. (2016). Sulfatides in extracellular vesicles isolated from plasma of multiple sclerosis patients. *Journal of Neuroscience Research*, *94*(12), 1579–1587. https://doi.org/10.1002/jnr.23899

Moyano, A. L., Pituch, K., Li, G., Breemen, R. van, Mansson, J. E., & Givogri, M. I. (2013). Levels of plasma sulfatides C18: 0 and C24 : 1 correlate with disease status in relapsing–remitting multiple sclerosis. *Journal of Neurochemistry*, *127*(5), 600–604. https://doi.org/10.1111/jnc.12341

Mukherjee, C., Kling, T., Russo, B., Miebach, K., Kess, E., Schifferer, M., Pedro, L. D., Weikert, U., Fard, M. K., Kannaiyan, N., Rossner, M., Aicher, M.-L., Goebbels, S., Nave, K.-A., Krämer-Albers, E.-M., Schneider, A., & Simons, M. (2020). Oligodendrocytes Provide Antioxidant Defense Function for Neurons by Secreting Ferritin Heavy Chain. *Cell Metabolism*, *32*(2), 259-272.e10. https://doi.org/10.1016/j.cmet.2020.05.019

Muzio, L., Viotti, A., & Martino, G. (2021). Microglia in Neuroinflammation and Neurodegeneration: From Understanding to Therapy. *Frontiers in Neuroscience*, *15*, 742065. https://doi.org/10.3389/fnins.2021.742065

Nagan, N., & Zoeller, R. A. (2001). Plasmalogens: Biosynthesis and functions. *Progress in Lipid Research*, *40*(3), 199–229. https://doi.org/10.1016/S0163-7827(01)00003-0

Nave, K. A., Lai, C., Bloom, F. E., & Milner, R. J. (1987). Splice site selection in the proteolipid protein (PLP) gene transcript and primary structure of the DM-20 protein of central nervous system myelin. *Proceedings of the National Academy of Sciences of the United States of America*, *84*(16), 5665–5669.

Nave, K.-A. (2010). Myelination and the trophic support of long axons. *Nature Reviews. Neuroscience*, *11*(4), 275–283. https://doi.org/10.1038/nrn2797

Norton, W. T., & Cammer, W. (1984). Isolation and Characterization of Myelin. In P. Morell (Ed.), *Myelin* (pp. 147–195). Springer US. https://doi.org/10.1007/978-1-4757-1830-0_5

Novakova, L., Henricsson, M., Björnson, E., Axelsson, M., Borén, J., Rosenstein, I., Lycke, J., Cardell, S. L., & Blomqvist, M. (2023). Cerebrospinal fluid sulfatide isoforms lack diagnostic utility in separating progressive from relapsing-remitting multiple sclerosis. *Multiple Sclerosis and Related Disorders*, *74*, 104705. https://doi.org/10.1016/j.msard.2023.104705

Novakova, L., Singh, A. K., Axelsson, M., Ståhlman, M., Adiels, M., Malmeström, C., Zetterberg, H., Borén, J., Lycke, J., Cardell, S. L., & Blomqvist, M. (2018). Sulfatide isoform pattern in cerebrospinal fluid discriminates progressive MS from relapsing-remitting MS. *Journal of Neurochemistry*, *146*(3), 322–332. https://doi.org/10.1111/jnc.14452

O'brien, J. S. (1965). STABILITY OF THE MYELIN MEMBRANE. *Science (New York, N.Y.)*, *147*(3662), 1099–1107. https://doi.org/10.1126/science.147.3662.1099

O'Brien, J. S., & Sampson, E. L. (1965). Lipid composition of the normal human brain: Gray matter, white matter, and myelin. *Journal of Lipid Research*, *6*(4), 537–544.

O'Connor, K. C., Bar-Or, A., & Hafler, D. A. (2001). The Neuroimmunology of Multiple Sclerosis: Possible Roles of T and B Lymphocytes in Immunopathogenesis. *Journal of Clinical Immunology*, *21*(2), 12.

Ogawa, Y., Schafer, D. P., Horresh, I., Bar, V., Hales, K., Yang, Y., Susuki, K., Peles, E., Stankewich, M. C., & Rasband, M. N. (2006). Spectrins and AnkyrinB Constitute a Specialized Paranodal Cytoskeleton. *Journal of Neuroscience*, *26*(19), 5230–5239. https://doi.org/10.1523/JNEUROSCI.0425-06.2006

Ohvo-Rekilä, H., Ramstedt, B., Leppimäki, P., & Slotte, J. P. (2002). Cholesterol interactions with phospholipids in membranes. *Progress in Lipid Research*, *41*(1), 66–97. https://doi.org/10.1016/s0163-7827(01)00020-0

Olsson, T., Barcellos, L. F., & Alfredsson, L. (2017). Interactions between genetic, lifestyle and environmental risk factors for multiple sclerosis. *Nature Reviews Neurology*, *13*(1), Article 1. https://doi.org/10.1038/nrneurol.2016.187

Omelchenko, A., Shrirao, A. B., Bhattiprolu, A. K., Zahn, J. D., Schloss, R. S., Dickson, S., Meaney, D. F., Boustany, N. N., Yarmush, M. L., & Firestein, B. L. (2019). Dynamin and reverse-mode sodium calcium exchanger blockade confers neuroprotection from diffuse axonal injury. *Cell Death & Disease*, *10*(10), 727. https://doi.org/10.1038/s41419-019-1908-3

Ovchinnikov, A., & Findling, O. (2022). An overview of pivotal trials and real-world evidence for CD20-depleting therapy in multiple sclerosis: Immunotherapy with rituximab, ocrelizumab, and ofatumumab. *Wiener Medizinische Wochenschrift (1946)*, *172*(15–16), 359–364. https://doi.org/10.1007/s10354-022-00939-w

Owen, T. (1957). Multiple sclerosis. *Canadian Journal of Occupational Therapy. Revue Canadienne D'ergotherapie*, *24*(4), 125–129. https://doi.org/10.1177/000841745702400404

Palavicini, J. P., Ding, L., Pan, M., Qiu, S., Wang, H., Shen, Q., Dupree, J. L., & Han, X. (2022). Sulfatide Deficiency, an Early Alzheimer's Lipidomic Signature, Causes Brain Ventricular Enlargement in the Absence of Classical Neuropathological Hallmarks. *International Journal of Molecular Sciences*, *24*(1), 233. https://doi.org/10.3390/ijms24010233

Palavicini, J. P., Wang, C., Chen, L., Ahmar, S., Higuera, J. D., Dupree, J. L., & Han, X. (2016). Novel molecular insights into the critical role of sulfatide in myelin maintenance/function. *Journal of Neurochemistry*, *139*(1), 40–54. https://doi.org/10.1111/jnc.13738

Pasquini, J. M., Guarna, M. M., Besio-Moreno, M. A., Iturregui, M. T., Oteiza, P. I., & Soto, E. F. (1989). Inhibition of the synthesis of glycosphingolipids affects the translocation of proteolipid protein to the myelin membrane. *Journal of Neuroscience Research*, *22*(3), 289–296. https://doi.org/10.1002/jnr.490220309

Peacock, J. D., Pridgeon, M. G., Tovar, E. A., Essenburg, C. J., Bowman, M., Madaj, Z., Koeman, J., Boguslawski, E. A., Grit, J., Dodd, R. D., Khachaturov, V., Cardona, D. M., Chen, M., Kirsch, D. G., Maina, F., Dono, R., Winn, M. E., Graveel, C. R., & Steensma, M. R. (2018). Genomic status of MET potentiates sensitivity to MET and MEK inhibition in NF1-related malignant peripheral nerve sheath tumors. *Cancer Research*, *78*(13), 3672–3687. https://doi.org/10.1158/0008-5472.CAN-17-3167

Pedraza, L., Owens, G. C., Green, L. A., & Salzer, J. L. (1990). The myelin-associated glycoproteins: Membrane disposition, evidence of a novel disulfide linkage between immunoglobulin-like domains, and posttranslational palmitylation. *Journal of Cell Biology*, *111*(6), 2651–2661. https://doi.org/10.1083/jcb.111.6.2651

Penfield, W. (1924). OLIGODENDROGLIA AND ITS RELATION TO CLASSICAL NEUROGLIA. *Brain*, *47*(4), 430–452. https://doi.org/10.1093/brain/47.4.430

Perge, J. A., Koch, K., Miller, R., Sterling, P., & Balasubramanian, V. (2009). How the Optic Nerve Allocates Space, Energy Capacity, and Information. *Journal of Neuroscience*, *29*(24), 7917–7928. https://doi.org/10.1523/JNEUROSCI.5200-08.2009

Pernber, Z., Molander-Melin, M., Berthold, C.-H., Hansson, E., & Fredman, P. (2002). Expression of the myelin and oligodendrocyte progenitor marker sulfatide in neurons and astrocytes of adult rat brain. *Journal of Neuroscience Research*, *69*(1), 86–93. https://doi.org/10.1002/jnr.10264

Peters, A. (1966). The Node of Ranvier in the Central Nervous System. *Quarterly Journal of Experimental Physiology and Cognate Medical Sciences*, *51*(3), 229–236. https://doi.org/10.1113/expphysiol.1966.sp001852

Peters, A., Palay, Sanford, & Webster, Henry. (1992). The Fine Structure of the Nervous System: Neurons and Their Supporting Cells. *The Quarterly Review of Biology*, *67*(1), 80.

Piehl, F. (2021). Current and emerging disease-modulatory therapies and treatment targets for multiple sclerosis. *Journal of Internal Medicine*, *289*(6), 771–791. https://doi.org/10.1111/joim.13215

Pillai, A. M., Thaxton, C., Pribisko, A. L., Cheng, J.-G., Dupree, J. L., & Bhat, M. A. (2009). Spatiotemporal Ablation of Myelinating Glia-Specific Neurofascin (NfascNF155) in Mice Reveals Gradual Loss of Paranodal Axoglial Junctions and Concomitant Disorganization of Axonal Domains. *Journal of Neuroscience Research*, *87*(8), 1773–1793. https://doi.org/10.1002/jnr.22015

Podbielska, M., Ariga, T., & Pokryszko-Dragan, A. (2022). Sphingolipid Players in Multiple Sclerosis: Their Influence on the Initiation and Course of the Disease. *International Journal of Molecular Sciences*, *23*(10), 5330. https://doi.org/10.3390/ijms23105330

Poduslo, S. E. (1975). The Isolation and Characterization of a Plasma Membrane and a Myelin Fraction Derived from Oligodendroglia of Calf Brain1. *Journal of Neurochemistry*, *24*(4), 647–654. https://doi.org/10.1111/j.1471-4159.1975.tb03842.x

Poliak, S., Gollan, L., Martinez, R., Custer, A., Einheber, S., Salzer, J. L., Trimmer, J. S., Shrager, P., & Peles, E. (1999). Caspr2, a new member of the neurexin superfamily, is localized at the juxtaparanodes of myelinated axons and associates with K+ channels. *Neuron*, *24*(4), 1037–1047. https://doi.org/10.1016/s0896-6273(00)81049-1

Poliak, S., Salomon, D., Elhanany, H., Sabanay, H., Kiernan, B., Pevny, L., Stewart, C. L., Xu, X., Chiu, S.-Y., Shrager, P., Furley, A. J. W., & Peles, E. (2003). Juxtaparanodal clustering of Shaker-like K+ channels in myelinated axons depends on Caspr2 and TAG-1. *The Journal of Cell Biology*, *162*(6), 1149–1160. https://doi.org/10.1083/jcb.200305018

Poliani, P. L., Wang, Y., Fontana, E., Robinette, M. L., Yamanishi, Y., Gilfillan, S., & Colonna, M. (2015). TREM2 sustains microglial expansion during aging and response to demyelination. *The Journal of Clinical Investigation*, *125*(5), 2161–2170. https://doi.org/10.1172/JCI77983

Pomicter, A. D., Shroff, S. M., Fuss, B., Sato-Bigbee, C., Brophy, P. J., Rasband, M. N., Bhat, M. A., & Dupree, J. L. (2010a). Novel forms of neurofascin 155 in the central nervous system: Alterations in paranodal disruption models and multiple sclerosis. *Brain*, *133*(2), 389–405. https://doi.org/10.1093/brain/awp341

Pomicter, A. D., Shroff, S. M., Fuss, B., Sato-Bigbee, C., Brophy, P. J., Rasband, M. N., Bhat, M. A., & Dupree, J. L. (2010b). Novel forms of neurofascin 155 in the central nervous system: Alterations in paranodal disruption models and multiple sclerosis. *Brain*, *133*(2), 389–405. https://doi.org/10.1093/brain/awp341

Pomicter, A., DeLoyht, J., Hackett, A., Purdie, N., Sato-Bigbee, C., Henderson, S., & Dupree, J. (2013). Nfasc155H and MAG are specifically susceptible to detergent extraction in the absence of the myelin sphingolipid sulfatide. *Neurochemical Research*, *38*(12), 2490–2502. https://doi.org/10.1007/s11064-013-1162-5

Previtali, S. C., Quattrini, A., & Bolino, A. (2007). Charcot–Marie–Tooth type 4B demyelinating neuropathy: Deciphering the role of MTMR phosphatases. *Expert Reviews in Molecular Medicine*, *9*(25), 1–16. https://doi.org/10.1017/S1462399407000439

Pronker, M. F., Lemstra, S., Snijder, J., Heck, A. J. R., Thies-Weesie, D. M. E., Pasterkamp, R. J., & Janssen, B. J. C. (2016). Structural basis of myelin-associated glycoprotein adhesion and signalling. *Nature Communications*, *7*(1), Article 1. https://doi.org/10.1038/ncomms13584

Qiu, S., Palavicini, J. P., Wang, J., Gonzalez, N. S., He, S., Dustin, E., Zou, C., Ding, L., Bhattacharjee, A., Van Skike, C. E., Galvan, V., Dupree, J. L., & Han, X. (2021). Adult-onset CNS myelin sulfatide deficiency is sufficient to cause Alzheimer's disease-like neuroinflammation and cognitive impairment. *Molecular Neurodegeneration*, *16*, 64. https://doi.org/10.1186/s13024-021-00488-7

Quarles, R. H. (2007). Myelin-associated glycoprotein (MAG): Past, present and beyond. *Journal of Neurochemistry*, *100*(6), 1431–1448. https://doi.org/10.1111/j.1471-4159.2006.04319.x

Quarles, R. H., Macklin, W. B., & Morell, P. (2006). Myelin Formation, Structure and Biochemistry. In *Basic Neurochemistry: Molecular, Cellular and Medical Aspects* (p. 21).

Rasband, M. N., Peles, E., Trimmer, J. S., Levinson, S. R., Lux, S. E., & Shrager, P. (1999). Dependence of Nodal Sodium Channel Clustering on Paranodal Axoglial Contact in the Developing CNS. *Journal of Neuroscience*, *19*(17), 7516–7528. https://doi.org/10.1523/JNEUROSCI.19-17-07516.1999

Rasband, M. N., Tayler, J., Kaga, Y., Yang, Y., Lappe-Siefke, C., Nave, K.-A., & Bansal, R. (2005). CNP is required for maintenance of axon–glia interactions at nodes of Ranvier in the CNS. *Glia*, *50*(1), 86–90. https://doi.org/10.1002/glia.20165

Rasband, M. N., & Trimmer, J. S. (2001). Developmental clustering of ion channels at and near the node of Ranvier. *Developmental Biology*, *236*(1), 5–16. https://doi.org/10.1006/dbio.2001.0326

Recks, M. S., Stormanns, E. R., Bader, J., Arnhold, S., Addicks, K., & Kuerten, S. (2013). Early axonal damage and progressive myelin pathology define the kinetics of CNS histopathology in a mouse model of multiple sclerosis. *Clinical Immunology (Orlando, Fla.)*, *149*(1), 32–45. https://doi.org/10.1016/j.clim.2013.06.004

Reeves, T. M., Phillips, L. L., & Povlishock, J. T. (2005). Myelinated and unmyelinated axons of the corpus callosum differ in vulnerability and functional recovery following traumatic brain injury. *Experimental Neurology*, *196*(1), 126–137. https://doi.org/10.1016/j.expneurol.2005.07.014

Ren, Q., & Bennett, V. (1998). Palmitoylation of Neurofascin at a Site in the Membrane-Spanning Domain Highly Conserved Among the L1 Family of Cell Adhesion Molecules. *Journal of Neurochemistry*, *70*(5), 1839–1849. https://doi.org/10.1046/j.1471-4159.1998.70051839.x

Rhodes, K. J., Strassle, B. W., Monaghan, M. M., Bekele-Arcuri, Z., Matos, M. F., & Trimmer, J. S. (1997). Association and Colocalization of the Kvβ1 and Kvβ2 β-Subunits with Kv1 α-Subunits in Mammalian Brain K+Channel Complexes. *Journal of Neuroscience*, *17*(21), 8246–8258. https://doi.org/10.1523/JNEUROSCI.17-21-08246.1997

Richert, S., Kleinecke, S., Günther, J., Schaumburg, F., Edgar, J., Nienhaus, G. U., Nave, K.-A., & Kassmann, C. M. (2014). In vivo labeling of peroxisomes by photoconvertible mEos2 in myelinating glia of mice. *Biochimie*, *98*, 127–134. https://doi.org/10.1016/j.biochi.2013.10.022

Rios, J. C., Melendez-Vasquez, C. V., Einheber, S., Lustig, M., Grumet, M., Hemperly, J., Peles, E., & Salzer, J. L. (2000). Contactin-Associated Protein (Caspr) and Contactin Form a Complex That Is Targeted to the Paranodal Junctions during Myelination. *The Journal of Neuroscience*, *20*(22), 8354–8364. https://doi.org/10.1523/JNEUROSCI.20-22-08354.2000

Rodi, P. M., Bocco Gianello, M. D., Corregido, M. C., & Gennaro, A. M. (2014). Comparative study of the interaction of CHAPS and Triton X-100 with the erythrocyte membrane. *Biochimica et Biophysica Acta (BBA) - Biomembranes*, *1838*(3), 859–866. https://doi.org/10.1016/j.bbamem.2013.11.006

Rodríguez Murúa, S., Farez, M. F., & Quintana, F. J. (2022). The Immune Response in Multiple Sclerosis. *Annual Review of Pathology*, *17*, 121–139. https://doi.org/10.1146/annurev-pathol-052920-040318

Rosenbluth, J. (1966). REDUNDANT MYELIN SHEATHS AND OTHER ULTRASTRUCTURAL FEATURES OF THE TOAD CEREBELLUM. *The Journal of Cell Biology*, *28*(1), 73–93.

Rosenbluth, J., Dupree, J. L., & Popko, B. (2003a). Nodal sodium channel domain integrity depends on the conformation of the paranodal junction, not on the presence of transverse bands. *Glia*, *41*(3), 318–325. https://doi.org/10.1002/glia.10179

Rosenbluth, J., Dupree, J. L., & Popko, B. (2003b). Nodal sodium channel domain integrity depends on the conformation of the paranodal junction, not on the presence of transverse bands. *Glia*, *41*(3), 318–325. https://doi.org/10.1002/glia.10179

Rosenbluth, J., Petzold, C., & Peles, E. (2012). Dependence of paranodal junctional gap width on transverse bands. *The Journal of Comparative Neurology*, *520*(12), 2774–2784. https://doi.org/10.1002/cne.23105

Roy, A., & Patra, S. K. (2023). Lipid Raft Facilitated Receptor Organization and Signaling: A Functional Rheostat in Embryonic Development, Stem Cell Biology and Cancer. *Stem Cell Reviews and Reports*, *19*(1), 2–25. https://doi.org/10.1007/s12015-022-10448-3

Rust, M. J., Bates, M., & Zhuang, X. (2006). Sub-diffraction-limit imaging by stochastic optical reconstruction microscopy (STORM). *Nature Methods*, *3*(10), 793–795. https://doi.org/10.1038/nmeth929

Saab, A. S., & Nave, K.-A. (2017). Myelin dynamics: Protecting and shaping neuronal functions. *Current Opinion in Neurobiology*, *47*, 104–112. https://doi.org/10.1016/j.conb.2017.09.013

Saliani, A., Perraud, B., Duval, T., Stikov, N., Rossignol, S., & Cohen-Adad, J. (2017). Axon and Myelin Morphology in Animal and Human Spinal Cord. *Frontiers in Neuroanatomy*, *11*, 129. https://doi.org/10.3389/fnana.2017.00129

Sankarshanan, M., Ma, Z., Iype, T., & Lorenz, U. (2007). Identification of a novel lipid raft-targeting motif in Src homology 2-containing phosphatase 1. *Journal of Immunology (Baltimore, Md.: 1950)*, *179*(1), 483–490. https://doi.org/10.4049/jimmunol.179.1.483

Schaeren-Wiemers, N., Bonnet, A., Erb, M., Erne, B., Bartsch, U., Kern, F., Mantei, N., Sherman, D., & Suter, U. (2004). The raft-associated protein MAL is required for maintenance of proper axon–glia interactions in the central nervous system. *The Journal of Cell Biology*, *166*(5), 731–742. https://doi.org/10.1083/jcb.200406092

Schafer, D. P. (2004). Does Paranode Formation and Maintenance Require Partitioning of Neurofascin 155 into Lipid Rafts? *Journal of Neuroscience*, *24*(13), 3176–3185. https://doi.org/10.1523/JNEUROSCI.5427-03.2004

Scherer, S. S., Braun, P. E., Grinspan, J., Collarini, E., Wang, D. Y., & Kamholz, J. (1994). Differential regulation of the 2',3'-cyclic nucleotide 3'-phosphodiesterase gene during oligodendrocyte development. *Neuron*, *12*(6), 1363–1375. https://doi.org/10.1016/0896-6273(94)90451-0

Schirmer, L., Merkler, D., König, F. B., Brück, W., & Stadelmann, C. (2012). Neuroaxonal Regeneration is More Pronounced in Early Multiple Sclerosis than in Traumatic Brain Injury Lesions. *Brain Pathology*, *23*(1), 2–12. https://doi.org/10.1111/j.1750-3639.2012.00608.x

Schnaar, R. L. (2010). Brain gangliosides in axon-myelin stability and axon regeneration. *FEBS Letters*, *584*(9), 1741–1747. https://doi.org/10.1016/j.febslet.2009.10.011

Schnapp, B., peracchia, camillo, & Mugnaini, E. (1976). THE PARANODAL AXO-GLIAL JUNCTION IN THE CENTRAL NERVOUS SYSTEM STUDIED WITH THIN SECTIONS AND FREEZE-FRACTURE. *Neuroscience*, *1*, 181–190.

Sezgin, E. (2017). Super-resolution optical microscopy for studying membrane structure and dynamics. *Journal of Physics. Condensed Matter: An Institute of Physics Journal*, *29*(27), 273001. https://doi.org/10.1088/1361-648X/aa7185

Shamshiev, A., Donda, A., Prigozy, T. I., Mori, L., Chigorno, V., Benedict, C. A., Kappos, L., Sonnino, S., Kronenberg, M., & De Libero, G. (2000). The alphabeta T cell response to self-glycolipids shows a novel mechanism of CD1b loading and a requirement for complex oligosaccharides. *Immunity*, *13*(2), 255–264. https://doi.org/10.1016/s1074-7613(00)00025-x

Sharma, G., Gopinath, S., & Lakshmi Narasimhan, R. (2022). Exploring the Molecular Aspects of Glycosylation in MOG Antibody Disease (MOGAD). *Current Protein & Peptide Science*, *23*(6), 384–394. https://doi.org/10.2174/1389203723666220815110509

Shepherd, M. N., Pomicter, A. D., Velazco, C. S., Henderson, S. C., & Dupree, J. L. (2012a). Paranodal reorganization results in the depletion of transverse bands in the aged central nervous system. *Neurobiology of Aging*, *33*(1), 203.e13-203.e24. https://doi.org/10.1016/j.neurobiolaging.2010.08.001

Shepherd, M. N., Pomicter, A. D., Velazco, C. S., Henderson, S. C., & Dupree, J. L. (2012b). Paranodal reorganization results in the depletion of transverse bands in the aged central nervous system. *Neurobiology of Aging*, *33*(1), 203.e13-203.e24. https://doi.org/10.1016/j.neurobiolaging.2010.08.001

Shinohara, M., Tachibana, M., Kanekiyo, T., & Bu, G. (2017). Role of LRP1 in the pathogenesis of Alzheimer's disease: Evidence from clinical and preclinical studies. *Journal of Lipid Research*, *58*(7), 1267–1281. https://doi.org/10.1194/jlr.R075796

Shroff, S. M., Pomicter, A. D., Chow, W. N., Fox, M. A., Colello, R. J., Henderson, S. C., & Dupree, J. L. (2009). Adult CST-null mice maintain an increased number of oligodendrocytes. *Journal of Neuroscience Research*, *87*(15), 3403–3414. https://doi.org/10.1002/jnr.22003

Simons, K., & Ikonen, E. (1997). Functional rafts in cell membranes. *Nature*, *387*(6633), 569–572. https://doi.org/10.1038/42408

Simons, M., Krämer, E.-M., Thiele, C., Stoffel, W., & Trotter, J. (2000). Assembly of Myelin by Association of Proteolipid Protein with Cholesterol- and Galactosylceramide-Rich Membrane Domains. *Journal of Cell Biology*, *151*(1), 143–154. https://doi.org/10.1083/jcb.151.1.143

Simons, M., & Trotter, J. (2007). Wrapping it up: The cell biology of myelination. *Current Opinion in Neurobiology*, *17*(5), 533–540. https://doi.org/10.1016/j.conb.2007.08.003

Sinha, K., Karimi-Abdolrezaee, S., Velumian, A. A., & Fehlings, M. G. (2006). Functional changes in genetically dysmyelinated spinal cord axons of shiverer mice: Role of juxtaparanodal Kv1 family K+ channels. *Journal of Neurophysiology*, *95*(3), 1683–1695. https://doi.org/10.1152/jn.00899.2005

Skotland, T., Hessvik, N. P., Sandvig, K., & Llorente, A. (2019). Exosomal lipid composition and the role of ether lipids and phosphoinositides in exosome biology. *Journal of Lipid Research*, *60*(1), 9–18. https://doi.org/10.1194/jlr.R084343

Smigiel, R., Sherman, D. L., Rydzanicz, M., Walczak, A., Mikolajkow, D., Krolak-Olejnik, B., Kosinska, J., Gasperowicz, P., Biernacka, A., Stawinski, P., Marciniak, M., Andrzejewski, W., Boczar, M., Krajewski, P., Sasiadek, M. M., Brophy, P. J., & Ploski, R. (2018). Homozygous mutation in the Neurofascin gene affecting the glial isoform of Neurofascin

causes severe neurodevelopment disorder with hypotonia, amimia and areflexia. *Human Molecular Genetics*, *27*(21), 3669–3674. https://doi.org/10.1093/hmg/ddy277

Smith, K. J. (2007). Sodium Channels and Multiple Sclerosis: Roles in Symptom Production, Damage and Therapy. *Brain Pathology*, *17*(2), 230–242. https://doi.org/10.1111/j.1750-3639.2007.00066.x

Snaidero, N., Möbius, W., Czopka, T., Hekking, L. H. P., Mathisen, C., Verkleij, D., Goebbels, S., Edgar, J., Merkler, D., Lyons, D. A., Nave, K.-A., & Simons, M. (2014). Myelin membrane wrapping of CNS axons by PI(3,4,5)P3-dependent polarized growth at the inner tongue. *Cell*, *156*(1–2), 277–290. https://doi.org/10.1016/j.cell.2013.11.044

Snaidero, N., Velte, C., Myllykoski, M., Raasakka, A., Ignatev, A., Werner, H. B., Erwig, M. S., Möbius, W., Kursula, P., Nave, K.-A., & Simons, M. (2017). Antagonistic Functions of MBP and CNP Establish Cytosolic Channels in CNS Myelin. *Cell Reports*, *18*(2), 314–323. https://doi.org/10.1016/j.celrep.2016.12.053

Soldan, S. S., & Lieberman, P. M. (2023). Epstein–Barr virus and multiple sclerosis. *Nature Reviews Microbiology*, *21*(1), Article 1. https://doi.org/10.1038/s41579-022-00770-5

Song, I., & Dityatev, A. (2018). Crosstalk between glia, extracellular matrix and neurons. *Brain Research Bulletin*, *136*, 101–108. https://doi.org/10.1016/j.brainresbull.2017.03.003

Song, J.-L., Westover, M. B., & Zhang, R. (2022). A mechanistic model of calcium homeostasis leading to occurrence and propagation of secondary brain injury. *Journal of Neurophysiology*, *128*(5), 1168–1180. https://doi.org/10.1152/jn.00045.2022

Sonnino, S., Aureli, M., Grassi, S., Mauri, L., Prioni, S., & Prinetti, A. (2014). Lipid Rafts in Neurodegeneration and Neuroprotection. *Molecular Neurobiology*, *50*(1), 130–148. https://doi.org/10.1007/s12035-013-8614-4

Sprong, H., Kruithof, B., Leijendekker, R., Slot, J. W., Meer, G. van, & Sluijs, P. van der. (1998). UDP-Galactose:Ceramide Galactosyltransferase Is a Class I Integral Membrane Protein of the Endoplasmic Reticulum. *Journal of Biological Chemistry*, *273*(40), 25880–25888. https://doi.org/10.1074/jbc.273.40.25880

Stadelmann, C., Timmler, S., Barrantes-Freer, A., & Simons, M. (2019). Myelin in the Central Nervous System: Structure, Function, and Pathology. *Physiological Reviews*, *99*(3), 1381–1431. https://doi.org/10.1152/physrev.00031.2018

Steinman, L. (2001). Multiple sclerosis: A two-stage disease. *Nature Immunology*, *2*(9), Article 9. https://doi.org/10.1038/ni0901-762

Steyer, A. M., Buscham, T. J., Lorenz, C., Hümmert, S., Eichel-Vogel, M. A., Schadt, L. C., Edgar, J. M., Köster, S., Möbius, W., Nave, K.-A., & Werner, H. B. (2023). Focused ion beam-scanning electron microscopy links pathological myelin outfoldings to axonal changes in mice lacking Plp1 or Mag. *Glia*, *71*(3), 509–523. https://doi.org/10.1002/glia.24290

Stifani, N. (2014). Motor neurons and the generation of spinal motor neuron diversity. *Frontiers in Cellular Neuroscience*, *8*, 293. https://doi.org/10.3389/fncel.2014.00293

Sturrock, R. R. (1980). Myelination of the mouse corpus callosum. *Neuropathology and Applied Neurobiology*, *6*(6), 415–420. https://doi.org/10.1111/j.1365-2990.1980.tb00219.x

Stys, P. K., Waxman, S. G., & Ransom, B. R. (1992). Ionic mechanisms of anoxic injury in mammalian CNS white matter: Role of Na + channels and Na + -Ca 2+ exchanger. *Journal of Neuroscience*, 430–439.

Su, L., Athamna, M., Wang, Y., Wang, J., Freudenberg, M., Yue, T., Wang, J., Moresco, E. M. Y., He, H., Zor, T., & Beutler, B. (2021). Sulfatides are endogenous ligands for the TLR4-MD-2 complex. *Proceedings of the National Academy of Sciences of the United States of America*, *118*(30), e2105316118. https://doi.org/10.1073/pnas.2105316118

Subczynski, W. K., & Kusumi, A. (2003). Dynamics of raft molecules in the cell and artificial membranes: Approaches by pulse EPR spin labeling and single molecule optical microscopy. *Biochimica Et Biophysica Acta*, *1610*(2), 231–243. https://doi.org/10.1016/s0005-2736(03)00021-x

Sun, X., Takagishi, Y., Okabe, E., Chishima, Y., Kanou, Y., Murase, S., Mizumura, K., Inaba, M., Komatsu, Y., Hayashi, Y., Peles, E., Oda, S., & Murata, Y. (2009). A Novel Caspr Mutation Causes the Shambling Mouse Phenotype by Disrupting Axoglial Interactions of Myelinated Nerves. *Journal of Neuropathology & Experimental Neurology*, *68*(11), 1207–1218. https://doi.org/10.1097/NEN.0b013e3181be2e96

Susuki, K., Baba, H., Tohyama, K., Kanai, K., Kuwabara, S., Hirata, K., Furukawa, K., Furukawa, K., Rasband, M. N., & Yuki, N. (2007). Gangliosides contribute to stability of paranodal junctions and ion channel clusters in myelinated nerve fibers. *Glia*, *55*(7), 746–757. https://doi.org/10.1002/glia.20503

Susuki, K., Chang, K.-J., Zollinger, D. R., Liu, Y., Ogawa, Y., Eshed-Eisenbach, Y., Dours-Zimmermann, M. T., Oses-Prieto, J. A., Burlingame, A. L., Seidenbecher, C. I., Zimmermann, D. R., Oohashi, T., Peles, E., & Rasband, M. N. (2013). Three mechanisms assemble central nervous system nodes of Ranvier. *Neuron*, *78*(3), 469–482. https://doi.org/10.1016/j.neuron.2013.03.005

Susuki, K., Zollinger, D. R., Chang, K.-J., Zhang, C., Huang, C. Y.-M., Tsai, C.-R., Galiano, M. R., Liu, Y., Benusa, S. D., Yermakov, L. M., Griggs, R. B., Dupree, J. L., & Rasband, M. N. (2018). Glial βII Spectrin Contributes to Paranode Formation and Maintenance. *The Journal of Neuroscience: The Official Journal of the Society for Neuroscience*, *38*(27), 6063–6075. https://doi.org/10.1523/JNEUROSCI.3647-17.2018

Suzuki, K., Andrews, J., Waltz, J., & Terry, R. (1969). Ultrastructural studies of multiple sclerosis. *International Academy of Pathology*, *20*(5), 444–454.

Tait, S., Gunn-Moore, F., Collinson, J. M., Huang, J., Lubetzki, C., Pedraza, L., Sherman, D. L., Colman, D. R., & Brophy, P. J. (2000). An Oligodendrocyte Cell Adhesion Molecule at the Site of Assembly of the Paranodal Axo-Glial Junction. *Journal of Cell Biology*, *150*(3), 657–666. https://doi.org/10.1083/jcb.150.3.657

Taylor, C. M., Coetzee, T., & Pfeiffer, S. E. (2002). Detergent-insoluble glycosphingolipid/cholesterol microdomains of the myelin membrane. *Journal of Neurochemistry*, *81*(5), 993–1004. https://doi.org/10.1046/j.1471-4159.2002.00884.x

Thaxton, C., & Bhat, M. A. (2009). Myelination and Regional Domain Differentiation of the Axon. *Results and Problems in Cell Differentiation*, *48*, 1–28. https://doi.org/10.1007/400_2009_3

Thaxton, C., Pillai, A. M., Pribisko, A. L., Dupree, J. L., & Bhat, M. A. (2011). Nodes of Ranvier act as barriers to restrict invasion of flanking paranodal domains in myelinated axons. *Neuron*, *69*(2), 244–257. https://doi.org/10.1016/j.neuron.2010.12.016

Thomason, E. J., Suárez-Pozos, E., Afshari, F. S., Rosenberg, P. A., Dupree, J. L., & Fuss, B. (2022). Deletion of the Sodium-Dependent Glutamate Transporter GLT-1 in Maturing Oligodendrocytes Attenuates Myelination of Callosal Axons During a Postnatal Phase of Central Nervous System Development. *Frontiers in Cellular Neuroscience*, *16*. https://www.frontiersin.org/articles/10.3389/fncel.2022.905299

Thompson, A. J., Banwell, B. L., Barkhof, F., Carroll, W. M., Coetzee, T., Comi, G., Correale, J., Fazekas, F., Filippi, M., Freedman, M. S., Fujihara, K., Galetta, S. L., Hartung, H. P., Kappos, L., Lublin, F. D., Marrie, R. A., Miller, A. E., Miller, D. H., Montalban, X., … Cohen, J. A. (2018). Diagnosis of multiple sclerosis: 2017 revisions of the McDonald criteria. *The Lancet. Neurology*, *17*(2), 162–173. https://doi.org/10.1016/S1474-4422(17)30470-2

Trajkovic, K., Dhaunchak, A. S., Goncalves, J. T., Wenzel, D., Schneider, A., Bunt, G., Nave, K.-A., & Simons, M. (2006). Neuron to glia signaling triggers myelin membrane exocytosis from endosomal storage sites. *The Journal of Cell Biology*, *172*(6), 937–948. https://doi.org/10.1083/jcb.200509022

Traka, M., Dupree, J. L., Popko, B., & Karagogeos, D. (2002). The neuronal adhesion protein TAG-1 is expressed by Schwann cells and oligodendrocytes and is localized to the juxtaparanodal region of myelinated fibers. *The Journal of Neuroscience: The Official Journal of the Society for Neuroscience*, *22*(8), 3016–3024. https://doi.org/10.1523/JNEUROSCI.22-08-03016.2002

Traka, M., Goutebroze, L., Denisenko, N., Bessa, M., Nifli, A., Havaki, S., Iwakura, Y., Fukamauchi, F., Watanabe, K., Soliven, B., Girault, J.-A., & Karagogeos, D. (2003). Association of TAG-1 with Caspr2 is essential for the molecular organization of juxtaparanodal regions of myelinated fibers. *The Journal of Cell Biology*, *162*(6), 1161–1172. https://doi.org/10.1083/jcb.200305078

Trapp, B. D., Bernier, L., Andrews, S. B., & Colman, D. R. (1988). Cellular and Subcellular Distribution of 2',3'-Cyclic Nucleotide 3'-Phosphodiesterase and Its mRNA in the Rat Central Nervous System. *Journal of Neurochemistry*, *51*(3), 859–868. https://doi.org/10.1111/j.1471-4159.1988.tb01822.x

Trapp, B. D., Nishiyama, A., Cheng, D., & Macklin, W. (1997). Differentiation and Death of Premyelinating Oligodendrocytes in Developing Rodent Brain. *The Journal of Cell Biology*, *137*(2), 459–468.

Trapp, B. D., Peterson, J., Ransohoff, R. M., Rudick, R., Mörk, S., & Bö, L. (1998). Axonal Transection in the Lesions of Multiple Sclerosis. *New England Journal of Medicine*, *338*(5), 278–285. https://doi.org/10.1056/NEJM199801293380502

Trapp, B. D., & Quarles, R. H. (1982). Presence of the myelin-associated glycoprotein correlates with alterations in the periodicity of peripheral myelin. *The Journal of Cell Biology*, *92*(3), 877–882. https://doi.org/10.1083/jcb.92.3.877

Tropak, M. B., & Roder, J. C. (1997). Regulation of myelin-associated glycoprotein binding by sialylated cis-ligands. *Journal of Neurochemistry*, *68*(4), 1753–1763. https://doi.org/10.1046/j.1471-4159.1997.68041753.x

Tsiotra, P. C., Theodorakis, K., Papamatheakis, J., & Karagogeos, D. (1996). The Fibronectin Domains of the Neural Adhesion Molecule TAX-1 Are Necessary and Sufficient for Homophilic Binding *. *Journal of Biological Chemistry*, *271*(46), 29216–29222. https://doi.org/10.1074/jbc.271.46.29216

Uchida, K., Obayashi, H., Minamihata, K., Wakabayashi, R., Goto, M., Shimokawa, N., Takagi, M., & Kamiya, N. (2022). Artificial Palmitoylation of Proteins Controls the Lipid Domain-Selective Anchoring on Biomembranes and the Raft-Dependent Cellular Internalization. *Langmuir: The ACS Journal of Surfaces and Colloids*, *38*(31), 9640–9648. https://doi.org/10.1021/acs.langmuir.2c01205

Valny, M., Honsa, P., Kirdajova, D., Kamenik, Z., & Anderova, M. (2016). Tamoxifen in the Mouse Brain: Implications for Fate-Mapping Studies Using the Tamoxifen-Inducible Cre-loxP System. *Frontiers in Cellular Neuroscience*, *10*. https://doi.org/10.3389/fncel.2016.00243

van Tilborg, E., de Theije, C. G. M., van Hal, M., Wagenaar, N., de Vries, L. S., Benders, M. J., Rowitch, D. H., & Nijboer, C. H. (2018). Origin and dynamics of oligodendrocytes in the developing brain: Implications for perinatal white matter injury. *Glia*, *66*(2), 221–238. https://doi.org/10.1002/glia.23256

Van Zyl, R., Gieselmann, V., & Eckhardt, M. (2010). Elevated sulfatide levels in neurons cause lethal audiogenic seizures in mice. *Journal of Neurochemistry*, *112*(1), 282–295. https://doi.org/10.1111/j.1471-4159.2009.06458.x

Venkatesh, K., Chivatakarn, O., Lee, H., Joshi, P. S., Kantor, D. B., Newman, B. A., Mage, R., Rader, C., & Giger, R. J. (2005). The Nogo-66 Receptor Homolog NgR2 Is a Sialic Acid-Dependent Receptor Selective for Myelin-Associated Glycoprotein. *Journal of Neuroscience*, *25*(4), 808–822. https://doi.org/10.1523/JNEUROSCI.4464-04.2005

Verreycken, J., Baeten, P., & Broux, B. (2022). Regulatory T cell therapy for multiple sclerosis: Breaching (blood-brain) barriers. *Human Vaccines & Immunotherapeutics*, *18*(7), 2153534. https://doi.org/10.1080/21645515.2022.2153534

Verrier, J. D., Jackson, T. C., Gillespie, D. G., Janesko-Feldman, K., Bansal, R., Goebbels, S., Nave, K.-A., Kochanek, P. M., & Jackson, E. K. (2013). Role of CNPase in the Oligodendrocytic Extracellular 2′,3′-cAMP-Adenosine Pathway. *Glia*, *61*(10), 1595–1606. https://doi.org/10.1002/glia.22523

Vinson, M., Rausch, O., Maycox, P. R., Prinjha, R. K., Chapman, D., Morrow, R., Harper, A. J., Dingwall, C., Walsh, F. S., Burbidge, S. A., & Riddell, D. R. (2003). Lipid rafts mediate the interaction between myelin-associated glycoprotein (MAG) on myelin and MAG-receptors on neurons. *Molecular and Cellular Neurosciences*, *22*(3), 344–352. https://doi.org/10.1016/s1044-7431(02)00031-3

Wahl, S. E., McLane, L. E., Bercury, K. K., Macklin, W. B., & Wood, T. L. (2014). Mammalian Target of Rapamycin Promotes Oligodendrocyte Differentiation, Initiation and Extent of CNS Myelination. *The Journal of Neuroscience*, *34*(13), 4453–4465. https://doi.org/10.1523/JNEUROSCI.4311-13.2014

Wallin, M. T., Culpepper, W. J., Campbell, J. D., Nelson, L. M., Langer-Gould, A., Marrie, R. A., Cutter, G. R., Kaye, W. E., Wagner, L., Tremlett, H., Buka, S. L., Dilokthornsakul, P., Topol, B., Chen, L. H., & LaRocca, N. G. (2019). The prevalence of MS in the United States: A population-based estimate using health claims data. *Neurology*, *92*(10), e1029–e1040. https://doi.org/10.1212/WNL.0000000000007035

Walton, C., King, R., Rechtman, L., Kaye, W., Leray, E., Marrie, R. A., Robertson, N., La Rocca, N., Uitdehaag, B., van der Mei, I., Wallin, M., Helme, A., Angood Napier, C., Rijke, N., & Baneke, P. (2020). Rising prevalence of multiple sclerosis worldwide: Insights from the Atlas of MS, third edition. *Multiple Sclerosis (Houndmills, Basingstoke, England)*, *26*(14), 1816–1821. https://doi.org/10.1177/1352458520970841

Wang, H., Kunkel, D. D., Schwartzkroin, P. A., & Tempel, B. L. (1994). Localization of Kv1.1 and Kv1.2, two K channel proteins, to synaptic terminals, somata, and dendrites in the mouse brain. *Journal of Neuroscience*, *14*(8), 4588–4599. https://doi.org/10.1523/JNEUROSCI.14-08-04588.1994

Wang, J.-Q., Gao, M.-Y., Gao, R., Zhao, K.-H., Zhang, Y., & Li, X. (2023). Oligodendrocyte lineage cells: Advances in development, disease, and heterogeneity. *Journal of Neurochemistry*, *164*(4), 468–480. https://doi.org/10.1111/jnc.15728

Wang, Y., Cella, M., Mallinson, K., Ulrich, J. D., Young, K. L., Robinette, M. L., Gilfillan, S., Krishnan, G. M., Sudhakar, S., Zinselmeyer, B. H., Holtzman, D. M., Cirrito, J. R., & Colonna, M. (2015). TREM2 Lipid Sensing Sustains the Microglial Response in an Alzheimer's Disease Model. *Cell*, *160*(6), 1061–1071. https://doi.org/10.1016/j.cell.2015.01.049

Ward, M., & Goldman, M. (2022). *Epidemiology and Pathophysiology of Multiple Sclerosis*. *28*(4), 988–1005.

Wee, P., & Wang, Z. (2017). Epidermal Growth Factor Receptor Cell Proliferation Signaling Pathways. *Cancers*, *9*(5), Article 5. https://doi.org/10.3390/cancers9050052

Westenbroek, R. E., Noebels, J. L., & Catterall, W. A. (1992). Elevated expression of type II Na+ channels in hypomyelinated axons of shiverer mouse brain. *The Journal of Neuroscience: The Official Journal of the Society for Neuroscience*, *12*(6), 2259–2267.

Wheeler, D., Bandaru, V. V. R., Calabresi, P. A., Nath, A., & Haughey, N. J. (2008a). A defect of sphingolipid metabolism modifies the properties of normal appearing white matter in multiple sclerosis. *Brain*, *131*(11), 3092–3102. https://doi.org/10.1093/brain/awn190

Wheeler, D., Bandaru, V. V. R., Calabresi, P. A., Nath, A., & Haughey, N. J. (2008b). A defect of sphingolipid metabolism modifies the properties of normal appearing white matter in multiple sclerosis. *Brain*, *131*(11), 3092–3102. https://doi.org/10.1093/brain/awn190

Whitehead, J. C., Hildebrand, B. A., Sun, M., Rockwood, M. R., Rose, R. A., Rockwood, K., & Howlett, S. E. (2014). A clinical frailty index in aging mice: Comparisons with frailty index data in humans. *The Journals of Gerontology. Series A, Biological Sciences and Medical Sciences*, *69*(6), 621–632. https://doi.org/10.1093/gerona/glt136

Wigger, D., Gulbins, E., Kleuser, B., & Schumacher, F. (2019). Monitoring the Sphingolipid de novo Synthesis by Stable-Isotope Labeling and Liquid Chromatography-Mass Spectrometry. *Frontiers in Cell and Developmental Biology*, *7*, 210. https://doi.org/10.3389/fcell.2019.00210

Wight, P. A., & Dobretsova, A. (2004). Where, when and how much: Regulation of myelin proteolipid protein gene expression. *Cellular and Molecular Life Sciences CMLS*, *61*(7), 810–821. https://doi.org/10.1007/s00018-003-3309-z

Williams, K. A., Deber, C. M., & Klrschner, O. A. (1993). The Structure and Function of Central Nervous System Myelin. *Critical Reviews in Clinical Laboratory Sciences*, *30*(1), 29–64. https://doi.org/10.3109/10408369309084665

Wilson, R., & Brophy, P. J. (1989). Role for the oligodendrocyte cytoskeleton in myelination. *Journal of Neuroscience Research*, *22*(4), 439–448. https://doi.org/10.1002/jnr.490220409

Yaghootfam, A., Sorkalla, T., Häberlein, H., Gieselmann, V., Havla, J., & Eckhardt*, M. (2007, July 21). *Cerebroside Sulfotransferase Forms Homodimers in Living Cells†* (world) [Research-article]. American Chemical Society. https://doi.org/10.1021/bi700014q

Yahara, S., Kawamura, N., Kishimoto, Y., Saida, T., & Tourtellotte, W. W. (1982). A change in the cerebrosides and sulfatides in a demyelinating nervous system. Development of the methodology and study of multiple sclerosis and Wallerian degeneration. *Journal of the Neurological Sciences*, *54*(2), 303–315. https://doi.org/10.1016/0022-510x(82)90191-5

Yamashita, T., Wada, R., Sasaki, T., Deng, C., Bierfreund, U., Sandhoff, K., & Proia, R. L. (1999). A vital role for glycosphingolipid synthesis during development and differentiation. *Proceedings of the National Academy of Sciences*, *96*(16), 9142–9147. https://doi.org/10.1073/pnas.96.16.9142

Yamate-Morgan, H., Lauderdale, K., Horeczko, J., Merchant, U., & Tiwari-Woodruff, S. K. (2019). Functional Effects of Cuprizone-Induced Demyelination in the Presence of the mTOR-Inhibitor Rapamycin ,. *Neuroscience*, *406*, 667–683. https://doi.org/10.1016/j.neuroscience.2019.01.038

Yang, J., Weimer, R. M., Kallop, D., Olsen, O., Wu, Z., Renier, N., Uryu, K., & Tessier-Lavigne, M. (2013). Regulation of axon degeneration after injury and in development by the endogenous calpain inhibitor calpastatin. *Neuron*, *80*(5), 1175–1189. https://doi.org/10.1016/j.neuron.2013.08.034

Yang, L. J., Zeller, C. B., Shaper, N. L., Kiso, M., Hasegawa, A., Shapiro, R. E., & Schnaar, R. L. (1996). Gangliosides are neuronal ligands for myelin-associated glycoprotein. *Proceedings of the National Academy of Sciences of the United States of America*, *93*(2), 814–818. https://doi.org/10.1073/pnas.93.2.814

Yang, Y., Lacas-Gervais, S., Morest, D. K., Solimena, M., & Rasband, M. N. (2004). BetaIV spectrins are essential for membrane stability and the molecular organization of nodes of Ranvier. *The Journal of Neuroscience: The Official Journal of the Society for Neuroscience*, *24*(33), 7230–7240. https://doi.org/10.1523/JNEUROSCI.2125-04.2004

Yermakov, L. M., Hong, L. A., Drouet, D. E., Griggs, R. B., & Susuki, K. (2019). Functional Domains in Myelinated Axons. *Advances in Experimental Medicine and Biology*, *1190*, 65–83. https://doi.org/10.1007/978-981-32-9636-7_6

Yin, X., Crawford, T. O., Griffin, J. W., Tu, P. h, Lee, V. M., Li, C., Roder, J., & Trapp, B. D. (1998). Myelin-associated glycoprotein is a myelin signal that modulates the caliber of myelinated axons. *The Journal of Neuroscience: The Official Journal of the Society for Neuroscience*, *18*(6), 1953–1962. https://doi.org/10.1523/JNEUROSCI.18-06-01953.1998

York, E. N., Martin, S.-J., Meijboom, R., Thrippleton, M. J., Bastin, M. E., Carter, E., Overell, J., Connick, P., Chandran, S., Waldman, A. D., & Hunt, D. P. J. (2021). MRI-derived g-ratio and lesion severity in newly diagnosed multiple sclerosis. *Brain Communications*, *3*(4), fcab249. https://doi.org/10.1093/braincomms/fcab249

Yu, F., Fan, Q., Tian, Q., Ngamsombat, C., Machado, N., Bireley, J. D., Russo, A. W., Nummenmaa, A., Witzel, T., Wald, L. L., Klawiter, E. C., & Huang, S. Y. (2019). Imaging G-Ratio in Multiple Sclerosis Using High-Gradient Diffusion MRI and Macromolecular Tissue Volume. *AJNR: American Journal of Neuroradiology*, *40*(11), 1871–1877. https://doi.org/10.3174/ajnr.A6283

Zajonc, D. M., Maricic, I., Wu, D., Halder, R., Roy, K., Wong, C.-H., Kumar, V., & Wilson, I. A. (2005). Structural basis for CD1d presentation of a sulfatide derived from myelin and its implications for autoimmunity. *The Journal of Experimental Medicine*, *202*(11), 1517–1526. https://doi.org/10.1084/jem.20051625

Zalc, B. (2006). The Acquisition of Myelin: A Success Story. In *Purinergic Signalling in Neuron–Glia Interactions* (pp. 15–25). John Wiley & Sons, Ltd. https://doi.org/10.1002/9780470032244.ch3

Zand, R., Li, M. X., Jin, X., & Lubman, D. (1998). Determination of the sites of posttranslational modifications in the charge isomers of bovine myelin basic protein by capillary electrophoresis-mass spectroscopy. *Biochemistry*, *37*(8), 2441–2449. https://doi.org/10.1021/bi972347t

Zeisel, A., Hochgerner, H., Lönnerberg, P., Johnsson, A., Memic, F., van der Zwan, J., Häring, M., Braun, E., Borm, L. E., La Manno, G., Codeluppi, S., Furlan, A., Lee, K., Skene, N., Harris, K. D., Hjerling-Leffler, J., Arenas, E., Ernfors, P., Marklund, U., & Linnarsson, S. (2018). Molecular Architecture of the Mouse Nervous System. *Cell*, *174*(4), 999-1014.e22. https://doi.org/10.1016/j.cell.2018.06.021

Zhang, B., Cao, Q., Guo, A., Chu, H., Chan, Y. G., Buschdorf, J. P., Low, B. C., Ling, E. A., & Liang, F. (2005). Juxtanodin: An oligodendroglial protein that promotes cellular arborization and 2′,3′-cyclic nucleotide-3′-phosphodiesterase

trafficking. *Proceedings of the National Academy of Sciences*, *102*(32), 11527–11532. https://doi.org/10.1073/pnas.0500952102

Zhang, C., Susuki, K., Zollinger, D. R., Dupree, J. L., & Rasband, M. N. (2013). Membrane domain organization of myelinated axons requires βII spectrin. *The Journal of Cell Biology*, *203*(3), 437–443. https://doi.org/10.1083/jcb.201308116

Zhang, K., Zhao, Y., Liang, Z., Wang, C., & Liu, X. (2020). Validity of the McDonald criteria in predicting second events in multiple sclerosis. *Multiple Sclerosis and Related Disorders*, *43*, 102223. https://doi.org/10.1016/j.msard.2020.102223

Zhang, L., Wang, Y., Liu, T., Mao, Y., & Peng, B. (2023). Novel Microglia-based Therapeutic Approaches to Neurodegenerative Disorders. *Neuroscience Bulletin*, *39*(3), 491–502. https://doi.org/10.1007/s12264-022-01013-6

Zhao, Y., Yamasaki, R., Yamaguchi, H., Nagata, S., Une, H., Cui, Y., Masaki, K., Nakamuta, Y., Iinuma, K., Watanabe, M., Matsushita, T., Isobe, N., & Kira, J.-I. (2020). Oligodendroglial connexin 47 regulates neuroinflammation upon autoimmune demyelination in a novel mouse model of multiple sclerosis. *Proceedings of the National Academy of Sciences of the United States of America*, *117*(4), 2160–2169. https://doi.org/10.1073/pnas.1901294117

Zöller, I., Meixner, M., Hartmann, D., Büssow, H., Meyer, R., Gieselmann, V., & Eckhardt, M. (2008). Absence of 2-Hydroxylated Sphingolipids Is Compatible with Normal Neural Development But Causes Late-Onset Axon and Myelin Sheath Degeneration. *The Journal of Neuroscience*, *28*(39), 9741–9754. https://doi.org/10.1523/JNEUROSCI.0458-08.2008

Aggarwal, S., Yurlova, L., Snaidero, N., Reetz, C., Frey, S., Zimmermann, J., Pähler, G., Janshoff, A., Friedrichs, J., Müller, D. J., Goebel, C., & Simons, M. (2011). A Size Barrier Limits Protein Diffusion at the Cell Surface to Generate Lipid-Rich Myelin-Membrane Sheets. *Developmental Cell*, *21*(3), 445–456. https://doi.org/10.1016/j.devcel.2011.08.001

Agrawal, H. C., Sprinkle, T. J., & Agrawal, D. (1994). In vivo phosphorylation of 2′,3′-cyclic nucleotide 3′-phosphohydrolase (CNP): CNP in brain myelin is phosphorylated by forskolin- and phorbol ester-sensitive protein kinases. *Neurochemical Research*, *19*(6), 721–728. https://doi.org/10.1007/BF00967712

Allt, G. (1969). Repair of segmental dehyelination in peripheral nerves: An electron microscope study. *Brain: A Journal of Neurology*, *92*(3), 639–646. https://doi.org/10.1093/brain/92.3.639

Alonso, A., & Goñi, F. M. (2018). The Physical Properties of Ceramides in Membranes. *Annual Review of Biophysics*, *47*, 633–654. https://doi.org/10.1146/annurev-biophys-070317-033309

Alpizar, S. A., Baker, A. L., Gulledge, A. T., & Hoppa, M. B. (2019). Loss of Neurofascin-186 Disrupts Alignment of AnkyrinG Relative to Its Binding Partners in the Axon Initial Segment. *Frontiers in Cellular Neuroscience*, *13*, 1. https://doi.org/10.3389/fncel.2019.00001

Alrashdi, B., Dawod, B., Schampel, A., Tacke, S., Kuerten, S., Marshall, J. S., & Côté, P. D. (2019). Nav1.6 promotes inflammation and neuronal degeneration in a mouse model of multiple sclerosis. *Journal of Neuroinflammation*, *16*(1), 215. https://doi.org/10.1186/s12974-019-1622-1

Amor, V., Feinberg, K., Eshed-Eisenbach, Y., Vainshtein, A., Frechter, S., Grumet, M., Rosenbluth, J., & Peles, E. (2014). Long-Term Maintenance of Na+ Channels at Nodes of Ranvier Depends on Glial Contact

Mediated by Gliomedin and NrCAM. *The Journal of Neuroscience*, *34*(15), 5089–5098. https://doi.org/10.1523/JNEUROSCI.4752-13.2014

Amor, V., Zhang, C., Vainshtein, A., Zhang, A., Zollinger, D. R., Eshed-Eisenbach, Y., Brophy, P. J., Rasband, M. N., & Peles, E. (2017). The paranodal cytoskeleton clusters Na+ channels at nodes of Ranvier. *ELife*, *6*, e21392. https://doi.org/10.7554/eLife.21392

Arélin, K., Kinoshita, A., Whelan, C. M., Irizarry, M. C., Rebeck, G. W., Strickland, D. K., & Hyman, B. T. (2002). LRP and senile plaques in Alzheimer's disease: Colocalization with apolipoprotein E and with activated astrocytes. *Brain Research. Molecular Brain Research*, *104*(1), 38–46. https://doi.org/10.1016/s0169-328x(02)00203-6

Arrenberg, P., Halder, R., Dai, Y., Maricic, I., & Kumar, V. (2010). Oligoclonality and innate-like features in the TCR repertoire of type II NKT cells reactive to a β-linked self-glycolipid. *Proceedings of the National Academy of Sciences*, *107*(24), 10984–10989. https://doi.org/10.1073/pnas.1000576107

Arvanitis, D. N., Min, W., Gong, Y., Heng, Y. M., & Boggs, J. M. (2005). Two types of detergent-insoluble, glycosphingolipid/cholesterol-rich membrane domains from isolated myelin. *Journal of Neurochemistry*, *94*(6), 1696–1710. https://doi.org/10.1111/j.1471-4159.2005.03331.x

Baba, H., & Ishibashi, T. (2019). The Role of Sulfatides in Axon–Glia Interactions. In K. Sango, J. Yamauchi, T. Ogata, & K. Susuki (Eds.), *Myelin* (Vol. 1190, pp. 165–179). Springer Singapore. https://doi.org/10.1007/978-981-32-9636-7_11

Babetto, E., & Beirowski, B. (2022). Of axons that struggle to make ends meet: Linking axonal bioenergetic failure to programmed axon degeneration. *Biochimica et Biophysica Acta. Bioenergetics*, *1863*(5), 148545. https://doi.org/10.1016/j.bbabio.2022.148545

Bagchi, B., Al-Sabi, A., Kaza, S., Scholz, D., O'Leary, V. B., Dolly, J. O., & Ovsepian, S. V. (2014). Disruption of myelin leads to ectopic expression of K(V)1.1 channels with abnormal conductivity of optic nerve axons in a cuprizone-induced model of demyelination. *PloS One*, *9*(2), e87736. https://doi.org/10.1371/journal.pone.0087736

Baker, A. J., Phan, N., Moulton, R. J., Fehlings, M. G., Yucel, Y., Zhao, M., Liu, E., & Tian, G. F. (2002). Attenuation of the Electrophysiological Function of the Corpus Callosum after Fluid Percussion Injury in the Rat. *Journal of Neurotrauma*, *19*(5), 587–599. https://doi.org/10.1089/089771502753754064

Bakiri, Y., Káradóttir, R., Cossell, L., & Attwell, D. (2011). Morphological and electrical properties of oligodendrocytes in the white matter of the corpus callosum and cerebellum. *The Journal of Physiology*, *589*(Pt 3), 559–573. https://doi.org/10.1113/jphysiol.2010.201376

Bano, D., Young, K. W., Guerin, C. J., Lefeuvre, R., Rothwell, N. J., Naldini, L., Rizzuto, R., Carafoli, E., & Nicotera, P. (2005). Cleavage of the plasma membrane Na+/Ca2+ exchanger in excitotoxicity. *Cell*, *120*(2), 275–285. https://doi.org/10.1016/j.cell.2004.11.049

Bansal, R., Winkler, S., & Bheddah, S. (1999). Negative Regulation of Oligodendrocyte Differentiation by Galactosphingolipids. *The Journal of Neuroscience*, *19*(18), 7913–7924. https://doi.org/10.1523/JNEUROSCI.19-18-07913.1999

Baron, W., Bijlard, M., Nomden, A., de Jonge, J. C., Teunissen, C. E., & Hoekstra, D. (2014). Sulfatide-mediated control of extracellular matrix-dependent oligodendrocyte maturation. *Glia*, *62*(6), 927–942. https://doi.org/10.1002/glia.22650

Baron, W., & Hoekstra, D. (2010). On the biogenesis of myelin membranes: Sorting, trafficking and cell polarity. *FEBS Letters*, *584*(9), 1760–1770. https://doi.org/10.1016/j.febslet.2009.10.085

Barratt, H. E., Budnick, H. C., Parra, R., Lolley, R. J., Perry, C. N., & Nesic, O. (2016). Tamoxifen promotes differentiation of oligodendrocyte progenitors in vitro. *Neuroscience*, *319*, 146–154. https://doi.org/10.1016/j.neuroscience.2016.01.026

Bartsch, U., Kirchhoff, F., & Schachner, M. (1989). Immunohistological localization of the adhesion molecules L1, N-CAM, and MAG in the developing and adult optic nerve of mice. *The Journal of Comparative Neurology*, *284*(3), 451–462. https://doi.org/10.1002/cne.902840310

Bazan, N. G., Colangelo, V., & Lukiw, W. J. (2002). Prostaglandins and other lipid mediators in Alzheimer's disease. *Prostaglandins & Other Lipid Mediators*, *68–69*, 197–210. https://doi.org/10.1016/s0090-6980(02)00031-x

Bei, F., & Smith, K. J. (2012). Axonal protection achieved by blockade of sodium/calcium exchange in a new model of ischemia in vivo. *Neuropharmacology*, *63*(3), 405–414. https://doi.org/10.1016/j.neuropharm.2012.04.019

Belachew, S., Yuan, X., & Gallo, V. (2001). Unraveling Oligodendrocyte Origin and Function by Cell-Specific Transgenesis. *Developmental Neuroscience*, *23*(4–5), 287–298. https://doi.org/10.1159/000048712

Benjamins, J. A., Murphy, E. J., & Seyfried, T. N. (2012). Chapter 5—Lipids. In S. T. Brady, G. J. Siegel, R. W. Albers, & D. L. Price (Eds.), *Basic Neurochemistry (Eighth Edition)* (pp. 81–100). Academic Press. https://doi.org/10.1016/B978-0-12-374947-5.00005-5

Benusa, S. D., George, N. M., Sword, B. A., DeVries, G. H., & Dupree, J. L. (2017). Acute neuroinflammation induces AIS structural plasticity in a NOX2-dependent manner. *Journal of Neuroinflammation*, *14*(1), 116. https://doi.org/10.1186/s12974-017-0889-3

Bercury, K. K., Dai, J., Sachs, H. H., Ahrendsen, J. T., Wood, T. L., & Macklin, W. B. (2014). Conditional Ablation of Raptor or Rictor Has Differential Impact on Oligodendrocyte Differentiation and CNS Myelination. *The Journal of Neuroscience*, *34*(13), 4466–4480. https://doi.org/10.1523/JNEUROSCI.4314-13.2014

Berger, T., & Reindl, M. (2015). Antibody biomarkers in CNS demyelinating diseases – a long and winding road. *European Journal of Neurology*, *22*(8), 1162–1168. https://doi.org/10.1111/ene.12759

Bhat, M. A., Rios, J. C., Lu, Y., Garcia-Fresco, G. P., Ching, W., St Martin, M., Li, J., Einheber, S., Chesler, M., Rosenbluth, J., Salzer, J. L., & Bellen, H. J. (2001). Axon-glia interactions and the domain organization of myelinated axons requires neurexin IV/Caspr/Paranodin. *Neuron*, *30*(2), 369–383. https://doi.org/10.1016/s0896-6273(01)00294-x

Bieberich, E. (2018). Sphingolipids and lipid rafts: Novel concepts and methods of analysis. *Chemistry and Physics of Lipids*, *216*, 114–131. https://doi.org/10.1016/j.chemphyslip.2018.08.003

Biffiger, K., Bartsch, S., Montag, D., Aguzzi, A., Schachner, M., & Bartsch, U. (2000). Severe Hypomyelination of the Murine CNS in the Absence of Myelin-Associated Glycoprotein and Fyn Tyrosine Kinase. *The Journal of Neuroscience*, *20*(19), 7430–7437. https://doi.org/10.1523/JNEUROSCI.20-19-07430.2000

Bizzozero, O. A., Malkoski, S. P., Mobarak, C., Bixler, H. A., & Evans, J. E. (2002). Mass-spectrometric analysis of myelin proteolipids reveals new features of this family of palmitoylated membrane proteins. *Journal of Neurochemistry*, *81*(3), 636–645. https://doi.org/10.1046/j.1471-4159.2002.00852.x

Bjornevik, K., Cortese, M., Healy, B. C., Kuhle, J., Mina, M. J., Leng, Y., Elledge, S. J., Niebuhr, D. W., Scher, A. I., Munger, K. L., & Ascherio, A. (2022). Longitudinal analysis reveals high prevalence of Epstein-Barr virus associated with multiple sclerosis. *Science (New York, N.Y.)*, *375*(6578), 296–301. https://doi.org/10.1126/science.abj8222

Bligh, E. G., & Dyer, W. J. (1959). A rapid method of total lipid extraction and purification. *Canadian Journal of Biochemistry and Physiology*, *37*(8), 911–917. https://doi.org/10.1139/o59-099

Block, M. L., & Hong, J.-S. (2005). Microglia and inflammation-mediated neurodegeneration: Multiple triggers with a common mechanism. *Progress in Neurobiology*, *76*(2), 77–98. https://doi.org/10.1016/j.pneurobio.2005.06.004

Boggs, J. M. (2014). Role of galactosylceramide and sulfatide in oligodendrocytes and CNS myelin: Formation of a glycosynapse. *Advances in Neurobiology*, *9*, 263–291. https://doi.org/10.1007/978-1-4939-1154-7_12

Boggs, J. M., Gao, W., & Hirahara, Y. (2008). Myelin glycosphingolipids, galactosylceramide and sulfatide, participate in carbohydrate–carbohydrate interactions between apposed membranes and may form glycosynapses between oligodendrocyte and/or myelin membranes. *Biochimica et Biophysica Acta (BBA) - General Subjects*, *1780*(3), 445–455. https://doi.org/10.1016/j.bbagen.2007.10.015

Boggs, J. M., Wang, H., Gao, W., Arvanitis, D. N., Gong, Y., & Min, W. (2004). A glycosynapse in myelin? *Glycoconjugate Journal*, *21*(3–4), 97–110. https://doi.org/10.1023/B:GLYC.0000044842.34958.f8

Boiko, T., Rasband, M. N., Levinson, S. R., Caldwell, J. H., Mandel, G., Trimmer, J. S., & Matthews, G. (2001). Compact Myelin Dictates the Differential Targeting of Two Sodium Channel Isoforms in the Same Axon. *Neuron*, *30*(1), 91–104. https://doi.org/10.1016/S0896-6273(01)00265-3

Boison, D., Bussow, H., D'Urso, D., Muller, H. W., & Stoffel, W. (1995). Adhesive properties of proteolipid protein are responsible for the compaction of CNS myelin sheaths. *Journal of Neuroscience*, *15*(8), 5502–5513. https://doi.org/10.1523/JNEUROSCI.15-08-05502.1995

Boison, D., & Stoffel, W. (1994). Disruption of the compacted myelin sheath of axons of the central nervous system in proteolipid protein-deficient mice. *Proceedings of the National Academy of Sciences of the United States of America*, *91*(24), 11709–11713.

Borges, B. C., Meng, X., Long, P., Kanold, P. O., & Corfas, G. (2023). Loss of oligodendrocyte ErbB receptor signaling leads to hypomyelination, reduced density of parvalbumin-expressing interneurons, and inhibitory function in the auditory cortex. *Glia*, *71*(2), 187–204. https://doi.org/10.1002/glia.24266

Borst, K., Dumas, A. A., & Prinz, M. (2021). Microglia: Immune and non-immune functions. *Immunity*, *54*(10), 2194–2208. https://doi.org/10.1016/j.immuni.2021.09.014

Bosio, A., Binczek, E., Haupt, W. F., & Stoffel, W. (1998). Composition and Biophysical Properties of Myelin Lipid Define the Neurological Defects in Galactocerebroside- and Sulfatide-Deficient Mice. *Journal of Neurochemistry*, *70*(1), 308–315. https://doi.org/10.1046/j.1471-4159.1998.70010308.x

Bouafia, A., Golmard, J.-L., Thuries, V., Sazdovitch, V., Hauw, J. J., Fontaine, B., & Seilhean, D. (2014). Axonal expression of sodium channels and neuropathology of the plaques in multiple sclerosis. *Neuropathology and Applied Neurobiology*, *40*(5), 579–590. https://doi.org/10.1111/nan.12059

Boullerne, A. I. (2016). The history of myelin. *Experimental Neurology*, *283*(Pt B), 431–445. https://doi.org/10.1016/j.expneurol.2016.06.005

Boyle, M. E., Berglund, E. O., Murai, K. K., Weber, L., Peles, E., & Ranscht, B. (2001). Contactin orchestrates assembly of the septate-like junctions at the paranode in myelinated peripheral nerve. *Neuron*, *30*(2), 385–397. https://doi.org/10.1016/s0896-6273(01)00296-3

Braun, P. E., De Angelis, D., Shtybel, W. W., & Bernier, L. (1991). Isoprenoid modification permits 2',3'-cyclic nucleotide 3'-phosphodiesterase to bind to membranes. *Journal of Neuroscience Research*, *30*(3), 540–544. https://doi.org/10.1002/jnr.490300311

Braun, P. E., Sandillon, F., Edwards, A., Matthieu, J. M., & Privat, A. (1988). Immunocytochemical localization by electron microscopy of 2'3'-cyclic nucleotide 3'-phosphodiesterase in developing oligodendrocytes of normal and mutant brain. *Journal of Neuroscience*, *8*(8), 3057–3066. https://doi.org/10.1523/JNEUROSCI.08-08-03057.1988

Britt, D. J., Farías, G. G., Guardia, C. M., & Bonifacino, J. S. (2016). Mechanisms of Polarized Organelle Distribution in Neurons. *Frontiers in Cellular Neuroscience*, *10*. https://www.frontiersin.org/articles/10.3389/fncel.2016.00088

Brown, D. A., & Rose, J. K. (1992). Sorting of GPI-anchored proteins to glycolipid-enriched membrane subdomains during transport to the apical cell surface. *Cell*, *68*(3), 533–544. https://doi.org/10.1016/0092-8674(92)90189-J

Brunner, C., Lassmann, H., Waehneldt, T. V., Matthieu, J. M., & Linington, C. (1989). Differential ultrastructural localization of myelin basic protein, myelin/oligodendroglial glycoprotein, and 2',3'-cyclic nucleotide 3'-phosphodiesterase in the CNS of adult rats. *Journal of Neurochemistry*, *52*(1), 296–304. https://doi.org/10.1111/j.1471-4159.1989.tb10930.x

Bujalka, H., Koenning, M., Jackson, S., Perreau, V. M., Pope, B., Hay, C. M., Mitew, S., Hill, A. F., Lu, Q. R., Wegner, M., Srinivasan, R., Svaren, J., Willingham, M., Barres, B. A., & Emery, B. (2013). MYRF Is a Membrane-Associated Transcription Factor That Autoproteolytically Cleaves to Directly Activate Myelin Genes. *PLOS Biology*, *11*(8), e1001625. https://doi.org/10.1371/journal.pbio.1001625

Burger, D., Steck, A. J., Bernard, C. C., & Kerlero de Rosbo, N. (1993). Human myelin/oligodendrocyte glycoprotein: A new member of the L2/HNK-1 family. *Journal of Neurochemistry*, *61*(5), 1822–1827. https://doi.org/10.1111/j.1471-4159.1993.tb09822.x

Burska, A. N., Hunt, L., Boissinot, M., Strollo, R., Ryan, B. J., Vital, E., Nissim, A., Winyard, P. G., Emery, P., & Ponchel, F. (2014). Autoantibodies to Posttranslational Modifications in Rheumatoid Arthritis. *Mediators of Inflammation*, *2014*, 492873. https://doi.org/10.1155/2014/492873

Buscham, T. J., Eichel-Vogel, M. A., Steyer, A. M., Jahn, O., Strenzke, N., Dardawal, R., Memhave, T. R., Siems, S. B., Müller, C., Meschkat, M., Sun, T., Ruhwedel, T., Möbius, W., Krämer-Albers, E.-M., Boretius, S., Nave, K.-A., & Werner, H. B. (2022). Progressive axonopathy when oligodendrocytes lack the myelin protein CMTM5. *ELife*, *11*, e75523. https://doi.org/10.7554/eLife.75523

Caldwell, J. H., Schaller, K. L., Lasher, R. S., Peles, E., & Levinson, S. R. (2000). Sodium channel Nav1.6 is localized at nodes of Ranvier, dendrites, and synapses. *Proceedings of the National Academy of Sciences*, *97*(10), 5616–5620. https://doi.org/10.1073/pnas.090034797

Campagnoni, A. T., & Skoff, R. P. (2001). The pathobiology of myelin mutants reveal novel biological functions of the MBP and PLP genes. *Brain Pathology (Zurich, Switzerland)*, *11*(1), 74–91. https://doi.org/10.1111/j.1750-3639.2001.tb00383.x

Cantoni, C., Bollman, B., Licastro, D., Xie, M., Mikesell, R., Schmidt, R., Yuede, C. M., Galimberti, D., Olivecrona, G., Klein, R. S., Cross, A. H., Otero, K., & Piccio, L. (2015). TREM2 regulates microglial cell activation in response to demyelination in vivo. *Acta Neuropathologica*, *129*(3), 429–447. https://doi.org/10.1007/s00401-015-1388-1

Capelluto, D. G. S. (2022). The repertoire of protein-sulfatide interactions reveal distinct modes of sulfatide recognition. *Frontiers in Molecular Biosciences*, *9*, 1080161. https://doi.org/10.3389/fmolb.2022.1080161

Caritá, A. C., Mattei, B., Domingues, C. C., de Paula, E., & Riske, K. A. (2017). Effect of Triton X-100 on Raft-Like Lipid Mixtures: Phase Separation and Selective Solubilization. *Langmuir: The ACS Journal of Surfaces and Colloids*, *33*(29), 7312–7321. https://doi.org/10.1021/acs.langmuir.7b01134

Casares, D., Escribá, P. V., & Rosselló, C. A. (2019). Membrane Lipid Composition: Effect on Membrane and Organelle Structure, Function and Compartmentalization and Therapeutic Avenues. *International Journal of Molecular Sciences*, *20*(9). https://doi.org/10.3390/ijms20092167

Castro, B. M., Prieto, M., & Silva, L. C. (2014). Ceramide: A simple sphingolipid with unique biophysical properties. *Progress in Lipid Research*, *54*, 53–67. https://doi.org/10.1016/j.plipres.2014.01.004

Chamberlain, K. A., & Sheng, Z.-H. (2019). Mechanisms for the maintenance and regulation of axonal energy supply. *Journal of Neuroscience Research*, *97*(8), 897–913. https://doi.org/10.1002/jnr.24411

Chang, K.-J., Zollinger, D. R., Susuki, K., Sherman, D. L., Makara, M. A., Brophy, P. J., Cooper, E. C., Bennett, V., Mohler, P. J., & Rasband, M. N. (2014). Glial ankyrins facilitate paranodal axoglial junction assembly. *Nature Neuroscience*, *17*(12), 1673–1681. https://doi.org/10.1038/nn.3858

Charcot, J.-M. (1868). *Histologie de la sclérose en plaques*. s.n.

Charles, P., Tait, S., Faivre-Sarrailh, C., Barbin, G., Gunn-Moore, F., Denisenko-Nehrbass, N., Guennoc, A.-M., Girault, J.-A., Brophy, P. J., & Lubetzki, C. (2002a). Neurofascin is a glial receptor for the

paranodin/Caspr-contactin axonal complex at the axoglial junction. *Current Biology: CB*, *12*(3), 217–220. https://doi.org/10.1016/s0960-9822(01)00680-7

Charles, P., Tait, S., Faivre-Sarrailh, C., Barbin, G., Gunn-Moore, F., Denisenko-Nehrbass, N., Guennoc, A.-M., Girault, J.-A., Brophy, P. J., & Lubetzki, C. (2002b). Neurofascin Is a Glial Receptor for the Paranodin/Caspr-Contactin Axonal Complex at the Axoglial Junction. *Current Biology*, *12*(3), 217–220. https://doi.org/10.1016/S0960-9822(01)00680-7

Chen, Y., Aulia, S., & Tang, B. L. (2006). Myelin-associated glycoprotein-mediated signaling in central nervous system pathophysiology. *Molecular Neurobiology*, *34*(2), 81–91. https://doi.org/10.1385/MN:34:2:81

Chen, Z., Yuan, Z., Yang, S., Zhu, Y., Xue, M., Zhang, J., & Leng, L. (2023). Brain Energy Metabolism: Astrocytes in Neurodegenerative Diseases. *CNS Neuroscience & Therapeutics*, *29*(1), 24–36. https://doi.org/10.1111/cns.13982

Chiu, S. Y., Zhou, L., Chuan-Li, Z., & Messing, A. (1999). Analysis of potassium channel functions in mammalian axons by gene knockouts. *Journal of Neurocytology*, *28*(4), 349–364.

Choi, S., Guo, L., & Cordeiro, M. F. (2021). Retinal and Brain Microglia in Multiple Sclerosis and Neurodegeneration. *Cells*, *10*(6), 1507. https://doi.org/10.3390/cells10061507

Chou, F. C., Chou, C. H., Shapira, R., & Kibler, R. F. (1976). Basis of microheterogeneity of myelin basic protein. *Journal of Biological Chemistry*, *251*(9), 2671–2679. https://doi.org/10.1016/S0021-9258(17)33540-8

Chrast, R., Saher, G., Nave, K.-A., & Verheijen, M. H. G. (2011). Lipid metabolism in myelinating glial cells: Lessons from human inherited disorders and mouse models. *Journal of Lipid Research*, *52*(3), 419–434. https://doi.org/10.1194/jlr.R009761

Clark, K. C., Josephson, A., Benusa, S. D., Hartley, R. K., Baer, M., Thummala, S., Joslyn, M., Sword, B. A., Elford, H., Oh, U., Dilsizoglu-Senol, A., Lubetzki, C., Davenne, M., DeVries, G. H., & Dupree, J. L. (2016). Compromised axon initial segment integrity in EAE is preceded by microglial reactivity and contact. *Glia*, *64*(7), 1190–1209. https://doi.org/10.1002/glia.22991

Coman, I., Aigrot, M. S., Seilhean, D., Reynolds, R., Girault, J. A., Zalc, B., & Lubetzki, C. (2006). Nodal, paranodal and juxtaparanodal axonal proteins during demyelination and remyelination in multiple sclerosis. *Brain: A Journal of Neurology*, *129*(Pt 12), 3186–3195. https://doi.org/10.1093/brain/awl144

Craner, M. J., Hains, B. C., Lo, A. C., Black, J. A., & Waxman, S. G. (2004). Co-localization of sodium channel Nav1.6 and the sodium-calcium exchanger at sites of axonal injury in the spinal cord in EAE. *Brain: A Journal of Neurology*, *127*(Pt 2), 294–303. https://doi.org/10.1093/brain/awh032

Craner, M. J., Lo, A. C., Black, J. A., & Waxman, S. G. (2003). Abnormal sodium channel distribution in optic nerve axons in a model of inflammatory demyelination. *Brain: A Journal of Neurology*, *126*(Pt 7), 1552–1561. https://doi.org/10.1093/brain/awg153

Craner, M. J., Newcombe, J., Black, J. A., Hartle, C., Cuzner, M. L., & Waxman, S. G. (2004). Molecular changes in neurons in multiple sclerosis: Altered axonal expression of Nav1.2 and Nav1.6 sodium channels and Na+/Ca2+ exchanger. *Proceedings of the National Academy of Sciences of the United States of America*, *101*(21), 8168–8173. https://doi.org/10.1073/pnas.0402765101

Cubí, R., Matas, L. A., Pou, M., Aguilera, J., & Gil, C. (2013). Differential sensitivity to detergents of actin cytoskeleton from nerve endings. *Biochimica Et Biophysica Acta*, *1828*(11), 2385–2393. https://doi.org/10.1016/j.bbamem.2013.06.022

Cunningham, M. E., McGonigal, R., Barrie, J. A., Campbell, C. I., Yao, D., & Willison, H. J. (2023). Axolemmal nanoruptures arising from paranodal membrane injury induce secondary axon degeneration in murine Guillain-Barré syndrome. *Journal of the Peripheral Nervous System*, *28*(1), 17–31. https://doi.org/10.1111/jns.12532

Curatolo, W., & Neuringer, L. J. (1986). The effects of cerebrosides on model membrane shape. *The Journal of Biological Chemistry*, *261*(36), 17177–17182.

Dai, G. (2022). Neuronal KCNQ2/3 channels are recruited to lipid raft microdomains by palmitoylation of BACE1. *The Journal of General Physiology*, *154*(4), e202112888. https://doi.org/10.1085/jgp.202112888

Dasgupta, S., Levery, S. B., & Hogan, E. L. (2002). 3-O-acetyl-sphingosine-series myelin glycolipids characterization of novel 3-O-acetyl-sphingosine galactosylceramide. *Journal of Lipid Research*, *43*(5), 751–761.

De Angelis, D. A., & Braun, P. E. (1996). 2′,3′-Cyclic Nucleotide 3′-Phosphodiesterase Binds to Actin-Based Cytoskeletal Elements in an Isoprenylation-Independent Manner. *Journal of Neurochemistry*, *67*(3), 943–951. https://doi.org/10.1046/j.1471-4159.1996.67030943.x

De Logu, F., De Prá, S. D.-T., de David Antoniazzi, C. T., Kudsi, S. Q., Ferro, P. R., Landini, L., Rigo, F. K., de Bem Silveira, G., Silveira, P. C. L., Oliveira, S. M., Marini, M., Mattei, G., Ferreira, J., Geppetti, P., Nassini, R., & Trevisan, G. (2020). Macrophages and Schwann cell TRPA1 mediate chronic allodynia in a mouse model of complex regional pain syndrome type I. *Brain, Behavior, and Immunity*, *88*, 535–546. https://doi.org/10.1016/j.bbi.2020.04.037

De Logu, F., Nassini, R., Materazzi, S., Carvalho Gonçalves, M., Nosi, D., Rossi Degl'Innocenti, D., Marone, I. M., Ferreira, J., Li Puma, S., Benemei, S., Trevisan, G., Souza Monteiro de Araújo, D., Patacchini, R., Bunnett, N. W., & Geppetti, P. (2017). Schwann cell TRPA1 mediates neuroinflammation that sustains macrophage-dependent neuropathic pain in mice. *Nature Communications*, *8*(1), Article 1. https://doi.org/10.1038/s41467-017-01739-2

del Rio-Hortega, P. (1924). *La glie à radiations peu nombreuses et la cellule de Schwann sontelles homologables? 91*, 818–820.

Denk, F., Ramer, L. M., Erskine, E. L. K. S., Nassar, M. A., Bogdanov, Y., Signore, M., Wood, J. N., McMahon, S. B., & Ramer, M. S. (2015). Tamoxifen induces cellular stress in the nervous system by inhibiting cholesterol synthesis. *Acta Neuropathologica Communications*, *3*. https://doi.org/10.1186/s40478-015-0255-6

Diaz-Rohrer, B., Castello-Serrano, I., Chan, S. H., Wang, H.-Y., Shurer, C. R., Levental, K. R., & Levental, I. (2023). Rab3 mediates a pathway for endocytic sorting and plasma membrane recycling of ordered microdomains. *Proceedings of the National Academy of Sciences of the United States of America*, *120*(10), e2207461120. https://doi.org/10.1073/pnas.2207461120

Doerflinger, N. H., Macklin, W. B., & Popko, B. (2003). Inducible site-specific recombination in myelinating cells. *Genesis*, *35*(1), 63–72. https://doi.org/10.1002/gene.10154

Domeniconi, M., Cao, Z., Spencer, T., Sivasankaran, R., Wang, K. C., Nikulina, E., Kimura, N., Cai, H., Deng, K., Gao, Y., He, Z., & Filbin, M. T. (2002). Myelin-Associated Glycoprotein Interacts with the Nogo66 Receptor to Inhibit Neurite Outgrowth. *Neuron*, *35*(2), 283–290. https://doi.org/10.1016/S0896-6273(02)00770-5

Domingues, H. S., Portugal, C. C., Socodato, R., & Relvas, J. B. (2016). Oligodendrocyte, Astrocyte, and Microglia Crosstalk in Myelin Development, Damage, and Repair. *Frontiers in Cell and Developmental Biology*, *4*, 71. https://doi.org/10.3389/fcell.2016.00071

Duncan, G. J., Simkins, T. J., & Emery, B. (2021). Neuron-Oligodendrocyte Interactions in the Structure and Integrity of Axons. *Frontiers in Cell and Developmental Biology*, *9*, 653101. https://doi.org/10.3389/fcell.2021.653101

Duncan, I. D., Radcliff, A. B., Heidari, M., Kidd, G., August, B. K., & Wierenga, L. A. (2018). The adult oligodendrocyte can participate in remyelination. *Proceedings of the National Academy of Sciences of the United States of America*, *115*(50), E11807–E11816. https://doi.org/10.1073/pnas.1808064115

Dupree, J. L., Coetzee, T., Blight, A., Suzuki, K., & Popko, B. (1998a). Myelin Galactolipids Are Essential for Proper Node of Ranvier Formation in the CNS. *Journal of Neuroscience*, *18*(5), 1642–1649. https://doi.org/10.1523/JNEUROSCI.18-05-01642.1998

Dupree, J. L., Coetzee, T., Blight, A., Suzuki, K., & Popko, B. (1998b). Myelin Galactolipids Are Essential for Proper Node of Ranvier Formation in the CNS. *Journal of Neuroscience*, *18*(5), 1642–1649. https://doi.org/10.1523/JNEUROSCI.18-05-01642.1998

Dupree, J. L., Coetzee, T., Suzuki, K., & Popko, B. (1998). Myelin abnormalities in mice deficient in galactocerebroside and sulfatide. *Journal of Neurocytology*, *27*(9), 649–659. https://doi.org/10.1023/A:1006908013972

Dupree, J. L., & Feinstein, D. L. (2018). Influence of diet on axonal damage in the EAE mouse model of multiple sclerosis. *Journal of Neuroimmunology*, *322*, 9–14. https://doi.org/10.1016/j.jneuroim.2018.05.010

Dupree, J. L., Girault, J. A., & Popko, B. (1999). Axo-glial interactions regulate the localization of axonal paranodal proteins. *The Journal of Cell Biology*, *147*(6), 1145–1152. https://doi.org/10.1083/jcb.147.6.1145

Dupree, J. L., Polak, P. E., Hensley, K., Pelligrino, D., & Feinstein, D. L. (2015). Lanthionine ketimine ester provides benefit in a mouse model of multiple sclerosis. *Journal of Neurochemistry*, *134*(2), 302–314. https://doi.org/10.1111/jnc.13114

Dupree, J. L., & Pomicter, A. D. (2010). Myelin, DIGs, and membrane rafts in the central nervous system. *Prostaglandins & Other Lipid Mediators*, *91*(3), 118–129. https://doi.org/10.1016/j.prostaglandins.2009.04.005

Dupree, J., Mason, J., Marcus, J., Stull, M., Levinson, R., Matsushima, G., & Popko, B. (2004). Oligodendrocytes assist in the maintenance of sodium channel clusters independent of the myelin sheath. *Neuron Glia Biology*, *1*(3), 179–192.

Dyer, C. A., & Benjamins, J. A. (1989). Organization of oligodendroglial membrane sheets. I: Association of myelin basic protein and 2′,3′-cyclic nucleotide 3′-phosphohydrolase with cytoskeleton. *Journal of Neuroscience Research*, *24*(2), 201–211. https://doi.org/10.1002/jnr.490240211

Eckhardt, M., Hedayati, K. K., Pitsch, J., Lüllmann-Rauch, R., Beck, H., Fewou, S. N., & Gieselmann, V. (2007). Sulfatide storage in neurons causes hyperexcitability and axonal degeneration in a mouse model of metachromatic leukodystrophy. *The Journal of Neuroscience: The Official Journal of the Society for Neuroscience*, *27*(34), 9009–9021. https://doi.org/10.1523/JNEUROSCI.2329-07.2007

Edgar, J. M., McLaughlin, M., Werner, H. B., McCulloch, M. C., Barrie, J. A., Brown, A., Faichney, A. B., Snaidero, N., Nave, K.-A., & Griffiths, I. R. (2009). Early ultrastructural defects of axons and axon–glia junctions in mice lacking expression of Cnp1. *Glia*, *57*(16), 1815–1824. https://doi.org/10.1002/glia.20893

Einheber, S., Bhat, M. A., & Salzer, J. L. (2006). Disrupted axo-glial junctions result in accumulation of abnormal mitochondria at nodes of ranvier. *Neuron Glia Biology*, *2*(3), 165–174. https://doi.org/10.1017/S1740925X06000275

Einheber, S., Meng, X., Rubin, M., Lam, I., Mohandas, N., An, X., Shrager, P., Kissil, J., Maurel, P., & Salzer, J. L. (2013). The 4.1B cytoskeletal protein regulates the domain organization and sheath thickness of myelinated axons. *Glia*, *61*(2), 240–253. https://doi.org/10.1002/glia.22430

Elazar, N., Vainshtein, A., Golan, N., Vijayaragavan, B., Schaeren-Wiemers, N., Eshed-Eisenbach, Y., & Peles, E. (2019). Axoglial Adhesion by Cadm4 Regulates CNS Myelination. *Neuron*, *101*(2), 224-231.e5. https://doi.org/10.1016/j.neuron.2018.11.032

Elazar, N., Vainshtein, A., Rechav, K., Tsoory, M., Eshed-Eisenbach, Y., & Peles, E. (2019). Coordinated internodal and paranodal adhesion controls accurate myelination by oligodendrocytes. *The Journal of Cell Biology*, *218*(9), 2887–2895. https://doi.org/10.1083/jcb.201906099

Emery, B. (2010). Regulation of oligodendrocyte differentiation and myelination. *Science (New York, N.Y.)*, *330*(6005), 779–782. https://doi.org/10.1126/science.1190927

Faivre-Sarrailh, C. (2020). Molecular organization and function of vertebrate septate-like junctions. *Biochimica et Biophysica Acta (BBA) - Biomembranes*, *1862*(5), 183211. https://doi.org/10.1016/j.bbamem.2020.183211

Falcão, A. M., van Bruggen, D., Marques, S., Meijer, M., Jäkel, S., Agirre, E., Samudyata, Floriddia, E. M., Vanichkina, D. P., ffrench-Constant, C., Williams, A., Guerreiro-Cacais, A. O., & Castelo-Branco, G. (2018). Disease-specific oligodendrocyte lineage cells arise in multiple sclerosis. *Nature Medicine*, *24*(12), Article 12. https://doi.org/10.1038/s41591-018-0236-y

Ferreira, H. B., Melo, T., Monteiro, A., Paiva, A., Domingues, P., & Domingues, M. R. (2021). Serum phospholipidomics reveals altered lipid profile and promising biomarkers in multiple sclerosis. *Archives of Biochemistry and Biophysics*, *697*, 108672. https://doi.org/10.1016/j.abb.2020.108672

Fewou, S. N., Fernandes, A., Stockdale, K., Francone, V. P., Dupree, J. L., Rosenbluth, J., Pfeiffer, S. E., & Bansal, R. (2010). Myelin protein composition is altered in mice lacking either sulfated or both sulfated and non-sulfated galactolipids. *Journal of Neurochemistry*, *112*(3), 599–610. https://doi.org/10.1111/j.1471-4159.2009.06464.x

Fiedler, K., Kobayashi, T., Kurzchalia, T. V., & Simons, K. (1993). Glycosphingolipid-enriched, detergent-insoluble complexes in protein sorting in epithelial cells. *Biochemistry*, *32*(25), 6365–6373. https://doi.org/10.1021/bi00076a009

Fisher, K. S., Cuascut, F. X., Rivera, V. M., & Hutton, G. J. (2020). Current Advances in Pediatric Onset Multiple Sclerosis. *Biomedicines*, *8*(4), 71. https://doi.org/10.3390/biomedicines8040071

Floriddia, E. M., Lourenço, T., Zhang, S., van Bruggen, D., Hilscher, M. M., Kukanja, P., Gonçalves dos Santos, J. P., Altınkök, M., Yokota, C., Llorens-Bobadilla, E., Mulinyawe, S. B., Grãos, M., Sun, L. O., Frisén, J., Nilsson, M., & Castelo-Branco, G. (2020). Distinct oligodendrocyte populations have spatial preference and different responses to spinal cord injury. *Nature Communications*, *11*, 5860. https://doi.org/10.1038/s41467-020-19453-x

Foran, D. R., & Peterson, A. C. (1992). Paper for timeline of myelination: Myelin acquisition in the central nervous system of the mouse revealed by an MBP-Lac Z transgene. *Journal of Neuroscience*, *12*(12), 4890–4897. https://doi.org/10.1523/JNEUROSCI.12-12-04890.1992

Ford, M. C., Alexandrova, O., Cossell, L., Stange-Marten, A., Sinclair, J., Kopp-Scheinpflug, C., Pecka, M., Attwell, D., & Grothe, B. (2015). Tuning of Ranvier node and internode properties in myelinated axons to adjust action potential timing. *Nature Communications*, *6*, 8073. https://doi.org/10.1038/ncomms9073

Freeman, S. A., Desmazières, A., Fricker, D., Lubetzki, C., & Sol-Foulon, N. (2016). Mechanisms of sodium channel clustering and its influence on axonal impulse conduction. *Cellular and Molecular Life Sciences*, *73*, 723–735. https://doi.org/10.1007/s00018-015-2081-1

Fruttiger, M., Montag, D., Schachner, M., & Martini, R. (1995). Crucial Role for the Myelin-associated Glycoprotein in the Maintenance of Axon-Myelin Integrity. *European Journal of Neuroscience*, *7*(3), 511–515. https://doi.org/10.1111/j.1460-9568.1995.tb00347.x

Fünfschilling, U., Supplie, L. M., Mahad, D., Boretius, S., Saab, A. S., Edgar, J., Brinkmann, B. G., Kassmann, C. M., Tzvetanova, I. D., Möbius, W., Diaz, F., Meijer, D., Suter, U., Hamprecht, B., Sereda, M. W., Moraes, C. T., Frahm, J., Goebbels, S., & Nave, K.-A. (2012). Glycolytic oligodendrocytes maintain myelin and long-term axonal integrity. *Nature*, *485*(7399), 517–521. https://doi.org/10.1038/nature11007

Furukawa, K., Takamiya, K., Okada, M., Inoue, M., Fukumoto, S., & Furukawa, K. (2001). Novel functions of complex carbohydrates elucidated by the mutant mice of glycosyltransferase genes. *Biochimica et Biophysica Acta (BBA) - General Subjects*, *1525*(1), 1–12. https://doi.org/10.1016/S0304-4165(00)00185-9

Gajate, C., Gonzalez-Camacho, F., & Mollinedo, F. (2009). Involvement of Raft Aggregates Enriched in Fas/CD95 Death-Inducing Signaling Complex in the Antileukemic Action of Edelfosine in Jurkat Cells. *PLOS ONE*, *4*(4), e5044. https://doi.org/10.1371/journal.pone.0005044

Gal, J., Katsumata, Y., Zhu, H., Srinivasan, S., Chen, J., Johnson, L. A., Wang, W.-X., Golden, L. R., Wilcock, D. M., Jicha, G. A., Cykowski, M. D., & Nelson, P. T. (2022). Apolipoprotein E Proteinopathy Is a Major Dementia-Associated Pathologic Biomarker in Individuals with or without the APOE Epsilon 4 Allele. *The American Journal of Pathology*, *192*(3), 564–578. https://doi.org/10.1016/j.ajpath.2021.11.013

Gallego-Delgado, P., James, R., Browne, E., Meng, J., Umashankar, S., Tan, L., Picon, C., Mazarakis, N. D., Faisal, A. A., Howell, O. W., & Reynolds, R. (2020a). Neuroinflammation in the normal-appearing white matter (NAWM) of the multiple sclerosis brain causes abnormalities at the nodes of Ranvier. *PLoS Biology*, *18*(12), e3001008. https://doi.org/10.1371/journal.pbio.3001008

Gallego-Delgado, P., James, R., Browne, E., Meng, J., Umashankar, S., Tan, L., Picon, C., Mazarakis, N. D., Faisal, A. A., Howell, O. W., & Reynolds, R. (2020b). Neuroinflammation in the normal-appearing white matter (NAWM) of the multiple sclerosis brain causes abnormalities at the nodes of Ranvier. *PLoS Biology*, *18*(12), e3001008. https://doi.org/10.1371/journal.pbio.3001008

García-Arribas, A. B., Alonso, A., & Goñi, F. M. (2016). Cholesterol interactions with ceramide and sphingomyelin. *Chemistry and Physics of Lipids*, *199*, 26–34. https://doi.org/10.1016/j.chemphyslip.2016.04.002

Garcia-Fresco, G. P., Sousa, A. D., Pillai, A. M., Moy, S. S., Crawley, J. N., Tessarollo, L., Dupree, J. L., & Bhat, M. A. (2006). Disruption of axo-glial junctions causes cytoskeletal disorganization and degeneration of Purkinje neuron axons. *Proceedings of the National Academy of Sciences of the United States of America*, *103*(13), 5137–5142. https://doi.org/10.1073/pnas.0601082103

Gardinier, M. V., Amiguet, P., Linington, C., & Matthieu, J. M. (1992). Myelin/oligodendrocyte glycoprotein is a unique member of the immunoglobulin superfamily. *Journal of Neuroscience Research*, *33*(1), 177–187. https://doi.org/10.1002/jnr.490330123

Gasser, A., Ho, T. S.-Y., Cheng, X., Chang, K.-J., Waxman, S. G., Rasband, M. N., & Dib-Hajj, S. D. (2012). An AnkyrinG-Binding Motif Is Necessary and Sufficient for Targeting Nav1.6 Sodium Channels to Axon Initial Segments and Nodes of Ranvier. *The Journal of Neuroscience*, *32*(21), 7232–7243. https://doi.org/10.1523/JNEUROSCI.5434-11.2012

Gbaguidi, B., Guillemin, F., Soudant, M., Debouverie, M., Mathey, G., & Epstein, J. (2022). Age-period-cohort analysis of the incidence of multiple sclerosis over twenty years in Lorraine, France. *Scientific Reports*, *12*(1), Article 1. https://doi.org/10.1038/s41598-022-04836-5

Grassi, S., Giussani, P., Mauri, L., Prioni, S., Sonnino, S., & Prinetti, A. (2020). Lipid rafts and neurodegeneration: Structural and functional roles in physiologic aging and neurodegenerative diseases: Thematic Review Series: Biology of Lipid Rafts. *Journal of Lipid Research*, *61*(5), 636–654. https://doi.org/10.1194/jlr.TR119000427

Grassi, S., Prioni, S., Cabitta, L., Aureli, M., Sonnino, S., & Prinetti, A. (2016). The Role of 3-O-Sulfogalactosylceramide, Sulfatide, in the Lateral Organization of Myelin Membrane. *Neurochemical Research*, *41*(1), 130–143. https://doi.org/10.1007/s11064-015-1747-2

Griffiths, I., Klugmann, M., Anderson, T., Yool, D., Thomson, C., Schwab, M. H., Schneider, A., Zimmermann, F., McCulloch, M., Nadon, N., & Nave, K. A. (1998). Axonal swellings and degeneration in mice lacking the major proteolipid of myelin. *Science (New York, N.Y.)*, *280*(5369), 1610–1613. https://doi.org/10.1126/science.280.5369.1610

Gutiérrez-Martín, Y., Martín-Romero, F. J., Henao, F., & Gutiérrez-Merino, C. (2005). Alteration of cytosolic free calcium homeostasis by SIN-1: High sensitivity of L-type Ca2+ channels to extracellular oxidative/nitrosative stress in cerebellar granule cells. *Journal of Neurochemistry*, *92*(4), 973–989. https://doi.org/10.1111/j.1471-4159.2004.02964.x

Haines, T. H. (2001). Do sterols reduce proton and sodium leaks through lipid bilayers? *Progress in Lipid Research*, *40*(4), 299–324. https://doi.org/10.1016/s0163-7827(01)00009-1

Han, X. (2004). The role of apolipoprotein E in lipid metabolism in the central nervous system. *Cellular and Molecular Life Sciences*, *61*(15), 1896–1906. https://doi.org/10.1007/s00018-004-4009-z

Han, X. (2007). Potential mechanisms contributing to sulfatide depletion at the earliest clinically recognizable stage of Alzheimer's disease: A tale of shotgun lipidomics. *Journal of Neurochemistry*, *103 Suppl 1*, 171–179. https://doi.org/10.1111/j.1471-4159.2007.04708.x

Han, X. (2010). The Pathogenic Implication of Abnormal Interaction Between Apolipoprotein E Isoforms, Amyloid-beta Peptides, and Sulfatides in Alzheimer's Disease. *Molecular Neurobiology*, *41*(2–3), 97–106. https://doi.org/10.1007/s12035-009-8092-x

Hanada, K., Kumagai, K., Tomishige, N., & Yamaji, T. (2009). CERT-mediated trafficking of ceramide. *Biochimica Et Biophysica Acta*, *1791*(7), 684–691. https://doi.org/10.1016/j.bbalip.2009.01.006

Hartline, D. K. (2008). What is myelin? *Neuron Glia Biology*, *4*(2), 153–163. http://dx.doi.org.proxy.library.vcu.edu/10.1017/S1740925X09990263

Hayashi, A., Kaneko, N., Tomihira, C., & Baba, H. (2013a). Sulfatide decrease in myelin influences formation of the paranodal axo-glial junction and conduction velocity in the sciatic nerve. *Glia*, *61*(4), 466–474. https://doi.org/10.1002/glia.22447

Hayashi, A., Kaneko, N., Tomihira, C., & Baba, H. (2013b). Sulfatide decrease in myelin influences formation of the paranodal axo-glial junction and conduction velocity in the sciatic nerve. *Glia*, *61*(4), 466–474. https://doi.org/10.1002/glia.22447

Hayes, L. W., & Jungawala, F. B. (1976). *Synthesis and Turnover of Cerebrosides and Phosphatidylserine of Myelin and Mcrosomal Fractions of Adult and Developing Rat Brain*. *160*, 10.

Hedstrom, K. L., Xu, X., Ogawa, Y., Frischknecht, R., Seidenbecher, C. I., Shrager, P., & Rasband, M. N. (2007). Neurofascin assembles a specialized extracellular matrix at the axon initial segment. *The Journal of Cell Biology*, *178*(5), 875–886. https://doi.org/10.1083/jcb.200705119

Hinman, J. D., Chen, C.-D., Oh, S.-Y., Hollander, W., & Abraham, C. R. (2008). Age-dependent accumulation of ubiquitinated 2',3'-cyclic nucleotide 3'-phosphodiesterase in myelin lipid rafts. *Glia*, *56*(1), 118–133. https://doi.org/10.1002/glia.20595

Hirahara, Y., Tsuda, M., Wada, Y., & Honke, K. (2000). CDNA cloning, genomic cloning, and tissue-specific regulation of mouse cerebroside sulfotransferase. *European Journal of Biochemistry*, *267*(7), 1909–1917. https://doi.org/10.1046/j.1432-1327.2000.01139.x

Hirahara, Y., Wakabayashi, T., Mori, T., Koike, T., Yao, I., Tsuda, M., Honke, K., Gotoh, H., Ono, K., & Yamada, H. (2017). Sulfatide species with various fatty acid chains in oligodendrocytes at different developmental stages determined by imaging mass spectrometry. *Journal of Neurochemistry*, *140*(3), 435–450. https://doi.org/10.1111/jnc.13897

Hirano, K., Kinoshita, M., & Matsumori, N. (2022). Impact of sphingomyelin acyl chain heterogeneity upon properties of raft-like membranes. *Biochimica Et Biophysica Acta. Biomembranes*, *1864*(12), 184036. https://doi.org/10.1016/j.bbamem.2022.184036

Hivert, B., Pinatel, D., Labasque, M., Tricaud, N., Goutebroze, L., & Faivre-Sarrailh, C. (2016). Assembly of juxtaparanodes in myelinating DRG culture: Differential clustering of the Kv1/Caspr2 complex and scaffolding protein 4.1B. *Glia*, *64*(5), 840–852. https://doi.org/10.1002/glia.22968

Holcomb, P. S., Deerinck, T. J., Ellisman, M. H., & Spirou, G. A. (2013). Construction of a polarized neuron. *The Journal of Physiology*, *591*(13), 3145–3150. https://doi.org/10.1113/jphysiol.2012.248542

Honke, K., Hirahara, Y., Dupree, J., Suzuki, K., Popko, B., Fukushima, K., Fukushima, J., Nagasawa, T., Yoshida, N., Wada, Y., & Taniguchi, N. (2002). Paranodal junction formation and spermatogenesis require sulfoglycolipids. *Proceedings of the National Academy of Sciences of the United States of America*, *99*(7), 4227–4232. https://doi.org/10.1073/pnas.032068299

Honke, K., Tsuda, M., Hirahara, Y., Ishii, A., Makita, A., & Wada, Y. (1997). Molecular cloning and expression of cDNA encoding human 3'-phosphoadenylylsulfate:galactosylceramide 3'-sulfotransferase. *The Journal of Biological Chemistry*, *272*(8), 4864–4868. https://doi.org/10.1074/jbc.272.8.4864

Hope, H. R., & Pike, L. J. (1996). Phosphoinositides and phosphoinositide-utilizing enzymes in detergent-insoluble lipid domains. *Molecular Biology of the Cell*, *7*(6), 843–851. https://doi.org/10.1091/mbc.7.6.843

Horbay, R., Hamraghani, A., Ermini, L., Holcik, S., Beug, S. T., & Yeganeh, B. (2022). Role of Ceramides and Lysosomes in Extracellular Vesicle Biogenesis, Cargo Sorting and Release. *International Journal of Molecular Sciences*, *23*(23), 15317. https://doi.org/10.3390/ijms232315317

Howell, O. W., Palser, A., Polito, A., Melrose, S., Zonta, B., Scheiermann, C., Vora, A. J., Brophy, P. J., & Reynolds, R. (2006a). Disruption of neurofascin localization reveals early changes preceding demyelination and remyelination in multiple sclerosis. *Brain*, *129*(12), 3173–3185. https://doi.org/10.1093/brain/awl290

Howell, O. W., Palser, A., Polito, A., Melrose, S., Zonta, B., Scheiermann, C., Vora, A. J., Brophy, P. J., & Reynolds, R. (2006b). Disruption of neurofascin localization reveals early changes preceding demyelination and remyelination in multiple sclerosis. *Brain*, *129*(12), 3173–3185. https://doi.org/10.1093/brain/awl290

Howell, Owain. W., Rundle, Jon. L., Garg, A., Komada, M., Brophy, Peter. J., & Reynolds, R. (2010). Activated microglia mediate axo-glial disruption that contributes to axonal injury in multiple sclerosis. *Journal of Neuropathology and Experimental Neurology*, *69*(10), 1017–1033. https://doi.org/10.1097/NEN.0b013e3181f3a5b1

Hughes, E. G., Kang, S. H., Fukaya, M., & Bergles, D. E. (2013). Oligodendrocyte progenitors balance growth with self-repulsion to achieve homeostasis in the adult brain. *Nature Neuroscience*, *16*(6), 668–676. https://doi.org/10.1038/nn.3390

Huxley, A. F., & Stämpeli, R. (1949). Evidence for saltatory conduction in peripheral myelinated nerve fibres. *The Journal of Physiology*, *108*(3), 315–339. https://doi.org/10.1113/jphysiol.1949.sp004335

Inglese, M., Fleysher, L., Oesingmann, N., & Petracca, M. (2018). Clinical applications of ultra-high field magnetic resonance imaging in multiple sclerosis. *Expert Review of Neurotherapeutics*, *18*(3), 221–230. https://doi.org/10.1080/14737175.2018.1433033

Isaac, G., Pernber, Z., Gieselmann, V., Hansson, E., Bergquist, J., & Månsson, J.-E. (2006). Sulfatide with short fatty acid dominates in astrocytes and neurons. *The FEBS Journal*, *273*(8), 1782–1790. https://doi.org/10.1111/j.1742-4658.2006.05195.x

Ishibashi, T., Dupree, J. L., Ikenaka, K., Hirahara, Y., Honke, K., Peles, E., Popko, B., Suzuki, K., Nishino, H., & Baba, H. (2002a). A myelin galactolipid, sulfatide, is essential for maintenance of ion channels on myelinated axon but not essential for initial cluster formation. *The Journal of Neuroscience: The Official Journal of the Society for Neuroscience*, *22*(15), 6507–6514. https://doi.org/20026705

Ishibashi, T., Dupree, J. L., Ikenaka, K., Hirahara, Y., Honke, K., Peles, E., Popko, B., Suzuki, K., Nishino, H., & Baba, H. (2002b). A Myelin Galactolipid, Sulfatide, Is Essential for Maintenance of Ion Channels on Myelinated Axon But Not Essential for Initial Cluster Formation. *The Journal of Neuroscience*, *22*(15), 6507–6514. https://doi.org/10.1523/JNEUROSCI.22-15-06507.2002

Isik, O. A., & Cizmecioglu, O. (2023). Rafting on the Plasma Membrane: Lipid Rafts in Signaling and Disease. *Advances in Experimental Medicine and Biology*. https://doi.org/10.1007/5584_2022_759

Jablonska, B., Gierdalski, M., Chew, L.-J., Hawley, T., Catron, M., Lichauco, A., Cabrera-Luque, J., Yuen, T., Rowitch, D., & Gallo, V. (2016). Sirt1 regulates glial progenitor proliferation and regeneration in white matter after neonatal brain injury. *Nature Communications*, *7*, 13866. https://doi.org/10.1038/ncomms13866

Jafari, A., Babajani, A., & Rezaei-Tavirani, M. (2021). Multiple Sclerosis Biomarker Discoveries by Proteomics and Metabolomics Approaches. *Biomarker Insights*, *16*, 11772719211013352. https://doi.org/10.1177/11772719211013352

Jahn, O., Tenzer, S., & Werner, H. B. (2009). Myelin Proteomics: Molecular Anatomy of an Insulating Sheath. *Molecular Neurobiology*, *40*(1), 55–72. https://doi.org/10.1007/s12035-009-8071-2

Jahng, A., Maricic, I., Aguilera, C., Cardell, S., Halder, R. C., & Kumar, V. (2004). Prevention of Autoimmunity by Targeting a Distinct, Noninvariant CD1d-reactive T Cell Population Reactive to Sulfatide. *The Journal of Experimental Medicine*, *199*(7), 947–957. https://doi.org/10.1084/jem.20031389

Janssen, B. J. C. (2018). Inside-out or outside-in, a new factor in MAG-mediated signaling in the nervous system: An Editorial for “High-affinity heterotetramer formation between the large myelin-associated glycoprotein and the dynein light chain DYNLL1” on page 764. *Journal of Neurochemistry*, *147*(6), 712–714. https://doi.org/10.1111/jnc.14597

Jeon, S.-B., Yoon, H. J., Park, S.-H., Kim, I.-H., & Park, E. J. (2008). Sulfatide, A Major Lipid Component of Myelin Sheath, Activates Inflammatory Responses As an Endogenous Stimulator in Brain-Resident Immune Cells. *The Journal of Immunology*, *181*(11), 8077–8087. https://doi.org/10.4049/jimmunol.181.11.8077

Johns, T. G., & Bernard, C. C. A. (1999). The Structure and Function of Myelin Oligodendrocyte Glycoprotein. *Journal of Neurochemistry*, *72*(1), 1–9. https://doi.org/10.1046/j.1471-4159.1999.0720001.x

Joseph, S., Vingill, S., Jahn, O., Fledrich, R., Werner, H. B., Katona, I., Möbius, W., Mitkovski, M., Huang, Y., Weis, J., Sereda, M. W., Schulz, J. B., Nave, K.-A., & Stegmüller, J. (2019). Myelinating Glia-Specific Deletion of Fbxo7 in Mice Triggers Axonal Degeneration in the Central Nervous System Together with Peripheral Neuropathy. *The Journal of Neuroscience: The Official Journal of the Society for Neuroscience*, *39*(28), 5606–5626. https://doi.org/10.1523/JNEUROSCI.3094-18.2019

Kapoor, R., Davies, M., Blaker, P. A., Hall, S. M., & Smith, K. J. (2003). Blockers of sodium and calcium entry protect axons from nitric oxide-mediated degeneration. *Annals of Neurology*, *53*(2), 174–180. https://doi.org/10.1002/ana.10443

Káradóttir, R., Hamilton, N. B., Bakiri, Y., & Attwell, D. (2008). Spiking and non-spiking classes of oligodendrocyte precursor glia in CNS white matter. *Nature Neuroscience*, *11*(4), 450–456. https://doi.org/10.1038/nn2060

Kim, J. K., Mastronardi, F. G., Wood, D. D., Lubman, D. M., Zand, R., & Moscarello, M. A. (2003). Multiple sclerosis: An important role for post-translational modifications of myelin basic protein in pathogenesis. *Molecular & Cellular Proteomics: MCP*, *2*(7), 453–462. https://doi.org/10.1074/mcp.M200050-MCP200

Kim, N.-S., & Chung, W.-S. (2023). Astrocytes regulate neuronal network activity by mediating synapse remodeling. *Neuroscience Research*, *187*, 3–13. https://doi.org/10.1016/j.neures.2022.09.007

Kim, T., & Pfeiffer, S. E. (1999). Myelin glycosphingolipid/cholesterol-enriched microdomains selectively sequester the non-compact myelin proteins CNP and MOG. *Journal of Neurocytology*, *28*(4), 281–293.

Kim, Y., Park, J., & Choi, Y. K. (2019). The Role of Astrocytes in the Central Nervous System Focused on BK Channel and Heme Oxygenase Metabolites: A Review. *Antioxidants*, *8*(5), 121. https://doi.org/10.3390/antiox8050121

Kister, A., & Kister, I. (2022). Overview of myelin, major myelin lipids, and myelin-associated proteins. *Frontiers in Chemistry*, *10*, 1041961. https://doi.org/10.3389/fchem.2022.1041961

Klar, T. A., Engel, E., & Hell, S. W. (2001). Breaking Abbe's diffraction resolution limit in fluorescence microscopy with stimulated emission depletion beams of various shapes. *Physical Review. E, Statistical, Nonlinear, and Soft Matter Physics*, *64*(6 Pt 2), 066613. https://doi.org/10.1103/PhysRevE.64.066613

Klingseisen, A., Ristoiu, A.-M., Kegel, L., Sherman, D. L., Rubio-Brotons, M., Almeida, R. G., Koudelka, S., Benito-Kwiecinski, S. K., Poole, R. J., Brophy, P. J., & Lyons, D. A. (2019). Oligodendrocyte Neurofascin Independently Regulates Both Myelin Targeting and Sheath Growth in the CNS. *Developmental Cell*, *51*(6), 730-744.e6. https://doi.org/10.1016/j.devcel.2019.10.016

Klugmann, M., Schwab, M. H., Pühlhofer, A., Schneider, A., Zimmermann, F., Griffiths, I. R., & Nave, K.-A. (1997). Assembly of CNS Myelin in the Absence of Proteolipid Protein. *Neuron*, *18*(1), 59–70. https://doi.org/10.1016/S0896-6273(01)80046-5

Knapp, P. E., Skoff, R. P., & Sprinkle, T. J. (1988). Differential expression of galactocerebroside, myelin basic protein, and 2′,3′-cyclic nucleotide 3′-phosphohydrolase during development of oligodendrocytes in vitro. *Journal of Neuroscience Research*, *21*(2–4), 249–259. https://doi.org/10.1002/jnr.490210217

Koch-Henriksen, N., & Sørensen, P. S. (2010). The changing demographic pattern of multiple sclerosis epidemiology. *The Lancet. Neurology*, *9*(5), 520–532. https://doi.org/10.1016/S1474-4422(10)70064-8

Kojima, W., & Hayashi, K. (2018). Changes in the axo-glial junctions of the optic nerves of cuprizone-treated mice. *Histochemistry and Cell Biology*, *149*(5), 529–536. https://doi.org/10.1007/s00418-018-1654-0

Kovacs, T., Zakany, F., & Nagy, P. (2022). It Takes More than Two to Tango: Complex, Hierarchal, and Membrane-Modulated Interactions in the Regulation of Receptor Tyrosine Kinases. *Cancers*, *14*(4), Article 4. https://doi.org/10.3390/cancers14040944

Krysko, K. M., Graves, J. S., Rensel, M., Weinstock-Guttman, B., Rutatangwa, A., Aaen, G., Belman, A., Benson, L., Chitnis, T., Gorman, M., Goyal, M. S., Harris, Y., Krupp, L., Lotze, T., Mar, S., Moodley, M., Ness, J., Rodriguez, M., Rose, J., … Centers, the U. N. of P. M. (2020). Real-World Effectiveness of

Initial Disease-Modifying Therapies in Pediatric Multiple Sclerosis. *Annals of Neurology*, *88*(1), 42–55. https://doi.org/10.1002/ana.25737

Kunz, B., Lierheimer, R., Rader, C., Spirig, M., Ziegler, U., & Sonderegger, P. (2002). Axonin-1/TAG-1 Mediates Cell-Cell Adhesion by a Cis-assisted Trans-interaction *. *Journal of Biological Chemistry*, *277*(6), 4551–4557. https://doi.org/10.1074/jbc.M109779200

Laganowsky, A., Reading, E., Allison, T. M., Ulmschneider, M. B., Degiacomi, M. T., Baldwin, A. J., & Robinson, C. V. (2014). Membrane proteins bind lipids selectively to modulate their structure and function. *Nature*, *510*(7503), Article 7503. https://doi.org/10.1038/nature13419

Lappe-Siefke, C., Goebbels, S., Gravel, M., Nicksch, E., Lee, J., Braun, P. E., Griffiths, I. R., & Nave, K.-A. (2003). Disruption of Cnp1 uncouples oligodendroglial functions in axonal support and myelination. *Nature Genetics*, *33*(3), 366–374. https://doi.org/10.1038/ng1095

Larson, V. A., Mironova, Y., Vanderpool, K. G., Waisman, A., Rash, J. E., Agarwal, A., & Bergles, D. E. (2018). Oligodendrocytes control potassium accumulation in white matter and seizure susceptibility. *ELife*, *7*, e34829. https://doi.org/10.7554/eLife.34829

Lassetter, A. P., Corty, M. M., Barria, R., Sheehan, A. E., Hill, J. Q., Aicher, S. A., Fox, A. N., & Freeman, M. R. (2023). Glial TGFβ activity promotes neuron survival in peripheral nerves. *The Journal of Cell Biology*, *222*(1), e202111053. https://doi.org/10.1083/jcb.202111053

Lee, J., Gravel, M., Gao, E., O'Neill, R. C., & Braun, P. E. (2001). Identification of Essential Residues in 2′,3′-Cyclic Nucleotide 3′-Phosphodiesterase: CHEMICAL MODIFICATION AND SITE-DIRECTED MUTAGENESIS TO INVESTIGATE THE ROLE OF CYSTEINE AND HISTIDINE RESIDUES IN ENZYMATIC ACTIVITY *. *Journal of Biological Chemistry*, *276*(18), 14804–14813. https://doi.org/10.1074/jbc.M009434200

Lee, Y., Morrison, B. M., Li, Y., Lengacher, S., Farah, M. H., Hoffman, P. N., Liu, Y., Tsingalia, A., Jin, L., Zhang, P.-W., Pellerin, L., Magistretti, P. J., & Rothstein, J. D. (2012). Oligodendroglia metabolically support axons and contribute to neurodegeneration. *Nature*, *487*(7408), 443–448. https://doi.org/10.1038/nature11314

Li, C., Tropak, M. B., Gerlai, R., Clapoff, S., Abramow-Newerly, W., Trapp, B., Peterson, A., & Roder, J. (1994). Myelination in the absence of myelin-associated glycoprotein. *Nature*, *369*(6483), 747–750. https://doi.org/10.1038/369747a0

Li, S., & Sheng, Z.-H. (2023). Oligodendrocyte-derived transcellular signaling regulates axonal energy metabolism. *Current Opinion in Neurobiology*, *80*, 102722. https://doi.org/10.1016/j.conb.2023.102722

Li, T., Wang, J., Wang, H., Yang, Y., Wang, S., Huang, N., Wang, F., Gao, X., Niu, J., Li, Z., Mei, F., & Xiao, L. (2018). The deletion of dicer in mature myelinating glial cells causes progressive axonal degeneration but not overt demyelination in adult mice. *Glia*, *66*(9), 1960–1971. https://doi.org/10.1002/glia.23450

Lichtenberg, D. (2005). *Detergent-resistant membranes should not be identified with membrane rafts*. 7.

Lim, B. C., & Rasband, M. N. (2020). Saltatory Conduction: Jumping to New Conclusions. *Current Biology*, *30*(7), R326–R328. https://doi.org/10.1016/j.cub.2020.02.037

Lin, S.-C., & Bergles, D. E. (2004). Synaptic signaling between neurons and glia. *Glia*, *47*(3), 290–298. https://doi.org/10.1002/glia.20060

Lopez, P. H. H. (2014). Role of myelin-associated glycoprotein (siglec-4a) in the nervous system. *Advances in Neurobiology*, *9*, 245–262. https://doi.org/10.1007/978-1-4939-1154-7_11

Luchicchi, A., Hart, B., Frigerio, I., van Dam, A., Perna, L., Offerhaus, H. L., Stys, P. K., Schenk, G. J., & Geurts, J. J. G. (2021a). Axon-Myelin Unit Blistering as Early Event in MS Normal Appearing White Matter. *Annals of Neurology*, *89*(4), 711–725. https://doi.org/10.1002/ana.26014

Luchicchi, A., Hart, B., Frigerio, I., van Dam, A.-M., Perna, L., Offerhaus, H. L., Stys, P. K., Schenk, G. J., & Geurts, J. J. G. (2021b). Axon-Myelin Unit Blistering as Early Event in MS Normal Appearing White Matter. *Annals of Neurology*, *89*(4), 711–725. https://doi.org/10.1002/ana.26014

Madsen, P. M., Desu, H. L., Vaccari, J. P. de R., Florimon, Y., Ellman, D. G., Keane, R. W., Clausen, B. H., Lambertsen, K. L., & Brambilla, R. (2020). Oligodendrocytes modulate the immune-inflammatory response in EAE via TNFR2 signaling. *Brain, Behavior, and Immunity*, *84*, 132–146. https://doi.org/10.1016/j.bbi.2019.11.017

Mahad, D. J., Ziabreva, I., Campbell, G., Lax, N., White, K., Hanson, P. S., Lassmann, H., & Turnbull, D. M. (2009). Mitochondrial changes within axons in multiple sclerosis. *Brain: A Journal of Neurology*, *132*(Pt 5), 1161–1174. https://doi.org/10.1093/brain/awp046

Maier, O., Hoekstra, D., & Baron, W. (2008). Polarity Development in Oligodendrocytes: Sorting and Trafficking of Myelin Components. *Journal of Molecular Neuroscience*, *35*(1), 35–53. https://doi.org/10.1007/s12031-007-9024-8

Makhani, N., & Tremlett, H. (2021). The multiple sclerosis prodrome. *Nature Reviews. Neurology*, *17*(8), 515–521. https://doi.org/10.1038/s41582-021-00519-3

Mallon, B. S., Shick, H. E., Kidd, G. J., & Macklin, W. B. (2002). Proteolipid Promoter Activity Distinguishes Two Populations of NG2-Positive Cells throughout Neonatal Cortical Development. *The Journal of Neuroscience*, *22*(3), 876–885. https://doi.org/10.1523/JNEUROSCI.22-03-00876.2002

Marbois, B. N., Faull, K. F., Fluharty, A. L., Raval-Fernandes, S., & Rome, L. H. (2000). Analysis of sulfatide from rat cerebellum and multiple sclerosis white matter by negative ion electrospray mass spectrometry. *Biochimica et Biophysica Acta (BBA) - Molecular and Cell Biology of Lipids*, *1484*(1), 59–70. https://doi.org/10.1016/S1388-1981(99)00201-2

Marcus, J., Dupree, J. L., & Popko, B. (2002). Myelin-associated glycoprotein and myelin galactolipids stabilize developing axo-glial interactions. *The Journal of Cell Biology*, *156*(3), 567–577. https://doi.org/10.1083/jcb.200111047

Marcus, J., Honigbaum, S., Shroff, S., Honke, K., Rosenbluth, J., & Dupree, J. L. (2006). Sulfatide is essential for the maintenance of CNS myelin and axon structure. *Glia*, *53*(4), 372–381. https://doi.org/10.1002/glia.20292

Maricic, I., Halder, R., Bischof, F., & Kumar, V. (2014). Dendritic cells and anergic type I NKT cells play a crucial role in sulfatide-mediated immune regulation in experimental autoimmune encephalomyelitis. *Journal of Immunology (Baltimore, Md. : 1950)*, *193*(3), 1035–1046. https://doi.org/10.4049/jimmunol.1302898

Marques, S., Zeisel, A., Codeluppi, S., van Bruggen, D., Mendanha Falcão, A., Xiao, L., Li, H., Häring, M., Hochgerner, H., Romanov, R. A., Gyllborg, D., Muñoz Manchado, A., La Manno, G., Lönnerberg, P.,

Floriddia, E. M., Rezayee, F., Ernfors, P., Arenas, E., Hjerling-Leffler, J., … Castelo-Branco, G. (2016). Oligodendrocyte heterogeneity in the mouse juvenile and adult central nervous system. *Science (New York, N.Y.)*, *352*(6291), 1326–1329. https://doi.org/10.1126/science.aaf6463

Martini, R., & Schachner, M. (1986). Immunoelectron microscopic localization of neural cell adhesion molecules (L1, N-CAM, and MAG) and their shared carbohydrate epitope and myelin basic protein in developing sciatic nerve. *The Journal of Cell Biology*, *103*(6 Pt 1), 2439–2448. https://doi.org/10.1083/jcb.103.6.2439

Mason, J. L., Langaman, C., Morell, P., Suzuki, K., & Matsushima, G. K. (2001). Episodic demyelination and subsequent remyelination within the murine central nervous system: Changes in axonal calibre. *Neuropathology and Applied Neurobiology*, *27*(1), 50–58. https://doi.org/10.1046/j.0305-1846.2001.00301.x

Maurel, P., Einheber, S., Galinska, J., Thaker, P., Lam, I., Rubin, M. B., Scherer, S. S., Murakami, Y., Gutmann, D. H., & Salzer, J. L. (2007). Nectin-like proteins mediate axon Schwann cell interactions along the internode and are essential for myelination. *The Journal of Cell Biology*, *178*(5), 861–874. https://doi.org/10.1083/jcb.200705132

Mayer, J. A., Larsen, E. C., Kondo, Y., & Duncan, I. D. (2011). Characterization of a PLP-overexpressing transgenic rat, a model for the connatal form of Pelizaeus-Merzbacher disease. *Neurobiology of Disease*, *44*(2), 231–238. https://doi.org/10.1016/j.nbd.2011.07.007

McGinley, M. P., & Cohen, J. A. (2021). Sphingosine 1-phosphate receptor modulators in multiple sclerosis and other conditions. *Lancet (London, England)*, *398*(10306), 1184–1194. https://doi.org/10.1016/S0140-6736(21)00244-0

McGonigal, R., Barrie, J. A., Yao, D., McLaughlin, M., Cunningham, M. E., Rowan, E. G., & Willison, H. J. (2019). Glial Sulfatides and Neuronal Complex Gangliosides Are Functionally Interdependent in Maintaining Myelinating Axon Integrity. *Journal of Neuroscience*, *39*(1), 63–77. https://doi.org/10.1523/JNEUROSCI.2095-18.2018

McGonigal, R., Cunningham, M. E., Smyth, D., Chou, M., Barrie, J. A., Wilkie, A., Campbell, C., Saatman, K. E., Lunn, M., & Willison, H. J. (2023). The endogenous calpain inhibitor calpastatin attenuates axon

degeneration in murine Guillain-Barré syndrome. *Journal of the Peripheral Nervous System: JPNS*, *28*(1), 4–16. https://doi.org/10.1111/jns.12520

McKie, S. J., Nicholson, A. S., Smith, E., Fawke, S., Caroe, E. R., Williamson, J. C., Butt, B. G., Kolářová, D., Peterka, O., Holčapek, M., Lehner, P. J., Graham, S. C., & Deane, J. E. (2023). Altered plasma membrane abundance of the sulfatide-binding protein NF155 links glycosphingolipid imbalances to demyelination. *Proceedings of the National Academy of Sciences*, *120*(14), e2218823120. https://doi.org/10.1073/pnas.2218823120

Mei, F., Wang, H., Liu, S., Niu, J., Wang, L., He, Y., Etxeberria, A., Chan, J. R., & Xiao, L. (2013). Stage-Specific Deletion of Olig2 Conveys Opposing Functions on Differentiation and Maturation of Oligodendrocytes. *Journal of Neuroscience*, *33*(19), 8454–8462. https://doi.org/10.1523/JNEUROSCI.2453-12.2013

Melkonian, K. A., Ostermeyer, A. G., Chen, J. Z., Roth, M. G., & Brown, D. A. (1999). Role of lipid modifications in targeting proteins to detergent-resistant membrane rafts. Many raft proteins are acylated, while few are prenylated. *The Journal of Biological Chemistry*, *274*(6), 3910–3917. https://doi.org/10.1074/jbc.274.6.3910

Meller, D., Eysel, U. T., & Schmidt-Kastner, R. (1994). Transient immunohistochemical labelling of rat retinal axons during Wallerian degeneration by a monoclonal antibody to neurofilaments. *Brain Research*, *648*(1), 162–166. https://doi.org/10.1016/0006-8993(94)91917-8

Micheva, K. D., Kiraly, M., Perez, M. M., & Madison, D. V. (2021). Conduction Velocity Along the Local Axons of Parvalbumin Interneurons Correlates With the Degree of Axonal Myelination. *Cerebral Cortex (New York, N.Y.: 1991)*, *31*(7), 3374–3392. https://doi.org/10.1093/cercor/bhab018

Mierzwa, A. J., Arevalo, J.-C., Schiff, R., Chao, M. V., & Rosenbluth, J. (2010a). Role of transverse bands in maintaining paranodal structure and axolemmal domain organization in myelinated nerve fibers: Effect on longevity in dysmyelinated mutant mice. *The Journal of Comparative Neurology*, *518*(14), 2841–2853. https://doi.org/10.1002/cne.22367

Mierzwa, A. J., Arevalo, J.-C., Schiff, R., Chao, M. V., & Rosenbluth, J. (2010b). Role of transverse bands in maintaining paranodal structure and axolemmal domain organization in myelinated nerve fibers: Effect

on longevity in dysmyelinated mutant mice. *The Journal of Comparative Neurology*, *518*(14), 2841–2853. https://doi.org/10.1002/cne.22367

Mierzwa, A. J., Marion, C. M., Sullivan, G. M., McDaniel, D. P., & Armstrong, R. C. (2015). Components of Myelin Damage and Repair in the Progression of White Matter Pathology After Mild Traumatic Brain Injury. *Journal of Neuropathology and Experimental Neurology*, *74*(3), 218–232. https://doi.org/10.1097/NEN.0000000000000165

Mierzwa, A. J., Zhou, Y.-X., Hibbits, N., Vana, A. C., & Armstrong, R. C. (2013). FGF2 and FGFR1 Signaling Regulate Functional Recovery Following Cuprizone Demyelination. *Neuroscience Letters*, *548*, 280–285. https://doi.org/10.1016/j.neulet.2013.05.010

Milner, R. J., Lai, C., Nave, K.-A., Lenoir, D., Ogata, J., & Sutcliffe, J. G. (1985). Nucleotide sequences of two mRNAs for rat brain myelin proteolipid protein. *Cell*, *42*(3), 931–939. https://doi.org/10.1016/0092-8674(85)90289-2

Moccia, M., Ruggieri, S., Ianniello, A., Toosy, A., Pozzilli, C., & Ciccarelli, O. (2019). Advances in spinal cord imaging in multiple sclerosis. *Therapeutic Advances in Neurological Disorders*, *12*, 1756286419840593. https://doi.org/10.1177/1756286419840593

Molander-Melin, M., Pernber, Z., Franken, S., Gieselmann, V., Månsson, J.-E., & Fredman, P. (2004). Accumulation of sulfatide in neuronal and glial cells of arylsulfatase A deficient mice. *Journal of Neurocytology*, *33*(4), 417–427. https://doi.org/10.1023/B:NEUR.0000046572.53905.2c

Mollinedo, F., & Gajate, C. (2020). Lipid rafts as signaling hubs in cancer cell survival/death and invasion: Implications in tumor progression and therapy. *Journal of Lipid Research*, *61*(5), 611–635. https://doi.org/10.1194/jlr.TR119000439

Moore, J. W., Joyner, R. W., Brill, M. H., Waxman, S. D., & Najar-Joa, M. (1978). Simulations of conduction in uniform myelinated fibers. Relative sensitivity to changes in nodal and internodal parameters. *Biophysical Journal*, *21*(2), 147–160. https://doi.org/10.1016/S0006-3495(78)85515-5

Morell, P., & Quarles, R. H. (1999). Characteristic Composition of Myelin. *Basic Neurochemistry: Molecular, Cellular and Medical Aspects. 6th Edition*. https://www.ncbi.nlm.nih.gov/books/NBK28221/

Morell, P., & Radin, N. S. (1969). Synthesis of cerebroside by brain from uridine diphosphate galactose and ceramide containing hydroxy fatty acid. *Biochemistry*, *8*(2), 506–512. https://doi.org/10.1021/bi00830a008

Morrison, B. M., Lee, Y., & Rothstein, J. D. (2013). Oligodendroglia metabolically support axons and maintain structural integrity. *Trends in Cell Biology*, *23*(12). https://doi.org/10.1016/j.tcb.2013.07.007

Moscatelli, E. A., & Isaacson, E. (1969). Gas liquid chromatographic analysis of sphingosine bases in sphingolipids of human normal and multiple sclerosis cerebral white matter. *Lipids*, *4*(6), 550–555. https://doi.org/10.1007/BF02531040

Moyano, A. L., Li, G., Boullerne, A. I., Feinstein, D. L., Hartman, E., Skias, D., Balavanov, R., van Breemen, R. B., Bongarzone, E. R., Månsson, J.-E., & Givogri, M. I. (2016). Sulfatides in extracellular vesicles isolated from plasma of multiple sclerosis patients. *Journal of Neuroscience Research*, *94*(12), 1579–1587. https://doi.org/10.1002/jnr.23899

Moyano, A. L., Pituch, K., Li, G., Breemen, R. van, Mansson, J. E., & Givogri, M. I. (2013). Levels of plasma sulfatides C18: 0 and C24 : 1 correlate with disease status in relapsing–remitting multiple sclerosis. *Journal of Neurochemistry*, *127*(5), 600–604. https://doi.org/10.1111/jnc.12341

Mukherjee, C., Kling, T., Russo, B., Miebach, K., Kess, E., Schifferer, M., Pedro, L. D., Weikert, U., Fard, M. K., Kannaiyan, N., Rossner, M., Aicher, M.-L., Goebbels, S., Nave, K.-A., Krämer-Albers, E.-M., Schneider, A., & Simons, M. (2020). Oligodendrocytes Provide Antioxidant Defense Function for Neurons by Secreting Ferritin Heavy Chain. *Cell Metabolism*, *32*(2), 259-272.e10. https://doi.org/10.1016/j.cmet.2020.05.019

Muzio, L., Viotti, A., & Martino, G. (2021). Microglia in Neuroinflammation and Neurodegeneration: From Understanding to Therapy. *Frontiers in Neuroscience*, *15*, 742065. https://doi.org/10.3389/fnins.2021.742065

Nagan, N., & Zoeller, R. A. (2001). Plasmalogens: Biosynthesis and functions. *Progress in Lipid Research*, *40*(3), 199–229. https://doi.org/10.1016/S0163-7827(01)00003-0

Nave, K. A., Lai, C., Bloom, F. E., & Milner, R. J. (1987). Splice site selection in the proteolipid protein (PLP) gene transcript and primary structure of the DM-20 protein of central nervous system myelin. *Proceedings of the National Academy of Sciences of the United States of America*, *84*(16), 5665–5669.

Nave, K.-A. (2010). Myelination and the trophic support of long axons. *Nature Reviews. Neuroscience*, *11*(4), 275–283. https://doi.org/10.1038/nrn2797

Norton, W. T., & Cammer, W. (1984). Isolation and Characterization of Myelin. In P. Morell (Ed.), *Myelin* (pp. 147–195). Springer US. https://doi.org/10.1007/978-1-4757-1830-0_5

Novakova, L., Henricsson, M., Björnson, E., Axelsson, M., Borén, J., Rosenstein, I., Lycke, J., Cardell, S. L., & Blomqvist, M. (2023). Cerebrospinal fluid sulfatide isoforms lack diagnostic utility in separating progressive from relapsing-remitting multiple sclerosis. *Multiple Sclerosis and Related Disorders*, *74*, 104705. https://doi.org/10.1016/j.msard.2023.104705

Novakova, L., Singh, A. K., Axelsson, M., Ståhlman, M., Adiels, M., Malmeström, C., Zetterberg, H., Borén, J., Lycke, J., Cardell, S. L., & Blomqvist, M. (2018). Sulfatide isoform pattern in cerebrospinal fluid discriminates progressive MS from relapsing-remitting MS. *Journal of Neurochemistry*, *146*(3), 322–332. https://doi.org/10.1111/jnc.14452

O'brien, J. S. (1965). STABILITY OF THE MYELIN MEMBRANE. *Science (New York, N.Y.)*, *147*(3662), 1099–1107. https://doi.org/10.1126/science.147.3662.1099

O'Brien, J. S., & Sampson, E. L. (1965). Lipid composition of the normal human brain: Gray matter, white matter, and myelin. *Journal of Lipid Research*, *6*(4), 537–544.

O'Connor, K. C., Bar-Or, A., & Hafler, D. A. (2001). The Neuroimmunology of Multiple Sclerosis: Possible Roles of T and B Lymphocytes in Immunopathogenesis. *Journal of Clinical Immunology*, *21*(2), 12.

Ogawa, Y., Schafer, D. P., Horresh, I., Bar, V., Hales, K., Yang, Y., Susuki, K., Peles, E., Stankewich, M. C., & Rasband, M. N. (2006). Spectrins and AnkyrinB Constitute a Specialized Paranodal Cytoskeleton. *Journal of Neuroscience*, *26*(19), 5230–5239. https://doi.org/10.1523/JNEUROSCI.0425-06.2006

Ohvo-Rekilä, H., Ramstedt, B., Leppimäki, P., & Slotte, J. P. (2002). Cholesterol interactions with phospholipids in membranes. *Progress in Lipid Research*, *41*(1), 66–97. https://doi.org/10.1016/s0163-7827(01)00020-0

Olsson, T., Barcellos, L. F., & Alfredsson, L. (2017). Interactions between genetic, lifestyle and environmental risk factors for multiple sclerosis. *Nature Reviews Neurology*, *13*(1), Article 1. https://doi.org/10.1038/nrneurol.2016.187

Omelchenko, A., Shrirao, A. B., Bhattiprolu, A. K., Zahn, J. D., Schloss, R. S., Dickson, S., Meaney, D. F., Boustany, N. N., Yarmush, M. L., & Firestein, B. L. (2019). Dynamin and reverse-mode sodium calcium exchanger blockade confers neuroprotection from diffuse axonal injury. *Cell Death & Disease*, *10*(10), 727. https://doi.org/10.1038/s41419-019-1908-3

Ovchinnikov, A., & Findling, O. (2022). An overview of pivotal trials and real-world evidence for CD20-depleting therapy in multiple sclerosis: Immunotherapy with rituximab, ocrelizumab, and ofatumumab. *Wiener Medizinische Wochenschrift (1946)*, *172*(15–16), 359–364. https://doi.org/10.1007/s10354-022-00939-w

Owen, T. (1957). Multiple sclerosis. *Canadian Journal of Occupational Therapy. Revue Canadienne D'ergotherapie*, *24*(4), 125–129. https://doi.org/10.1177/000841745702400404

Palavicini, J. P., Ding, L., Pan, M., Qiu, S., Wang, H., Shen, Q., Dupree, J. L., & Han, X. (2022). Sulfatide Deficiency, an Early Alzheimer's Lipidomic Signature, Causes Brain Ventricular Enlargement in the Absence of Classical Neuropathological Hallmarks. *International Journal of Molecular Sciences*, *24*(1), 233. https://doi.org/10.3390/ijms24010233

Palavicini, J. P., Wang, C., Chen, L., Ahmar, S., Higuera, J. D., Dupree, J. L., & Han, X. (2016). Novel molecular insights into the critical role of sulfatide in myelin maintenance/function. *Journal of Neurochemistry*, *139*(1), 40–54. https://doi.org/10.1111/jnc.13738

Pasquini, J. M., Guarna, M. M., Besio-Moreno, M. A., Iturregui, M. T., Oteiza, P. I., & Soto, E. F. (1989). Inhibition of the synthesis of glycosphingolipids affects the translocation of proteolipid protein to the myelin membrane. *Journal of Neuroscience Research*, *22*(3), 289–296. https://doi.org/10.1002/jnr.490220309

Peacock, J. D., Pridgeon, M. G., Tovar, E. A., Essenburg, C. J., Bowman, M., Madaj, Z., Koeman, J., Boguslawski, E. A., Grit, J., Dodd, R. D., Khachaturov, V., Cardona, D. M., Chen, M., Kirsch, D. G., Maina, F., Dono, R., Winn, M. E., Graveel, C. R., & Steensma, M. R. (2018). Genomic status of MET

potentiates sensitivity to MET and MEK inhibition in NF1-related malignant peripheral nerve sheath tumors. *Cancer Research*, *78*(13), 3672–3687. https://doi.org/10.1158/0008-5472.CAN-17-3167

Pedraza, L., Owens, G. C., Green, L. A., & Salzer, J. L. (1990). The myelin-associated glycoproteins: Membrane disposition, evidence of a novel disulfide linkage between immunoglobulin-like domains, and posttranslational palmitylation. *Journal of Cell Biology*, *111*(6), 2651–2661. https://doi.org/10.1083/jcb.111.6.2651

Penfield, W. (1924). OLIGODENDROGLIA AND ITS RELATION TO CLASSICAL NEUROGLIA. *Brain*, *47*(4), 430–452. https://doi.org/10.1093/brain/47.4.430

Perge, J. A., Koch, K., Miller, R., Sterling, P., & Balasubramanian, V. (2009). How the Optic Nerve Allocates Space, Energy Capacity, and Information. *Journal of Neuroscience*, *29*(24), 7917–7928. https://doi.org/10.1523/JNEUROSCI.5200-08.2009

Pernber, Z., Molander-Melin, M., Berthold, C.-H., Hansson, E., & Fredman, P. (2002). Expression of the myelin and oligodendrocyte progenitor marker sulfatide in neurons and astrocytes of adult rat brain. *Journal of Neuroscience Research*, *69*(1), 86–93. https://doi.org/10.1002/jnr.10264

Peters, A. (1966). The Node of Ranvier in the Central Nervous System. *Quarterly Journal of Experimental Physiology and Cognate Medical Sciences*, *51*(3), 229–236. https://doi.org/10.1113/expphysiol.1966.sp001852

Peters, A., Palay, Sanford, & Webster, Henry. (1992). The Fine Structure of the Nervous System: Neurons and Their Supporting Cells. *The Quarterly Review of Biology*, *67*(1), 80.

Piehl, F. (2021). Current and emerging disease-modulatory therapies and treatment targets for multiple sclerosis. *Journal of Internal Medicine*, *289*(6), 771–791. https://doi.org/10.1111/joim.13215

Pillai, A. M., Thaxton, C., Pribisko, A. L., Cheng, J.-G., Dupree, J. L., & Bhat, M. A. (2009). Spatiotemporal Ablation of Myelinating Glia-Specific Neurofascin (NfascNF155) in Mice Reveals Gradual Loss of Paranodal Axoglial Junctions and Concomitant Disorganization of Axonal Domains. *Journal of Neuroscience Research*, *87*(8), 1773–1793. https://doi.org/10.1002/jnr.22015

Podbielska, M., Ariga, T., & Pokryszko-Dragan, A. (2022). Sphingolipid Players in Multiple Sclerosis: Their Influence on the Initiation and Course of the Disease. *International Journal of Molecular Sciences*, *23*(10), 5330. https://doi.org/10.3390/ijms23105330

Poduslo, S. E. (1975). The Isolation and Characterization of a Plasma Membrane and a Myelin Fraction Derived from Oligodendroglia of Calf Brain1. *Journal of Neurochemistry*, *24*(4), 647–654. https://doi.org/10.1111/j.1471-4159.1975.tb03842.x

Poliak, S., Gollan, L., Martinez, R., Custer, A., Einheber, S., Salzer, J. L., Trimmer, J. S., Shrager, P., & Peles, E. (1999). Caspr2, a new member of the neurexin superfamily, is localized at the juxtaparanodes of myelinated axons and associates with K+ channels. *Neuron*, *24*(4), 1037–1047. https://doi.org/10.1016/s0896-6273(00)81049-1

Poliak, S., Salomon, D., Elhanany, H., Sabanay, H., Kiernan, B., Pevny, L., Stewart, C. L., Xu, X., Chiu, S.-Y., Shrager, P., Furley, A. J. W., & Peles, E. (2003). Juxtaparanodal clustering of Shaker-like K+ channels in myelinated axons depends on Caspr2 and TAG-1. *The Journal of Cell Biology*, *162*(6), 1149–1160. https://doi.org/10.1083/jcb.200305018

Poliani, P. L., Wang, Y., Fontana, E., Robinette, M. L., Yamanishi, Y., Gilfillan, S., & Colonna, M. (2015). TREM2 sustains microglial expansion during aging and response to demyelination. *The Journal of Clinical Investigation*, *125*(5), 2161–2170. https://doi.org/10.1172/JCI77983

Pomicter, A. D., Shroff, S. M., Fuss, B., Sato-Bigbee, C., Brophy, P. J., Rasband, M. N., Bhat, M. A., & Dupree, J. L. (2010a). Novel forms of neurofascin 155 in the central nervous system: Alterations in paranodal disruption models and multiple sclerosis. *Brain*, *133*(2), 389–405. https://doi.org/10.1093/brain/awp341

Pomicter, A. D., Shroff, S. M., Fuss, B., Sato-Bigbee, C., Brophy, P. J., Rasband, M. N., Bhat, M. A., & Dupree, J. L. (2010b). Novel forms of neurofascin 155 in the central nervous system: Alterations in paranodal disruption models and multiple sclerosis. *Brain*, *133*(2), 389–405. https://doi.org/10.1093/brain/awp341

Pomicter, A., DeLoyht, J., Hackett, A., Purdie, N., Sato-Bigbee, C., Henderson, S., & Dupree, J. (2013). Nfasc155H and MAG are specifically susceptible to detergent extraction in the absence of the myelin sphingolipid sulfatide. *Neurochemical Research*, *38*(12), 2490–2502. https://doi.org/10.1007/s11064-013-1162-5

Previtali, S. C., Quattrini, A., & Bolino, A. (2007). Charcot–Marie–Tooth type 4B demyelinating neuropathy: Deciphering the role of MTMR phosphatases. *Expert Reviews in Molecular Medicine*, *9*(25), 1–16. https://doi.org/10.1017/S1462399407000439

Pronker, M. F., Lemstra, S., Snijder, J., Heck, A. J. R., Thies-Weesie, D. M. E., Pasterkamp, R. J., & Janssen, B. J. C. (2016). Structural basis of myelin-associated glycoprotein adhesion and signalling. *Nature Communications*, *7*(1), Article 1. https://doi.org/10.1038/ncomms13584

Qiu, S., Palavicini, J. P., Wang, J., Gonzalez, N. S., He, S., Dustin, E., Zou, C., Ding, L., Bhattacharjee, A., Van Skike, C. E., Galvan, V., Dupree, J. L., & Han, X. (2021). Adult-onset CNS myelin sulfatide deficiency is sufficient to cause Alzheimer's disease-like neuroinflammation and cognitive impairment. *Molecular Neurodegeneration*, *16*, 64. https://doi.org/10.1186/s13024-021-00488-7

Quarles, R. H. (2007). Myelin-associated glycoprotein (MAG): Past, present and beyond. *Journal of Neurochemistry*, *100*(6), 1431–1448. https://doi.org/10.1111/j.1471-4159.2006.04319.x

Quarles, R. H., Macklin, W. B., & Morell, P. (2006). Myelin Formation, Structure and Biochemistry. In *Basic Neurochemistry: Molecular, Cellular and Medical Aspects* (p. 21).

Rasband, M. N., Peles, E., Trimmer, J. S., Levinson, S. R., Lux, S. E., & Shrager, P. (1999). Dependence of Nodal Sodium Channel Clustering on Paranodal Axoglial Contact in the Developing CNS. *Journal of Neuroscience*, *19*(17), 7516–7528. https://doi.org/10.1523/JNEUROSCI.19-17-07516.1999

Rasband, M. N., Tayler, J., Kaga, Y., Yang, Y., Lappe-Siefke, C., Nave, K.-A., & Bansal, R. (2005). CNP is required for maintenance of axon–glia interactions at nodes of Ranvier in the CNS. *Glia*, *50*(1), 86–90. https://doi.org/10.1002/glia.20165

Rasband, M. N., & Trimmer, J. S. (2001). Developmental clustering of ion channels at and near the node of Ranvier. *Developmental Biology*, *236*(1), 5–16. https://doi.org/10.1006/dbio.2001.0326

Recks, M. S., Stormanns, E. R., Bader, J., Arnhold, S., Addicks, K., & Kuerten, S. (2013). Early axonal damage and progressive myelin pathology define the kinetics of CNS histopathology in a mouse model of multiple sclerosis. *Clinical Immunology (Orlando, Fla.)*, *149*(1), 32–45. https://doi.org/10.1016/j.clim.2013.06.004

Reeves, T. M., Phillips, L. L., & Povlishock, J. T. (2005). Myelinated and unmyelinated axons of the corpus callosum differ in vulnerability and functional recovery following traumatic brain injury. *Experimental Neurology*, *196*(1), 126–137. https://doi.org/10.1016/j.expneurol.2005.07.014

Ren, Q., & Bennett, V. (1998). Palmitoylation of Neurofascin at a Site in the Membrane-Spanning Domain Highly Conserved Among the L1 Family of Cell Adhesion Molecules. *Journal of Neurochemistry*, *70*(5), 1839–1849. https://doi.org/10.1046/j.1471-4159.1998.70051839.x

Rhodes, K. J., Strassle, B. W., Monaghan, M. M., Bekele-Arcuri, Z., Matos, M. F., & Trimmer, J. S. (1997). Association and Colocalization of the Kvβ1 and Kvβ2 β-Subunits with Kv1 α-Subunits in Mammalian Brain K+Channel Complexes. *Journal of Neuroscience*, *17*(21), 8246–8258. https://doi.org/10.1523/JNEUROSCI.17-21-08246.1997

Richert, S., Kleinecke, S., Günther, J., Schaumburg, F., Edgar, J., Nienhaus, G. U., Nave, K.-A., & Kassmann, C. M. (2014). In vivo labeling of peroxisomes by photoconvertible mEos2 in myelinating glia of mice. *Biochimie*, *98*, 127–134. https://doi.org/10.1016/j.biochi.2013.10.022

Rios, J. C., Melendez-Vasquez, C. V., Einheber, S., Lustig, M., Grumet, M., Hemperly, J., Peles, E., & Salzer, J. L. (2000). Contactin-Associated Protein (Caspr) and Contactin Form a Complex That Is Targeted to the Paranodal Junctions during Myelination. *The Journal of Neuroscience*, *20*(22), 8354–8364. https://doi.org/10.1523/JNEUROSCI.20-22-08354.2000

Rodi, P. M., Bocco Gianello, M. D., Corregido, M. C., & Gennaro, A. M. (2014). Comparative study of the interaction of CHAPS and Triton X-100 with the erythrocyte membrane. *Biochimica et Biophysica Acta (BBA) - Biomembranes*, *1838*(3), 859–866. https://doi.org/10.1016/j.bbamem.2013.11.006

Rodríguez Murúa, S., Farez, M. F., & Quintana, F. J. (2022). The Immune Response in Multiple Sclerosis. *Annual Review of Pathology*, *17*, 121–139. https://doi.org/10.1146/annurev-pathol-052920-040318

Rosenbluth, J. (1966). REDUNDANT MYELIN SHEATHS AND OTHER ULTRASTRUCTURAL FEATURES OF THE TOAD CEREBELLUM. *The Journal of Cell Biology*, *28*(1), 73–93.

Rosenbluth, J., Dupree, J. L., & Popko, B. (2003a). Nodal sodium channel domain integrity depends on the conformation of the paranodal junction, not on the presence of transverse bands. *Glia*, *41*(3), 318–325. https://doi.org/10.1002/glia.10179

Rosenbluth, J., Dupree, J. L., & Popko, B. (2003b). Nodal sodium channel domain integrity depends on the conformation of the paranodal junction, not on the presence of transverse bands. *Glia*, *41*(3), 318–325. https://doi.org/10.1002/glia.10179

Rosenbluth, J., Petzold, C., & Peles, E. (2012). Dependence of paranodal junctional gap width on transverse bands. *The Journal of Comparative Neurology*, *520*(12), 2774–2784. https://doi.org/10.1002/cne.23105

Roy, A., & Patra, S. K. (2023). Lipid Raft Facilitated Receptor Organization and Signaling: A Functional Rheostat in Embryonic Development, Stem Cell Biology and Cancer. *Stem Cell Reviews and Reports*, *19*(1), 2–25. https://doi.org/10.1007/s12015-022-10448-3

Rust, M. J., Bates, M., & Zhuang, X. (2006). Sub-diffraction-limit imaging by stochastic optical reconstruction microscopy (STORM). *Nature Methods*, *3*(10), 793–795. https://doi.org/10.1038/nmeth929

Saab, A. S., & Nave, K.-A. (2017). Myelin dynamics: Protecting and shaping neuronal functions. *Current Opinion in Neurobiology*, *47*, 104–112. https://doi.org/10.1016/j.conb.2017.09.013

Saliani, A., Perraud, B., Duval, T., Stikov, N., Rossignol, S., & Cohen-Adad, J. (2017). Axon and Myelin Morphology in Animal and Human Spinal Cord. *Frontiers in Neuroanatomy*, *11*, 129. https://doi.org/10.3389/fnana.2017.00129

Sankarshanan, M., Ma, Z., Iype, T., & Lorenz, U. (2007). Identification of a novel lipid raft-targeting motif in Src homology 2-containing phosphatase 1. *Journal of Immunology (Baltimore, Md.: 1950)*, *179*(1), 483–490. https://doi.org/10.4049/jimmunol.179.1.483

Schaeren-Wiemers, N., Bonnet, A., Erb, M., Erne, B., Bartsch, U., Kern, F., Mantei, N., Sherman, D., & Suter, U. (2004). The raft-associated protein MAL is required for maintenance of proper axon–glia interactions in the central nervous system. *The Journal of Cell Biology*, *166*(5), 731–742. https://doi.org/10.1083/jcb.200406092

Schafer, D. P. (2004). Does Paranode Formation and Maintenance Require Partitioning of Neurofascin 155 into Lipid Rafts? *Journal of Neuroscience*, *24*(13), 3176–3185. https://doi.org/10.1523/JNEUROSCI.5427-03.2004

Scherer, S. S., Braun, P. E., Grinspan, J., Collarini, E., Wang, D. Y., & Kamholz, J. (1994). Differential regulation of the 2',3'-cyclic nucleotide 3'-phosphodiesterase gene during oligodendrocyte development. *Neuron*, *12*(6), 1363–1375. https://doi.org/10.1016/0896-6273(94)90451-0

Schirmer, L., Merkler, D., König, F. B., Brück, W., & Stadelmann, C. (2012). Neuroaxonal Regeneration is More Pronounced in Early Multiple Sclerosis than in Traumatic Brain Injury Lesions. *Brain Pathology*, *23*(1), 2–12. https://doi.org/10.1111/j.1750-3639.2012.00608.x

Schnaar, R. L. (2010). Brain gangliosides in axon-myelin stability and axon regeneration. *FEBS Letters*, *584*(9), 1741–1747. https://doi.org/10.1016/j.febslet.2009.10.011

Schnapp, B., peracchia, camillo, & Mugnaini, E. (1976). THE PARANODAL AXO-GLIAL JUNCTION IN THE CENTRAL NERVOUS SYSTEM STUDIED WITH THIN SECTIONS AND FREEZE-FRACTURE. *Neuroscience*, *1*, 181–190.

Sezgin, E. (2017). Super-resolution optical microscopy for studying membrane structure and dynamics. *Journal of Physics. Condensed Matter: An Institute of Physics Journal*, *29*(27), 273001. https://doi.org/10.1088/1361-648X/aa7185

Shamshiev, A., Donda, A., Prigozy, T. I., Mori, L., Chigorno, V., Benedict, C. A., Kappos, L., Sonnino, S., Kronenberg, M., & De Libero, G. (2000). The alphabeta T cell response to self-glycolipids shows a novel mechanism of CD1b loading and a requirement for complex oligosaccharides. *Immunity*, *13*(2), 255–264. https://doi.org/10.1016/s1074-7613(00)00025-x

Sharma, G., Gopinath, S., & Lakshmi Narasimhan, R. (2022). Exploring the Molecular Aspects of Glycosylation in MOG Antibody Disease (MOGAD). *Current Protein & Peptide Science*, *23*(6), 384–394. https://doi.org/10.2174/1389203723666220815110509

Shepherd, M. N., Pomicter, A. D., Velazco, C. S., Henderson, S. C., & Dupree, J. L. (2012a). Paranodal reorganization results in the depletion of transverse bands in the aged central nervous system. *Neurobiology of Aging*, *33*(1), 203.e13-203.e24. https://doi.org/10.1016/j.neurobiolaging.2010.08.001

Shepherd, M. N., Pomicter, A. D., Velazco, C. S., Henderson, S. C., & Dupree, J. L. (2012b). Paranodal reorganization results in the depletion of transverse bands in the aged central nervous system. *Neurobiology of Aging*, *33*(1), 203.e13-203.e24. https://doi.org/10.1016/j.neurobiolaging.2010.08.001

Shinohara, M., Tachibana, M., Kanekiyo, T., & Bu, G. (2017). Role of LRP1 in the pathogenesis of Alzheimer's disease: Evidence from clinical and preclinical studies. *Journal of Lipid Research*, *58*(7), 1267–1281. https://doi.org/10.1194/jlr.R075796

Shroff, S. M., Pomicter, A. D., Chow, W. N., Fox, M. A., Colello, R. J., Henderson, S. C., & Dupree, J. L. (2009). Adult CST-null mice maintain an increased number of oligodendrocytes. *Journal of Neuroscience Research*, *87*(15), 3403–3414. https://doi.org/10.1002/jnr.22003

Simons, K., & Ikonen, E. (1997). Functional rafts in cell membranes. *Nature*, *387*(6633), 569–572. https://doi.org/10.1038/42408

Simons, M., Krämer, E.-M., Thiele, C., Stoffel, W., & Trotter, J. (2000). Assembly of Myelin by Association of Proteolipid Protein with Cholesterol- and Galactosylceramide-Rich Membrane Domains. *Journal of Cell Biology*, *151*(1), 143–154. https://doi.org/10.1083/jcb.151.1.143

Simons, M., & Trotter, J. (2007). Wrapping it up: The cell biology of myelination. *Current Opinion in Neurobiology*, *17*(5), 533–540. https://doi.org/10.1016/j.conb.2007.08.003

Sinha, K., Karimi-Abdolrezaee, S., Velumian, A. A., & Fehlings, M. G. (2006). Functional changes in genetically dysmyelinated spinal cord axons of shiverer mice: Role of juxtaparanodal Kv1 family K+ channels. *Journal of Neurophysiology*, *95*(3), 1683–1695. https://doi.org/10.1152/jn.00899.2005

Skotland, T., Hessvik, N. P., Sandvig, K., & Llorente, A. (2019). Exosomal lipid composition and the role of ether lipids and phosphoinositides in exosome biology. *Journal of Lipid Research*, *60*(1), 9–18. https://doi.org/10.1194/jlr.R084343

Smigiel, R., Sherman, D. L., Rydzanicz, M., Walczak, A., Mikolajkow, D., Krolak-Olejnik, B., Kosinska, J., Gasperowicz, P., Biernacka, A., Stawinski, P., Marciniak, M., Andrzejewski, W., Boczar, M., Krajewski, P., Sasiadek, M. M., Brophy, P. J., & Ploski, R. (2018). Homozygous mutation in the Neurofascin gene affecting the glial isoform of Neurofascin causes severe neurodevelopment disorder with hypotonia, amimia and areflexia. *Human Molecular Genetics*, *27*(21), 3669–3674. https://doi.org/10.1093/hmg/ddy277

Smith, K. J. (2007). Sodium Channels and Multiple Sclerosis: Roles in Symptom Production, Damage and Therapy. *Brain Pathology*, *17*(2), 230–242. https://doi.org/10.1111/j.1750-3639.2007.00066.x

Snaidero, N., Möbius, W., Czopka, T., Hekking, L. H. P., Mathisen, C., Verkleij, D., Goebbels, S., Edgar, J., Merkler, D., Lyons, D. A., Nave, K.-A., & Simons, M. (2014). Myelin membrane wrapping of CNS axons by PI(3,4,5)P3-dependent polarized growth at the inner tongue. *Cell*, *156*(1–2), 277–290. https://doi.org/10.1016/j.cell.2013.11.044

Snaidero, N., Velte, C., Myllykoski, M., Raasakka, A., Ignatev, A., Werner, H. B., Erwig, M. S., Möbius, W., Kursula, P., Nave, K.-A., & Simons, M. (2017). Antagonistic Functions of MBP and CNP Establish Cytosolic Channels in CNS Myelin. *Cell Reports*, *18*(2), 314–323. https://doi.org/10.1016/j.celrep.2016.12.053

Soldan, S. S., & Lieberman, P. M. (2023). Epstein–Barr virus and multiple sclerosis. *Nature Reviews Microbiology*, *21*(1), Article 1. https://doi.org/10.1038/s41579-022-00770-5

Song, I., & Dityatev, A. (2018). Crosstalk between glia, extracellular matrix and neurons. *Brain Research Bulletin*, *136*, 101–108. https://doi.org/10.1016/j.brainresbull.2017.03.003

Song, J.-L., Westover, M. B., & Zhang, R. (2022). A mechanistic model of calcium homeostasis leading to occurrence and propagation of secondary brain injury. *Journal of Neurophysiology*, *128*(5), 1168–1180. https://doi.org/10.1152/jn.00045.2022

Sonnino, S., Aureli, M., Grassi, S., Mauri, L., Prioni, S., & Prinetti, A. (2014). Lipid Rafts in Neurodegeneration and Neuroprotection. *Molecular Neurobiology*, *50*(1), 130–148. https://doi.org/10.1007/s12035-013-8614-4

Sprong, H., Kruithof, B., Leijendekker, R., Slot, J. W., Meer, G. van, & Sluijs, P. van der. (1998). UDP-Galactose:Ceramide Galactosyltransferase Is a Class I Integral Membrane Protein of the Endoplasmic Reticulum. *Journal of Biological Chemistry*, *273*(40), 25880–25888. https://doi.org/10.1074/jbc.273.40.25880

Stadelmann, C., Timmler, S., Barrantes-Freer, A., & Simons, M. (2019). Myelin in the Central Nervous System: Structure, Function, and Pathology. *Physiological Reviews*, *99*(3), 1381–1431. https://doi.org/10.1152/physrev.00031.2018

Steinman, L. (2001). Multiple sclerosis: A two-stage disease. *Nature Immunology*, *2*(9), Article 9. https://doi.org/10.1038/ni0901-762

Steyer, A. M., Buscham, T. J., Lorenz, C., Hümmert, S., Eichel-Vogel, M. A., Schadt, L. C., Edgar, J. M., Köster, S., Möbius, W., Nave, K.-A., & Werner, H. B. (2023). Focused ion beam-scanning electron microscopy links pathological myelin outfoldings to axonal changes in mice lacking Plp1 or Mag. *Glia*, *71*(3), 509–523. https://doi.org/10.1002/glia.24290

Stifani, N. (2014). Motor neurons and the generation of spinal motor neuron diversity. *Frontiers in Cellular Neuroscience*, *8*, 293. https://doi.org/10.3389/fncel.2014.00293

Sturrock, R. R. (1980). Myelination of the mouse corpus callosum. *Neuropathology and Applied Neurobiology*, *6*(6), 415–420. https://doi.org/10.1111/j.1365-2990.1980.tb00219.x

Stys, P. K., Waxman, S. G., & Ransom, B. R. (1992). Ionic mechanisms of anoxic injury in mammalian CNS white matter: Role of Na + channels and Na + -Ca 2+ exchanger. *Journal of Neuroscience*, 430–439.

Su, L., Athamna, M., Wang, Y., Wang, J., Freudenberg, M., Yue, T., Wang, J., Moresco, E. M. Y., He, H., Zor, T., & Beutler, B. (2021). Sulfatides are endogenous ligands for the TLR4-MD-2 complex. *Proceedings of the National Academy of Sciences of the United States of America*, *118*(30), e2105316118. https://doi.org/10.1073/pnas.2105316118

Subczynski, W. K., & Kusumi, A. (2003). Dynamics of raft molecules in the cell and artificial membranes: Approaches by pulse EPR spin labeling and single molecule optical microscopy. *Biochimica Et Biophysica Acta*, *1610*(2), 231–243. https://doi.org/10.1016/s0005-2736(03)00021-x

Sun, X., Takagishi, Y., Okabe, E., Chishima, Y., Kanou, Y., Murase, S., Mizumura, K., Inaba, M., Komatsu, Y., Hayashi, Y., Peles, E., Oda, S., & Murata, Y. (2009). A Novel Caspr Mutation Causes the Shambling Mouse Phenotype by Disrupting Axoglial Interactions of Myelinated Nerves. *Journal of Neuropathology & Experimental Neurology*, *68*(11), 1207–1218. https://doi.org/10.1097/NEN.0b013e3181be2e96

Susuki, K., Baba, H., Tohyama, K., Kanai, K., Kuwabara, S., Hirata, K., Furukawa, K., Furukawa, K., Rasband, M. N., & Yuki, N. (2007). Gangliosides contribute to stability of paranodal junctions and ion channel clusters in myelinated nerve fibers. *Glia*, *55*(7), 746–757. https://doi.org/10.1002/glia.20503

Susuki, K., Chang, K.-J., Zollinger, D. R., Liu, Y., Ogawa, Y., Eshed-Eisenbach, Y., Dours-Zimmermann, M. T., Oses-Prieto, J. A., Burlingame, A. L., Seidenbecher, C. I., Zimmermann, D. R., Oohashi, T., Peles, E.,

& Rasband, M. N. (2013). Three mechanisms assemble central nervous system nodes of Ranvier. *Neuron*, *78*(3), 469–482. https://doi.org/10.1016/j.neuron.2013.03.005

Susuki, K., Zollinger, D. R., Chang, K.-J., Zhang, C., Huang, C. Y.-M., Tsai, C.-R., Galiano, M. R., Liu, Y., Benusa, S. D., Yermakov, L. M., Griggs, R. B., Dupree, J. L., & Rasband, M. N. (2018). Glial βII Spectrin Contributes to Paranode Formation and Maintenance. *The Journal of Neuroscience: The Official Journal of the Society for Neuroscience*, *38*(27), 6063–6075. https://doi.org/10.1523/JNEUROSCI.3647-17.2018

Suzuki, K., Andrews, J., Waltz, J., & Terry, R. (1969). Ultrastructural studies of multiple sclerosis. *International Academy of Pathology*, *20*(5), 444–454.

Tait, S., Gunn-Moore, F., Collinson, J. M., Huang, J., Lubetzki, C., Pedraza, L., Sherman, D. L., Colman, D. R., & Brophy, P. J. (2000). An Oligodendrocyte Cell Adhesion Molecule at the Site of Assembly of the Paranodal Axo-Glial Junction. *Journal of Cell Biology*, *150*(3), 657–666. https://doi.org/10.1083/jcb.150.3.657

Taylor, C. M., Coetzee, T., & Pfeiffer, S. E. (2002). Detergent-insoluble glycosphingolipid/cholesterol microdomains of the myelin membrane. *Journal of Neurochemistry*, *81*(5), 993–1004. https://doi.org/10.1046/j.1471-4159.2002.00884.x

Thaxton, C., & Bhat, M. A. (2009). Myelination and Regional Domain Differentiation of the Axon. *Results and Problems in Cell Differentiation*, *48*, 1–28. https://doi.org/10.1007/400_2009_3

Thaxton, C., Pillai, A. M., Pribisko, A. L., Dupree, J. L., & Bhat, M. A. (2011). Nodes of Ranvier act as barriers to restrict invasion of flanking paranodal domains in myelinated axons. *Neuron*, *69*(2), 244–257. https://doi.org/10.1016/j.neuron.2010.12.016

Thomason, E. J., Suárez-Pozos, E., Afshari, F. S., Rosenberg, P. A., Dupree, J. L., & Fuss, B. (2022). Deletion of the Sodium-Dependent Glutamate Transporter GLT-1 in Maturing Oligodendrocytes Attenuates Myelination of Callosal Axons During a Postnatal Phase of Central Nervous System Development. *Frontiers in Cellular Neuroscience*, *16*. https://www.frontiersin.org/articles/10.3389/fncel.2022.905299

Thompson, A. J., Banwell, B. L., Barkhof, F., Carroll, W. M., Coetzee, T., Comi, G., Correale, J., Fazekas, F., Filippi, M., Freedman, M. S., Fujihara, K., Galetta, S. L., Hartung, H. P., Kappos, L., Lublin, F. D.,

Marrie, R. A., Miller, A. E., Miller, D. H., Montalban, X., … Cohen, J. A. (2018). Diagnosis of multiple sclerosis: 2017 revisions of the McDonald criteria. *The Lancet. Neurology*, *17*(2), 162–173. https://doi.org/10.1016/S1474-4422(17)30470-2

Trajkovic, K., Dhaunchak, A. S., Goncalves, J. T., Wenzel, D., Schneider, A., Bunt, G., Nave, K.-A., & Simons, M. (2006). Neuron to glia signaling triggers myelin membrane exocytosis from endosomal storage sites. *The Journal of Cell Biology*, *172*(6), 937–948. https://doi.org/10.1083/jcb.200509022

Traka, M., Dupree, J. L., Popko, B., & Karagogeos, D. (2002). The neuronal adhesion protein TAG-1 is expressed by Schwann cells and oligodendrocytes and is localized to the juxtaparanodal region of myelinated fibers. *The Journal of Neuroscience: The Official Journal of the Society for Neuroscience*, *22*(8), 3016–3024. https://doi.org/10.1523/JNEUROSCI.22-08-03016.2002

Traka, M., Goutebroze, L., Denisenko, N., Bessa, M., Nifli, A., Havaki, S., Iwakura, Y., Fukamauchi, F., Watanabe, K., Soliven, B., Girault, J.-A., & Karagogeos, D. (2003). Association of TAG-1 with Caspr2 is essential for the molecular organization of juxtaparanodal regions of myelinated fibers. *The Journal of Cell Biology*, *162*(6), 1161–1172. https://doi.org/10.1083/jcb.200305078

Trapp, B. D., Bernier, L., Andrews, S. B., & Colman, D. R. (1988). Cellular and Subcellular Distribution of 2',3'-Cyclic Nucleotide 3'-Phosphodiesterase and Its mRNA in the Rat Central Nervous System. *Journal of Neurochemistry*, *51*(3), 859–868. https://doi.org/10.1111/j.1471-4159.1988.tb01822.x

Trapp, B. D., Nishiyama, A., Cheng, D., & Macklin, W. (1997). Differentiation and Death of Premyelinating Oligodendrocytes in Developing Rodent Brain. *The Journal of Cell Biology*, *137*(2), 459–468.

Trapp, B. D., Peterson, J., Ransohoff, R. M., Rudick, R., Mörk, S., & Bö, L. (1998). Axonal Transection in the Lesions of Multiple Sclerosis. *New England Journal of Medicine*, *338*(5), 278–285. https://doi.org/10.1056/NEJM199801293380502

Trapp, B. D., & Quarles, R. H. (1982). Presence of the myelin-associated glycoprotein correlates with alterations in the periodicity of peripheral myelin. *The Journal of Cell Biology*, *92*(3), 877–882. https://doi.org/10.1083/jcb.92.3.877

Tropak, M. B., & Roder, J. C. (1997). Regulation of myelin-associated glycoprotein binding by sialylated cis-ligands. *Journal of Neurochemistry*, *68*(4), 1753–1763. https://doi.org/10.1046/j.1471-4159.1997.68041753.x

Tsiotra, P. C., Theodorakis, K., Papamatheakis, J., & Karagogeos, D. (1996). The Fibronectin Domains of the Neural Adhesion Molecule TAX-1 Are Necessary and Sufficient for Homophilic Binding *. *Journal of Biological Chemistry*, *271*(46), 29216–29222. https://doi.org/10.1074/jbc.271.46.29216

Uchida, K., Obayashi, H., Minamihata, K., Wakabayashi, R., Goto, M., Shimokawa, N., Takagi, M., & Kamiya, N. (2022). Artificial Palmitoylation of Proteins Controls the Lipid Domain-Selective Anchoring on Biomembranes and the Raft-Dependent Cellular Internalization. *Langmuir: The ACS Journal of Surfaces and Colloids*, *38*(31), 9640–9648. https://doi.org/10.1021/acs.langmuir.2c01205

Valny, M., Honsa, P., Kirdajova, D., Kamenik, Z., & Anderova, M. (2016). Tamoxifen in the Mouse Brain: Implications for Fate-Mapping Studies Using the Tamoxifen-Inducible Cre-loxP System. *Frontiers in Cellular Neuroscience*, *10*. https://doi.org/10.3389/fncel.2016.00243

van Tilborg, E., de Theije, C. G. M., van Hal, M., Wagenaar, N., de Vries, L. S., Benders, M. J., Rowitch, D. H., & Nijboer, C. H. (2018). Origin and dynamics of oligodendrocytes in the developing brain: Implications for perinatal white matter injury. *Glia*, *66*(2), 221–238. https://doi.org/10.1002/glia.23256

Van Zyl, R., Gieselmann, V., & Eckhardt, M. (2010). Elevated sulfatide levels in neurons cause lethal audiogenic seizures in mice. *Journal of Neurochemistry*, *112*(1), 282–295. https://doi.org/10.1111/j.1471-4159.2009.06458.x

Venkatesh, K., Chivatakarn, O., Lee, H., Joshi, P. S., Kantor, D. B., Newman, B. A., Mage, R., Rader, C., & Giger, R. J. (2005). The Nogo-66 Receptor Homolog NgR2 Is a Sialic Acid-Dependent Receptor Selective for Myelin-Associated Glycoprotein. *Journal of Neuroscience*, *25*(4), 808–822. https://doi.org/10.1523/JNEUROSCI.4464-04.2005

Verreycken, J., Baeten, P., & Broux, B. (2022). Regulatory T cell therapy for multiple sclerosis: Breaching (blood-brain) barriers. *Human Vaccines & Immunotherapeutics*, *18*(7), 2153534. https://doi.org/10.1080/21645515.2022.2153534

Verrier, J. D., Jackson, T. C., Gillespie, D. G., Janesko-Feldman, K., Bansal, R., Goebbels, S., Nave, K.-A., Kochanek, P. M., & Jackson, E. K. (2013). Role of CNPase in the Oligodendrocytic Extracellular 2′,3′-cAMP-Adenosine Pathway. *Glia*, *61*(10), 1595–1606. https://doi.org/10.1002/glia.22523

Vinson, M., Rausch, O., Maycox, P. R., Prinjha, R. K., Chapman, D., Morrow, R., Harper, A. J., Dingwall, C., Walsh, F. S., Burbidge, S. A., & Riddell, D. R. (2003). Lipid rafts mediate the interaction between myelin-associated glycoprotein (MAG) on myelin and MAG-receptors on neurons. *Molecular and Cellular Neurosciences*, *22*(3), 344–352. https://doi.org/10.1016/s1044-7431(02)00031-3

Wahl, S. E., McLane, L. E., Bercury, K. K., Macklin, W. B., & Wood, T. L. (2014). Mammalian Target of Rapamycin Promotes Oligodendrocyte Differentiation, Initiation and Extent of CNS Myelination. *The Journal of Neuroscience*, *34*(13), 4453–4465. https://doi.org/10.1523/JNEUROSCI.4311-13.2014

Wallin, M. T., Culpepper, W. J., Campbell, J. D., Nelson, L. M., Langer-Gould, A., Marrie, R. A., Cutter, G. R., Kaye, W. E., Wagner, L., Tremlett, H., Buka, S. L., Dilokthornsakul, P., Topol, B., Chen, L. H., & LaRocca, N. G. (2019). The prevalence of MS in the United States: A population-based estimate using health claims data. *Neurology*, *92*(10), e1029–e1040. https://doi.org/10.1212/WNL.0000000000007035

Walton, C., King, R., Rechtman, L., Kaye, W., Leray, E., Marrie, R. A., Robertson, N., La Rocca, N., Uitdehaag, B., van der Mei, I., Wallin, M., Helme, A., Angood Napier, C., Rijke, N., & Baneke, P. (2020). Rising prevalence of multiple sclerosis worldwide: Insights from the Atlas of MS, third edition. *Multiple Sclerosis (Houndmills, Basingstoke, England)*, *26*(14), 1816–1821. https://doi.org/10.1177/1352458520970841

Wang, H., Kunkel, D. D., Schwartzkroin, P. A., & Tempel, B. L. (1994). Localization of Kv1.1 and Kv1.2, two K channel proteins, to synaptic terminals, somata, and dendrites in the mouse brain. *Journal of Neuroscience*, *14*(8), 4588–4599. https://doi.org/10.1523/JNEUROSCI.14-08-04588.1994

Wang, J.-Q., Gao, M.-Y., Gao, R., Zhao, K.-H., Zhang, Y., & Li, X. (2023). Oligodendrocyte lineage cells: Advances in development, disease, and heterogeneity. *Journal of Neurochemistry*, *164*(4), 468–480. https://doi.org/10.1111/jnc.15728

Wang, Y., Cella, M., Mallinson, K., Ulrich, J. D., Young, K. L., Robinette, M. L., Gilfillan, S., Krishnan, G. M., Sudhakar, S., Zinselmeyer, B. H., Holtzman, D. M., Cirrito, J. R., & Colonna, M. (2015). TREM2 Lipid

Sensing Sustains the Microglial Response in an Alzheimer's Disease Model. *Cell*, *160*(6), 1061–1071. https://doi.org/10.1016/j.cell.2015.01.049

Ward, M., & Goldman, M. (2022). *Epidemiology and Pathophysiology of Multiple Sclerosis*. *28*(4), 988–1005.

Wee, P., & Wang, Z. (2017). Epidermal Growth Factor Receptor Cell Proliferation Signaling Pathways. *Cancers*, *9*(5), Article 5. https://doi.org/10.3390/cancers9050052

Westenbroek, R. E., Noebels, J. L., & Catterall, W. A. (1992). Elevated expression of type II Na+ channels in hypomyelinated axons of shiverer mouse brain. *The Journal of Neuroscience: The Official Journal of the Society for Neuroscience*, *12*(6), 2259–2267.

Wheeler, D., Bandaru, V. V. R., Calabresi, P. A., Nath, A., & Haughey, N. J. (2008a). A defect of sphingolipid metabolism modifies the properties of normal appearing white matter in multiple sclerosis. *Brain*, *131*(11), 3092–3102. https://doi.org/10.1093/brain/awn190

Wheeler, D., Bandaru, V. V. R., Calabresi, P. A., Nath, A., & Haughey, N. J. (2008b). A defect of sphingolipid metabolism modifies the properties of normal appearing white matter in multiple sclerosis. *Brain*, *131*(11), 3092–3102. https://doi.org/10.1093/brain/awn190

Whitehead, J. C., Hildebrand, B. A., Sun, M., Rockwood, M. R., Rose, R. A., Rockwood, K., & Howlett, S. E. (2014). A clinical frailty index in aging mice: Comparisons with frailty index data in humans. *The Journals of Gerontology. Series A, Biological Sciences and Medical Sciences*, *69*(6), 621–632. https://doi.org/10.1093/gerona/glt136

Wigger, D., Gulbins, E., Kleuser, B., & Schumacher, F. (2019). Monitoring the Sphingolipid de novo Synthesis by Stable-Isotope Labeling and Liquid Chromatography-Mass Spectrometry. *Frontiers in Cell and Developmental Biology*, *7*, 210. https://doi.org/10.3389/fcell.2019.00210

Wight, P. A., & Dobretsova, A. (2004). Where, when and how much: Regulation of myelin proteolipid protein gene expression. *Cellular and Molecular Life Sciences CMLS*, *61*(7), 810–821. https://doi.org/10.1007/s00018-003-3309-z

Williams, K. A., Deber, C. M., & Klrschner, O. A. (1993). The Structure and Function of Central Nervous System Myelin. *Critical Reviews in Clinical Laboratory Sciences*, *30*(1), 29–64. https://doi.org/10.3109/10408369309084665

Wilson, R., & Brophy, P. J. (1989). Role for the oligodendrocyte cytoskeleton in myelination. *Journal of Neuroscience Research*, *22*(4), 439–448. https://doi.org/10.1002/jnr.490220409

Yaghootfam, A., Sorkalla, T., Häberlein, H., Gieselmann, V., Havla, J., & Eckhardt*, M. (2007, July 21). *Cerebroside Sulfotransferase Forms Homodimers in Living Cells†* (world) [Research-article]. American Chemical Society. https://doi.org/10.1021/bi700014q

Yahara, S., Kawamura, N., Kishimoto, Y., Saida, T., & Tourtellotte, W. W. (1982). A change in the cerebrosides and sulfatides in a demyelinating nervous system. Development of the methodology and study of multiple sclerosis and Wallerian degeneration. *Journal of the Neurological Sciences*, *54*(2), 303–315. https://doi.org/10.1016/0022-510x(82)90191-5

Yamashita, T., Wada, R., Sasaki, T., Deng, C., Bierfreund, U., Sandhoff, K., & Proia, R. L. (1999). A vital role for glycosphingolipid synthesis during development and differentiation. *Proceedings of the National Academy of Sciences*, *96*(16), 9142–9147. https://doi.org/10.1073/pnas.96.16.9142

Yamate-Morgan, H., Lauderdale, K., Horeczko, J., Merchant, U., & Tiwari-Woodruff, S. K. (2019). Functional Effects of Cuprizone-Induced Demyelination in the Presence of the mTOR-Inhibitor Rapamycin ,. *Neuroscience*, *406*, 667–683. https://doi.org/10.1016/j.neuroscience.2019.01.038

Yang, J., Weimer, R. M., Kallop, D., Olsen, O., Wu, Z., Renier, N., Uryu, K., & Tessier-Lavigne, M. (2013). Regulation of axon degeneration after injury and in development by the endogenous calpain inhibitor calpastatin. *Neuron*, *80*(5), 1175–1189. https://doi.org/10.1016/j.neuron.2013.08.034

Yang, L. J., Zeller, C. B., Shaper, N. L., Kiso, M., Hasegawa, A., Shapiro, R. E., & Schnaar, R. L. (1996). Gangliosides are neuronal ligands for myelin-associated glycoprotein. *Proceedings of the National Academy of Sciences of the United States of America*, *93*(2), 814–818. https://doi.org/10.1073/pnas.93.2.814

Yang, Y., Lacas-Gervais, S., Morest, D. K., Solimena, M., & Rasband, M. N. (2004). BetaIV spectrins are essential for membrane stability and the molecular organization of nodes of Ranvier. *The Journal of Neuroscience: The Official Journal of the Society for Neuroscience*, *24*(33), 7230–7240. https://doi.org/10.1523/JNEUROSCI.2125-04.2004

Yermakov, L. M., Hong, L. A., Drouet, D. E., Griggs, R. B., & Susuki, K. (2019). Functional Domains in Myelinated Axons. *Advances in Experimental Medicine and Biology*, *1190*, 65–83. https://doi.org/10.1007/978-981-32-9636-7_6

Yin, X., Crawford, T. O., Griffin, J. W., Tu, P. h, Lee, V. M., Li, C., Roder, J., & Trapp, B. D. (1998). Myelin-associated glycoprotein is a myelin signal that modulates the caliber of myelinated axons. *The Journal of Neuroscience: The Official Journal of the Society for Neuroscience*, *18*(6), 1953–1962. https://doi.org/10.1523/JNEUROSCI.18-06-01953.1998

York, E. N., Martin, S.-J., Meijboom, R., Thrippleton, M. J., Bastin, M. E., Carter, E., Overell, J., Connick, P., Chandran, S., Waldman, A. D., & Hunt, D. P. J. (2021). MRI-derived g-ratio and lesion severity in newly diagnosed multiple sclerosis. *Brain Communications*, *3*(4), fcab249. https://doi.org/10.1093/braincomms/fcab249

Yu, F., Fan, Q., Tian, Q., Ngamsombat, C., Machado, N., Bireley, J. D., Russo, A. W., Nummenmaa, A., Witzel, T., Wald, L. L., Klawiter, E. C., & Huang, S. Y. (2019). Imaging G-Ratio in Multiple Sclerosis Using High-Gradient Diffusion MRI and Macromolecular Tissue Volume. *AJNR: American Journal of Neuroradiology*, *40*(11), 1871–1877. https://doi.org/10.3174/ajnr.A6283

Zajonc, D. M., Maricic, I., Wu, D., Halder, R., Roy, K., Wong, C.-H., Kumar, V., & Wilson, I. A. (2005). Structural basis for CD1d presentation of a sulfatide derived from myelin and its implications for autoimmunity. *The Journal of Experimental Medicine*, *202*(11), 1517–1526. https://doi.org/10.1084/jem.20051625

Zalc, B. (2006). The Acquisition of Myelin: A Success Story. In *Purinergic Signalling in Neuron–Glia Interactions* (pp. 15–25). John Wiley & Sons, Ltd. https://doi.org/10.1002/9780470032244.ch3

Zand, R., Li, M. X., Jin, X., & Lubman, D. (1998). Determination of the sites of posttranslational modifications in the charge isomers of bovine myelin basic protein by capillary electrophoresis-mass spectroscopy. *Biochemistry*, *37*(8), 2441–2449. https://doi.org/10.1021/bi972347t

Zeisel, A., Hochgerner, H., Lönnerberg, P., Johnsson, A., Memic, F., van der Zwan, J., Häring, M., Braun, E., Borm, L. E., La Manno, G., Codeluppi, S., Furlan, A., Lee, K., Skene, N., Harris, K. D., Hjerling-Leffler,

J., Arenas, E., Ernfors, P., Marklund, U., & Linnarsson, S. (2018). Molecular Architecture of the Mouse Nervous System. *Cell*, *174*(4), 999-1014.e22. https://doi.org/10.1016/j.cell.2018.06.021

Zhang, B., Cao, Q., Guo, A., Chu, H., Chan, Y. G., Buschdorf, J. P., Low, B. C., Ling, E. A., & Liang, F. (2005). Juxtanodin: An oligodendroglial protein that promotes cellular arborization and 2′,3′-cyclic nucleotide-3′-phosphodiesterase trafficking. *Proceedings of the National Academy of Sciences*, *102*(32), 11527–11532. https://doi.org/10.1073/pnas.0500952102

Zhang, C., Susuki, K., Zollinger, D. R., Dupree, J. L., & Rasband, M. N. (2013). Membrane domain organization of myelinated axons requires βII spectrin. *The Journal of Cell Biology*, *203*(3), 437–443. https://doi.org/10.1083/jcb.201308116

Zhang, K., Zhao, Y., Liang, Z., Wang, C., & Liu, X. (2020). Validity of the McDonald criteria in predicting second events in multiple sclerosis. *Multiple Sclerosis and Related Disorders*, *43*, 102223. https://doi.org/10.1016/j.msard.2020.102223

Zhang, L., Wang, Y., Liu, T., Mao, Y., & Peng, B. (2023). Novel Microglia-based Therapeutic Approaches to Neurodegenerative Disorders. *Neuroscience Bulletin*, *39*(3), 491–502. https://doi.org/10.1007/s12264-022-01013-6

Zhao, Y., Yamasaki, R., Yamaguchi, H., Nagata, S., Une, H., Cui, Y., Masaki, K., Nakamuta, Y., Iinuma, K., Watanabe, M., Matsushita, T., Isobe, N., & Kira, J.-I. (2020). Oligodendroglial connexin 47 regulates neuroinflammation upon autoimmune demyelination in a novel mouse model of multiple sclerosis. *Proceedings of the National Academy of Sciences of the United States of America*, *117*(4), 2160–2169. https://doi.org/10.1073/pnas.1901294117

Zöller, I., Meixner, M., Hartmann, D., Büssow, H., Meyer, R., Gieselmann, V., & Eckhardt, M. (2008). Absence of 2-Hydroxylated Sphingolipids Is Compatible with Normal Neural Development But Causes Late-Onset Axon and Myelin Sheath Degeneration. *The Journal of Neuroscience*, *28*(39), 9741–9754. https://doi.org/10.1523/JNEUROSCI.0458-08.2008

APPENDIX ONE

Developmental Study of Myelination and Compound Action Potentials (CAP)

Background: g-ratios are the gold standard in the myelin field of assessing myelin health, and proper conduction of action potentials in myelinated fibers. Recently, our work has shown that g-ratios are not an indicator of axonal function, and ion channel mis-localization may be a more sensitive indicator of axonal health. During early post-natal development, the myelination is not complete in the corpus callosum and proper myelin domains (Node of Ranvier, paranode, and juxtaparanode) have not been set up yet.

Rational: Therefore, we want to compare g-ratios, nodal domain localization, and electrophysiological function of developing brains. *I contributed electrophysiological studies which will be described below*

Methods: Post natal day 14, 21, and 28 day old wild-type c57black/6J mice were initially anesthetized with the volatile anesthetic isoflurane followed by an intraperitoneal injection of ketamine (200 mg/kg) and xylazine (20 mg/kg). Mice were then transcardially perfused with ice-cold sucrose artificial cerebrospinal fluid (sucrose-aCSF), which contained (in mM): 206 sucrose, 25 glucose, 25 $NaHCO_3$, 4 $MgSO_4$, 3 KCl, 1.25 NaH_2PO_4, 1.2 $CaCl_2$ saturated with 95% O_2 and 5% CO_2. Following perfusion, mice were decapitated and the brain removed to produce ex vivo brain slices. Coronal brain slices of 350μm thickness were sectioned in the same ice-cold sucrose-aCSF using a vibratome (Leica VT1200, Leica Biosystems, Deer Park, IL). Slices between 1.0 mm anterior to bregma and -2.5 mm posterior to bregma were collected for recording and maintained in an incubation chamber for at least 30 min before recording. The incubation chamber contained room temperature aCSF (~21° C) consisting of (in mM): 125 NaCl, 25 $NaHCO_3$, 25 glucose, 3 KCl, 1.2 NaH_2PO_4, 1.2 $CaCl_2$, 1.2 $MgSO_4$ bubbled with 95% O_2 and 5% CO_2. For recording, slices were transferred to a recording chamber mounted on the stage of an Olympus BX51WI microscope (Olympus Life Science Solutions, Bartlett, TN) equipped with a 10x (0.3 NA) water immersion objective and perfused with oxygenated room temperature aCSF. For electrophysiology studies, an n = 3 mice per timepoint was used.

To stimulate corpus callosal fibers, a bipolar stimulating electrode (FHC Neural Microtargeting, Bowdoin, ME; matrix electrode; cat #30250) was placed approximately 1 mm from a glass micropipette recording electrode

filled with extracellular solution (1.65 mm OD, 1.0 mm ID, 8250 capillary glass, King Precision Glass, Claremont, CA). Micropipettes were pulled on a horizontal electrode puller (P1000; Sutter Instruments, Novato, CA) to produce tip diameters of approximately 2µm that resulted in ~3 MΩ resistances when filled with aCSF. Compound action potentials (CAPs) were evoked with a DS3 Isolated Current Stimulator (Digitimer, Ft. Lauderdale, FL) and measured with a Model 2400 patch clamp amplifier (A-M Systems; Sequim, WA). The resultant extracellular analog signals were converted into a digital signal by a PCI-6040E A/D board (National Instruments, Austin, TX), and stored and analyzed on a PC computer using WCP Strathclyde Software (courtesy of Dr. J Dempster, Strathclyde University, Glasgow, Scotland). CAPs were elicited using a stimulation protocol consisting of five consecutive sweeps, 100µs in duration, with a 10s delay between sweeps ranging from 100µA to 500µA. An average of three recordings from one slice was used to reduce signal to noise ratio. CAPs were analyzed using the WinWCP program (courtesy of Dr. J Dempster, Strathclyde University, Glasgow, Scotland). Graphpad prism (San Diego, CA) was used to graph the ratio of N1 (myelinated axons) to N2 (unmyelinated axons) and for statistical analysis. Analysis was performed using a 2-way ANOVA comparing genotypes across stimulus current. Representative traces were superimposed using Origin2020b software (Origin, Northampton, MA).

Results: At 7 days of age, the mice presented with no N1, only one singular peak was observed. This peak occurred 3 milliseconds after the stimulus artifact which is consistent with N2 peaks. At 21 days of age the average stimulus current was 0.147 ± 0.02 and at 28 days the average stimulus current was 0.2358 ± 0.02. The ratio of N1/N2 averaged across all stimulus currents for 7, 21, and 28 day old mice were significantly different (appendix figure 1).

Moving forward: The data is highly variable, increase ‘n’ at each timepoint as well as performing electrophysiology on 7 day old mice would give clearer picture on the relationship between myelination state indicated by g-ratio, and CAP. IHC and EM still need to be conducted to compare g-ratio, ion channel localization, and CAP along development

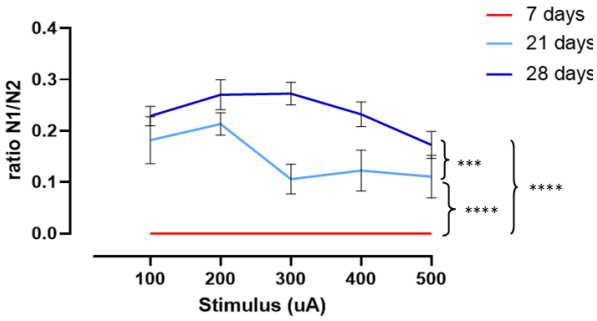

Appendix figure 1: Compound action potential (CAP) recordings demonstrate an increase in the ratio of N1:N2 with development. Analyzed using a 2-way ANOVA. ***p<0.0005 ****p<0.0001

Primary Mouse OL Culture

Primary Mouse Oligodendrocyte Culture

(Protocol adapted from Dr. Pam Knapp Lab) Red font are E.D suggestions

Oligodendrocyte cell culture protocol

In advance:

Sterilize hood with 70% EtOH

Sterilize instruments (10 min to warm sterilizer, 10 sec to sterilize)

Prepare 2 35 mm dishes: one with 3 mL sterile SFM, one with 2 mL SFM + 1 mL Trypsin/DNase

Prepare a 15 mL conical tube with 7 mL SFM

Cover a small piece of cardboard with gauze and soak with 70% EtOH

1. Decapitate p0-p2 mouse pups (n of 2-3), pin the heads to the gauze pad and spritz with 70% EtOH
2. Remove the skin and the skull, then transfer the brain into one of the 35 mm dishes
3. Divide the hemispheres with a scalpel and remove the cerebellum, then remove the meninges under the dissection scope (thin membranous layer, most visible by vasculature)
4. Transfer the clean (meninges removed) brains into the second dish of SFM with Trypsin/DNase
5. Dice the brains into small pieces and transfer them to the 15 mL tube with p1000
6. Loosen the cap and place in the incubator – incubate for 30 minutes, gently mixing by inversion every 10 minutes
7. Centrifuge for 5 min at 1000 rpm
8. Pour off supernatant and resuspend pellet in 9 mL of 10% FBM
9. Triturate the tissue 12-15 times with a 10 mL stripette – allow large pieces to settle, then filter TOP 4 mL through a pre-wet 100 µm filter
10. Triturate the tissue 12-15 times with a 5 mL stripette – allow large pieces to settle, then filter another 4 mL

11. Triturate the remaining tissue with a 1000 µL pipette then filter
12. Centrifuge filtrate for 5 min at 1000 rpm
13. Pour off supernatant and resuspend cells in 10% FBM and filter through a 40 µm filter (resuspend in at least 1 mL)
14. Plate on PLL coated T25, ~ 1 brain per flask (4mL total, add 2mL media)
15. Feed cells 24 hours later, washing debris if necessary, then every 2-3 days with 10% FBM – 3-5 days post plating, switch to OGM (usually around ~60% confluency)

Harvesting OPC's

16. After 7-10 DIV, shake off microglia for 1 hr at 120 rpm, 37˚C (cells should be confluent with plentiful progenitor on top of the astrocyte bed layer when ready to harvest, should see some sizable progenitor clumps)
    a. Aspirate media containing microglia and replace with fresh ODM FBM
17. Bang flask on the bench (thigh works better for me, softer surface decreases contaminating cells) 5-10 times to lift oligodendrocyte progenitors and transfer media containing OPCs to conical tube
    a. *For this step, it's best to look at the flask, do a few bangs, and check to see what cells have lifted and assess from there – the bang uses substantial force, not enough to like bruise but it does hurt*
18. DIFFERENTIAL ADHESION STEP transfer harvested cells to a non-TC treated petri dish (100 mm) and incubate for at least 2 hr
19. Gently tap/swirl the dish to lift the unadhered oligodendrocytes (astrocytes and microglia will adhere quickly to the dish while OPCs will take longer and will not adhere as strongly)
20. Pellet OPCs at 1000 rpm for 5 minutes – pour off supernatant and resuspend cells in the volume of media remaining in the tube (~300uL)
    a. Count cells and calculate at a density of 50,000 cells per 1mL I calculated 50,000 cells per 0.1mL. Spot 80 µL of ODM onto coverslips, then spot cells into the meniscus of media on PLL coated 12mm coverslip. After 30 min to an hour flood the wells with 750 µL of ODM
    b. Check cells at 24 hours but do not change media until 48 hours after

c. After change media every 2-3 days, OLs should begin to differentiate after 5 days.

d. I find the OLs look best when there is a higher density, but over crowded and not good for imaging. Therefore, when cells are differentiated, I would GENTLY wash cells trying to knock a few off to get separated OLs

- Once OLs are differentiated, fix with 4% PFA, I had issues with OLs dying right after differentiation
- For imaging, before PFA fixing, take media and wash cells gently to try to knock off a few cells to get the OLs more sparse. This will allow better imaging of single OLs

NOTE: Poly-L-Lysine (Sigma #p2636-100mg) should be done at concentration of i.e 100 mg/mL stock diluted in 20 mL borate buffer and sterile filter

PLL coverslip (CS) coating

1. ***Prepare Borate Buffer: to 1L of water, add 3.1g of Boric acid (Sigma, cat#B6768) and 4.75g Sodium Borate (Sigma, cat# 221732). Note* I always had trouble getting this to issolve completely***
2. ***Aliquot into 50mL conical tubes and store at -20°C.***
3. ***CS stored in 100% Etoh, place CS into 24 well plate and wash with sterile H2O***
4. ***Let completely dry (overnight) under hood***
5. ***Put 100uL of PLL on CS and let sit 3hrs or overnight***
6. ***Wash CS 3x 5min each with sterile H2O***
7. ***Let completely dry overnight***
8. ***Can store at 4°C up to one month***

SFM

190 mL DMEM

3.5 mL 7.5% $NaHCO_3$

2 mL 50% glucose

1 mL Pen/Strep

Sterile filter

10% FBM

175 mL DMEM

3.5 mL 7.5% $NaHCO_3$

2 mL 50% glucose

1 mL Pen/Strep

20 mL FBS

Sterile filter

Trypsin/DNase

20 mL DMEM

3 mg DNase

500 mg Trypsin

Sterile filter and aliquot – store at -20˚C

Borate Buffer

3.1 g boric acid

4.75 g Na Borate

1 L ddH_2O

pH 8.5, store in fridge

Oligodendrocyte growth media (OGM)

190 mL DMEM

2 mL N2 supplement

2 mL L-Glutamine (100X)

2 mL Sodium Pyruvate (100X)

3 mL Sodium Bicarbonate (7.5%)

1 mL Pen/Strep

100 µL PDGF-AA (10 µg/mL)

100 µL NT-3 (2 µg/mL)

50 µL bFGF (20 µg/mL)

100 µL Insulin (5 µg/mL)

Sterile filter

Oligodendrocyte Differentiation media (ODM)

190 mL DMEM

2 mL N2 supplement

2 mL L-Glutamine (200X)

2 mL Sodium Pyruvate (100X)

3 mL Sodium Bicarbonate (7.5%)

1 mL Pen/Strep

100 µL Insulin (5 µg/mL)

200 µL NAC (5 mg/mL)

100 µL CNTF (20 ng/mL)

2.4 µL T3 (thyroid hormone, 15 mg/mL)

Sterile filter

OL media stocks

PDGF-AA (peprotech cat# 100-13A-10UG)

- Reconstitute in 100 µL ddH_2O
- Dilute with 900 µL 0.1% BSA to final concentration of 10 µg/mL
- *Aliquot to 100 µL and store at -20 ˚C for up to 12 months*

- NT-3 (peprotech cat# 450-03-2UG)
  - Reconstitute in 20 µL ddH_2O
  - Dilute with 980 µL 0.1% BSA to final concentration of 2 µg/mL
  - *Aliquot to 100 µL and store at -20 ˚C for up to 6 months*
- CNTF (peprotech cat# 450-13-20UG)
  - Reconstitute in 200 µL ddH_2O
  - Dilute with 800 µL 0.1% BSA to final concentration of 20 µg/mL
  - *Aliquot to 100 µL and store at -20 ˚C for up to 12 months*
- NAC (sigma cat#)
  - Reconstitute 50 mg NAC in 5 mL ddH_2O and 5 mL 0.1% BSA (final conc. 5 mg/mL)
  - *Aliquot to 200 µL and store at -20 ˚C for up to 12 months*
- Insulin (sigma cat# I6634-50MG)
  - Reconstitute 15 mg insulin in 3 mL ddH_2O – drop in 1M HCL until solution clears (insulin has a neutral pH and requires an acidic solution to dissolve, ~0.1M HCL)
  - *Aliquot to 100 µL and store at -20 ˚C for up to 6 months*
- bFGF (peprotech cat# 100-18B-10UG)
  - Reconstitute in 100 µL 5mM Tris (pH 7.6)
  - Dilute in 400 µL 0.1% BSA to final concentration of 20 µg/mL
  - *Aliquot to 50 µL and store at -20 ˚C for up to 12 months*
- T3 (tocris cat# 6666)

Vita

Elizabeth Dustin was born in Raleigh, North Carolina in 1994 and raised in Fuquay-Varina, NC. She received a Bachelor's with honors in Biological Science with a concentration in Integrative Physiology and Neurobiology with a minor in Biomanufacturing from North Carolina State University in 2016. After college, Elizabeth worked as a Biomanufacturing Training Associate at Biomanufacturing Training and Education Center at NCSU. In 2018, Elizabeth was accepted into the Biomedical Sciences Doctoral Portal at the Virginia Commonwealth University School of Medicine, where she completed her neuroscience graduate training under the mentorship of Jeffery Dupree, PhD. This thesis was defended on May 4th, 2023 before the PhD committee.